

# Summary of FY 2000 Geosciences Research

November 2001



U.S. Department of Energy

Office of Science  
Office of Basic Energy Sciences  
Division of Engineering and Geosciences  
Washington, D.C. 20585

# Table of Contents

<b>TABLE OF CONTENTS</b>	<b>I</b>
<b>FORWARD</b>	<b>X</b>
<b>THE GEOSCIENCES RESEARCH PROGRAM IN THE OFFICE OF BASIC ENERGY SCIENCES</b>	<b>11</b>
<b>CONTRACTOR: ARGONNE NATIONAL LABORATORY</b>	<b>12</b>
CATEGORY: Geochemistry	12
Mineral-Fluid Interactions: Synchrotron Radiation Studies at the Advanced Photon Source	12
<b>CONTRACTOR: BROOKHAVEN NATIONAL LABORATORY</b>	<b>14</b>
CATEGORY: Geophysics	14
Study of the Microgeometry of Geological Materials Using Synchrotron Computed Microtomography	14
CATEGORY: Geochemistry	16
Geochemistry of Organic Sulfur in Marine Sediments	16
<b>CONTRACTOR: LAWRENCE BERKELEY NATIONAL LABORATORY</b>	<b>17</b>
CATEGORY: Geophysics	17
Joint Inversion for Subsurface Imaging	17
Center for Computational Seismology (CCS)	19
Deformation and Fracture of Poorly Consolidated Media	20
Decomposition of Scattering and Intrinsic Attenuation on Rock with Heterogeneous Multiphase Fluids Distributions	22
Unsaturated Fast Flow in Fractured Rock: Testing Film Flow and Aperture Influences	24
Prediction and Evaluation of Coupled Processes for CO <sub>2</sub> Disposal in Aquifers	26
Colloid Transport in Unsaturated Porous Media and Rock Fractures	27
CATEGORY: Geochemistry	28
Integrated Isotopic Studies of Geochemical Processes	28
Clay Mineral Surface Geochemistry	30
Molecular-level studies of Fe-Al oxyhydroxide coating formation on quartz	31
Development of Isotope Techniques for Reservoir and Aquifer Characterization	33
Geochemical and Isotopic Constraints on Processes in Oil Hydrogeology	33
Reactive Chemical Transport in Structured Porous Media: X-ray Microprobe and Micro-XANES Studies	35
<b>CONTRACTOR: LAWRENCE LIVERMORE NATIONAL LABORATORY</b>	<b>37</b>
CATEGORY: Geophysics	37
Pore-scale Simulations of Rock Deformation, Fracture and Fluid Flow in Three Dimensions	37

Three-dimensional Analysis of Seismic Signatures and Characterizations of Fluids and Fractures in Anisotropic Formations	38
Physical Properties of Heterogeneous Rocks Containing Fluids	39
Geophysical Monitoring of Carbon Dioxide Sequestration using Electrical Resistance Tomography (ERT)	40
Water Distribution in Partially Saturated Porous Materials	41
CATEGORY: Geochemistry	42
Reactive Transport of CO <sub>2</sub> -Rich Fluids and Precipitation and Dissolution in Rock Fractures	42
The Role of Carbon and Temperature in Determining Electrical Conductivity of Basins, Crust, and Mantle.	43
Thermodynamic and Transport Properties of Aqueous Geochemical Systems	44
Collaborative Research: Studies for Surface Exposure Dating in Geomorphology	45
In-Situ CO <sub>2</sub> -sequestration: Measurement of Coupled Silicate Dissolution and Carbonate Precipitation	46
Mineral Dissolution and Precipitation Kinetics: A Combined Atomic-Scale and Macro-Scale Investigation	47
Determining the Physical Controls on Biomineralization	49
Testing Deep Saline Aquifers for Long-term CO <sub>2</sub> Leakage Using In-Situ Noble Gases	51
<b>CONTRACTOR: LOS ALAMOS NATIONAL LABORATORY</b>	<b>52</b>
CATEGORY: Geophysics	52
Fast 3D Seismic Modeling and Prestack Depth Migration Using Generalized Screen Methods	52
The Role of Carbon and Temperature in Determining Electrical Conductivity of Basins, Crust, and Mantle.	53
Nonlinear Elasticity in Earth Materials	54
Nonlinear Dynamics of Contaminant Transport	55
Energy Transport in Space Plasma	56
The Solar Wind-Magnetospheric Interaction	56
Energetic Particle Acceleration and Transport	57
CATEGORY Geochemistry	58
Uranium Series Concordance Studies	58
Surface Exposure Dating in Geomorphology	59
Dissolution of Fe(III)(hydr)oxides by Aerobic Microorganisms	59
<b>CONTRACTOR: OAK RIDGE NATIONAL LABORATORY</b>	<b>61</b>
CATEGORY: Geochemistry	61
Volumetric Properties, Phase Relations and Reaction Kinetics of CO <sub>2</sub> -CH <sub>4</sub> -H <sub>2</sub> -H <sub>2</sub> O Fluids: Effects of Injecting CO <sub>2</sub> into Geological Reservoirs	61
Fundamental Research in the Geochemistry of Geothermal Systems	62
Ion Microprobe Studies of Fluid-Rock Interaction	63
Fundamental Research in Isotopic Fractionation of Carbonate Systems Relevant Subsurface CO <sub>2</sub> -Sequestration	65
Experimental studies of Hydrothermal Fluid Speciation and Fluid/Solid Interaction Employing Potentiometric Methods	66
Mechanisms and Rates of Isotope Exchange in Mineral-Fluid Systems	67
Nanoscale Complexity at the Oxide-Water Interface	68

<b>CONTRACTOR: PACIFIC NORTHWEST LABORATORY</b>	<b>70</b>
CATEGORY: Geochemistry	70
Local Reactions on Carbonate Surfaces: Structure, Reactivity, and Solution	70
Structure and Reactivity of Iron Oxide and Oxyhydroxide Surface	72
Molecular Basis for Microbial Adhesion and Geochemical Surface Reactions in Fe-Reducing Bacteria	74
Electron Transfer at the Fe(III) Oxide-Microbe Interface	75
<b>CONTRACTOR: SANDIA NATIONAL LABORATORIES</b>	<b>77</b>
CATEGORY: Geophysics	77
Forward modeling and inversion of seismic data in 3D isotropic elastic media	77
Three Dimensional Transient Electromagnetic Inversion	78
Micromechanical Processes in Porous Geomaterials	79
The Role of Fracture Intersections in the Flow and Transport Properties of Rock	80
Continuum and Particle Level Modeling of Concentrated Suspension Flows	82
Transport Visualization for Studying Mass Transfer and Solute Transport in Permeable Media	83
Investigation of Permeability Upscaling	85
The Physics of Two-Phase Immiscible Fluid Flow in Single Fractures and Fractured Rock	86
CATEGORY: Geochemistry	88
Atomistic Simulations of Clay Minerals and Their Interaction with Hazardous Wastes: Molecular Orbital and Empirical Methods	88
<b>PART II: OFF-SITE</b>	<b>90</b>
<b>GRANTEE: AMERICAN MUSEUM OF NATURAL HISTORY</b>	<b>90</b>
The Influence of Carbon on the Electrical Properties of Crustal Rocks	90
<b>GRANTEE: ARIZONA STATE UNIVERSITY</b>	<b>91</b>
A Sims Study of the Chemical Dynamics of Organic/Inorganic Interactions in Sedimentary Basins	91
<b>GRANTEE: BOSTON UNIVERSITY</b>	<b>93</b>
Analysis and Interpretation of Multi-Scale Phenomena in Crustal Deformation Processes: Using Numerical Simulations of Complex Nonlinear Earth Systems	93
<b>GRANTEE: CALIFORNIA INSTITUTE OF TECHNOLOGY</b>	<b>94</b>
Infrared Spectroscopy and Stable Isotope Geochemistry of Hydrrous Silicate Glasses	94
Isotope Tracer Studies of Diffusion in Silicates and of Geological Transport Processes Using Actinide Elements	96
<b>GRANTEE: UNIVERSITY OF CALIFORNIA AT BERKELEY</b>	<b>98</b>
Advective-Diffusive/Dispersive Transport of Chemically Reacting Species in Hydrothermal System	98
Collaborative Research: Studies for Surface Exposure Dating in Geomorphology	100
Dissolution of Fe(III)(hydr)Oxides by Aerobic Microorganisms	101

<b>GRANTEE: UNIVERSITY OF CALIFORNIA AT DAVIS</b>	<b>103</b>
The Kinetics of Dissociation of Aluminum-Oxygen Bonds in Aqueous Complexes: An NMR Study	103
Thermodynamics of Minerals Stable Near the Earth's Surface	105
Electrochemical Measurements of Thermodynamics Properties of Minerals and the Processes of Reconstruction at Mineral Surfaces	106
<b>GRANTEE: UNIVERSITY OF CALIFORNIA AT LOS ANGELES</b>	<b>108</b>
Application of $^{40}\text{Ar}/^{39}\text{Ar}$ Thermochronometry and Ion Microprobe Stable Isotope Geochemistry to the Evolution of Petroleum Reservoirs and Hydrothermal Systems	108
<b>GRANTEE: UNIVERSITY OF CALIFORNIA AT SANTA BARBARA</b>	<b>110</b>
Fluid Flow in Faults: Estimating Permeability and Diagenetic Effects in a Transpressional Setting, Southern California	110
<b>GRANTEE: UNIVERSITY OF CALIFORNIA AT SANTA BARBARA</b>	<b>111</b>
Three-Dimensional Miscible Porous Media Flows with Viscosity Contrasts and Gravity Override	111
Magma Rheology, Mixing of Rheological Fluids, Molecular Dynamics Simulation, and Lithospheric Dynamics	112
<b>GRANTEE: UNIVERSITY OF CALIFORNIA AT SANTA CRUZ</b>	<b>114</b>
Fast 3D Modeling and Prestack Depth Migration Using Generalized Screen Methods	114
<b>GRANTEE: THE UNIVERSITY OF CHICAGO</b>	<b>116</b>
Kinetic Isotope Fractionation	116
GeoSoilEnviroCARS: A National Resource for Earth, Planetary, Soil and Environmental Science Research at the Advanced Photon Source	117
Synchrotron X-ray Microprobe and Microspectroscopy Research in Low Temperature Geochemistry	120
<b>GRANTEE: THE CITY COLLEGE OF THE CITY UNIVERSITY OF NEW YORK</b>	<b>123</b>
Particulate Dynamics in Filtration and Granular Flow	123
<b>GRANTEE: UNIVERSITY OF COLORADO</b>	<b>124</b>
Analysis and Interpretation of Multi-Scale Phenomena in Crustal Deformation Processes: Using Numerical Simulations of Complex Nonlinear Earth Systems	124
Evolution of Rock Fracture Permeability During Shearing	125
Nucleation and Growth Kinetics of Clays and Carbonates on Mineral Substrates	127
Two-Phase Immiscible Fluid Flow in Fractured Rock: The Physics of Two-Phase Flow Processes in Single Fractures	128
Seismic Absorption and Modulus Measurements in Single Cracks and Porous Rocks: Physical and Chemical Effects of Fluids	130

<b>GRANTEE: COLORADO SCHOOL OF MINES</b>	<b>131</b>
Possible Vertical Migration of CO <sub>2</sub> Associated with Large-Scale Injection into Subsurface Geologic Formations	131
Three-dimensional Analysis of Seismic Signatures and Characterization of Fluids and Fractures in Anisotropic Formations	132
<b>GRANTEE: COLUMBIA UNIVERSITY</b>	<b>134</b>
Rock Varnish Record of Holocene Climate Variations in the Great Basin of Western US	134
<b>GRANTEE: UNIVERSITY OF CONNECTICUT</b>	<b>136</b>
Geochemical and Isotopic Constraints on Processes in Oil Hydrogeology	136
<b>GRANTEE: UNIVERSITY OF DELAWARE</b>	<b>139</b>
Development of an Experimental Database and Theories For Prediction of Thermodynamic Properties of Aqueous Electrolytes and Nonelectrolytes of Geochemical Significance at Supercritical Temperatures and Pressures	139
<b>GRANTEE: UNIVERSITY OF FLORIDA</b>	<b>141</b>
Pore Scale Simulations of Rock Deformation, Fracture, and Fluid Flow in Three Dimensions	141
<b>GRANTEE: GEORGIA INSTITUTE OF TECHNOLOGY</b>	<b>143</b>
Biomineralization: Organic-Directed Controls on Carbonate Growth Structures and Kinetics Determined by <i>In situ</i> Atomic Force Microscopy	143
<b>GRANTEE: UNIVERSITY OF HAWAII</b>	<b>145</b>
Growth of Faults, Scaling of Fault Structure, and Hydrologic Implications	145
<b>GRANTEE: UNIVERSITY OF ILLINOIS AT URBANA-CHAMPAIGN</b>	<b>146</b>
Computational and Spectroscopic Investigations of Water-Carbon Dioxide Fluids and Surface Sorption Processes	146
<b>GRANTEE: INDIANA UNIVERSITY</b>	<b>148</b>
Self-Organized Mega-Structures in Sedimentary Basins	148
Isotopically Labile Organic Hydrogen in Thermal Maturation of Organic Matter	150
<b>GRANTEE: THE JOHNS HOPKINS UNIVERSITY</b>	<b>152</b>
Fluid Flow in Faults: Estimating Permeability and Diagenetic Effects in a Transpressional Setting, Southern California	152
Predictive Single-Site Protonation and Cation Adsorption Modeling	153
Reactions and Transport of Toxic Metals in Rock-Forming Silicates at 25°C	154
<b>GRANTEE: KENT STATE UNIVERSITY</b>	<b>156</b>
Dissolution of Fe(III)(hydr)oxides by Aerobic Microorganisms	156
<b>GRANTEE: LEHIGH UNIVERSITY</b>	<b>159</b>
Reactions and Transport of Toxic Metals in Rock-Forming Silicates at 25°C	159

<b>GRANTEE: UNIVERSITY OF MARYLAND</b>	<b>161</b>
Theoretical Studies on Metal Species in Solution and on Mineral Surfaces	161
<b>GRANTEE: MASSACHUSETTS INSTITUTE OF TECHNOLOGY</b>	<b>164</b>
Evolution of Pore Structure and Permeability of Rocks under Hydrothermal Conditions	164
Transport Visualization for Studying Mass Transfer and Solute Transport in Permeable Media	166
Theoretical Studies of Landscape Erosion	167
Fluid Mobility Estimation From Electroseismic Measurements: Laboratory, Field, and Theoretical Study	168
<b>GRANTEE: UNIVERSITY OF MINNESOTA, TWIN CITIES</b>	<b>169</b>
Magma Rheology, Mixing of Rheological Fluids, Molecular Dynamics Simulation , and Lithospheric Dynamics	169
<b>GRANTEE: NATIONAL ACADEMY OF SCIENCES, BOARD ON EARTH SCIENCES AND RESOURCES</b>	<b>171</b>
Board on Earth Sciences and Resources and Its Activities	171
<b>GRANTEE: UNIVERSITY OF NEVADA at RENO</b>	<b>172</b>
Growth of Faults, Scaling of Fault Structure, and Hydrologic Implications	172
<b>GRANTEE: NEW ENGLAND RESEARCH</b>	<b>173</b>
The Role of Fracture Intersections in the Flow and Transport Properties of Rock	173
<b>GRANTEE: UNIVERSITY OF NEW MEXICO</b>	<b>175</b>
Continuum and Particle Level Modeling of Concentrated Suspension Flows	175
<b>GRANTEE: NEW MEXICO INSTITUTE OF MINING AND TECHNOLOGY</b>	<b>177</b>
Investigation of Permeability Upscaling	177
<b>GRANTEE: STATE UNIVERSITY OF NEW YORK AT STONY BROOK</b>	<b>179</b>
High Precision Radiometric Dating of Sedimentary Materials	179
Medial Axis Analysis of Porous Media	181
Surface Chemistry of Pyrite: An Interdisciplinary Approach	182
Micromechanical Processes in Porous Geomaterials	184
<b>GRANTEE: NORTHWESTERN UNIVERSITY</b>	<b>186</b>
Interactions of Pore Fluid Pressure and Inelastic Deformation of Dilating and Compacting Rock	186
<b>GRANTEE: OKLAHOMA STATE UNIVERSITY</b>	<b>187</b>
The Physics of Two-Phase Immiscible Fluid Flow in Single Fractures and Fractured Rock	187
<b>GRANTEE: UNIVERSITY OF OKLAHOMA</b>	<b>189</b>
Development and Application of a Paleomagnetic/Geochemical Method for Constraining the Timing of Fluid Migration and Other Diagenetic Events	189

<b>GRANTEE: OREGON STATE UNIVERSITY</b>	<b>191</b>
Transport Visualization for Studying Mass Transfer and Solute Transport in Permeable Media	191
<b>GRANTEE: THE PENNSYLVANIA STATE UNIVERSITY</b>	<b>192</b>
Dissolution of Feldspar in the Field and Laboratory	192
Critical Chemical-Mechanical Couplings that Define Permeability Modification in Pressure-Sensitive Rock Fractures	194
<b>GRANTEE: PRINCETON UNIVERSITY</b>	<b>195</b>
In-situ Evaluation of Soil Organic Molecules: Functional Group Chemistry, Aggregates Structures, Metal and Mineral Surface Complexation using Soft X-rays	195
<b>GRANTEE: PURDUE UNIVERSITY</b>	<b>196</b>
Mechanical Models of Fault-Related Folding	196
Seismic Monitoring of Time-Dependent, Multi-Scale Heterogeneity in Fractured Rock	197
<b>GRANTEE: RENSSELAER POLYTECHNIC INSTITUTE</b>	<b>199</b>
Transport Phenomena in Fluid-Bearing Rocks	199
<b>GRANTEE: RICE UNIVERSITY</b>	<b>201</b>
Transition Metal Catalysis in the Generation of Petroleum and Natural Gas	201
<b>GRANTEE: SCRIPPS INSTITUTION OF OCEANOGRAPHY</b>	<b>203</b>
Joint Inversion of Acoustic and Induction Log Data for Enhanced Resistivity Structure	203
<b>GRANTEE: SMITHSONIAN INSTITUTION</b>	<b>204</b>
Low-T, Fluid-Ashflow-Tuff Interactions : How Rock Textures, Chemistry, and Mineralogy Reflect Reaction Pathways and Influence Rock Response to Heating	204
<b>GRANTEE: UNIVERSITY OF SOUTHERN CALIFORNIA</b>	<b>205</b>
Three-Dimensional Miscible Porous Media Flows with Viscosity Contrast and Gravity Override	205
<b>GRANTEE: STANFORD UNIVERSITY</b>	<b>206</b>
Metal Ion Sorption at Oxide Surfaces and Oxide-Water Interfaces: Spectroscopic Studies and Modelling”	206
Seismic Signatures of Fluids in Anisotropic Rocks	208
Porous Rocks with Fluids: Seismic and Transport Properties	210
Diffusion of CO <sub>2</sub> during Hydrate Formation and Dissolution	211
Development of Fracture Networks and Clusters: Their Role in Channelized Flow in Reservoirs and Aquifers	213
Coupled Fluid Deformation Effects in Earthquakes and Energy Extraction	215
<b>GRANTEE: TEMPLE UNIVERSITY</b>	<b>216</b>
Surface Chemistry of Pyrite: An Interdisciplinary Approach	216

<b>GRANTEE: THE UNIVERSITY OF TENNESSEE</b>	<b>218</b>
Development of Laser-Based Resonance Ionization Techniques for $^{81}\text{Kr}$ and $^{85}\text{Kr}$ in the Geosciences	218
<b>GRANTEE: TEXAS A&amp;M UNIVERSITY</b>	<b>220</b>
Time-Lapse Seismic Monitoring and Performance Assessment of $\text{CO}_2$ Sequestration in Hydrocarbon Reservoirs	220
Fluid-Assisted Compaction and Deformation of Reservoir Lithologies	222
Experimental and Analytic Studies to Model Reaction Kinetics and Mass Transport of Carbon Dioxide Sequestration in Depleted Carbonate Reservoirs	224
<b>GRANTEE: UNIVERSITY OF TEXAS</b>	<b>225</b>
High-Resolution Temporal Variations in Groundwater Chemistry: Tracing the Links between Climate, Hydrology, and Element Mobility in the Vadose Zone.	225
Thermohaline Convection in the Gulf of Mexico Sedimentary Basin, South Texas	226
<b>GRANTEE: THE UNIVERSITY OF TEXAS AT DALLAS</b>	<b>228</b>
Integrated 3-D, Ground-penetrating Radar, Outcrop, and Borehole Data Applied to Reservoir Characterization and Flow Simulation	228
<b>GRANTEE: TEXAS TECH UNIVERSITY</b>	<b>230</b>
Continuum and Particle Level Modeling of Concentrated Suspension Flows	230
<b>GRANTEE: UNIVERSITY OF UTAH</b>	<b>232</b>
A Comparative Study of the Feasibility for $\text{CO}_2$ Sequestration in Faulted and Fractured Sandstones in Eolian and Fluvial Deltaic Deposits	232
High Resolution Imaging of Electrical Conductivity using Low-Frequency Electromagnetic Fields	234
<b>GRANTEE: UTAH STATE UNIVERSITY</b>	<b>235</b>
A Comparative Study of the Feasibility for $\text{CO}_2$ Sequestration in Faulted and Fractured Sandstones in Eolian and Fluvial Deltaic Deposits	235
Growth of Faults and Scaling of Fault Structure	237
<b>GRANTEE: VIRGINIA POLYTECHNIC INSTITUTE &amp; STATE UNIVERSITY</b>	<b>239</b>
Experimental Studies in the System $\text{H}_2\text{O}-\text{CH}_4$ -“Petroleum”-Salt Using Synthetic Fluid Inclusions	239
Microbial Community Acquisition of Nutrients from Mineral Surfaces	241
<b>GRANTEE: UNIVERSITY OF WASHINGTON</b>	<b>242</b>
Two and Three-dimensional Magnetotelluric and Controlled Source Electromagnetic Inversion	242
Electromagnetic Imaging of Fluids in the San Andreas Fault	244

<b>GRANTEE: UNIVERSITY OF WISCONSIN</b>	<b>246</b>
Three Dimensional Transient Electromagnetic Inversion	246
Precipitation at the Microbe-Mineral Interface	248
Deformation and Fracture of Poorly Consolidated Media	250
Microanalysis of Stable Isotope Ratios in Low Temperature Rocks	252
Pore-Scale Simulations of Rock Deformation, Fracture, and Fluid Flow in Three Dimensions	254
<b>GRANTEE: WOODS HOLE OCEANOGRAPHIC INSTITUTION</b>	<b>255</b>
Laboratory Constraints on the Stability of Petroleum at Elevated Temperatures: Implications for the Origin of Natural Gas	255
Organic Geochemistry of Outer Continental Margins and Deep-Water Sediments	256
Evolution of Pore Structure and Permeability of Rocks under Hydrothermal Conditions	258
<b>GRANTEE: UNIVERSITY OF WYOMING</b>	<b>259</b>
Mineral Dissolution and Precipitation Kinetics: A Combined Atomic-Scale and Macro-Scale Investigation Targeted Toward CO <sub>2</sub> Sequestration Data Needs	259
<b>GRANTEE: YALE UNIVERSITY</b>	<b>261</b>
A Field Experiment on Plants and Weathering	261
Reactive Fluid Flow and Applications to Diagenesis, Mineral Deposits, and Crustal Rocks	262
<b>SUBJECT INDEX</b>	<b>264</b>
<b>AUTHOR INDEX</b>	<b>270</b>
<b>DOE/OBES GEOSCIENCES RESEARCH: HISTORICAL BUDGET SUMMARY</b>	<b>276</b>

## FORWARD

The Department of Energy supports research in the geosciences in order to provide a sound foundation of fundamental knowledge in those areas of the geosciences that are germane to the Department of Energy's many missions, and those which provide stewardship for geosciences research capabilities, primarily at the DOE National Laboratories. The Geosciences Research Program resides within the Division of Chemical Sciences, Geosciences and Biosciences, part of the Office of Basic Energy Sciences of the Office of Science. The participants in this program include researchers at Department of Energy laboratories, academic institutions, and other governmental agencies. These activities are formalized by a contract or grant between the Department of Energy and the organization performing the work, providing funds for salaries, equipment, research materials, and overhead. Collaborative work among these institutions is encouraged. The summaries in this document, prepared by the investigators, describe the scope of the individual projects. The Geosciences Research Program includes research in the two broad areas of geophysics and geochemistry. Within these areas, topics of research interest include Earth dynamics, properties of Earth materials, rock mechanics, seismic, electromagnetic and radar underground imaging, geochemistry, biogeochemistry, rock-fluid interactions, hydrogeology, coupled reactive fluid flow and transport, resource exploration and evaluation, and geomagnetic solar-terrestrial interactions. All such research is related either directly or indirectly to the Department of Energy's long-range technological needs. Because of the variety of the research needs in the different applied DOE programs, fundamental approaches with multiple potential applications are favored. Further information on the Geosciences Research Program, including recent program activities and highlights, may be found on the Geosciences Programs home page at: <http://www.sc.doe.gov/production/bes/geo/geohome.html>

## THE GEOSCIENCES RESEARCH PROGRAM IN THE OFFICE OF BASIC ENERGY SCIENCES

The Geosciences Research Program is directed by the Department of Energy's (DOE's) Office of Science (SC) through its Office of Basic Energy Sciences (OBES). The Geosciences Research Program emphasizes research leading to fundamental understanding of Earth's natural processes and properties that will advance the forefront of scientific knowledge, as well as help solve geosciences-related problems in multiple DOE mission areas. Activities in the Geosciences Research Program are directed toward building the long-term fundamental knowledge base necessary to provide for energy technologies of the future. Future energy technologies and their individual roles in satisfying the nation's energy needs cannot be easily predicted. It is clear, however, that these future energy technologies will involve consumption of energy and mineral resources and generation of technological wastes. The Earth is a source for energy and mineral resources, and is also the host for wastes generated by technological enterprise. Viable energy technologies for the future must contribute to a national energy enterprise that is efficient, economical, and environmentally sound.

The Geosciences Research Program is divided into two broad categories *Geophysics* and *Geochemistry*.

***Geophysics***: Improving geophysical interrogation of the Earth's crust through better collection and analysis of seismic and electromagnetic data; improving understanding of geophysical signatures of fluids and fluid-bearing reservoirs; and characterizing geologic structures better.

***Geochemistry***: Investigating geochemistry of mineral-fluid interactions through studies of rates and mechanisms of reactions at the atomistic/molecular scale; studying coupled flow and reactivity in porous and fractured rocks; and tracking of mineral-mineral and mineral-fluid processes using isotopes.

The program evolves with time and progress in these and related fields. Individual research projects supported by this program at DOE national laboratories, academic institutions, research centers, and other federal agencies typically have components in more than one of the categories or subcategories listed. In addition, it is common for research activities to involve a high level of collaboration between investigators and different institutions. Cross-cutting issues include: improving understanding of basic properties of rocks, minerals, and fluids; determining physical, chemical, and mechanical properties of multi-phase, heterogeneous, anisotropic systems; improving analysis of rock deformation, flow, fracture, and failure, and characterization of fluid transport properties of large-scale geologic structures. Research progress, in addition, will be based on developing advanced analytical instrumentation and computational methods, including: higher-resolution geophysical imaging and inversion tools, angstrom-scale resolution analysis of heterogeneous minerals with x-ray and neutron methods, and advancing computational modeling and algorithm development.

## **PART I: ON-SITE**

### **CONTRACTOR: ARGONNE NATIONAL LABORATORY**

Environmental Research Division, Bldg. 203  
Argonne, Illinois 60439

**CONTRACT:** W-31-109-Eng-38

**CATEGORY:** Geochemistry

**PERSON IN CHARGE:** P. Fenter

### **Mineral-Fluid Interactions: Synchrotron Radiation Studies at the Advanced Photon Source**

*Paul Fenter, 630-252-7053, fax 630-252-7415, Fenter@anl.gov; Neil C. Sturchio, University of Illinois at Chicago; Michael J. Bedzyk, Northwestern University*

**Website:** [http://www.anl.gov/ER/GPG\\_wp/index.html](http://www.anl.gov/ER/GPG_wp/index.html)

**Objectives:** The objective of this program is to advance the basic understanding of rock-fluid and soil-fluid interactions through experimental studies of atomic-scale processes at mineral-fluid interfaces. This is crucial to establishing the relation between atomic-scale processes and macroscopic geochemical transport in natural systems.

**Project Description:** The principal approach is to observe single-crystal mineral surfaces *in situ* during chemically controlled reactions with fluids, using X-ray scattering, standing-wave, and absorption techniques with high-brilliance synchrotron radiation. These techniques provide high-resolution atomic-scale structural information that cannot be acquired by any other means. Experiments are being performed on common rock- and soil-forming minerals under conditions representative of geochemical environments near the earth's surface. Types of reactions being investigated include dissolution-precipitation, adsorption-desorption, and oxidation-reduction.

**Results:** Progress during the past year included further successful demonstrations of the ability to perform *in situ* X-ray reflectivity, diffraction, and standing-wave studies of reacting mineral surfaces under chemically controlled conditions. Experiments were conducted to characterize the dissolution mechanisms of the orthoclase (001) cleavage plane in contact with aqueous solutions. Distinct dissolution mechanisms were identified at acidic and basic pH through real-time measurements with x-ray reflectivity and atomic force microscopy. The dissolution kinetics were also measured as a function of temperature at acidic and basic pH and the structure of reacted orthoclase (001) surfaces were characterized with high-resolution x-ray reflectivity. X-ray reflectivity was used to probe the structure of the barite (001) and (210) cleavage surfaces and the fluorapatite (100) growth surface in contact with aqueous solutions. Measurements of organic-mineral interactions were also performed on the barite and fluorapatite surfaces. X-ray standing waves and surface X-ray absorption spectroscopy were combined to determine the structure of Zn adsorbed onto rutile as a function of ionic strength. Experimental

studies of ion adsorption on muscovite substrates using X-ray reflectivity techniques were continued, in collaboration with K. L. Nagy (University of Colorado).

**CONTRACTOR: BROOKHAVEN NATIONAL LABORATORY**

Upton, New York 11973-5000

**CONTRACT:** DE-AC02-98CH10886

**CATEGORY: Geophysics**

**Study of the Microgeometry of Geological Materials Using Synchrotron Computed Microtomography**

*K. W. Jones, 631-344-4588, fax 631-344-5271, kwj@bnl.gov*

**Website:** <http://www.rocks.bnl.gov>

**Objectives:** The objective of this project is to gain improved knowledge of the properties and behavior of geological materials on a grain-size scale. Measurements are made to determine: 1) the microgeometry of typical rock types, 2) changes in the microgeometry of the rocks as a function of applied pressure, 3) fluid-flow paths through the rocks, 4) changes in rock composition caused by fluid-rock interactions, and 5) determination of fracture structures and growth as a function of pressure.

**Project Description:** The work in this program is focused on the determination of the microgeometry and microcomposition of different types of geological materials. The results help to improve understanding of the formation mechanisms of different geological materials and fluid flow at a microscopic scale. The experimental work includes: 1) measurement of the structure of rocks from different geological formations to determine the extent of the variability of porosity, permeability, and connectivity of the pore space; 2) structure determinations of sediments, sandstones, carbonates, and limestones following laboratory modification by application of pressure and temperature; 3) fluid-flow measurements using Wood's metal, oil, and water to investigate fluid-rock and fluid-fluid interactions; 4) determination of the composition and structure of micrometeorites; 5) study of vesicles in volcanic basalts to gain refined understanding of the eruption processes; and 6) investigation of other samples as time permits. The experimental approach is based on application of synchrotron computed microtomography (CMT) at the Brookhaven National Laboratory (BNL) National Synchrotron Light Source (NSLS) and other similar facilities. The interpretation of the tomographic measurements is facilitated by the use of data obtained through application of other synchrotron x-ray methods including x-ray fluorescence, x-ray absorption spectroscopy, high-resolution x-ray microscopy, and Fourier Transform Infrared Spectroscopy. The experiments and analyses are carried out in collaboration with scientists from universities, national laboratories, and industry.

**Results:** Experiments were carried out at the BNL NSLS, the Argonne Advanced Photon Source (APS), and the European Synchrotron Radiation Facility (ESRF). The APS and ESRF were used to obtain x-ray beams with characteristics not provided at the NSLS. In particular, a bending magnet at the APS gave high intensity monoenergetic beams at energies above 50 KeV that are suitable for investigation of high-attenuation samples. An undulator beam line at the ESRF was used to obtain intense beams with a size of a few micrometers to make fluorescent tomography measurements of trace metal distributions.

We investigated a Wood's metal filled sandstone sample at both the NSLS and the APS. The Wood's

metal is a surrogate for use of high-contrast fluids to enhance the separation of pores from solids. It is particularly useful since it can be used to give a picture of a particular instant in a fluid-flow process that can be studied at leisure. The measurements represent a convolution of instrumental spatial resolution with the pore-size distribution in the rock. The pixel sizes used were about 0.035 to 0.060 mm so that the results are relevant to the larger pores. The results show the grain structure of the sandstone, unfilled pore space, and the pores filled with Wood's metal so that their x-ray attenuation coefficient is larger than that for the rock. In addition, the percolation front of the Wood's metal was clearly defined. Further measurements will be made with higher resolutions to look at the transport along rock-pore surfaces and the filling of the smaller pores.

Several experiments were carried out to investigate questions related to the microstructure of sediments to provide an experimental basis for modeling the microgeometry for application in fluid flow calculations and for understanding interactions between dissolved metals and grain surfaces. Theoretical models of the sedimentation process have been developed that predict values for quantities such as the 2-point correlation function, conductivity, and permeability. Experimental investigations of sediments can be made using computed microtomography and the results compared to the theoretical predictions.

We determined the distribution of metals in sediment grains from the New York/New Jersey Harbor and from the North Sea using fluorescent tomography at the ESRF. The two sites contrast grains from a location with major input from anthropogenic materials with grains from a relatively pristine location. The measured metals were K, Ca, Ti, Cr, V, Fe, Ni, Cu, and Zn with a pixel size of 0.002 mm. The results did not show clear evidence for increased concentrations at the surface of the particles that might result from metals contained in a coating of organic compounds.

At the NSLS we investigated sieved samples of sands from Cancun, Mexico, in the size range from 0.250 to 0.500  $\mu\text{m}$ . These were contained in a plastic tube with provision for adding and draining fluids so that the wet ability and interfaces between the different fluids used in the experiment, air, iodooctane and water, could be measured. The relatively large grain size was chosen to facilitate identification of pore space and grain surfaces. The voxel size was about 0.010 mm. Tomographic volumes were obtained for a column of dry sand. Then, sedimentation was simulated by filling the tube with liquid and sand and letting the sand settle after shaking. To achieve a two-liquid phase distribution in the pore space of the sand columns, a non-wetting fluid was forced through the sand columns: water in the case of iodooctane-wet sand and iodooctane in the case of water-wet sand. The resulting pore-space fluid distribution was analyzed. This initial investigation yielded a number of tomographic volumes and radiographs of the sand column for different conditions of the fluids in the sand column. Work on comparing this data to the theoretical model predictions is now in progress.

## **CATEGORY: Geochemistry**

### **Geochemistry of Organic Sulfur in Marine Sediments**

*Murthy A. Vairavamurthy 631-344-5337; fax 631-344-5526; vmurthy@bnl.gov*

**Objectives:** The overall objective is to gain a fuller understanding of the geochemical role of the sulfur system in transforming sedimentary organic matter from organized structures typical of biopolymers (*e.g.* proteins and carbohydrates) to heterogeneous sedimentary geopolymers, such as humic substances and kerogen. A major emphasis is placed on understanding the abiotic mechanisms of sulfur incorporation into organic matter and its influence in the preservation of organic matter in marine sediments.

**Program Description:** Sulfur is believed to be involved in preserving organic matter in sediments, in converting this organic matter to petroleum and in controlling the timing of petroleum generation from a source rock. A fundamental geochemical issue is the mechanism of incorporation of sulfur into sedimentary organic matter. Although it is accepted that H<sub>2</sub>S and its partial oxidation products (such as polysulfide ions) are involved, there is controversy about its molecular mechanism, and the active species involved. This project, which is aimed at understanding the formation and transformation of sedimentary organic sulfur during early diagenesis, has four major components: (1) studies of sulfur speciation in sediments, (2) mechanistic studies of organic sulfur formation, (3) mechanistic studies of the pathways of transformation of organic sulfur compounds in sediments, and (4) development of analytical methods. The suite of complementary spectroscopic and chromatographic techniques used (particularly synchrotron-radiation-based XANES spectroscopy for sulfur speciation and liquid chromatography combined with mass spectrometry, LC-MS) give detailed structural information on sulfur and its associated organic moiety.

**Results:** Major types of organic sulfur compounds in soils and sediments include thiols, organic sulfides, di- and poly-sulfides, thiophenes, sulfonates and ester-linked sulfate. Although there is some contribution of the organic sulfur from the original biological organic matter, the dominant fraction is generated through abiotic reactions of inorganic sulfur nucleophiles with functionalized organic matter. Since H<sub>2</sub>S is the predominant sulfur nucleophile, thiols are expected to be the leading products of the initial incorporation of sulfur into organic matter. Thiols also can be formed biotically from the microbial degradation of sulfur-containing biochemicals. Although it is known that thiols can be oxidized to disulfides, the pathways of oxidation in sediments are unclear. Using XANES spectroscopy to determine sulfur speciation, our results with various model thiols establish that iron oxide could be a potential oxidant for forming disulfides from thiols. Thus, the oxic-anoxic interface is probably the primary site for major transformations involving disulfide cross-linking that augments humification.

Furthermore, our results suggest that geochemical catalysis involving transition metal oxides, particularly birnessite, could be important for forming the heterocyclic thiophenic compounds. We used 3-mercaptopropionic acid (3-MPA) as a simple model to understand the transformations of thiols mediated by birnessite. The disulfide was the main product when the thiol was reacted alone with birnessite. However, in the presence of catechol, an important lignin derivative, a thiophenic end product was formed. Evidence suggests that the mechanism involves ring cleavage of catechol forming unsaturated products followed by reaction with 3-MPA. Our results illustrate the importance of mineral catalysis in the transformation of organic sulfur compounds in the geosphere.

**CONTRACTOR: LAWRENCE BERKELEY NATIONAL LABORATORY**

University of California  
Berkeley, CA 94720

CONTRACT: DE-AC03-76SF00098

**CATEGORY: Geophysics**

PERSON IN CHARGE: S. M. Benson

**Joint Inversion for Subsurface Imaging**

*K.H.Lee 510-486-7468, fax 510-486-5686, KHLee@lbl.gov; H.F.Morrison, M.Hoversten, and D.Vasco*

**Objectives:** The objective of this project is to develop a joint inversion methodology using geophysical data to predict the subsurface hydrologic properties. Specifically the data are from in-hole, surface-to-borehole and borehole-to-borehole electromagnetic and seismic surveys, and the in-hole gravity survey, to extrapolate borehole log or core data to the interwell volume. The underlying concept of using the geophysical data to predict the hydrologic properties is borrowed directly from the well-established field of well logging. Here borehole geophysical measurements of sonic velocity, electrical resistivity and density are used jointly to estimate porosity and saturation (usually oil/water saturation). Cross-plots of different physical properties are often reliable site-specific indicators of lithology and, in conjunction with pumping tests, site-specific correlations can be established between the physical properties and permeability. It is the objective of this proposal to extend these concepts to the mapping of hydrological properties in the interwell volume using both in-hole and large-scale cross-hole and hole-to-surface geophysics.

**Project Description:** Accurate mapping of geophysical and hydrological parameters are increasingly more important in the broader study of groundwater supply, development of long-term injection strategy for CO<sub>2</sub> sequestration, characterization and monitoring of petroleum reservoirs and environmental remediation processes, and in almost all aspects of subsurface engineering in general. Geophysical methods can map the distribution of seismic velocity and electrical conductivity beneath the surface and between holes. These physical properties are dependent on density, porosity, fluid saturation, clay content, and in some circumstances, permeability. While general quantitative relationships are elusive, on a site-specific basis this geophysical data can provide spatial information that is ideal for the interpolation of well log data and for constraining or conditioning the inversion of data from pumping tests. The relationship between seismic properties, conductivity, and the hydrologic parameters are now so well known that we propose to develop a means to jointly invert the geophysical and well data to a distribution of properties that satisfies all the field data.

**Results:** A two-dimensional joint inversion algorithm is under development (Dr. Hung-Wen Tseng) using electromagnetic (EM) and seismic traveltimes data. Inversion parameters are the rock porosity and the fluid electrical conductivity instead of the usual bulk electrical conductivity and seismic velocity. The substitution is based on simple empirical relationships such as Arch's law and the time average

equation. To begin we chose a simplest earth model in which the formation is fully saturated and the P-wave velocities in the rock matrix and pore fluid are fixed, so the traveltime is only a function of porosity. For this simple model the bulk electrical conductivity is a function of fluid conductivity and porosity.

A crosshole configuration is used to produce synthetic data and test the inversion algorithm. Two boreholes, 20 m apart and both 60 m deep, are located in a half space with a pore fluid conductivity of 0.1 S/m and a porosity of 0.1. The P-wave velocities are fixed at 5486 m/s and 1692 m/s for the rock matrix and fluid, respectively. A thin anomalous zone of 1 S/m and 0.4 in fluid conductivity and porosity, respectively, is centered at the source borehole at 30 m depth with a 10 m radial extension. Twenty-three source positions for both methods are distributed at 2.5 m intervals between the depths of 5 m and 60 m. As many receivers are located in the other borehole. For the EM method, the source is a 10 kHz vertical magnetic dipole and vertical magnetic fields are calculated at the receivers. Several inversion schemes have been tried, and the best image was obtained by alternately finding the distribution of one parameter while holding that of the other parameter. The two central panels, (b) and (c), in Figure 1 present the inverted rock porosity and fluid conductivity, respectively, between the two boreholes. The location of the anomalous body is precisely retrieved. The velocity and bulk conductivity shown in (a) and (d) are derived from the porosity and fluid conductivity based on the time average equation and the simplified Arch's law, respectively.

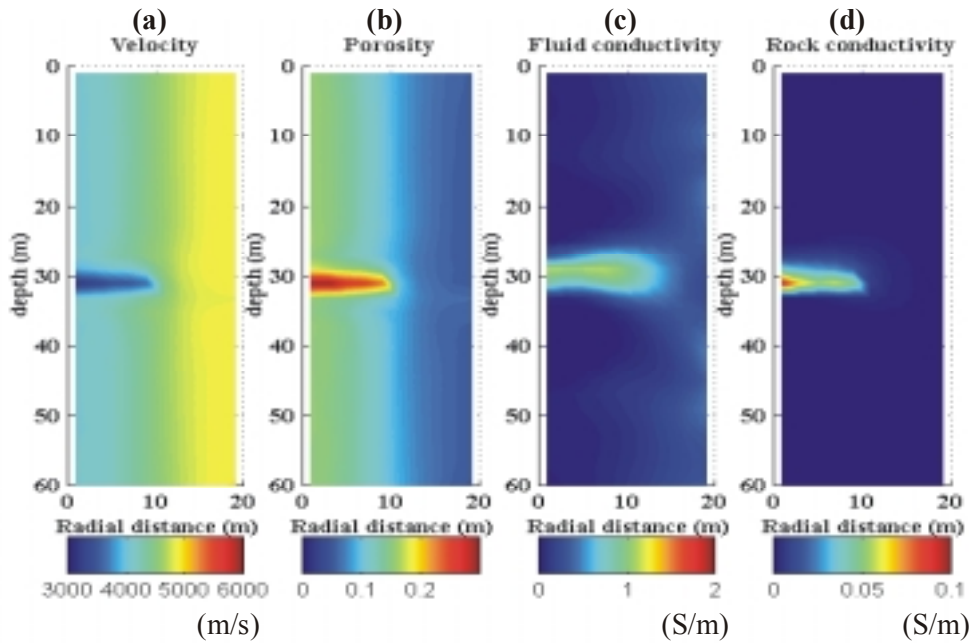


Figure 1. Result of joint inversion using synthetic data. (a) formation velocity, (b) porosity, (c) fluid conductivity, and (d) rock conductivity. (a) and (d) are calculated based on the inverted results of the rock porosity and fluid conductivity, respectively.

## Center for Computational Seismology (CCS)

*T.V. McEvilly, 510-486-7316, fax 510-486-5686, tvmcevilly@lbl.gov; E.L. Majer; L.R. Johnson*

**Objectives:** The Center for Computational Seismology (CCS) serves as the core data processing, computation and visualization facility for seismology-related research at LBNL. As such, it will be integral to our critical efforts in mapping the distribution and migration of fluids in the subsurface, a problem requiring new approaches in seismic waveform inversion techniques that can take into account the presence and effects of diffracted waves. A wide range of research projects relies upon CCS resources for development and application of methods for characterization, process definition, and process monitoring in the rock-fluid-thermochemical subsurface environment. Pursuing an objective of providing modern tools for seismological research, the Center is designed and operated to provide a focused environment for research in modern computational seismology by scientists whose efforts at any time may be distributed among diverse research projects. A large number of varied, separately funded research projects, from many different sponsors, rely upon this resource for intellectual exchange as well as computational needs. Ph.D. theses and journal publications reveal a spectrum of effort from the most fundamental theoretical studies to field applications at all scales.

**Project Description:** CCS provides a specially equipped and staffed computational facility to support and advance a wide-ranging program of seismological research. Beyond computers, work stations, seismic processing packages and visualization capabilities, it is a physical facility in which scientists pursuing individual research interact with other scientists and technical support staff in a multidisciplinary intellectual environment. CCS supports research in the general areas of wave propagation, geophysical inverse methods, earthquake and explosion source theory, seismic imaging, borehole geophysics, four-dimensional process monitoring and visualization technology.

**Results:** Results from the diverse seismological program at CCS are best demonstrated in the CCS research output. Major accomplishments flow largely from the breadth of research support provided by CCS, and the cross-fertilization between applications and fundamental studies. Significant recent results involve successful imaging of contaminant flow zones in fractured basalt, development of borehole orbital vibrator technology and promising results in CO<sub>2</sub> monitoring with borehole imaging methodology.

Findings for a facility and scientific environment such as that provided by CCS must be defined in the context of the multidisciplined research base that is supported there, rather than project-specific accomplishments (those appear in other sections of this report). It is fair to attribute a large part of the scientific reputation in seismology at LBNL to the CCS environment.

## Deformation and Fracture of Poorly Consolidated Media

*L.R.Myer 510-486-6456, fax 510-486-5686, LRMyer@lbl.gov*

**Objectives:** Rocks with small intergranular cohesion can be a potential threat to the stability of boreholes and other stress-bearing rock structures. Their mechanical behavior is intermediate between that of rock and soil. This study examines the effect of micromechanical properties of weak granular rock on macroscopic properties such as load-displacement response, ultimate strength, and failure mode.

**Project Description:** In order to examine the mechanical and acoustic properties of weakly cemented granular rocks, artificial sandstone samples were fabricated using pure silica sand with sodium silicate cement. Both intergranular cohesion strength and porosity of the samples could be controlled independently by changing the amount of cement and the degree of compaction. Both mechanical tests (uniaxial compression tests and fracture toughness tests) and acoustic tests (seismic wave propagation tests) were conducted upon samples for a range of cohesion strength and porosity. For acoustic tests, samples were tested both under dry and 100% liquid-saturated conditions. 99%-pure isopropyl alcohol was used as pore fluid because the sodium silicate cement is soluble in water.

**Results:** Uniaxial compression tests showed that until the grains achieve a certain degree of intergranular cohesion, samples with different cementation follow an identical load-displacement path, but with different final strengths ( $U_c$ ) and deformations. Once this critical cohesion was achieved, displacement due to the intergranular slip decreased monotonically, and the sample's behavior became rock-like (Figure 1). Both mode I critical fracture toughness and  $U_c$  increased monotonically with increasing intergranular cohesion but particularly,  $U_c$  increased linearly with cement volume (C). For a constant cementation,  $U_c$  decreased linearly with an increase in porosity for a range of 32-39%.

An increase in intergranular cementation resulted in a significant increase in velocity, amplitude, and high-frequency spectral content of both P and S-waves for dry samples. The measured results showed good agreement with predictions by a model (Dvorkin and Nur, 1996) that assumes a coating of cement around individual grains. Despite the large changes in velocities over a range of intergranular cementation, Poisson's ratio remained virtually constant, at about 0.13. This result is interesting because it indicates a possibility of a unique relationship between porosity and Poisson's ratio. The classical Biot's model successfully predicted the wave velocities of liquid-saturated samples using the measurements from dry samples. However, the model grossly underestimated the observed attenuation and velocity dispersion of fast P-waves. In addition, the attenuation of high frequency waves (~1MHz) increased dramatically for a very small amount of intergranular cementation but rapidly decreased with increasing cohesion strength of the material.

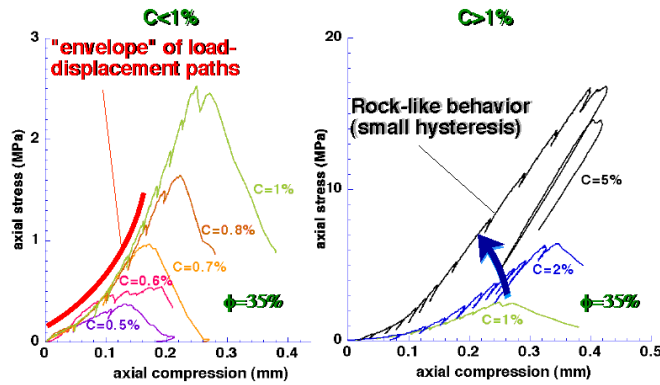


Figure 1 Uniaxial compression test results on weakly cemented artificial sandstone samples. With increasing sodium silicate cement content (solution volume per pore space in C%), the load-displacement behavior of the samples becomes from soil-like to rock-like.

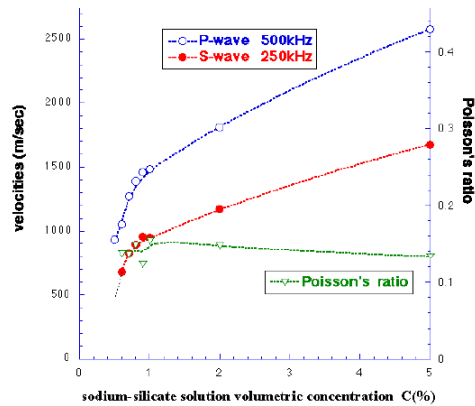


Figure 2 Measured velocities and dynamic Poisson's ratios for a range of intergranular cementation. Both P and S-velocities increase rapidly with increasing intergranular bond strength but Poisson's ratio remains constant.

## **Decomposition of Scattering and Intrinsic Attenuation on Rock with Heterogeneous Multiphase Fluids Distributions**

*K.T.Nihei, 510-486-5349, fax 510-486-5686; KTNihei@lbl.gov, L.R.Myer 510-486-6456, fax 510-486-5686, LRMyer@lbl.gov*

**Objectives:** The overall focus of this project is a fundamental investigation of scattering and intrinsic attenuation of seismic waves in rock with heterogeneous distributions of fluids and gas. This research represents a departure from past rock physics studies on seismic attenuation in that the emphasis here is not a detailed study of a specific attenuation mechanism, but rather to investigate theoretical and laboratory methods for obtaining separate estimates of scattering and intrinsic attenuation in rock with heterogeneous pore fluid distributions. It is anticipated that methods for obtaining separate estimates of intrinsic and scattering attenuation may lead to higher resolution methods for monitoring the movement of fluids in the subsurface.

This project combines laboratory, numerical, and theoretical studies to the investigation of scattering and intrinsic attenuation in rock with heterogeneous fluid distributions. The objectives of this project are threefold: (1) to adapt and further refine methods for decomposing scattering and intrinsic attenuation in rock with heterogeneous multiphase fluids, (2) to apply these methods to laboratory seismic measurements in porous rock with heterogeneous fluid distributions and compare these results with direct laboratory measurements, and (3) to examine a new method for focusing seismic waves in heterogeneous media using time reversal mirrors. These objectives are addressed in three tasks to be performed over a period of three years.

**Project Description:** In this project, laboratory, theoretical, and numerical studies are combined to investigate methods for estimating scattering and intrinsic attenuation in rock with heterogeneous distributions of gas and fluid. The focus is on sandstone and carbonates under conditions in which the relative saturation of miscible and immiscible liquids (*e.g.*, water and oil) and gas (*e.g.*, CO<sub>2</sub>) vary. Decomposition of the attenuation will be conducted to compare the contributions from scattering and intrinsic attenuation and related to the characteristics of introduced heterogeneity obtained from X-ray CT images. Numerical and theoretical models will be performed to help interpret the results of the laboratory experiments and to investigate the effect of both attenuation mechanisms on the characteristics of the waves. Laboratory and numerical studies of wave focusing on selected heterogeneities using elastic time reversal mirrors will also be investigated. The effects of intrinsic attenuation on the time reversal focusing process and methods for correcting for intrinsic attenuation will be examined.

**Results:** Work to date consists primarily of experimental design and set-up, and numerical code development. Efforts have focused on the following three efforts: (1) bar resonance and pulse transmission tests on intact and fractured acrylic bars to investigate the possibility of separately estimating Q-intrinsic and Q-scattering from lab measurements, (2) physical model development of an acoustic medium with variable Q-intrinsic and embedded heterogeneities to test Q estimation using an acoustic full waveform imaging algorithm, and (3) computer simulations in layered media with time reversal mirrors.

Here, we will briefly summarize our efforts on item 1. We have assembled laboratory resonant bar and pulse transmission systems capable of operating in the 1-50 kHz frequency range. The first series of laboratory experiments focused on determining if reliable estimates of Q-intrinsic could be obtained with the resonant bar method. To test this hypothesis, we performed tests on 0.813 m acrylic bars with

and without localized scatterers (bars with a circumferential notch and a planar array of 1/8” diameter holes). The resonance spectra, shown in Fig. 1, were used to compute the quality factors via the half-power method. The quality factors (ranging from 25 to 35) shown in Fig. 2 are very similar for the intact bar and the two bars with localized scattering planes. These preliminary tests support 1D computer simulations for highly fractured bars that show discrete scatters do not influence the Q estimate obtained from the resonant bar method. That is, the Q estimate obtained from the resonant bar method is a direct measure of Q-intrinsic.

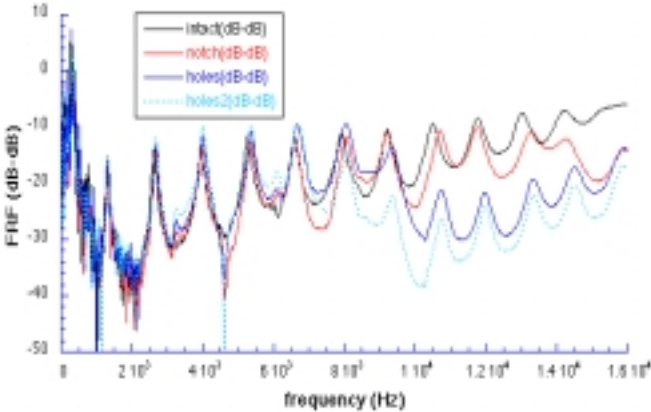


Figure 1. Resonance spectra for intact and fractured acrylic bars.

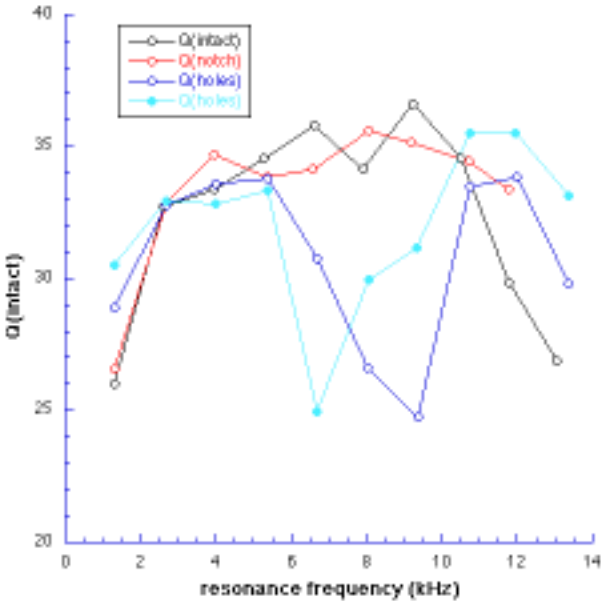


Figure 2. Quality factors for intact and fractured acrylic bars obtained from the resonance spectra in Fig. 1.

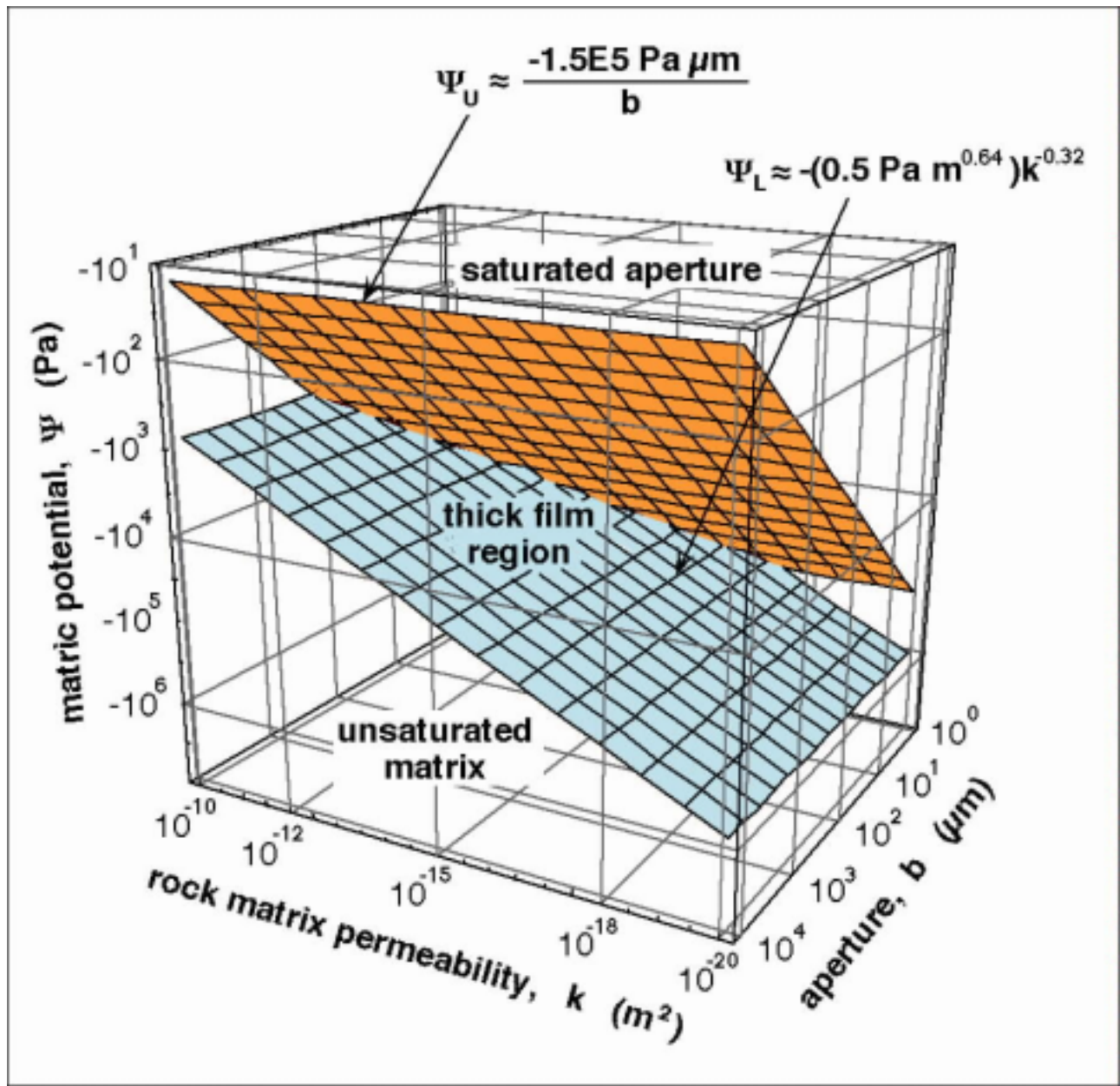
## Unsaturated Fast Flow in Fractured Rock: Testing Film Flow and Aperture Influences

*T.K. Tokunaga, 510-486-7176, fax 510-486-7797; tktokunaga@lbl.gov*

**Objectives:** The nature of unsaturated fast-flow in fractured rocks needs to be understood in order to obtain reasonable constraints on vadose zone transport. Water films along unsaturated fractures have recently been shown to be capable of supporting fast flow and transport, and revealed limitations of existing aperture-based models. In this project, theoretical considerations and experiments are combined to improve our understanding of unsaturated flow in fractured rocks.

**Project Description:** Recently, the concept of film flow was introduced as a possible process by which preferential flow could occur along truly unsaturated fractured rock. Our work concerns water films on fracture surfaces under near-zero (negative) matric potentials, and examines the possibility of fast, unsaturated flow under "tension". "Films" in this context are a complex network of thick pendular regions that form within topographic depressions and thin films on topographic ridges. Thus, the thickness and connectivity of pendular film regions is expected to be important in controlling film flow on individual fracture surfaces. We showed that at matric potentials greater than that needed to saturate the rock matrix, transmissive water films can develop on fracture surfaces. The matric potential dependence of the average film thickness, the film transmissivity and film hydraulic diffusivity have been measured on fracture surfaces of Bishop Tuff, a basalt, and roughened glass, using equilibrium, steady-state and transient methods. The water "films" investigated in the previous study as well as the present one develop on rough surfaces, range in average thickness from about 1 to 50  $\mu\text{m}$ , and flow in the laminar regime. In the FY 2000 work, studies were continued on the general conditions necessary for stable film flow.

**Results:** Flow through unsaturated fractured rock occurs via a number of processes, including film flow. Approximate ranges of conditions necessary for the presence of thick water films along unsaturated fracture surfaces were investigated through considering rock matrix and fracture aperture saturation criteria. Stable thick films exist when the matric potential is high enough to effectively saturate the immediately underlying rock matrix, yet low enough not to saturate the fracture aperture. The lower energy limit for stable thick films was estimated through correlations between air-entry matric potentials and matrix permeabilities. A survey of saturated-unsaturated hydraulic property information in the literature (117 data sets, covering 9 orders of magnitude in permeability), showed an approximately 0.32 power law correlation. The upper matric potential limit was estimated from the Laplace-Young predicted inverse fracture aperture dependence of capillary filling. With these two limiting relations, the domain for stable thick films was identified in the parameter space defined by matrix permeability, fracture aperture, and matric potential (Figure 1). These results show that thick films are stable over a moderate range of matric potentials when the rock matrix permeability is less than about  $10^{-14} \text{ m}^2$  and the fracture aperture is greater than about 30  $\mu\text{m}$ . Such combinations of permeabilities and apertures are common in fractured rock vadose zones. Thus, thick water films can form in these environments within the matric potential ranges identified here. However, near-zero matric potentials are necessary for the possible development of fast film flow. Within this narrow energy region, the nature of film hydraulic properties is very dependent on fracture surface topography. Current studies concern fracture surface topography influences on film flow.



## **Prediction and Evaluation of Coupled Processes for CO<sub>2</sub> Disposal in Aquifers**

*Karsten Pruess, 510-486-6732, fax 510-486-5686, K\_Pruess@lbl.go, Chin-Fu Tsang 510-486-5782, fax 510-486-5686, CFTsang@lbl.gov*

**Objective:** Evaluate the physical and chemical processes that would be induced by large-scale CO<sub>2</sub> injection into brine aquifers. Develop and demonstrate numerical simulation capabilities for CO<sub>2</sub> disposal.

**Project Description:** The purpose of the research is to develop a systematic, rational, and mechanistic understanding of the coupled processes that would be induced by injection of CO<sub>2</sub> into aquifers. This will be accomplished by means of conceptual, mathematical, and numerical models that are based on rigorous continuum theories of fluid dynamics, coupled with detailed rock fracture mechanics and chemical speciation and reaction path analyses. Field experience and data from natural CO<sub>2</sub> reservoirs and engineered aquifer gas storage systems will be used, as will be laboratory data and generally accepted physical and chemical principles for multiphase flow, geochemical alteration, and rock mechanical effects. By developing a mechanistic understanding of the relevant processes, this research will provide a sound basis for evaluating the feasibility of CO<sub>2</sub> disposal in different hydrogeologic environments, including fractured rock systems, and will provide engineering tools for the design, implementation, and monitoring of CO<sub>2</sub> disposal systems in brine aquifers.

**Results:** The accuracy of published data and correlations for thermophysical properties of CO<sub>2</sub> (density, viscosity, enthalpy) was evaluated for the range of pressure and temperature conditions of interest in aquifer disposal. Suitable correlations were implemented in our multi-purpose simulator TOUGH2. Pre-existing models for CO<sub>2</sub> dissolution in aqueous fluids were enhanced by incorporating salinity and fugacity effects. Special techniques were developed for describing the movement of sharp CO<sub>2</sub>-water interfaces during immiscible displacement of saline brines by CO<sub>2</sub>. Numerical simulations of CO<sub>2</sub> injection for typical brine formation conditions showed (1) average CO<sub>2</sub> saturations in the region swept during the operational period of a CO<sub>2</sub> disposal system are in the range of from 15 – 35 %; (2) phase segregation due to gravity override will substantially reduce CO<sub>2</sub> injection pressures; (3) the capacity factor for storing CO<sub>2</sub> by dissolution in the aqueous phase depends strongly on salinity, but is only weakly dependent on pressure and temperature; (4) the amount of CO<sub>2</sub> dissolving in formation waters is equivalent to an average gas saturation of from 2 – 7.5 %, the lower value corresponding to saturated NaCl solutions, the higher to dilute waters. Loss of CO<sub>2</sub> from storage along leaky faults may be a self-enhancing process. A comprehensive survey of rock-forming minerals indicated that minerals with potential for substantial CO<sub>2</sub> sequestration are not plentiful in common aquifer lithologies. Under favorable conditions, the amount of CO<sub>2</sub> that could be sequestered by mineral phases may be comparable to what can dissolve in pore waters. Reaction path calculations showed the precipitation of siderite (FeCO<sub>3</sub>) to be sensitive to the reactivity of organic material. General aspects of coupled thermo-hydro-mechanical (THM) processes were reviewed, and modeling of CO<sub>2</sub> injection with coupling to associated stress effects was initiated.

## Colloid Transport in Unsaturated Porous Media and Rock Fractures

*Jiamin Wan, 510-486-6004, fax 510-495-7797, jwan@lbl.gov*

**Objectives:** The current understanding of colloid transport is largely based on the classic filtration theory used in saturated porous media. Some recent studies have led to identification of several important aspects of vadose zone colloid transport that still need to be understood. The overall objective of this project is to obtain a comprehensive understanding of colloid transport in partially saturated porous media and rock fractures.

**Project Description:** The basic physics and chemistry unique to vadose zone colloid transport is a consequence of the existence of a second immiscible fluid phase, gas. Traditional filtration theory cannot be directly applied in the vadose zone colloid transport because of the coexistence of air and water. In the 1997 to 1999 period, we focused on studies of colloids being strained by becoming trapped within thin water films in unsaturated porous media, and introduced the concept of “film straining”. Our recent research has been focused on quantifying the partitioning of surface-active colloids at the air-water interfaces. Much effort has been devoted to characterizing surface accumulations of colloids. Previously developed methods include surface microlayer sampling and jet drop collection. Because of the large uncertainties in thicknesses and interfacial areas, results are often reported as the enrichment factors for a given estimated thickness. We have recently developed a simple dynamic method to quantify colloid surface excesses at air-water interfaces without requiring assumptions concerning the thickness of interfacial regions. During the 1999 to 2000 period, we measured partition coefficients of different clay minerals at the air-water interface, primarily under environmentally relevant solution chemistry conditions.

**Results:** The affinity of clay colloids to the air-water interface was quantitatively measured using a bubble column method. The affinities of clay particles to the air-water interface are reported as partition coefficients ( $K$ ), in a manner analogous to surface-active solutes. Five types of dilute clay suspensions were measured: Ca-montmorillonite, Na-montmorillonite, bentonite clay, illite, and kaolinite, under varying pH and ionic strength conditions. In order to obtain results that are directly relevant to typical subsurface environments, no surfactants were used, and most experiments were conducted at low values of ionic strength. Na-montmorillonite and bentonite clay were found surface excluded from the air-water interface at any given pH and ionic strength. Ca-montmorillonite and bentonite clay are slightly surface-active at the air-water interface with increased  $K$  values at lower pH. Kaolinite exhibited extremely high affinity to the air-water interface at pH below 7. The strong pH dependence of the  $K$  values suggests that electrostatic force might be the governing force for partitioning of the clay colloids at the air-water interface.

## **CATEGORY: Geochemistry**

PERSON IN CHARGE: S. M. Benson

### **Integrated Isotopic Studies of Geochemical Processes**

*Donald J. DePaolo 510-486-4975, 510-643-5064, fax 510-642-9520, depaolo@socrates.berkeley.edu or djdepaolo@lbl.gov; B. Mack Kennedy 510-486-6451, fax 510-486-5496, bmkennedy@lbl.gov*

**Objective:** Combine high-precision measurements of isotopic ratios in natural materials with mathematical models to understand the spatial and time scales of geochemical processes of interest for energy management.

**Project Description:** Isotopic measurements of Sr, Ca, O, C, He, Ne, Ar, Xe, Pb, Nd, and U are used to address problems of mass transport in fluid-rock systems, interpretation of past global climatic change, crustal magmatic and tectonic processes, and Quaternary geochronology. Mathematical models are developed to extend the application of isotopic measurements for field-scale parameterization of hydrological systems. Modeling is accompanied by systematic measurements of simple natural systems, and by efforts to improve sampling methodologies and measurement techniques such as microsampling of geological materials, high-precision measurement of the small samples, and rapid low-blank chemical separation of trace metals. Other efforts are aimed at improving techniques for dating and correlation of sedimentary and volcanic rocks, and for understanding the time scales and mechanisms of crustal processes such as extensional faulting, mountain building, and volcanism. All efforts are aimed at improved characterization of natural rock and fluid systems relevant to environmental remediation, geothermal and fossil energy resources, climate change science, and nuclear waste isolation.

**Results:** (1) A difficulty in making models for reactive chemical transport is the inability to accurately predict fluid-solid reaction rates, particularly for dissolution and precipitation reactions. The approach we have taken to address the issue is to use isotopic tracers (primarily Sr, but also U and Nd) to determine fluid-solid exchange rates in various natural situations. The isotopic methods characterize the reaction rates in the system at the scale of the "reaction length," which can be anywhere from a few centimeters to hundreds of meters depending on the element used and the natural environment. The ultimate objective is to understand the microscopic (as well as pore scale and mesoscale) characteristics of natural systems that have been characterized in terms of "field scale" measures of reaction rates. An intermediate goal is to establish empirically the natural range of fluid-solid reaction rates.

Sr and U isotopic composition of fluids and rocks have been measured in saturated zone groundwater, vadose zone groundwater, geothermal systems, deep sea pore fluids, and in metamorphic rocks. The groundwater and geothermal systems are advective, the fluid velocities are meters to 100's of meters per year (less in the vadose zone), and the reaction lengths for Sr are in the range of km's to hundreds of km. In deep sea pore fluids and metamorphic systems, the transport in the fluid phase is mainly by diffusion; the reaction lengths vary from 10's of cm to 10's of meters. To determine the rates, the groundwater flow velocity (or fluid phase diffusivity) must be constrained. Uncertainties in these values are typically less than a factor of  $\pm 3$ . Deduced fluid-solid exchange rates correspond to mineral dissolution time constants (grams dissolved/gram/yr) in the range  $3 \times 10^{-9} \text{ yr}^{-1}$  for the slowest low temperature systems to about  $5 \times 10^{-6} \text{ yr}^{-1}$  for the fastest high temperature systems (at 500 - 600°C). The rates are not highly variable, show a significant but relatively weak temperature dependence, and are 2 to 8 orders of

magnitude smaller than typical laboratory rates measured far from equilibrium. In some cases, empirically inferred rates combined with isotopic measurements can serve to constrain groundwater flow velocities; this is particularly useful for cases where the velocities are very small, such as the vadose zone at Yucca Mountain. The differing reaction lengths for different elements (eg. Sr and O; or Sr and Nd) in the same system can also be exploited to extract information on the mesoscale hydrology (e.g. fracture spacing) of some fluid-rock systems.

The isotope  $^{234}\text{U}$  decays radioactively, and at the same time is injected into pore fluids by recoil from the solid phase. Recoil leakage from the solid phase drives the pore fluid  $^{234}\text{U}/^{238}\text{U}$  up, whereas solid phase dissolution drives the pore fluid toward the equilibrium activity ratio of 1. Fluid phase  $^{234}\text{U}/^{238}\text{U}$  ratios are therefore a measure of solid dissolution rates. Measurements were made of pore fluids from fine-grained deep-sea sediments composed of ca. 70-90% silicates and 10-20% carbonate. The fluid-solid exchange for U is rapid in comparison to diffusional transport, and hence the fluid isotopic values give estimates for the local solid dissolution rates as a function of depth in the sediment. The deduced rates are  $7 \times 10^{-7}$  to  $3 \times 10^{-6}$  g/g/yr, decreasing with depth between 6 and 54 meters below the sediment-water interface. These rates are higher than those deduced from Sr isotopes for older sediments. The results suggest that U isotopes can be used in groundwater systems to determine local dissolution rates, which can then be combined with Sr isotopes to measure fluid migration velocities.

(2) Noble gases, carbon dioxide, nitrogen and  $^{14}\text{C}$  are being monitored in gas discharging from Mammoth Mountain. The helium and carbon isotopic compositions and the  $^3\text{He}/\text{CO}_2$  ratio are indicative of a magmatic source. Variations in noble gas abundances,  $^3\text{He}/\text{CO}_2$ , and excess  $\text{N}_2$  indicate that the anomalous gas discharge is derived from a combination of magmatic degassing and thermal metamorphism of carbonates. The persistently high  $^3\text{He}/^4\text{He}$  ratio combined with the magnitude and duration of gas emission at the surface and estimates of the size of the emplaced dike requires continued degassing from a deeper magma system. A more rapid increase in  $\text{CO}_2/^3\text{He}$  relative to  $\text{CO}_2/^4\text{He}$  combined with a gradual decrease in the helium isotopic composition suggests that the influence of the crustal gas source is increasing. Recent efforts have concentrated on quantifying the magmatic carbon discharge in cold groundwater around Mammoth Mountain. The total water flow from all the sampled cold springs is ~70-100% of the total annual precipitation hence the springs are an excellent sampling of the groundwater. Some of the waters contain magmatic helium ( $R \leq 4.5 \text{ Ra}$ ) and carbon. Isotopes can identify magmatic volatiles in waters that otherwise look like normal groundwater. Such waters have previously escaped notice at Mammoth Mountain, and possibly at other volcanoes, because the  $\text{CO}_2$  is rapidly lost to the air as water flows away from the springs, leaving neutral pH waters that contain only 1-4 mmol/L  $\text{HCO}_3^-$ . We estimate the total discharge of magmatic carbon in the cold groundwater system to be ~ 20,000 t/yr (as  $\text{CO}_2$ ).

(3) Although there are extensive data on past variations in the isotopic ratios of such elements as Sr, C, and O, in the oceans, there are few data that relate to changes in the major and minor cation concentrations in ocean water. Calcium ( $\text{Ca}^{2+}$ ) is a particularly interesting species because of its relation to both the rates of weathering of silicate rocks and the deposition of carbonate materials on the seafloor; processes that control atmospheric  $\text{CO}_2$  concentration<sup>1-4</sup> and hence strongly influence global temperature. We have measured significant variations in the isotopic composition of marine calcium over the last 80 Ma. The isotopic variations indicate that there have been significant changes in the Ca concentration in the oceans. The calcium isotopic ratio of paleo-seawater may be a direct indicator of past changes in atmospheric  $\text{CO}_2$  when combined with paleo-pH determinations.

## Clay Mineral Surface Geochemistry

Garrison Sposito 510-643-8297, fax 510-643-2940, [gsposito@lbl.gov](mailto:gsposito@lbl.gov)

**Website:** <http://esd.lbl.gov/GEO/geo.shtml>

**Objectives:** The current objectives of this project are to investigate the structures of clay minerals using *ab initio* molecular simulation, with principal focus on the effect of interlayer cations.

**Project Description:** The simulation method involves *ab initio* energy minimization calculations based on local density approximation, gradient-corrected density functional theory. These first-principles calculations, which involve no adjustable parameters, are based on an explicit quantum-mechanical treatment of the electrons in a clay mineral system, which means solving the Schrodinger eigenvalue problem for the electronic ground state. This approach was applied to simulate the structure of the important clay mineral, montmorillonite, with the results then compared to X-ray crystallographic data. We hope to be able to answer not only questions about the structure of montmorillonite itself, but also about the hydration of its interlayer cations and its swelling behavior.

**Results:** Equilibrium structures of Na-montmorillonite with varying  $\text{Al}^{3+} \rightarrow \text{Mg}^{2+}$  isomorphic substitution at octahedral sites were investigated. Our calculations indicated that there is a significant structural change with respect to varying the charge substitution pattern. The most significant change occurred at the structural hydroxyl group in the octahedral sheet. Figure 1 shows the four of the structures simulated. The structure of a half unit cell, with formula  $\text{Si}_4(\text{Al}_{1.0}\text{Mg}_{1.0})\text{O}_{10}(\text{OH})_2$ , was first optimized in a uniform positively-charged background (*i.e.*, without an interlayer cation) for a high charge ( $x = -2$ ;  $x \equiv$  the number of moles of excess electron charge per unit cell produced by isomorphic substitution.) montmorillonite (Fig. 1a). A full unit cell expansion by doubling the structure in Fig. 1a was made to simulate montmorillonite with a layer charge of  $x = -1$  (Fig. 1c). An interlayer sodium ion was then added for these two cases to balance the layer charge (yellow sphere in Figs. 1b and 1d). A fifth simulation was performed by doubling the full unit cell to give the chemical formula,  $\text{Si}_{16}(\text{Al}_{7.0}\text{Mg}_{1.0})\text{O}_{40}(\text{OH})_8$ , both with and without  $\text{Na}^+$  ( $x = -0.5$ , structure not shown). Interlayer  $\text{Na}^+$  strongly influenced the position of the proton in the structural OH group. The protons nearest to  $\text{Na}^+$  (upper layer in Fig. 1b; bottom layer in Fig. 1d) moved toward the octahedral sheet and away from the interlayer cation because of coulomb repulsion. However, protons not close to  $\text{Na}^+$  (*i.e.*, all other protons in Figs. 1b, 1d) either moved similarly (Fig. 1b) or even moved toward the interlayer region (Fig. 1d). The optimized structure was compared to the structure of pyrophyllite, a 2:1 layer type aluminosilicate isomorphic to montmorillonite, but without charge substitutions. For example, the angle of corrugation of the surface was less for montmorillonite ( $\sim 5^\circ$ ) than for pyrophyllite ( $\sim 6.7^\circ$ ).

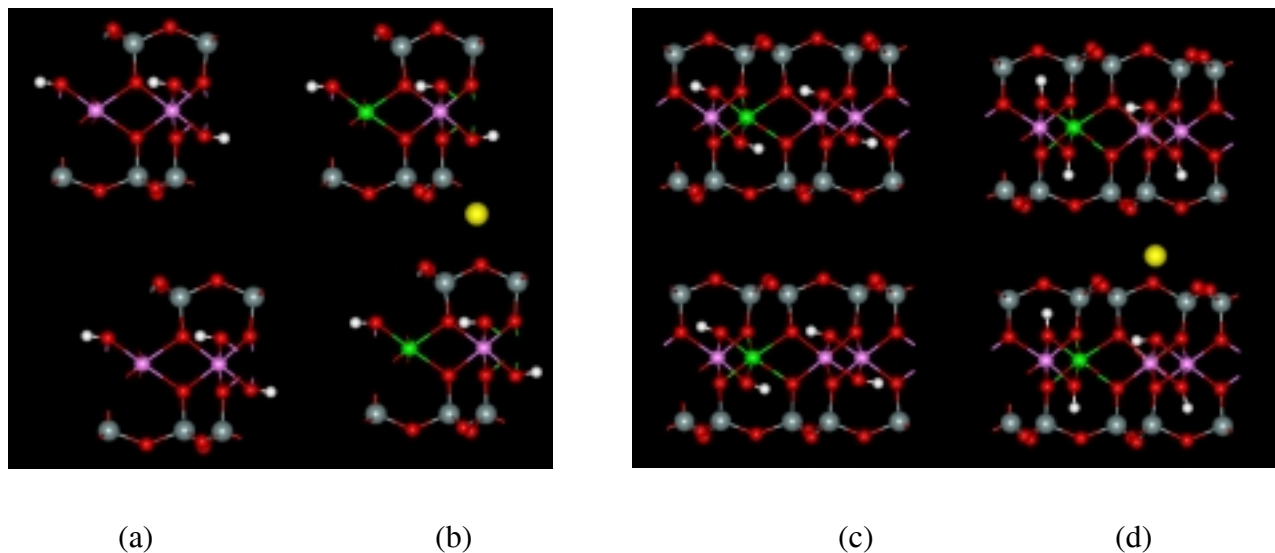


**Figure 1.** Optimized structures of montmorillonite as determined by *ab initio* energy minimization based on local density approximation, gradient-corrected density functional theory. [Si are shown in gray and O are shown in red. The substituted octahedral-sheet cation is  $\text{Mg}^{2+}$  (green) and the interlayer cation is  $\text{Na}^+$  (yellow). Octahedral-sheet  $\text{Al}^{3+}$  cations are shown in pink.] Note the positions of the protons (white) and the angles made by the structural OH relative to horizontal.

### Molecular-level studies of Fe-Al oxyhydroxide coating formation on quartz

Glenn A. Waychunas, 510-495-2224, fax 510-486-7152, [GAWaychunas@lbl.gov](mailto:GAWaychunas@lbl.gov); James A. Davis, Rebecca Reitmeyer, USGS Menlo Park, CA

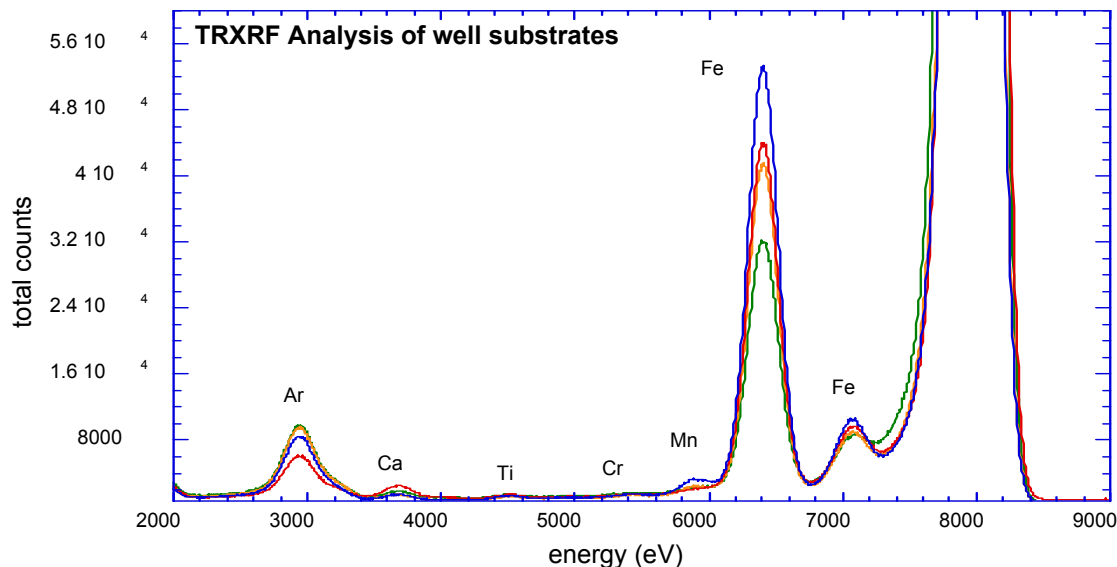
**Website:** [http://www-esd.lbl.gov/GEO/aqueous\\_geochem/synbased\\_gaw.shtml](http://www-esd.lbl.gov/GEO/aqueous_geochem/synbased_gaw.shtml)

**Objectives:** Determination of the molecular structure of initial sorbed and precipitated Fe-Al oxyhydroxides on quartz surfaces; Comparison of perfect surface reactivity with degraded perfect surfaces and with perfect surfaces exposed to natural conditions; Characterization of the effects of undersaturation on precipitate formation; Exploration of coating sorption properties to specific toxic metals and organic species.

**Project Description:** Fe oxyhydroxides are potent scavengers of toxic oxyanions (arsenite, selenite, chromate) over a large pH range, and can also incorporate or sorb toxic metal cations under appropriate conditions. Recent work has shown that coatings of these materials, down to nanometer thicknesses, can be ubiquitous even in the cleanest sediments, effectively creating a large surface area sorbant that dominates mineral-water interface reactivity. This project combines three efforts to understand the nature, formation and alteration of these coatings in aquifer sediments: 1) laboratory sample preparation and characterization including both perfect single crystal surfaces and high surface area silica (Aerosil). 2) emplacement of perfect single crystal surfaces into sampling wells at two aquifers where the sediments, conditions and chemistry are well described. These samples are withdrawn periodically to reveal coating formation and quartz surface degradation. 3) Characterization of coatings on natural quartz grains from these aquifers and elsewhere representing a range of formation environments. Characterization methods include synchrotron-based x-ray absorption spectroscopy in grazing incidence

mode (GIXAS) and total reflection x-ray fluorescence spectroscopy (TRXRF), transmission electron microscopy (TEM) and atomic force microscopy (AFM).

**Results:** Perfect quartz wafers extracted from the Cape Cod site aquifer had sufficient Fe after 8 months to obtain excellent GIXAS and TRXRF spectra using beamline 9-3 at SSRL. Data collection for TRXRF required about 30 minutes per sample, while GIXAS collection required about 8 hours per sample. The figure below shows the overall TRXRF spectra for 4 different samples, with the inset showing a blowup of the Ca to Mn fluorescence regions. The amount of Fe on the sample surfaces was estimated to be  $10^{13}$  atoms, while the Mn was estimated to be on the order of  $10^{11}$  atoms or about 100 femtomoles. Despite this low density, well below the monolayer regime, excellent EXAFS and Fourier transforms could be calculated. Mn and Fe were found to be correlated with each other, but anticorrelated with Ca, suggesting that formation of Ca phases block surface growth or sorption of Fe-Mn phases. The Fe GIXAS radial structure functions do not closely resemble either goethite or hematite, and show a decrease in the degree of Fe-O-Fe polymerization with increasing Mn content and decreasing Ca content. Hence, Ca composition on the surface reduces the amount of Fe and Mn on the quartz surface but does not retard crystallization. However increasing Mn does affect Fe oxide crystallization. Simulation and AFM studies are in progress to identify the specific Fe, Mn and Ca phases involved at the surfaces. It is anticipated that the next GIXAS/TRXRF run may allow spectra from both the Fe and Mn edges to be collected if ion uptake has proceeded at the same rate.



## Development of Isotope Techniques for Reservoir and Aquifer Characterization

*B. Mack Kennedy 510-486-6451, fax 510-486-5496, bmkenedy@lbl.gov*

**Website:** <http://www-esd.lbl.gov/CIG/noblegas/noblegas.shtml>

**Objectives:** Based on results from prior studies, isotopic characterization of fluids associated with hydrocarbons and groundwater aquifers are useful for mapping regional fluid migration and preferred flow paths, identifying fluid sources, and estimating fluid flow rates. However, the potential utility of isotope techniques to identify reservoir flow units, compartments, and fluid loss to overlying strata has not been extensively exploited.

**Project Description:** Efficient and safe sequestration of large quantities of CO<sub>2</sub> will require reliable characterization of potential storage formations, reservoirs and aquifers. Many oil and gas reservoirs are complexly partitioned by differing structural, petrologic and stratigraphic controls that will inhibit efficient CO<sub>2</sub> injection and limit reservoir potential. In groundwater aquifers, long term storage requires effective traps with minimal leakage to overlying strata. To maximize CO<sub>2</sub> sequestration efficiency, it will be necessary to address these and similar issues related to reservoir and aquifer characterization. We believe this can be accomplished by merging geophysical techniques, which provide structural and imaging information, with isotope and tracer techniques, that can identify fluid sources and flow paths, zones of fluid mixing, and isolated fluid compartments, and 2-D fluid flow models that can set limits on fluid transit times and leakage rates.

**Results:** During FY2000, we joined a pilot field scale test of a CO<sub>2</sub> injection in the Lost Hills oil and gas field in the San Joaquin Basin, California. The test consists of three parallel projects: seismic and electrical imaging, co-injection of chemical and isotopic tracers, and chemical and isotopic analyses of production fluids before, during and after CO<sub>2</sub> injection. As samples become available they will be analyzed for bulk gas chemistry, noble gas abundance and isotopic compositions, and the isotopic compositions of carbon in CO<sub>2</sub> and CH<sub>4</sub>.

## Geochemical and Isotopic Constraints on Processes in Oil Hydrogeology

*B. Mack Kennedy, 510-486-6451; fax 510-486-5496; bmkenedy@lbl.gov; T. Torgersen, University of Connecticut, 860-405-9094, fax 860-405-9153, Thomas.Torgersen@Uconn.edu*

**Website:** <http://www-esd.lbl.gov/CIG/noblegas/noblegas.shtml>

**Objectives:** This research project (with the University of Connecticut) evaluates the processes which produce, dissolve and distribute noble gases and noble gas isotopes among liquid hydrocarbon, gaseous hydrocarbon and aqueous phases. This project also uses the abundances and isotopic composition of noble gases in hydrocarbon systems to evaluate hydrocarbon sources and characteristics, groundwater end-members, and migration processes, mechanisms, and time scales.

**Project Description:** The mechanisms, processes, and time scales of fluid flow in sedimentary basins represent a fundamental question in the Earth Sciences with direct application to exploration and exploitation strategies for energy and mineral resources. This project investigates the noble gas composition of hydrocarbon samples on a basin and field scale where adequate commercial production

and ancillary information are available, to provide a test of the use and applicability of noble gases to delineate end members, migration mechanism and migration paths for hydrocarbons. Samples are analyzed for the five stable noble gases (He, Ne, Ar, Kr, Xe) and their isotopes.

Results: (1) *Sources of Air-Like Noble Gases in Hydrocarbon Reservoirs*: The atmospheric component is identified primarily by isotopic composition and by relative gas abundances (e.g. Ne/Kr/Xe/Ar), determined from the abundances of non-radiogenic isotopes, typically  $^{20,22}\text{Ne}$ ,  $^{36}\text{Ar}$ ,  $^{84}\text{Kr}$ , and  $^{130}\text{Xe}$ . It is generally assumed that the source for all atmospheric noble gases in subsurface fluids is air-saturated sea, meteoric or connate water. Evidence for water-derived noble gases in hydrocarbon systems is extensive and provides strong support that water plays an important role in hydrocarbon systems. However, evidence has surfaced suggesting that the hydrocarbons themselves are also a source of atmospheric derived noble gases (Torgersen and Kennedy, 1999) with a relative abundance pattern that is highly enriched in the heavy noble gases (Kr and Xe).  $^{130}\text{Xe}/^{36}\text{Ar}$  enrichment factors up to ~600 relative to air have been observed. This component cannot be derived from air-saturated water by distillation and/or solubility driven equilibration with oil, gas, or oil-gas systems. Instead, we believe this fractionated air component is derived from the petroleum source rock. Support for this hypothesis is provided by laboratory studies of noble gases in carbon-rich and petroleum source rocks.

We now have evidence for a third air-like noble gas component, identified by an unusual Ne/Kr/Xe/Ar relative abundance pattern that is unlike air saturated water or the highly fractionated source rock component. Systematic field-wide trends in noble gas compositions suggest that this third air-like component may be derived from the reservoir sediments. Understanding the formation and occurrence of these atmospheric noble gas sources and their interaction with oil and natural gas systems will lead to a better understanding of the processes and scales related to primary and secondary migration, basin scale fluid movement, gain or loss of secondary porosity, and biodegradation.

(2) *Noble Gas Evolution in Hydrocarbon Fields: Secondary Migration Processes and End-member Characterization*: Hydrocarbons carry an indigenous noble gas component acquired from the hydrocarbon source area. Typically, this component contains radiogenic noble gases (e.g.  $^4\text{He}$  and  $^{40}\text{Ar}$ ) and an air-like component characterized by highly fractionated abundance patterns ( $^{130}\text{Xe}/^{36}\text{Ar}$  ratios > 600 times the ratio in air have been observed). The solubility of noble gases in hydrocarbons and water dictate that noble gases will be stripped from groundwater (air saturated water, ASW) during secondary migration, and will dilute the indigenous noble gas signature in the hydrocarbon. The composition of ASW is also be modified in the carrier strata by basal fluxes and *in situ* production. The degree of dilution by the modified ASW component is a function of the total amount of water with which the hydrocarbon interacts during secondary migration (water/hydrocarbon interaction ratio). Systematic trends in noble gas composition ( $F[\text{Ng}]$  and isotopic compositions vs.  $1/[^{36}\text{Ar}]$ ) identify wells which produce hydrocarbons originating from common source areas and that interact with a common groundwater. Zeroth order interpretation of noble gas evolution as simple mixing can characterize noble gas composition of the source area (slope of the line) and modified groundwater with which it interacts (the intercept at  $1/[^{36}\text{Ar}]\sim 0$ ). Application of the concept to multiple data sets (published and unpublished) provides proof of concept and identifies distinct and readable noble gas evolution trends that are interpretable as secondary migration paths.

In the gas fields of Alberta, Canada, evolution trends defined by noble gas compositions support the hydrologically defined secondary migration flow paths of Garven (1989) and Hitchon (1984). Two groups of wells have source areas (distinct from source rock) that are characterized by very large but different enrichment factors of radiogenic  $^4\text{He}$  and  $^{40}\text{Ar}$  (as well as  $^{21}\text{Ne}$ ,  $^{136}\text{Xe}$ ) that could not have been

derived solely from the source rock. These large enrichments suggest that Tertiary orogeny, preceding secondary migration, degassed large volumes of old crust into the source areas. This noble gas evolution defined scenario supports a role for tectonics in the accumulation of hydrocarbons (Oliver, 1986, 1989). Noble gas evolution analysis can thus provide a fundamental constraint on models of hydrocarbon migration and emplacement.

## **Reactive Chemical Transport in Structured Porous Media: X-ray Microprobe and Micro-XANES Studies**

*T.K. Tokunaga, 510-486-7176, fax 510-486-7797; tktokunaga@lbl.gov*

**Objectives:** In subsurface reactive transport, large differences in chemical composition can be sustained in boundary regions such as sediment-water interfaces, interior regions of soil aggregates, and surfaces of fractured rocks. Studies of reactive transport in such boundary zones require information on chemical speciation with appropriate spatial and temporal resolution.

**Project Description:** Predicting transport of trace elements between various environmental compartments is currently often unsuccessful, partly due to lack of relevant information at compartment boundaries. Batch studies can yield insights into kinetics and equilibrium in well-mixed systems, but much of the subsurface is very poorly mixed. Without in-situ, spatially- and temporally-resolved chemical information, transport between compartments can only be described with system-specific, nonmechanistic, mass transfer models. In this project, the synchrotron x-ray microprobe and micro-XANES techniques are used to obtain such measurements in a variety of critical microenvironments. Past efforts in this project focused on selenium transport and reduction in two types of microenvironments, that found at surface water-sediment boundaries, and that found within soil aggregates. In FY 1998, the project emphasis shifted to consider reactive transport of Cr included flow-through experiments in columns of aggregated soils, including spatially resolved, real-time tracking of initial contamination processes within soil aggregates, and later characterization of Cr redistribution upon long-term drying. The complexity of reactive transport in such systems with macropore flow and intraaggregate diffusion-redox motivated simpler FY 1999-2000 studies focused only on the latter processes.

**Results:** The FY 2000 studies focused on Cr(VI) diffusion and reduction to Cr(III) within natural soil aggregates, in order to test the validity of our previously reported results from synthetic soil aggregates. Those earlier studies showed greater Cr transport into aggregates, shorter transport distances, and more complete reduction to Cr(III) with increasing available soil organic carbon (OC). Experiments were conducted on intact aggregates of Altamont clay. The alkalinity of this soil minimized the extent of Cr(VI) sorption on mineral surfaces. A range of initial redox conditions was established within aggregates by infusing solutions containing different concentrations of organic carbon (0 to 800 ppm, as tryptic soy broth). Cr(VI) was diffused into the aggregates at initial concentrations of 1,000 ppm, along with a nonreactive bromide trace. Aggregates were sampled at 3 and 30 days after Cr-exposure, freeze-dried, resin-fixed, and sliced to permit 2-dimensional elemental and Cr oxidation state mapping with an x-ray microprobe. Micro-XANES mapping was done at beamline X26A, National Synchrotron Light Source. Micro-XANES mapping of Cr in aggregates showed (1) deeper Cr diffusion in systems with lower organic carbon, (2) reduction of Cr(VI) to Cr(III) during transport, and (3) very sharp termination

of Cr fronts in more reducing aggregates. The latter phenomenon results from rapidly increasing reduction rates over very short distances (< 10 mm). These results are consistent with our earlier work on synthetic aggregates, and show that larger-scale, aggregate-averaged information on Cr concentrations and oxidation states in contaminated soil profiles can be inadequate for understanding reactive transport.

**CONTRACTOR: LAWRENCE LIVERMORE NATIONAL LABORATORY**

University of California  
Livermore, California 94550

**CONTRACT:** W-6405-ENG-48

**CATEGORY:** Geophysics

PERSON IN CHARGE: F. J. Ryerson

**Pore-scale Simulations of Rock Deformation, Fracture and Fluid Flow in Three Dimensions**

*S. C. Blair 925-422-6467, fax 925-423-1057, blair5@llnl.gov; J. P. Morris, A. L. Ladd, Univ. of Florida; H. F Wang, Univ. of Wisconsin*

**Objective:** The objective of this research is to provide new fundamental understanding of the coupling of localized rock deformation and fracture behavior to macroscopic rock properties and to and fluid flow. During this fiscal year, the project focussed on simulation of the effect of shear deformation on flow in fractures.

**Project Description:** This project is concerned with simulation of rock deformation and fracture at grain and larger scales. This project builds on an earlier OBES project in which a 2-dimensional field-theory model for rock fracture was developed and then used to determine how heterogeneity in different microscale parameters affects rock behavior in compression, and how macroscopic stress strain behavior is related to the formation of cracks. More recently, we have extended our work to include simulation of flow in fractures during shear behavior

**Results:** We have performed preliminary simulations of flow in fractures using the distinct element method (DEM). We have chosen the DEM because it allows us to simulate directly the changing morphology of opposing fracture surfaces and the void space between them with a limited number of initial assumptions. This micromechanical approach simplifies the calculation of permeability and lends itself to fully coupled mechanical-flow problems. The versatility of the DEM accommodates a precise description of fracture surface roughness. Preliminary microscale two-dimensional simulations of a single, sinusoidal fracture in shear showed the expected periodic variation in shear stress as the fracture surfaces undergo shear-slip.

The versatility of a DEM approach using basic principles also permits investigation of many coupled phenomena. For example, the effect of gouge material is readily investigated by introducing free elements into the void space. The DEM can also simulate erosion of asperities and dynamic generation of fines by splitting the discrete blocks in response to excessive stress. We have performed preliminary simulations of a sinusoidal fracture with a number of small round distinct elements within the initial void space. These simulations exhibited a substantially different shear behavior with a dramatic (six-fold for this case) reduction in shear stress as expected.

The microscale DEM results have provided boundary conditions for other computer codes that can be used to evaluate various properties of the fracture network. For example, existing computational fluid

dynamics (CFD) codes were applied directly to the detailed description of the changing void space to give accurate estimates of permeability during shear.

### **Three-dimensional Analysis of Seismic Signatures and Characterizations of Fluids and Fractures in Anisotropic Formations**

*P.A. Berge 925-423-4829, fax 925-423-1057, berge@llnl.gov; J. G. Berryman 925-423-2905, fax 925-422-1002; berryman1@llnl.gov*

**Objectives:** Our major objective is to obtain constraints on lithology in fluid-filled anisotropic rocks by using rock physics theories for anisotropic and poroelastic media. We are collaborating with investigators on related OBES projects at the Colorado School of Mines and Stanford University, who are developing techniques for obtaining anisotropy parameters from seismic reflection data (CSM) and relating laboratory measurement information to modeling and field data (Stanford). By using our theoretical methods to model the anisotropy parameters recovered from seismic data, we can find ways to improve analysis of seismic reflection data collected in areas where the geology is complicated by anisotropy and heterogeneity.

**Project Description:** CSM collaborators are generalizing anisotropic velocity analysis techniques to account properly for vertical inhomogeneity and dipping structure, so that the technique will be applicable to a wide range of exploration problems. The LLNL/Stanford group is working on developing and analyzing rock physics models that describe transversely isotropic media, particularly to determine how these models may constrain lithology. Stanford is focusing more on laboratory measurements and anisotropic signatures of fractured rocks, and LLNL is focusing on fluid effects and poroelasticity in anisotropic rocks. Topics of research include determining what constraints on lithology can be found from the anisotropy and poroelasticity parameters and what information is sufficient and necessary for the constraints. The overlying questions are how to do lithologic interpretation of the anisotropic parameters obtained from field data, and the possibility of incorporating shear-wave data into the velocity analysis and lithology interpretation.

**Results:** LLNL researchers have developed a new method for using P and S velocities to obtain information about rock saturation. This work was published in the Journal of the Acoustical Society of America and was also submitted to Geophysics. Results relating the fluid distribution in partially saturated anisotropic rocks to measured seismic parameters, and the effects of fluids on anisotropy parameters were presented at an OBES symposium and manuscripts for journal papers on these results are in preparation.

## Physical Properties of Heterogeneous Rocks Containing Fluids

*J. G. Berryman, 925-423-2905; fax 925-423-6907, berryman1@llnl.gov*

**Objectives:** Our main objective is to understand significant factors affecting physical properties of heterogeneous rocks in order (1) to improve our ability to predict rock behavior from knowledge of rock components and pore fluids and (2) to improve our ability to interpret geophysical field data. One new tool developed to accomplish this objective is the discovery by the PI of exact results in poroelasticity and thermoelasticity for two component composite rocks and the application of these ideas to effective medium theories for poroelastic composites. This project exploits these as well as other new results, with the expectation that new insight into the elasticity and poroelasticity of rocks will result. Such insight has proven to be important for understanding partial melt in both the upper and lower mantle, for clarifying earthquake source mechanisms, for interpreting seismic reflection survey data for oil and gas exploration, for oil field engineering practices related to drilling and pumping, and for related issues in environmental cleanup of DOE sites. This type of information is important for interpretation of both seismic and electrical geophysical field data, and is useful to both oil reservoir engineers and hazard cleanup activities.

**Project Description:** Four major approaches are being considered in this project: (1) partial saturation data analysis showing that the Lamé' lambda parameter is most important for analyzing liquid content of rocks and that shear modulus predictions for higher frequency data needs to incorporate changes caused by liquid content, (2) continuing development and use of a generalization of Eshelby's formula from elasticity theory for poroelastic and thermoelastic composite inclusions analysis problems, (3) double-porosity/dual-permeability methods for fractured reservoirs, and (4) applications of rigorous viscoelastic bounds to rock/fluid mixtures. These types of results are all of interest in the oil and gas industry. The same basic framework can also be employed to treat reservoir characterization problems, especially regarding the effects of changing stress on matrix and fracture permeability in double-porosity models used for reservoir pumpdown studies. In addition to single-fluid reservoir analysis, related ideas have been applied to partial saturation problems, in which both gas and oil, or gas and water may be present and distributed throughout the reservoir volume in a complicated, inhomogeneous manner. Related ideas (Gassmann's fluid-substitution formulas) can play a very significant role in interpretation of seismic AVO (amplitude versus offset) data used as direct hydrocarbon indicators.

**Results:** One exciting area of the work this year has been analysis of partial and patchy saturation of rocks. This work had built on previously funded BES work in anisotropy, wherein it was determined that the most important variable determining Thomsen's parameters in anisotropy analysis is surprisingly Lamé's elasticity parameter known as lambda. For rocks containing fluids, we have shown theoretically, and by extensive studies of published laboratory data, that this is also the parameter that depends most sensitively on the pore fluid's physical properties. Thus, plots of seismic velocity (both compressional and shear are required) emphasizing changes in lambda have the power not only to determine the magnitude of the liquid saturation present, but also (and this was also a big surprise to all of us) to distinguish homogeneous from inhomogeneous (patchy) saturation. One paper on this topic has now been published in Journal of the Acoustical Society of America and another has been submitted to Geophysics. Our most recent work in this area shows that seismic impedance (density times velocity) data that are typically obtained in seismic reflection surveys for oil exploration can also be used to accomplish the same results. This fact has significant implications for improvements to seismic AVO analysis. We also published a paper in Geophysical Research Letters this year showing that it is

possible to use Gassmann's equations to study seismic velocity decrements due to partial melt in the lower mantle. The new approach takes advantage of the fact that Gassmann's equations do not depend explicitly on the microstructure of the porous earth, but only on the fact that the pores are connected and the pertinent time scales long. In collaboration with researchers at the University of Wisconsin, we had previously developed methods to determine and in some cases drastically reduce the number of elastic coefficients required to describe the behavior of a double-porosity system in the presence of changing pore pressure for applications to reservoir pumpdown. An extension of this work in collaboration with Steven Pride (from France, currently on sabbatical at Stanford) has been submitted to the Journal of Geophysical Research. Other related work has been published now in International Journal of Rock Mechanics describing methods to study elastic wave propagation through such media. The resulting equations permit the parameters determining wave speed and attenuation to be decoupled in a significant new way. Extensions of this work continue through studies of methods to estimate coefficients in these equations that can be computed from knowledge of the constituents and their physical properties. A number of surprising results have been obtained, including some new exact results for multicomponent systems that had not been previously anticipated.

### **Geophysical Monitoring of Carbon Dioxide Sequestration using Electrical Resistance Tomography (ERT)**

*R.L. Newmark, 925-423-3644, fax 925-422-3925, newmark@llnl.gov; A.L. Ramirez 925-42-6909, fax 925-422-3925, ramirez3@llnl.gov; W. D. Daily 925-422-8623, fax 925 422-2495, daily1@llnl.gov*

**Objectives:** The objective of this project is to evaluate the applicability of high resolution electrical imaging techniques to monitor CO<sub>2</sub> injection and migration and to evaluate their potential for detecting leaks or leak pathways.

**Project Description:** Numerical simulations and bench-scale modeling will be used to investigate the range of conditions and configurations under which electrical resistance tomography (ERT) methods may be used to monitor the geophysical changes resulting from CO<sub>2</sub> injection and migration. The results of these studies will be directed toward the design of a field survey. The primary activities and goals of the research will be to:

1. Investigate the sensitivity of high-resolution electrical imaging methods to key geophysical and chemical parameters pertinent to CO<sub>2</sub> injection scenarios.
2. Determine the operational issues pertinent to process control and performance assessment.
3. Determine the sensitivity of high-resolution electrical imaging methods to different measurement configurations, reflecting operational field survey design constraints.
4. Design and conduct a field survey to demonstrate the applicability of high-resolution electrical imaging methods to monitor CO<sub>2</sub> injection and migration, and to evaluate their potential for detecting leaks or leak pathways.

**Results:** Using published field data and unpublished information obtained through communication with industry researchers, we developed a set of target scenarios, indicative of realistic CO<sub>2</sub> injection projects. We then conducted a series of sensitivity studies to map the ERT performance envelope and evaluate the effectiveness of 3D ERT as a potential monitoring approach for CO<sub>2</sub> sequestration. ERT resolution is affected by a number of factors, including resistivity contrast, anomaly location (proximity to electrodes), anomaly size and shape, noise level and measurement configuration; sensitivity studies were designed to explore all of these factors in a methodical manner, so as to permit quantitative evaluation of the relative influence of each. Using a model patterned after an oil field undergoing CO<sub>2</sub> flood, forward and inverse simulations of ERT surveys were run to test the sensitivity of the method to detect the changes resulting from CO<sub>2</sub> migration. The initial model approximates the complexity of a layered reservoir, and is consistent with previously published results. Carbon dioxide migration is introduced into a thin layer (~7 m thick) by changing the resistivity in the targeted layer, producing an anomalous region. The anomalous region's resistivity ranges from 0.2 to 10 times that of the initial value. Its geometry ranges from a thin, horizontal finger to a planar, horizontal mass having vertical protrusions simulating leakage of CO<sub>2</sub>. The measurement configuration involves a nine-spot of vertical measurement locations (simulating wells), each separated by 140 m. Simulations were run either with arrays of point electrodes (simulating high resolution surveys) or assuming the well casings are used as long electrodes (1480 m long). Results of simulations run assuming both point electrode arrays, and long electrodes show good detection for even the narrowest simulated CO<sub>2</sub> fingers. The initial results of this work were presented at the Fall AGU Meeting (December, 2000).

### **Water Distribution in Partially Saturated Porous Materials**

*J. J. Roberts, 925-422-7108, fax 925-423-1057, roberts17@llnl.gov*

**Objective:** To determine the electrical properties of water and CO<sub>2</sub> saturated porous materials at a variety of experimental conditions and to utilize the experimentally determined electrical properties to investigate the relationships between electrical transport and other transport properties in materials with well-characterized microstructures. Results will be used in conjunction with field EM measurements to track flow and injection processes at EOR and CO<sub>2</sub> sequestration sites.

**Project Description:** The purpose of this project is to measure the frequency dependent electrical properties of porous materials and relate the results to other transport properties and to improve the interpretation of field EM measurements through better understanding of physical properties of partially saturated porous media. Measurements include dielectric constant and electrical resistivity as functions of saturation, temperature and microstructural properties and include monitoring the resistivity of materials as they become fluid-, steam-, and CO<sub>2</sub>-saturated. The complex impedance is measured because impedance spectra provide information regarding the number and arrangement of conduction mechanisms, distribution of liquid phase, and microstructural properties. The fluids used to saturate the samples have a range of ionic composition, and hence, electrical conductivity. This permits the comparison of impedance spectra of samples at similar saturations to better understand the relationship between fluid distribution and the corresponding conduction mechanisms. These measurements are of particular importance because field electrical measurements in unsaturated regions (including electrical resistance tomography, electromagnetic depth sounding, and induced polarization) depend on reliable laboratory measurements for accurate interpretation. A number of geophysical problems including

remediation, enhanced oil recovery, geothermal reservoir evaluation and site monitoring depend on reliable information regarding the interconnectedness and distribution of the fluid phase.

**Results:** Laboratory impedance measurements have been performed on samples of geologic interest including sandstones, welded tuffs, siltstones, and serpentinites. Results on the electrical properties of geothermal reservoir rocks during boiling were presented at the Geothermal Resources Council Annual Meeting, Reno, NV, October 17-20, 1999, and the Twenty-Fifth Workshop on Geothermal Reservoir Engineering, Stanford University, January, 2000, resulting in two conference proceedings papers and a journal article.

Preliminary results on samples from the Lost Hills EOR site have been used by the Fossil Energy Program to better understand their crosswell EM inversions and have been presented at the National Petroleum Technology Office, FE Annex IV review at LLNL.

The pressure vessel and pumping system used for the laboratory electrical measurements has been modified to accommodate the injection and flow of both gaseous and liquid CO<sub>2</sub> into and through samples. Initial measurements of electrical properties during CO<sub>2</sub> injection were performed. The focus in the upcoming year will be on improvement of this type of measurement.

Collaborations with WHOI investigators on the electrical properties of serpentinites were performed. The results are applicable to studies of hydrothermal systems near mid-ocean ridge spreading centers.

## **CATEGORY: Geochemistry**

PERSON IN CHARGE: F.J.Ryerson

### **Reactive Transport of CO<sub>2</sub>-Rich Fluids and Precipitation and Dissolution in Rock Fractures**

*W. B. Durham, 925-422-7046, fax 925-423-1057, durham1@llnl.gov; W. L. Bourcier; E. A. Burton*

**Objective:** The objective of this research is to measure local rates of dissolution and precipitation on the walls of individual fractures and the presence of CO<sub>2</sub>-rich fluids and correlate differences in reaction rates to changes local fracture aperture. Much use will be made of high-resolution physical topography measurement and numerical simulation of reactive flow.

**Project Description:** The project entails refurbishing a hot-reactive-flow pressure vessel used in earlier years in this laboratory and applying it to the reactive flow problem. We will build on past successes using a similar experimental strategy, with the main difference being the high concentration of CO<sub>2</sub> in the reactive fluid, a condition that requires the use of elevated temperature and pressure. The experiments and simulations will be done on rock samples containing a single laboratory-made or natural fracture. Detailed imaging of the fracture aperture before and after alteration will be coordinated with measurements of fracture deformation, permeability, dispersivity, and effluent composition, all as functions of pressure, temperature, temperature gradient, time, rock composition, fluid velocity, and fluid composition. For the most part, we will work with simple but relevant systems in order to maximize our understanding and impact: samples will be monomineralic rocks with low porosity and

low bulk permeability (such as quartzites and marbles), under fully saturated, single-phase flow conditions. We will attempt measurements in undersaturated, dual-porosity, and more chemically complex settings as success dictates.

**Results:** The experimental apparatus has now been thoroughly rebuilt with new plumbing, new pressure sensors, and a new sample assembly adapted to the use of hot, CO<sub>2</sub>-rich fluids. In keeping with the philosophy of beginning with simple, well-defined systems, the first samples prepared for testing are of Carrara marble. The first of these is a calibration sample prepared with a fracture aperture that is simply two wide, flat grooves about 0.25 mm deep running the length of the sample. A second core of Carrara marble with a more realistic rough fracture has also been prepared and its surface digitized with our specialized profilometer to produce a detailed topographic map of its aperture.

### **The Role of Carbon and Temperature in Determining Electrical Conductivity of Basins, Crust, and Mantle.**

*A. G. Duba, LLNL, 510-422-7306, fax 510-423-1057, alduba@llnl.gov; T. J. Shankland, 505-667-4907, fax 505-667-8487, shankland@lanl.gov; E. A. Mathez, American Museum of Natural History 212-769-5379; fax 212-769-5339; mathez@amnh.org*

**Objectives:** The intent of this work is to comprehend the electrical conduction mechanisms in carbon-bearing rocks and in mantle minerals to relate electrical conductivity ( $\sigma$ ) measured in the field to the nature and origin of carbon in crustal rocks and to temperature in the mantle.

**Project Description:** Electrical conductivity depends strongly on temperature and on the presence of other phases such as carbon, fluids, or ore minerals at the lower temperatures of the crust and basins. One research approach is to measure  $\sigma$  of mantle minerals as functions of temperature, orientation, oxygen fugacity  $f(\text{O}_2)$  and iron content. These data supply the best models for "electrogeotherms" yet available. Another approach is to document textures of carbon in crustal rocks from basins and metamorphic zones and relate them to rock conductivity. In this case, the nature of the carbon is determined by time-of-flight mass spectroscopy and its distribution determined by electron microbeam techniques in the same samples used for conductivity measurement.

**Results:** Amphibolites from 4.6 and 9.1 km depth in the KTB borehole have developed extensive, interconnected networks of carbonaceous films on cracks and grain boundaries as determined by electron probe and time-of-flight secondary ion mass spectrometry. In the sample from 9.1 km depth, the carbon is almost completely elemental. In contrast, the carbonaceous matter in the samples from 4.6 km depth is a mixture of elemental carbon and simple hydrocarbons such as alkanes, and possibly C-O-H compounds. The microcracks in the 4.6 km sample also contain a retrograde micro-assemblage consisting of ferri-oxy-hydroxide, calcite, and possibly clay minerals, suggesting that the carbonaceous matter and retrograde minerals formed together at relatively high crustal levels and at a time much later than peak metamorphism. Because the carbon films likely influence the electrical conductivity of the rocks *in situ*, it is proposed that production of hydrocarbons (which are insulating materials) during retrograde metamorphism of grain boundary and microcrack carbon tends to increase the resistivity of the rocks. This chemical destruction of the interconnectivity of electrical pathways may contribute to the observed diminished electrical conductivity of the shallow crust relative to the deep crust.

## Thermodynamic and Transport Properties of Aqueous Geochemical Systems

*Joseph A. Rard, 510-422-6872, fax 510-423-6907, rard1@llnl.gov; Donald G. Miller 510-422-8074, fax 510-422-0208, dmiller@llnl.gov*

**Objectives:** The objectives are to (1) measure precise and accurate osmotic/activity coefficients, solubilities, densities, and mutual (Fick's law) diffusion coefficients for aqueous brine salt mixtures and osmotic/activity coefficients for acidic and nonacidic sulfate mixtures; (2) develop reliable methods to estimate such properties for multicomponent solutions from binary solution properties; and (3) calculate trace diffusion coefficients and generalized transport coefficients.

**Project Description:** The general techniques of classical thermodynamics and of linear irreversible thermodynamics are used to model equilibrium and transport processes in brines and other aqueous electrolyte mixtures relevant to energy programs. Highly precise osmotic/activity coefficients and solubilities are being measured by the isopiestic method, densities by vibrating-tube densimetry, and diffusion coefficients by Rayleigh interferometry. We use our accurate new data for developing and testing estimation methods for accurate predictions of these properties for mixtures of arbitrary complexity. Osmotic/activity coefficients are being analyzed using extended forms of Pitzer's equations, and transport data are being analyzed as Onsager transport coefficients.

**Results:** We extended our diffusion and density experiments for aqueous mixtures of NaCl and Na<sub>2</sub>SO<sub>4</sub> at 25°C up to a total molarity of 5.0 mol/dm<sup>3</sup>, at NaCl molarity fractions of 0.90 and 0.95, using Rayleigh interferometry. The measurements at high concentrations were made for solutions containing high molar ratios of NaCl to Na<sub>2</sub>SO<sub>4</sub>, because of solubility limitations due to precipitation of mirabilite. These experiments supplement our previous results at 0.5 – 1.5 mol/dm<sup>3</sup> at 25°C for the full composition fraction range, and were made using the Gosting diffusimeter with computer-controlled data collection. Above 3.0 mol/dm<sup>3</sup> the NaCl cross term diffusion coefficient exceeds the Na<sub>2</sub>SO<sub>4</sub> main term coefficient, which indicates that any gradient of Na<sub>2</sub>SO<sub>4</sub> will cause the transport of more NaCl than of itself. Extrapolation of these combined results to Na<sub>2</sub>SO<sub>4</sub> molarity fractions of zero yield the trace diffusion coefficient of the sulfate ion in aqueous NaCl at molar concentrations of 0.5 to 5.0 mol/dm<sup>3</sup>. These trace diffusion coefficients were obtained without using a radioactive tracer, and are probably more precise and accurate than those obtained by conventional methods. The diffusion experiments were performed in collaboration with Professor John G. Albright and a graduate student at Texas Christian University.

Isopiestic vapor-pressure experiments were finished for aqueous Na<sub>2</sub>SO<sub>4</sub> + MgSO<sub>4</sub> mixtures at equal molal concentrations at 25 °C, and extend to the supersaturated molality corresponding to spontaneous crystallization. We started isopiestic experiments for aqueous H<sub>2</sub>SO<sub>4</sub> + Al<sub>2</sub>(SO<sub>4</sub>)<sub>3</sub> mixtures at 25 °C, in part to understand the dissolution of aluminum minerals in acid mine waste. Isopiestic measurements were made at three ionic molality fractions  $z$  of H<sub>2</sub>SO<sub>4</sub> of  $z \approx 6/7$ ,  $5/7$ , and  $4/7$  for total molalities from 0.50 to 1.64 mol/kg.

During this period, two journal articles and one book were published, and two other journal articles were written and accepted for publication. The first of the published journal articles is an extensive critical review of the published thermodynamic data for aqueous Na<sub>2</sub>SO<sub>4</sub>, and reports a mole-fraction based equation of state that represents the available results accurately from freezing temperatures to 150.5°C.

This review was done in collaboration with Simon Clegg (University of East Anglia) and Donald Palmer (Oak Ridge National Laboratory). The second journal article reports diffusion data for aqueous mixtures of NaCl and Na<sub>2</sub>SO<sub>4</sub> at 25°C and at 1.5 mol/dm<sup>3</sup>, at various ratios of the solutes, and was done in collaboration with John G. Albright's research group. The book "Chemical Thermodynamics of Technetium" was published by Elsevier/ North Holland. Its authors are Joseph A. Rard, Malcolm H. Rand, Giorgio Anderegg, and Hans Wanner.

A new paper reporting diffusion data for aqueous mixtures of NaCl and Na<sub>2</sub>SO<sub>4</sub> at 25°C at fixed NaCl molarity fraction of 0.90, and at concentrations of 0.5 to 5.0 mol/dm<sup>3</sup>, was accepted for publication by the Journal of Chemical and Engineering Data. Another paper, accepted for publication by the Journal of Chemical Thermodynamics, reports apparent molar heat capacities and apparent molar volumes of aqueous trivalent rare earth sulfate solutions at 25°C and was done in collaboration with Professor Andrew W. Hakin and Robert Marriott of the University of Lethbridge (Canada).

### **Collaborative Research: Studies for Surface Exposure Dating in Geomorphology**

*R.C. Finkel, 925-422-2044, fax 925-422-0208, rfinkel@llnl.gov; M. Caffee, 925-423-7896, fax 925-422-1002, caffee1@llnl.gov*

**Objective:** The objective of this research is an experimental and theoretical program to fully develop the systematics of *in situ* produced cosmogenic nuclides in terrestrial surface samples and their application to the dating of surface features and processes. This work includes determination of precise production rates and production depth profiles, studies of altitude and latitude effects, intercalibration with other methods, isolation of *in situ* produced nuclides from other lithologies and development of *in situ* produced <sup>14</sup>C. This research is a collaborative endeavor between LLNL (Caffee, Finkel, AMS), UC Berkeley (Dietrich, geomorphology; Nishiizumi, geochemistry) and LANL (Reedy, cosmogenic nuclide modeling; Poths, noble gas mass spectrometry).

**Project Description:** The measurement of in-situ produced radiocarbon in the quartz from rocks exposed to cosmic rays will provide more thorough understanding of surface processes of the Earth. Despite the widely recognized potential of this method, it has not been possible to measure the abundance of in-situ <sup>14</sup>C, due to the technical difficulty of extracting it from the quartz matrix. This can be contrasted with <sup>10</sup>Be and <sup>26</sup>Al, which have found routine application. We are establishing a reliable measurement system for radiocarbon extraction from quartz at the Lawrence Livermore National Laboratory.

**Results:** The main difficulties in extracting in-situ produced cosmogenic <sup>14</sup>C are all related to its relative scarcity in quartz. This scarcity is aggravated by the abundance of meteoric <sup>14</sup>C, a contaminant for our purposes. To resolve these problems, we assembled a high-vacuum <sup>14</sup>C-extraction line dedicated for only in-situ <sup>14</sup>C experiments.

The system consists two parts, a high-temperature furnace that can attain temperatures of up to 1,700 °C, and a purification line. The purification line serves several purposes. C-14 released from quartz during heating can exist as <sup>14</sup>CO or <sup>14</sup>CO<sub>2</sub>. Although an oxidizing gas, which also contains the carrier C, is flowed through the systems at all times this may be insufficient to convert all CO to CO<sub>2</sub>. Pt chips,

heated to ~600 C serve to complete the oxidation of CO to CO<sub>2</sub>. The CO<sub>2</sub> is then cryogenically concentrated. Until recently, the line had high and variable background levels (equivalent to ca. 18,000-25,000 yrs <sup>14</sup>C BP). Extensive leak tests and replacement of many parts have been conducted, including careful selection of the Pt chips, which were cleaned at 1,000 °C prior to the installation. As discussed below, this work has yielded significant reductions in the <sup>14</sup>C backgrounds.

Since quartz is extremely low in carbon, it is necessary to use a carrier gas that contains no <sup>14</sup>C. With the exception of the CO<sub>2</sub> concentration, which is enhanced relative to the atmosphere, the carrier gas is atmospheric in composition. In some laboratories (*e.g.* University of Arizona's group), ultra-purified-oxygen is used for extraction of <sup>14</sup>C, but we employed a 4:1 N<sub>2</sub>/O<sub>2</sub> gas mixture with trace amounts of CO and CO<sub>2</sub> carrier. Because the O fugacity of atmospheric gas suffices to oxidize <sup>14</sup>C released from the rock quartz, this mixture is preferable, not only because it ameliorates safety concerns, but it is less reactive with components of the furnace. The Arizona group observed in their experiments that the alumina tube became chemically activated and adsorbed CO<sub>2</sub>. No detailed explanation for their results has been given however we have not seen similar behavior in our furnace.

A critical issue is the activity of the carrier gas. The <sup>14</sup>C activity of the gas was tested using the AMS preparation line at CAMS, LLNL and we obtained results indicating that the <sup>14</sup>C activity of the carrier gas was indistinguishable from the system background.

During in-situ <sup>14</sup>C extraction, a known amount of carrier gas is continuously flowed through the high-temperature furnace. The effect of degassing the furnace at the various temperatures was determined. All temperature steps provide similar and low background <sup>14</sup>C ages, indicating the reliability of the high-vacuum line used for the current project.

After the demonstration of low backgrounds, we used quartzite samples taken from the Homestake mine in South Dakota (-1,600 m from the surface), presumed to be in-situ <sup>14</sup>C-free, as a test for the effectiveness of step-wise heating to eliminate meteoric <sup>14</sup>C in real quartz. The results show that most of the meteoric contamination can be outgassed at temperatures < 500 °C in the furnace. Step-wise heating experiments revealed a constant background level of ca. 38,000-40,000 yrs BP above 500 °C. This background corresponds to about 1-2 x 10<sup>5</sup> atoms of <sup>14</sup>C. Thus backgrounds achieved to date will enable us to perform experiments on samples of geologic significance. Although our goal is further reduction of backgrounds from a practical viewpoint, we ready to move on to the next phase of the experiment, which is to use quartz samples collected from the Dry Valleys in Antarctica. These are demonstrably saturated in <sup>14</sup>C activity (based on <sup>10</sup>Be and <sup>26</sup>Al concentrations), and will provide a test of the extraction efficiency of our technique.

### **In-Situ CO<sub>2</sub>-sequestration: Measurement of Coupled Silicate Dissolution and Carbonate Precipitation**

*Susan A. Carroll 510-423-5694, carroll6@llnl.gov; Kevin Knauss, knauss1@llnl.gov*

**Objectives:** The objective of this research is to measure dissolution and precipitation rates important to the mineralization of dissolved carbon at conditions relevant to CO<sub>2</sub> sequestration. Determination of

mineral dissolution and precipitation kinetics is fundamental to the successful disposal of greenhouse CO<sub>2</sub>-rich gases in aquifers, because reservoir storage capacity is directly related to the conversion rates of CO<sub>2</sub> to carbonate minerals. The reaction of CO<sub>2</sub> and water with unstable silicate minerals to produce more stable silicates (*e.g.* clays) and solid carbonates is the natural weathering process which is a dominant part of the long-term global geochemical cycling process. Our kinetic research will feed directly into promising reaction-transport codes that will evaluate aquifer storage of dissolved CO<sub>2</sub> and mineral carbonates, and resulting changes in porosity and permeability.

**Project Description:** Our approach is to conduct single and multi-mineral dissolution and precipitation experiments and reaction transport experiments in Ca-Al-Si-CO<sub>2</sub> and CaCO<sub>3</sub> systems as a function of pCO<sub>2</sub>, pH and temperature. Supercritical CO<sub>2</sub> experiments simulate the reactive front of CO<sub>2</sub> plume and aquifer water and are designed to measure the available source of calcium for storage of CO<sub>2</sub> as carbonates and the source of aluminum and silica for the precipitation of secondary minerals that will effect aquifer porosity and permeability.

**Results:** We have experimentally measured the dissolution rate of labradorite (Ca<sub>0.6</sub>Na<sub>0.4</sub>Al<sub>1.6</sub>Si<sub>2.4</sub>O<sub>8</sub>) in waters saturated with and without supercritical CO<sub>2</sub> at pH 3.2 and at 30, 60, 100 and 130°C using mixed flow-through reactors. To-date we have two important findings: (1) Any enhanced dissolution of labradorite in waters saturated with supercritical CO<sub>2</sub> can be attributed directly to acid pH from the high concentrations of dissolved CO<sub>2</sub> (about 0.6 M CO<sub>2</sub> in our experiments). There is no direct effect of dissolved CO<sub>2</sub> on mineral dissolution. We measured similar dissolution rates in pH 3.2 solutions saturated with atmospheric CO<sub>2</sub> and with supercritical CO<sub>2</sub> (1400 psi). (2) Labradorite dissolution rates are dependent on temperature and dissolved aluminum concentrations. To model geologic CO<sub>2</sub> sequestration accurately, reactive-transport codes need to account for the temperature dependence of incongruent and congruent dissolution of these minerals. We observe incongruent dissolution of labradorite at 30 and 60°C, in which the Ca, Al, and Na dissolve faster than Si. At 100°C, labradorite dissolution is congruent with no precipitation of secondary phases. At 130°C, dissolution is incongruent, in which net Al rates are about 20 times less than the Ca, Na, and Si rates, indicating precipitation of a secondary aluminum phase. Labradorite dissolution is dependent on dissolved aluminum concentration and is consistent with model proposed by Oelkers et al.(1994) in which alumino-silicate dissolution is dependent on the decomposition of an Al-deficient, silica-rich surface complex.

### **Mineral Dissolution and Precipitation Kinetics: A Combined Atomic-Scale and Macro-Scale Investigation**

*Kevin G. Knauss, 510-422-1372, fax 510-422-0208, knauss@llnl.gov; Carrick M. Eggleston 307-766-6769; fax 307-766-6679, carrick @uwyo.edu; Steven R. Higgins, 307-766-3318; fax 307-766-6679, shiggins@uwyo.edu*

**Objectives:** The primary objective for this research program is to develop an appropriate mechanistic understanding of carbonate mineral dissolution and growth through extensive experimentation at both microscopic and macroscopic length-scales.

**Project Description:** This project utilizes a combined atomic-scale and macro-scale study of mineral/fluid interaction that is designed to improve our understanding of, and ability to predict the course of, mineral dissolution and precipitation processes specifically affecting coupled silicate mineral

dissolution and carbonate mineral growth expected as part of a CO<sub>2</sub> sequestration strategy of injection into deep aquifers. Our atomic-scale studies utilize a Hydrothermal Atomic Force Microscope (HAFM) for molecular-level experiments on the kinetics of nucleation, step motion and other phenomena on mineral surfaces under conditions relevant to CO<sub>2</sub>-sequestration. The same conditions used in HAFM experiments will also be investigated with macroscopic hydrothermal reactors (for stoichiometric rate data) and geochemical reactive transport codes. This approach will allow us to address many still-open questions concerning the exact forms for rate laws near and far from equilibrium, the microscopic interpretation of these rate laws, the activation energies and formation energies for key microscopic surface structures (*e.g.*, steps, kinks), and the impact of specific aquifer solute catalysts and inhibitors on the dissolution and growth processes.

**Results:** Our objectives for FY 2000 involved both research and instrumentation development. On the research front, our goal was to obtain experimental data on the dissolution and precipitation kinetics of magnesite and calcite as a function of solution composition and temperature, all in well-defined hydrodynamics. These experimental goals required that significant improvements to the fluid delivery system be made to the original HAFM developed earlier under this grant number.

We have updated and improved the HAFM technology with a new fluid inlet that creates hydrodynamic conditions, modeled extensively by Dr. Richard Compton's group at Oxford University. This improvement permits well-constrained kinetic data to be obtained from the HAFM. We have conducted studies of magnesite and calcite dissolution in aqueous solution at temperatures up to 90 °C. The step directions defining etch pits on magnesite (see Figure 1) are sensitive to the extent of surface protonation with little resultant change in overall dissolution flux. The experimental results suggest a fundamental difference in mechanism between acidic dissolution of calcite and magnesite – calcite follows a first-order heterogeneous proton promoted mechanism whereas magnesite displays a much weaker dependence on surface proton concentration; indicative of a pre-equilibrium or surface complexation mechanism.

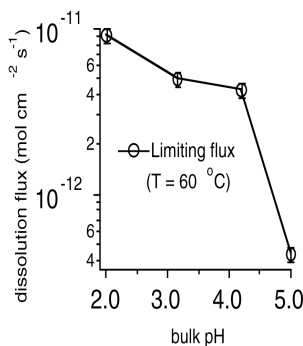
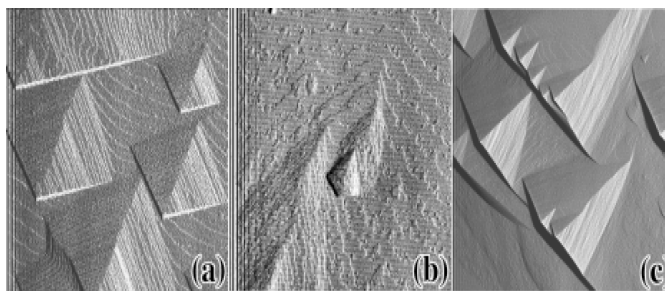


**Figure 1.** Magnesite *in-situ* etch pit morphology (6000 nm x 6000 nm images) at 60°C using the HAFM at (a) pH = 4.2, (b) pH = 3.1, and (c) pH = 2.0. (left) limiting dissolution flux vs. bulk pH.

## Determining the Physical Controls on Biomineralization

Jim De Yoreo, 925-423-4240; fax 925-422-6892; [deyoreo1@llnl.gov](mailto:deyoreo1@llnl.gov); Patricia Dove 404-894-6043, fax 404-894-5638, [dove@eas.gatech.edu](mailto:dove@eas.gatech.edu)

**Objectives:** Since the emergence of life on earth, organisms have directed the crystallization of inorganic ions from solution to form minerals that meet specific biological needs. The resulting materials often exhibit remarkable properties, making the processes involved in biomineralization of interest to a wide array of scientific disciplines. From a geochemical standpoint, perhaps the most important consequence is that  $\text{CaCO}_3$  biomineral formation occurs in the oceans on such a large scale that it influences many aspects of seawater chemistry and results in sequestration of carbon in the form of carbonate sediments. In this manner, the products of biomineralization are preserved in the rock record and serve as an extensive chronicle of the interplay between biota and the earth system environment.

From the point of view of materials synthesis, biological control over epitaxy is an elegant example of self-organization in complex molecular systems. Through selective introduction of peptides and proteins, living organisms deterministically modify nucleation, step kinetics, surface morphologies, and facet stabilities to produce nanophase materials, topologically complex single-crystals, and multi-layer composites. The resulting materials have biological functions as diverse as structural supports, porous filtration media, grinding and cutting tools, lenses, gravity sensors and magnetic guidance systems.

Calcium carbonate minerals are ubiquitous amongst biomineral structures. In addition, calcium carbonate is a well studied material that is easily crystallized and has known solution chemistry. Consequently, the calcium carbonate system provides an excellent model for investigating biomineralization processes. Surprisingly, in spite of the identification of carbonate biogenesis as a critical contributor to the carbon reservoir mediating climate change, and the enormous potential of biomimetic synthesis for production of tailored, crystalline nano- and micro-structured materials, the fundamental physical controls on carbonate biomineral formation remain poorly understood.

The objective of this project is to obtain a microscopic understanding of the reaction mechanisms and physical controls on calcium carbonate biomineral formation, recognizing the fact that mineralization is, above all, a thermodynamic phase transition. As such, rates of nucleation and growth as well as the resulting crystal structure, surface morphology, and habit are controlled by the energetics and kinetics of ad molecules and steps on the crystal surface. Our hypothesis is that biomineralization of  $\text{CaCO}_3$  is successful because functional groups on protein chains are able to provide preferential sites for nucleation by changing the interfacial energies and are able to alter growth rates and surface morphologies by selectively binding to kink sites on the  $\text{CaCO}_3$  surface. Our approach is designed to test this hypothesis.

**Project Description:** Our primary tool is *in situ* atomic force microscopy (AFM). Using this method to measure the dependence of critical step length and terrace width on supersaturation, we are able to determine the step edge energy of the system. This parameter describes the equilibrium thermodynamic state of the system determines the equilibrium surface morphology. From the dependence of step speed on concentration, we can extract the kinetic coefficient for elementary step motion. The latter provides a measure of the activation barrier to step motion. By examining the effect of the organic fraction on these parameters, we can gain an understanding of their effects on the energetic and kinetic factors controlling the growth phase. To take into account the effect of Mg, a common component of both ocean waters and biogenic calcite, we will also examine the effect of Mg on these parameters.

**Results:** The addition of Mg to calcite solutions leads to an upward shift in the concentration at which the step speed passes through zero, but has little or no effect on the kinetic coefficient. This result demonstrates that the well-known inhibition of calcite growth by Mg addition is a result not due to step pinning as is often assumed. Rather it is a thermodynamic effect associated with the higher affinity of the Mg-bearing calcite for aqueous solvation. Measurements of the Mg content of calcite crystals grown under conditions identical to those used in the AFM experiments show that the observed increase is consistent with the trends observed in macroscopic crystallization experiments as well as in biogenic calcite.

The effects of glycine, aspartic acid and glutamic acid on step speed, critical length and growth hillock, etchpit and crystal morphology were examined as a function of amino acid chirality and concentration. Addition of all amino acids during growth, led to stabilization of the  $\{hk0\}$  family of planes. When the amino acid had a chiral structure, the addition of pure L- and D- forms resulted in anisotropic expression of these planes. The resulting growth hillock, etchpits and crystal morphologies displayed a left/right asymmetry about the glide plane of calcite that depended upon the amino acid enantiomer. The addition of glycine, an achiral molecule, or D and L mixtures of aspartic and glutamic acid, led to symmetric forms. Because the overall facet shape exhibited the same shape as the growth hillocks, we were able to use the growth hillock geometry to construct the modified Wulff diagram for the orientational dependence of the step edge energy

For any site on one side of the glide plane, an equivalent site on the other side can be found for which the geometric relationship with neighboring sites is related by mirror symmetry. Furthermore, the geometrical relationship between a single functional group of the amino acid with any single site on one side of the glide plane can be matched at the equivalent site on the other side. Consequently, the results of this study show unequivocally that the interaction of the amino acid with the calcite surface must involve both the chiral center of the amino acid (*i.e.*, multiple functional groups) and multiple sites on the calcite surface. Using molecular modeling, we calculated the binding energy for aspartic acid to both the  $\{104\}$  face and the two acute step edges. These results mimic the AFM experiments; L and D Asp show preferential binding to the step edges predominantly expressed in experiments. Furthermore, binding across two carboxyl groups at the step riser was preferred over binding to the face, a result that explains why surface spectroscopic methods reveal little or no Asp coverage on the  $\{104\}$  face, despite its dramatic effect on growth morphology.

Finally, we found that the addition of aspartic and glutamic acid had little effect on the step speeds showing that the growth kinetics are relatively unchanged. In contrast, the dramatic change in morphology and orientational dependence of the step edge energy shows that the equilibrium thermodynamic state of the crystal is strongly altered. These results suggest that the organic fraction in biomineralizing systems exert thermodynamic rather than kinetic controls over crystallization. The organic molecules bind preferentially to the acute steps, acting as the 1D equivalent of a surfactant to lower the step edge energies and produce new equilibrium shapes.

## Testing Deep Saline Aquifers for Long-term CO<sub>2</sub> Leakage Using *In-Situ* Noble Gases

*G.J. Nimz, 925-423-2766; fax 925-422-0208; nimz1@llnl.gov; G.B. Hudson, 925-423-2947, hudson5@llnl.gov, M.W. Caffee 925-423-8395, caffee1@llnl.gov*

**Objectives:** The intent of this project is to develop techniques based on noble gas isotopes for the purpose of testing deep saline aquifers for long-term leakage of gases. Such aquifers have been suggested as repositories for industry-derived CO<sub>2</sub> effectively sequestering this “greenhouse” gas rather than releasing it to the atmosphere. Some noble gas nuclides, notably <sup>4</sup>He, <sup>21</sup>Ne, <sup>40</sup>Ar, and <sup>134,136</sup>Xe, are produced in-situ in aquifers continuously over geologic time, and accumulate in measurable excess abundances. If CO<sub>2</sub> is capable of leaking as a gas either continuously or episodically, these noble gas nuclides would likely also be affected, and their full accumulation would not be observed.

**Project Description:** There are two primary methods by which the nuclides of interest to this project are produced in the subsurface, neutron nuclear reactions (<sup>21</sup>Ne, <sup>40</sup>Ar) and natural spontaneous fission of <sup>238</sup>U (<sup>134,136</sup>Xe). As a measure of the expected subsurface production of these gaseous species, two non-gaseous nuclides which are also produced by these two methods can also be measured (<sup>36</sup>Cl produced by neutron reactions, <sup>129</sup>I produced by fission). In addition, a positive correlation might also be expected between <sup>4</sup>He, produced during the radioactive decay of <sup>238</sup>U and the fission-produced nuclides, providing another measure of expected subsurface production. The approach taken in this project is to measure the relative abundances of these nuclides in geologic materials and deep saline fluids to investigate the possible usefulness of the gaseous nuclides in testing deep aquifers for leakage.

**Results:** In order to assess neutron flux in aquifers of various lithologies, and to confirm calculated fluxes based on U and Th concentrations, measurements of <sup>36</sup>Cl were made in fluids from 20 deep carbonate aquifers associated with oil production in Louisiana and Gulf of Mexico, and from deep basin-and-range aquifers in northern (2500-3000m depth) and southern Nevada (600-1000m depth). With very few exceptions, measured fluxes confirm the calculated fluxes. Low flux rates require <sup>129</sup>I/I sensitivity in the low 10<sup>-13</sup> range. This is near the common background for <sup>129</sup>I by accelerator mass spectrometry (~10<sup>-14</sup>), and required a stabilization of our analytical abilities for <sup>129</sup>I. This was accomplished this year by an enhanced beamline and adjustments to an ESA analyzer. Repeatable backgrounds of ~10<sup>-14</sup> are now available for use in this project. An assessment was also made of the relationship between <sup>129</sup>I concentrations and stable iodine concentrations in deep aquifers, based on published data. The results indicate the need for a different emanation efficiency of <sup>129</sup>I compared to stable iodine, implying preferential removal of <sup>129</sup>I. The mechanism for this removal requires further investigation pertinent to the use of <sup>129</sup>I in this project. This assessment resulted in a manuscript entitled “Numerical models for <sup>129</sup>I behavior in deep saline aquifers”, which is being prepared as a LLNL-UCRL document. Significant time was spent this year attempting to gain access to non-carbonate aquifers associated with oil production in the Elk Hills and Sacramento fields of Central Valley of California. We will continue to pursue this in FY01.

## **CONTRACTOR: LOS ALAMOS NATIONAL LABORATORY**

University of California  
Los Alamos, New Mexico 87545

CONTRACT: W-7405-ENG-36

## **CATEGORY: Geophysics**

PERSON IN CHARGE: D. R. Janecky

**Website:** <http://www-emtd.lanl.gov/bes/Program.html>

### **Fast 3D Seismic Modeling and Prestack Depth Migration Using Generalized Screen Methods**

*M. Fehler 505-667-1925, fax 505-667-8487, fehler@seismo5.lanl.gov; Ru-Shan Wu, U.C. Santa Cruz; M.N. Toksoz, Massachusetts Institute of Technology*

**Website:** <http://www-emtd.lanl.gov/bes/Program.html>

**Objectives:** To develop and test new methods based on the wave equation for modeling seismic wave propagation and processing of seismic data to obtain images of the Earth's subsurface. These methods will be used to investigate physics of wave propagation in the Earth's lithosphere and to image seismic data of importance to the petroleum industry.

**Project Description:** Modeling and migration of seismic data are among the two most important ways we learn about the structure of the earth and the effects of the structure on wave propagation. The finite difference method is the most popular method for modeling wave propagation through complex structures. This method has limitations due to the large amount of computation and memory requirements that tax even the largest computers. State-of-the-art migration techniques using the wave equation are now becoming popular as replacements for the previously used ray-based Kirchhoff approach. We have been developing a suite of methods for doing efficient and reliable wave-equation-based modeling and migration. The methods are implemented in the dual (frequency-space; frequency-wavenumber) domain and are solutions of the one-way wave equation. We have been investigating applications of these methods to modeling and migration.

**Results:** We continued work on our Rytov and Born-based methods. We extended our work to 3D and migrated portions of a numerical 3D reflection dataset. We developed a new method based on the Fourier-finite difference method, which is a dual domain solution of the one-wave wave equation. The method consists of a combination of the well-known split-step operator, which is fast and easy to implement but relatively unreliable, with an additional finite-difference calculation to improve the reliability of the overall propagator. This method works extremely well for migrating data collected over complex structures and the cost is only slightly larger than the split-step approach. We modeled regional seismic wave propagation in a random medium model of the Earth using our Rytov-based solution. For suitable description of random media, we found that ensemble-average envelopes calculated for several realizations of random media are in agreement with envelopes calculated using a theory based on a the Markov approximation. While the Markov-based approach is faster computationally, it is unable to model more realistic Earth structures. When one-way propagation

dominates seismic waveforms, the Rytov-base method may be used to investigate wave propagation in realistic Earth structures at a fraction of the computational cost of finite difference based solutions.

### **The Role of Carbon and Temperature in Determining Electrical Conductivity of Basins, Crust, and Mantle.**

*T. J. Shankland, 505-667-4907, fax 505-667-8487, shankland@lanl.gov; A. G. Duba, LLNL, 510-422-7306; fax 510-423-1057; alduba@llnl.gov; E. A. Mathez, American Museum of Natural History 212-769-5379, fax 212-769-5339, mathez@amnh.org*

**Website:** <http://www-emtd.lanl.gov/bes/Program.html>

**Objectives:** The intent of this work is to comprehend the electrical conduction mechanisms in carbon-bearing rocks and in mantle minerals to relate electrical conductivity ( $\sigma$ ) measured in the field to the nature and origin of carbon in crustal rocks and to temperature in the mantle.

**Project Description:** Electrical conductivity depends strongly on temperature  $T$  and on the presence of other phases such carbon, fluids, or ore minerals at the lower temperatures of the crust and basins. One research approach is to measure  $\sigma$  of mantle minerals as functions of temperature, orientation, oxygen fugacity  $fO_2$ , and iron content. These data supply the best models for "electrogeotherms" yet available. Another approach is to document textures of carbon in crustal rocks from basins and metamorphic zones and relate them to rock conductivity. In this case, the nature of the carbon is determined by time-of-flight mass spectroscopy, and its distribution is determined by electron microbeam techniques in the same samples used for conductivity measurement.

**Results:** Amphibolites from 4.6 and 9.1 km depth in the KTB borehole have developed extensive, interconnected networks of carbonaceous films on cracks and grain boundaries as determined by electron probe and time-of-flight secondary ion mass spectrometry. In the sample from 9.1 km depth, the carbon is almost completely elemental. In contrast, the carbonaceous matter in the samples from 4.6 km depth is a mixture of elemental carbon and simple hydrocarbons such as alkanes, and possibly C-O-H compounds. The microcracks in the 4.6 km sample also contain a retrograde micro-assemblage consisting of ferri-oxy-hydroxide, calcite, and possibly clay minerals, suggesting that the carbonaceous matter and retrograde minerals formed together at relatively high crustal levels and at a time much later than peak metamorphism. Because the carbon films likely influence the electrical conductivity of the rocks *in situ*, it is proposed that production of hydrocarbons (which are insulating materials) during retrograde metamorphism of grain boundary and microcrack carbon tends to increase the resistivity of the rocks. This chemical destruction of the interconnectivity of electrical pathways may contribute to the observed diminished electrical conductivity of the shallow crust relative to the deep crust. The paper may be seen at:

<http://146.201.254.53/publicationsfinal/articles/2000GC000081/article2000GC000081.pdf>

## Nonlinear Elasticity in Earth Materials

*P. A. Johnson, 505-667-8936, fax 505-667-8487, paj@lanl.gov; J. A. TenCate; T. J. Shankland; E. Smith; R. A. Guyer*

**Website:** <http://www-emtd.lanl.gov/bes/Program.html>

**Objectives:** Research objectives are to investigate the physical manifestations of nonlinear elasticity in rock, and to characterize nonlinear properties of rocks and other solids that exhibit similar behavior, such as compressed powdered metals and materials that are damaged. Of primary importance is determining the mechanism of nonlinear behavior, relating this quantitatively to nonlinear response, and developing and applying a holistic model describing the nonlinear response of rock over broad stress-strain-frequency ranges so that practical applications can proceed.

**Project Description:** Increasingly rapid progress is being made in the field of dynamic nonlinear elasticity of earth materials. Roughly fifteen years ago, three groups of scientists (at Los Alamos, at the Institute of Applied Physics, and the Institute of Physics of the Earth in Russia) independently initiated this research field. Early and continued OBES support has been instrumental in making it possible for this research field to flourish. Today the field of dynamic nonlinear elasticity of earth materials has recognized importance in the domains of geomaterials, materials science, and strong ground motion, and there are an ever-increasing number of researchers working within it.

Rocks display unique elastic behavior. They are extremely nonlinear, being hysteretic, possessing discrete memory, and having slow dynamics [a long term memory of strain]. Although some of these types of nonlinearities may exist in, for example, powdered metals, it is rocks where these characteristics were first observed. It is now clear that rocks are part of a large class of materials, in fact a **universality** class, that exhibit the same type of nonlinear behavior. The class of materials includes rock, damaged solids, compressed powdered metals, and we are finding others as we study more and more materials. Further, nonlinear behavior plays a central role in developing new methods with which to characterize material properties, for instance, interrogating the elastic microstructure of rock, determining if a material is damaged, or monitoring progressive damage. Nonlinear attributes of rock have important consequences on processes in the earth such as earthquake strong ground motion, reservoir subsidence, seismic wave propagation and attenuation, stress fatigue damage, hydraulic fracturing, *etc.* Our work involves developing a comprehensive theoretical and experimental framework that (1) employs static and dynamic laboratory investigation of materials to provide a macroscopic and microscopic description of the elastic state, and (2) provides for turning the microscopic description into a prescription for material properties that can be used to predict change in stress state, both static and dynamic.

**Results:** The features in an earth solid that determine its elasticity are the same features that control access by fluids, aging, chemical reaction, *etc.* (flat pores, grain contacts, cracks, *etc.*). These features commonly make up 1% or less of the total volume. Understanding how these “soft” portions of the material behave is the key to understanding how the bulk material behaves. We have discovered a remarkable tool for probing the elastically soft portion of geomaterials, called slow dynamics. Surprisingly, we have discovered that many other materials respond like earth materials in their slow dynamical behavior, including certain ceramics and metals, at the very least. Remarkably, this behavior takes place in materials that are wildly diverse in their physical, meso-geometrical and chemical makeup, *e.g.*, the strain memory of an object composed of a pearlitic steel/graphite alloy is manifest like that of sandstone, limestone, granite, concrete, and martensitic 5180 steel. In contrast, an object

composed of ordinary 5180 (mostly) pearlitic steel, for instance, exhibits no memory of dynamic wave excitation; however, if the pearlite contains even a very small crack, the macroscopic strain memory of the object, due to the crack, appears like that of the martensite, the rock, *etc.* Our group is the first ever to report such findings. We have recently discovered that this behavior originates at the nanoscale. Slow dynamics are destined to be a sensitive probe of the micromechanics of material systems, and appear to be the primary manifestation of a new universality class. The use of slow dynamics as a probe of nanoscale material properties will become a new domain of research.

### **Nonlinear Dynamics of Contaminant Transport**

*B. J. Travis, 505-667-1254, fax 505-665-3687, bjt@vega.lanl.gov; D. Yuen U. of Minnesota, 612-624-1868 ; fax 612-624-8861, davey@krissy.msi.umn.edu*

**Website:** <http://www-emtd.lanl.gov/bes/Program.html>

**Objectives:** The goal of this work is to develop multi-scale algorithms for the governing equations of flow and transport in porous media and related processes in the Earth's crust.

**Project Description:** This is a collaborative effort with Prof. David Yuen of the University of Minnesota, Geophysics Dept, to develop and apply computational models to capture interaction of fluid flow processes in the earth's crust over a range of scales. Prof. Yuen's focus is on multi-scale particle methods. My part focuses on multi-scale continuum methods, in particular, use of fractal functions in a predictive mode, *i.e.*, as solutions of governing equations in which the coefficients of the equations are fractal functions. Important properties of geologic media, such as permeability, are known to be approximately fractal over a wide range of length scales, from mm to km.

**Results:** FY2000 was the first year of this project. Fractal interpolating functions (fif) have been developed for porous media. Given a set of measurements, such as permeability, for a subsurface region, an fif set can be obtained in one, two or three dimensions. Various computational tools needed for dealing with (continuous but not differentiable in the classical sense) fractal functions have been created, namely, integrals of fractal functions and integrals of products of fractal functions, as well as fractional derivatives, over the entire domain or over sub-domains. These have been applied to simple 1-D flow and transport equations, providing solutions that capture dynamics at all scales. These results will be extended to 2- and 3-D geometries. Initial results were reported in: Travis, B.J., 2000. "Using Fractal Functions to Capture Subgridscale Dynamics in Porous Flow and Transport Numerical Models", *Computational Methods in Water Resources XIII*, pp. 849-854. Also, D. Yuen and I organized a special session at the 2000 Fall Meeting of the AGU (American Geophysical Union) on "Nonlinear Simulation and Visualization".

## Energy Transport in Space Plasma

*S. P. Gary, 505-667-3807, fax 505-665-7395, pgary@lanl.gov; URL: <http://nis-www.lanl.gov/~pgary>*

**Website:** <http://www-emtd.lanl.gov/bes/Program.html>

**Objectives:** The long-term goal of this research is to understand the flow of plasma energy in the near-Earth space environment from a small-scale point of view. The objective of this research is to use plasma theory, simulations, and data analysis to express the consequences of plasma microinstabilities as concise relationships that may be used in large-scale models of space plasmas that describe the solar-terrestrial interaction.

**Project Description:** Particle velocity distributions and parameters observed by Los Alamos plasma instruments on scientific spacecraft as well as computer simulations are used to carry out fundamental studies of plasma instabilities and associated transport in and near the solar wind, the Earth's bow shock, and the terrestrial magnetosphere.

**Results:** Our most important accomplishment in 2000 was our use of plasma hybrid simulations to yield a simple analytic expression for the rate at which proton temperature anisotropies are reduced by the electromagnetic proton cyclotron instability. This expression will permit incorporation of the consequences of this wave-particle scattering process into large-scale models of the terrestrial magnetosphere, the solar wind, and perhaps the solar corona. We have recently used Ulysses spacecraft data to show that this process should operate in the solar wind, and have used simulations to show that similar scattering of heavy ions should also take place in the corona.

## The Solar Wind-Magnetospheric Interaction

*J. Birn 505-667-9232, fax 505-665-3332; jbirn@lanl.gov*

**Website:** <http://www-emtd.lanl.gov/bes/Program.html>

**Objectives:** The goal of this research is to further the understanding of the structure and dynamics of the Earth's magnetosphere, coupled to the fast-flowing solar wind plasma on the one hand and to the ionosphere on the other.

**Project Description:** The focus of this research is the investigation of the large-scale structure and evolution of the Earth's magnetosphere, using theory, numerical modeling, and correlative studies of data from multiple sites within and near the magnetosphere (including the Earth itself as well as scientific satellites).

**Results:** Our most significant accomplishment in 2000 was a significantly improved understanding of magnetic reconnection in space plasmas, using various plasma simulation codes. Reconnection is the core process that couples the solar wind with the magnetosphere and that enables explosive magnetospheric energy releases and dynamics (substorms). The key element is a threefold embedding structure of the reconnection site, which develops when the magnetic field becomes significantly distorted by external forces. The innermost region is governed by electron inertia, which enables anomalous dissipation. The electron region is embedded in a region governed by unmagnetized ions,

while electrons become tied to the magnetic field. This ion region is embedded in an even wider region, where both ions and electrons are tied to the magnetic field and the plasma is governed by fluid-like behavior. Despite the crucial role of electrons in the dissipation, the overall dynamics is governed by ions.

### **Energetic Particle Acceleration and Transport**

*G. D. Reeves, 505-665-3877, fax 505-665-7395, reeves@lanl.gov; URL:  
<http://leadbelly.lanl.gov/reeves.html>*

**Website:** <http://www-emtd.lanl.gov/bes/Program.html>

**Objectives:** The overall goals of this project are (1) to better understand the acceleration and transport of energetic particles during magnetic storms, substorms, relativistic electron enhancements, solar energetic particle events, and other magnetospheric processes, (2) to develop empirical models of the structure and dynamics of the Earth's radiation belts and other energetic particle regions, and (3) to develop a better understanding of the space environment as a system and to better understand the effects of the space environment on spacecraft and their operations.

**Project Description:** This effort concerns the analysis of energetic particle data from a variety of US programmatic and NASA scientific satellites. Those include the series of geosynchronous spacecraft that carry Los Alamos energetic particle detectors, the GPS satellites which also carry Los Alamos energetic particle detectors, NASA's POLAR satellite, and others. The energies of the particles of interest range from keV to hundreds of MeV. The lower end of this range lies somewhat above the thermal plasma energies and is therefore sensitive to local acceleration processes such as magnetospheric substorms. The higher end of the energy range is well suited to the study of energetic particles in the earth's radiation belts and those that can penetrate the Earth's magnetic field, such as galactic cosmic rays and particles produced in solar flares. We also investigate the effects of those particles on spacecraft systems and instrumentation.

**Results:** Our most important accomplishment in 2000 was the further development of a new technique to remotely image the energetic particle populations in the Earth's magnetosphere using Energetic Neutral Atom (ENA) Imaging. The most recent result concerns the similarities and differences between energetic particle injections in geomagnetic storms and the smaller and less energetic "substorms". In other recent work we have used simultaneous measurements of the Earth's relativistic electron belts from up to 11 satellites to create time-dependent "data synthesis" models of the Van Allen radiation belts. We have also applied that technique to four different relativistic electron events, which provided the first evidence for several common, underlying characteristics of relativistic electron acceleration.

## CATEGORY Geochemistry

### Uranium Series Concordance Studies

*M.T. Murrell, 505-667-4299, fax 505-665-4955, mmurrell@lanl.gov; S.J. Goldstein, 505-665-4793*

**Website:** <http://www-emtd.lanl.gov/bes/Program.html>

**Objectives:** The goal of this project is to provide unique information on the behavior of U-series members in the environment using improved capabilities for Quaternary dating.

**Project Description:** Uranium-series disequilibria techniques are well-established and valuable tools for geochronology and geochemistry. Such measurements have typically been made by decay counting; however, there are considerable advantages in using mass spectrometric techniques. We have previously used BES funding to develop such techniques. The general goal of the current project is to apply mass spectrometric methods to answer basic questions in Quaternary dating and geochemistry. Emphasis is placed on a multi-element concordia approach. This work provides information on the recent evolution of magmatic systems and also has application to natural hazard risk assessment, paleoclimate studies, and the carbon cycle.

**Results:** A number of projects are ongoing including studies to determine: 1) the residence time of Hawaiian magmas at different stages of volcano evolution and in different settings in the same volcano; 2) the spatial and temporal evolution of travertines in central Italy and Nevada; 3) temporal and spatial evolution of MORB at the Northern Gorda Ridge, the Axial Valley of the Mid-Atlantic Ridge, and the EPR, and 4) ventilation ages for deep-ocean water, both presently and during the past glacial maximum using U-series dates for deep-sea corals.

Here we highlight our U-series dating results for ice samples. Improved radiometric dating methods for polar ice are needed to improve correlation of paleoenvironmental records from the cryosphere with other media, and for basic studies in glaciology and the terrestrial history of meteorites. Such methods would be of greatest utility for older ice deposits where radiocarbon dating or counting layers are not possible. We have applied uranium-series disequilibria techniques to age-date near-surface ice samples from Allan Hills, Antarctica, an ablation area known for its abundance of old meteorites. Prior studies (Fireman, 1986) on dusty samples based on alpha spectrometry and a recoil model for uranium series nuclides dissolved in ice suggested an old 325 ka age for ice from this area. However, our results for three Allan Hills samples failed to confirm these results based on alpha spectrometry. Our mass spectrometric data are most consistent with a young age for these ice samples, with their large U-series disequilibria inherited from precipitation. These data suggest that dating large samples of polar ice based on U-series disequilibria inherited from precipitation may be feasible. We are presently applying these techniques to date extremely dusty ice found at the base of the GISP2 ice core, thought to have an age of >150 ka based on ice accumulation models. These results should further constrain U-series techniques for dating dusty polar ice and provide valuable age constraints for a section of ice core that is not precisely dated by other techniques.

## Surface Exposure Dating in Geomorphology

*Robert Reedy, 505-667-5446, fax 505-665-4414, rreedy@lanl.gov; K. Nishiizumi, Univ. Calif., Berkeley, 510-643-9361, kuni@ssl.berkeley.edu; W. E. Dietrich, UCB, R. C. Finkel, LLNL, M. W. Caffee, LLNL*

**Website:** <http://www-emtd.lanl.gov/bes/Program.html>

**Objectives:** The production of cosmogenic nuclides in terrestrial surface samples and the use of these nuclides to date and characterize young (<1 Ma) surfaces are studied.

**Project Description:** Geological samples start accumulating cosmogenic stable and radioactive nuclides such as 0.7-Ma <sup>26</sup>Al once they are formed very near the surface or brought to the surface from depths of many meters. These nuclides are often the only way to characterize the recent surface record of such samples, such as dating when they were exposed on the Earth's surface or inferring erosion rates. To interpret the measurements of the concentrations of these nuclides in surface samples requires good rates for their production. This project uses measurements of cosmogenic nuclides in well-characterized samples plus numerical simulations using computer codes developed at Los Alamos to get better production systematics for many in-situ-produced cosmogenic nuclides as a function of target composition, elevation, and geomagnetic latitude.

**Results:** The code recently developed at Los Alamos, MCNPX, is being used in this work. Calculations made with MCNPX are being compared with measurements of cosmogenic nuclides in documented samples and calculations done with other codes.

Recently-measured cross sections for the production of these nuclides continue to be compiled and evaluated. Many of these neutron-induced cross sections are different than the proton-induced ones that were often assumed to apply for neutrons. Work is being done with Dr. J. Sisterson on measuring more needed neutron cross sections at the Los Alamos Neutron Scattering Center and other sources of energetic neutrons.

Contacts have been maintained with groups exposing artificial samples on the Earth's surface and with others measuring cosmogenic nuclides in natural samples. These measurements are being modeled using MCNPX in testing the ability of the code to model the production of in-situ-produced cosmogenic nuclides.

## Dissolution of Fe(III)(hydr)oxides by Aerobic Microorganisms

*Larry Hersman 505-667-2779; fax 505-665-6894; hersman@lanl.gov; P. Maurice, Kent State University; Garrison Sposito, U.C., Berkeley*

**Website:** <http://www-emtd.lanl.gov/bes/Program.html>

**Objectives:** Our overall objective is to determine the mechanisms of iron release during microbially enhanced iron oxide dissolution by an aerobic microorganism. The results of several of our experiments performed in our first funding cycle lead us to believe that aerobic microorganisms used a reductive dissolution process to acquire iron from hematite ( $\alpha$ -Fe<sub>2</sub>O<sub>3</sub>). We therefore proposed to use a combination of biochemical and analytical techniques to determine the compounds and conditions

responsible for the microbially enhanced dissolution. We report here the progress of our work to date, at LANL.

**Project Description:** The purpose of this research is to investigate the mechanisms used by aerobic microorganisms to obtain Fe for growth. Currently little is known about Fe oxide dissolution processes in oxic environments. Understanding these mechanisms is fundamental to a wide range of bio-geochemical processes. For example, Fe oxides sorb a variety organic and inorganic pollutants, therefore understanding the mechanisms of dissolution is important to understanding pollutant transport phenomena. Los Alamos National Laboratory is investigating the growth characteristics of a *Pseudomonas* sp. whose only source of Fe is either hematite or goethite. Additionally, we supply siderophore for siderophore-mediated investigations at UC Berkeley and provide microbially reacted, Fe oxide surfaces for AFM analysis at Kent State University.

**Results:** In aerobic environments microorganisms are faced with approximately ten orders of magnitude discrepancy between available Fe ( $\sim 10^{-17}$  M) and their metabolic requirement ( $\sim 10^{-7}$  M). In contrast to facultative anaerobic environments, where dissimilatory iron reducing bacteria (DIRB) are often abundant, few studies have detailed microbial interactions with Fe(III)(hydr)oxides in aerobic environments. In the first study, *P. mendocina* was grown in batch culture with hematite, goethite, or ferrihydrite as Fe sources. *P. mendocina* obtained Fe from these minerals in the following order: goethite > hematite > ferrihydrite, exerting  $3.2 \times 10^{16}$ ,  $3.9 \times 10^{16}$ , or  $5.5 \times 10^{16}$  cell h ( $\mu\text{mol Fe}$ )<sup>-1</sup> kcal<sup>-1</sup> to obtain the Fe, respectively. Furthermore, Fe dissolution for each of the minerals appears to have occurred in excess, as evidenced by the growth of *P. mendocina* in the medium above the sediments. These results demonstrate that an aerobic microorganism is able to obtain Fe for growth from different insoluble Fe minerals, with varying dissolution rates.

In our second set of experiments, we investigated the production of siderophore and Fe(III) reduction by a strict aerobe in the presence of synthetic hematite as a source of Fe. *Pseudomonas mendocina* grew best when Fe was supplied as FeEDTA (approximately  $1.8 \times 10^8$  CFU mL<sup>-1</sup>), grew abundantly when Fe was supplied as hematite (approximately  $1.2 \times 10^8$  CFU mL<sup>-1</sup>), and grew poorly when Fe was withheld from the medium (approximately  $5.5 \times 10^7$  CFU mL<sup>-1</sup>). As expected, negligible siderophore was produced per cell when Fe was supplied as FeEDTA and more siderophore was produced in the hematite flasks than in the controls. Thus, growth on and the production of siderophore in the presence of hematite present compelling evidence that siderophore was produced as a mechanism to acquire Fe from hematite. For the Fe reduction experiments, Fe reduction by components of the supernatant fluid was induced weakly when Fe was supplied as hematite or as FeEDTA, but much more so when the cells were cultured under extreme Fe deprivation. In fact, 16 times as much Fe reduction occurred in the controls than for either of the FeEDTA or hematite amendments. Our results provide a new perspective regarding microbial interactions with Fe bearing minerals.

## **CONTRACTOR: OAK RIDGE NATIONAL LABORATORY**

University of Tennessee-Battelle LLC  
Oak Ridge, Tennessee 37831

**CONTRACT:** DE-AC05-96OR22464

**CATEGORY:** Geochemistry

PERSON IN CHARGE: David. R. Cole

### **Volumetric Properties, Phase Relations and Reaction Kinetics of CO<sub>2</sub>-CH<sub>4</sub>-H<sub>2</sub>-H<sub>2</sub>O Fluids: Effects of Injecting CO<sub>2</sub> into Geological Reservoirs**

*J.G. Blencoe 865-574-7041, fax 865-574-4961; blencoejg@ornl.gov, L.M. Anovitz; M.T. Naney*

**Objectives:** Experiments, thermodynamic analyses, and equation-of-state (EOS) modeling are being performed to gain a predictive understanding of the geochemical behavior of CO<sub>2</sub> and CH<sub>4</sub> in deep porous and permeable rocks. Results of the research will have numerous practical applications in technologies for sequestering CO<sub>2</sub> in geological reservoirs.

**Project Description:** Experiments are conducted with binary and ternary mixtures of CO<sub>2</sub>, CH<sub>4</sub>, and H<sub>2</sub>O at temperature-pressure conditions similar to those encountered in deep aquifers, sedimentary basins, and geothermal resource areas. Volumetric properties and liquid-vapor phase relations are determined with high precision and accuracy using a unique vibrating-tube densimeter (VTD) designed for operation at 50-500°C and 5-200 MPa. The activity-composition relations of the fluids are measured using another unique facility: a hydrogen-service internally heated pressure vessel (IHPV) capable of operation at high hydrogen fugacities, with an overall operating range of 100-1100°C and 5-800 MPa. Experimentally measured thermophysical properties for fluid mixtures are modeled using theoretically based (semi-empirical) formulations. Laboratory experiments and thermodynamic modeling are closely integrated to optimize the efficiency and effectiveness of data acquisition and EOS development.

**Results:** This year important progress was made in: (i) modeling the thermophysical properties of binary, mixed-volatile fluids; and (ii) determining the upper baric stabilities of liquid-vapor assemblages in the CO<sub>2</sub>-H<sub>2</sub>O system.

Rigorous analysis of highly accurate and precise density data for CO<sub>2</sub>-H<sub>2</sub>O mixtures at 400°C, 10-400 MPa—obtained from experiments performed with our VTD—yielded a new, three-term semi-empirical (modified, B-truncated virial, or “MBV”) formulation for binary, mixed-volatile fluids. It is explicit in excess pressure ( $P^{\text{ex}}$ ), applicable over wide ranges of temperature and pressure, and can accurately represent the excess volumetric properties of binary fluid mixtures at  $P$ - $T$ - $X$  conditions close to the critical point of a pure fluid. It’s first term, derived from basic virial theory, accurately represents  $P^{\text{ex}}$  from 0 MPa to pressures where “liquid-like behavior” is first manifested. The second and third terms permit accurate correlation of volumetric data for high pressures.

The MBV EOS has numerous advantages over alternative semi-empirical models for binary mixed-volatile fluids. Because it is explicit in  $P^{\text{ex}}$  rather than  $P$ , it is used exclusively to represent the excess volumetric properties of binary fluid mixtures. The properties of the two pure-component fluids are

represented by separate and completely independent EOSs, which may be semi-empirical or empirical, and of any suitable mathematical form. Used together, the set of equations behaves as a single EOS. This “modular approach” to EOS development circumvents many of the problems encountered in modeling the behavior of strongly nonideal binary volatile fluids using a single, semi-empirical,  $P$ -explicit EOS. Finally, the MBV model can be integrated analytically to develop an expression explicit in excess Helmholtz free energy, which in turn can be used to compute other thermodynamic mixing properties of interest (*e.g.*, excess Gibbs free energies, and activity-composition relations).

Laboratory work this year emphasized acquisition of liquid-vapor equilibrium data for CO<sub>2</sub>-H<sub>2</sub>O fluids. This led to the discovery—and subsequent refinement—of a new vibrating U-tube technique for determining the upper baric stabilities of liquid-vapor assemblages in the CO<sub>2</sub>-H<sub>2</sub>O system at high subcritical temperatures (~275-360°C). In the procedure, the first step is to create an isobaric-isothermal, physically isolated and chemically homogeneous sample of “high-pressure” CO<sub>2</sub>-H<sub>2</sub>O fluid of known composition. Fluid pressure ( $P$ ) is then lowered slowly at constant temperature. Pressure readings and matching values for  $\tau$  (the period of vibration of the U-tube) are recorded at 0.1 or 0.2 MPa intervals. When the fluid begins to separate into two phases (liquid + vapor), a distinct inflection is observed in the trend of  $P$  vs.  $\tau$ . Performing such experiments for fluid compositions at 0.05 mole fraction CO<sub>2</sub> ( $X_{\text{CO}_2}$ ) intervals in the range  $0.05 \leq X_{\text{CO}_2} \leq 0.40$  at 300°C produced a complete high- $P$  liquid-vapor boundary curve for the CO<sub>2</sub>-H<sub>2</sub>O system at that temperature. Agreement with corresponding curves determined in previous studies ranges from poor to excellent.

## Fundamental Research in the Geochemistry of Geothermal Systems

*J. Horita 865-576-2750, fax 865-574-4961, horitaj@ornl.gov ; D. R. Cole*

**Objectives:** The objective of this project is to provide fundamental information on geochemical reactions that play pivotal roles in a wide range of geological processes, but that specifically impact reservoir dynamics, corrosion, and heat extraction in active geothermal systems. Kinetic and equilibrium partitioning of stable C-O-H isotopes, and other fluid-solid interactions are primary subject areas for this research.

**Project Description:** At Oak Ridge National Laboratory, a long-term basic research program in experimental hydrothermal geochemistry, stable isotope geochemistry, and igneous petrology has led to the development of unique methodologies for extracting rigorous and unambiguous information on a wide range of geochemical processes. This capability permits the efficient and definitive examination of specific problems hampering the ability to quantitatively model fluid-rock interaction processes related to the discovery and exploitation of geothermal resources. Research topics in this project are selected in close cooperation with geothermal industry representatives and are frequently augmented by parallel research on more applied aspects of the same problems funded by the U.S. Department of Energy’s Geothermal and Wind Technologies Program.

**Results** A series of hydrothermal experiments were completed to determine pressure effects on D/H isotope fractionation between brucite [Mg(OH)<sub>2</sub>] and water in the temperature of 200 to 600°C and pressures to 300 MPa (up to 800 MPa at 380°C). At all the temperatures investigated, the measured D/H fractionation factors between brucite and water increased systematically with increasing pressure,

ranging in the magnitude from 4.37‰ at 600°C to 12.44‰ at 380°C. The observed pressure effects on the D/H fractionation are more pronounced in the low-pressure range (<100 MPa) than in the high pressure range (>100 MPa). When the same results are plotted as a function of the density of pure water at experimental conditions, a good linear relation was observed at each temperature. Theoretical calculations suggest that isotope pressure effects on brucite are small, in the range of 1-2‰ at the experimental conditions, and that pressure increases to 1 kbars decreases the partition function ratios of water by 4-5‰, thus increasing combined brucite-water D/H fractionation factors by 5-6‰. These calculations agree well with those experimental results.

Similar hydrothermal experiments were conducted to examine the effect of dissolved NaCl on <sup>18</sup>O/<sup>16</sup>O isotope fractionation between calcite (CaCO<sub>3</sub>) and water at 600-800°C and at 100 MPa. Our results of fractionation factors for pure water agree well with those in the literature. Dissolved NaCl up to 5 molal was found to change little the <sup>18</sup>O/<sup>16</sup>O isotope fractionation between calcite and water at 600 and 700°C, but the results at 800°C are not conclusive yet.

### **Ion Microprobe Studies of Fluid-Rock Interaction**

*L.R. Riciputi, 865-574-2449, fax 865-576-8559, i79@ornl.gov; D. R. Cole*

**Objectives:** The objective of this research is to investigate how the microscale elemental and isotopic record, accessible using ion microprobe analysis, can be used to understand mass transfer processes occurring during fluid-rock interaction at low to moderate temperatures in the earth's crust, studying both natural and experimental samples.

**Project Description:** In this project, the ability of ORNL's Cameca 4f ion microprobe to obtain quantitative element and light (H, B, C, O, S) isotope ratio analyses with a 5-30 micron spatial resolution are being developed and applied to studies of fluid-rock interactions in a variety of settings, in both natural and experimental systems. The ion microprobe data is typically integrated with information obtained using a variety of other techniques, petrographic studies, conventional bulk gas source and thermal ionization isotope ratio analyses, electron microprobe, and fluid inclusion analysis. Primary areas of investigation include (1) use of the microscale isotope record to study mass transport during large-scale fluid-rock events, (2) determination of both diffusion rates and equilibrium water-mineral isotope partitioning factors in the O, H, and C systems, and (3) utilizing microscale isotopic and elemental disequilibrium in natural settings to study the duration of fluid-rock events.

**Results:** We have continued our study of authigenic K-feldspar and quartz cements from the Mount Simon Sandstone in the Illinois Basin (and surrounding areas) to resolve the multiple the regional events that precipitated the widespread K-feldspar and quartz cements across the mid-continent at ~400Ma. Thus far, we have analyzed over 20 samples in a 600km, south-north traverse from southern Illinois to mid-Wisconsin. Cathodoluminescence shows that there are two generations of quartz cements, but only one generation of authigenic K-feldspar. Stage 1 quartz appears texturally to be associated with the K-spar overgrowths. Average K-feldspar oxygen isotope values increase over 10‰ δ<sup>18</sup>O from the southernmost, most deeply buried sample (+14‰) to outcrop samples from the Wisconsin Arch (+24‰), with oxygen isotope values from stage-1 quartz cements displaying similar trends (23‰ to 28‰). Stage 2 quartz postdates stage 1 quartz and the K-feldspar cements. Fluid inclusion data suggests two different sets of fluids, one (early with temperatures between 60 and 100°C, and a later stage with higher (110-140°C) temperatures. Geographic trends suggest that there might be a slight

gradient (20°C total) of decreasing temperatures northward for both fluid generations. Calculated average  $\delta^{18}\text{O}$  values for stage 1 quartz and contemporaneous K-feldspar range from -2‰ in samples from the south to +8‰ in the north. Although our data is limited, stage 2 quartz suggests that  $\delta^{18}\text{O}_{\text{fluid}}$  increased from +4 to +10‰ northward. These observations suggest that there are two distinct episodes of regional fluid migration from south to north in the Illinois Basin recorded in quartz overgrowths, with widespread K-feldspar cementation associated with the first event, and that the regional gradient in oxygen isotope values is due to increasing  $\delta^{18}\text{O}$  values associated with progressive diagenetic modification. A possible source of the superheated fluids is deeply buried sediments in the Reelfoot rift.

We have made considerable progress in our study of hydration rates and mechanisms in obsidian glasses in both natural and experimental samples. Analysis of obsidian artifacts from a number of sites in Mesoamerica, hydrated for 500-2500 years under ambient conditions, all display similar relationships between hydration depth and elapsed time, although there are clear differences that correlate with average site temperature. Although we only have preliminary results from our experimental studies, they have already yielded valuable information, including (1) confirmation that diffusion rates are hydrogen concentration dependent, (2) that the process is actually hydrogenation, rather than hydration *sensu stricto*, (3) the presence of critical kinetic effects, some of which may be defect density related, and (4) that simple extrapolation of short-term experiments will yield incorrect diffusion rates and activation energies for long-term hydration processes.

Depth profiles were measured on a number of experimental run products. Hydrothermal isotope exchange experiments involving epidote+D<sub>2</sub>O, amphibole+D<sub>2</sub>O and biotite+D<sub>2</sub>O were conducted at elevated temperatures (up to 800°C) and pressures (up to 300 MPa). The diffusion coefficients for D in these phases were calculated from the fits to the inverse error function. For example, the diffusivities for epidote range from 10<sup>-17</sup> to 10<sup>-13.5</sup> cm<sup>2</sup>/s for temperatures between 200 and 600°C, respectively. A similar range in D values was determined for amphibole. The activation energy for the hydrogen exchange process was estimated to be 67 kJ/mole.

We have obtained a series of uraninite crystals that have been prepared for oxygen diffusion experiments. In addition, we obtained and begun to characterize the U-Th standard that will be used to obtain U-Th isotopic data from uraninite. Preliminary results from exchange experiments using the double capsule, buffered cold seal hydrothermal method were promising. Three 4-mm<sup>3</sup> crystals of uraninite were placed in 1mm diameter platinum capsule with 10 mg of water. The capsule was sealed and placed in a 3 mm diameter gold capsule along with Fe metal powder (buffer) and 10 mg of water. The gold capsule was also sealed and the entire assembly was placed in a cold seal bomb at a temperature of 600°C for 48 hrs. The exchange products were re-examined and showed no signs of oxidation.

We continue to try to improve the capabilities of our instrument. We are presently upgrading our oxygen primary ion source to provide a better source of O<sub>2</sub><sup>-</sup>. We have installed an upgraded Faraday cup counting amplifier and electrostatic faraday-electron multiplier switching. We are in the process of building climate controlled detector housing to improve the stability of the electronics. Although we only have preliminary results, experiments using low energy ions and our improved electron gun indicate that it may be feasible to obtain better than ±1‰ precision for  $\delta^{18}\text{O}$  measurements on <5 μm spots. These modifications promise to enhance sensitivity by increasing primary ion yields and improved precision for isotopic analyses.

## Fundamental Research in Isotopic Fractionation of Carbonate Systems Relevant Subsurface CO<sub>2</sub>-Sequestration

*J. Horita, 865-576-2750, fax 865-574-4961, horitaj@ornl.gov; D. R. Cole*

**Objectives:** The objective of this project is to understand and quantify several key reactions controlling kinetic and equilibrium isotope partitioning during the precipitation, recrystallization, and transformation of carbonate minerals (calcite, dolomite, siderite) in CO<sub>2</sub>-rich fluids at conditions encountered in various geologic settings (groundwater, deep aquifers, sedimentary basins, geothermal systems, etc). This information is needed to monitor and model large volumes of CO<sub>2</sub> injected into the subsurface.

**Project Description:** This project is currently focused on: a) mechanisms, rates, and isotopic fractionation during slow to rapid precipitation of calcite from CO<sub>2</sub>-rich solutions at low temperatures (<100°C) and b) recrystallization and replacement of calcite and dolomite in CO<sub>2</sub>-rich fluids at moderately elevated temperatures (100-300°C), both as function of several key variables (temperature, pCO<sub>2</sub>, ionic strength, microbial activity, *etc.*).

**Results:** Design and installation of a “chemo-stat” system was completed, which is used for the investigation of the kinetics and mechanisms of heterogeneous precipitation of carbonate minerals from CO<sub>2</sub>-rich aqueous fluids over a wide range of constant conditions throughout an experiment. This system was tested for its real-time monitoring and controlling capabilities of several variables (temperature, pH, select ionic concentrations) for an extended period of time (>several hours). Our preliminary results of precipitation rates of calcite in circum-neutral Na-Ca-HCO<sub>3</sub>-Cl solutions at 25°C appear consistent with those in the literature. This system is being further developed to maintain constant isotopic compositions of water and dissolved CO<sub>2</sub> during the precipitation of carbonates.

In collaboration with C. Zhang of University of Missouri, we have investigated carbon and oxygen isotope partitioning during microbial siderite (FeCO<sub>3</sub>) precipitation in the temperature range from 15 to 75°C, using several strains of mesophilic and thermophilic iron-reducing bacteria. During an early stage of incubation, Fe(III) is rapidly reduced to Fe(II) and siderite was precipitated. Then, microbial activity slowed down, and the amount of siderite appeared to stay constant or slightly decreased. <sup>18</sup>O/<sup>16</sup>O isotopic composition of siderite precipitated in the early stage from HCO<sub>3</sub>-rich (>120mM) solutions are much greater (>10‰) than expected equilibrium values, and slowly declined toward an equilibrium value with time. Thus, <sup>18</sup>O/<sup>16</sup>O isotopic fractionation in early stages appears to be controlled by kinetic processes, while <sup>13</sup>C/<sup>12</sup>C composition of siderite is very close to an equilibrium value. Different strains of bacteria didn't affect isotope fractionation. Our long-term culturing experiments resulted in <sup>18</sup>O/<sup>16</sup>O isotopic fractionation at 15-75°C in good agreement with those obtained from inorganic precipitation of siderite.

In collaboration with D. Allen of University of Minnesota, we studied kinetics and <sup>13</sup>C/<sup>12</sup>C isotope fractionation during hydrothermal conversion of dissolved CO<sub>2</sub> to formate (HCOOH) at 200-400°C and at 500 bars. Formate was formed at all the temperatures catalyzed by MgO or other solids present in the system. <sup>13</sup>C/<sup>12</sup>C ratios of formate formed are always lower than that of an initial dissolved CO<sub>2</sub> by 25‰ (200°C) to 3‰ (400°C). These fractionations are much larger than expected equilibrium partitioning between the two compounds, especially at 200°C, suggesting a kinetic isotope fractionation.

A number of preliminary 25°C experiments have been carried out to determine the C and O isotope partitioning between CO<sub>2</sub> and a variety of potential reservoir phases. The intent here is to quantify the partitioning as a function of mineral type, surface area, P<sub>CO<sub>2</sub></sub>, presence or absence of an organic phase (as might be encountered during an injection scenario involving a hydrocarbon reservoir such as in Enhanced Oil Recovery). Powders of known surface area of calcite, quartz and montmorillonite were exposed to CO<sub>2</sub> gas of varying C and O isotope composition for varying lengths of time. Different isotopically labeled CO<sub>2</sub> gases were used to see if the partitioning was reversible, which it turned out to be. These batch experiments demonstrated that in every case the “free” gas (*i.e.*, gas sampled over the solid) was isotopically enriched in both <sup>18</sup>O and <sup>13</sup>C relative to CO<sub>2</sub> sorbed onto the mineral surface. The partitioning was greatest between the CO<sub>2</sub> and the clay (roughly 4 to 8 per mil for C; 23 to 27 per mil for O), followed by CO<sub>2</sub> – calcite (roughly 2 to 3.5 per mil for C; 6 to 12 per mil for O), and finally CO<sub>2</sub> – quartz (roughly 1 to 2.5 per mil for C; 2 to 4 per mil for O).

### **Experimental studies of Hydrothermal Fluid Speciation and Fluid/Solid Interaction Employing Potentiometric Methods**

*D.J. Wesolowski, 865-574-6903, fax 865-574- 4961, wesolowskid@ornl.gov; P. Bénézech*

**Objective:** The objective of this project is to utilize ORNL’s unique, high temperature, hydrogen-electrode, pH-measurement cells and other potentiometric approaches to study aqueous reactions and water/mineral interactions relevant to DOE’s geoscience mission areas. The results find broad application in waste isolation, geothermal and fossil fuel utilization, and electrical power generation.

**Project Description:** The pH is considered the master variable in aqueous systems, controlling the nature of dissolved species, the rates of homogeneous and heterogeneous reactions, the solubility and absorbtivity of rock minerals, the transport and deposition of contaminants and ore components, the volatility of mineral acids and the thermal stability of organic acids. In this program we develop and use unique experimental facilities to directly measure the pH of aqueous solutions and the activities of important dissolved ions over broad ranges of temperature, salinity and pH, and use these measurements to quantify the dissociation constants of inorganic and organic acids and bases, the hydrolysis and complexation of metal ions in solution and the solubilities and surface adsorption properties of minerals.

**Results:** A major focus of our recent studies had been the protonation and sorption of ions on minerals surfaces at elevated temperatures, which plays a major role in mineral dissolution/precipitation kinetics and the transport of dissolved contaminants in subsurface environments. We have developed a method of predicting the protonation constants of individual surface oxygen sites on various crystal faces at elevated temperatures, using the MUSIC Model, and have experimentally calibrated the approach with rutile (TiO<sub>2</sub>) and magnetite (Fe<sub>3</sub>O<sub>4</sub>) to 290°C, and ZrO<sub>2</sub> to 150°C. We have also demonstrated that different surface morphologies lead to predicted changes in the surface protonation behavior of metal oxides, by comparing the surface charging characteristics of magnetite with a similar inverse spinel, NiFe<sub>2</sub>O<sub>4</sub>, to 290°C. In collaboration with Dr. Jeremy Fein of the University of Notre Dame, we have conducted the first studies of the surface protonation and cation adsorption (Nd<sup>3+</sup>) on bacterial surfaces ever reported at conditions above room temperature (30-75°C), using the aerobic, gram-positive species *Bacillus Subtilis* and the thermophilic anaerobe TOR-39. Finally, we have begun investigating the

sorption of aqueous anions on mineral surfaces at elevated temperatures, with investigations of the sorption of oxalate and sulfate on TiO<sub>2</sub> and ZrO<sub>2</sub> surfaces to 150°C in NaCl brines.

Using a newly developed mercury/mercurous chloride concentration cell, we completed studies on the complexation of Al<sup>3+</sup>, Fe<sup>2+</sup> and Zn<sup>2+</sup> by the sulfate anion (SO<sub>4</sub><sup>2-</sup>) in the 0-75°C range in dilute to very saline aqueous solutions. These results are needed in order to quantitatively model phase equilibria and contaminant transport in acid mine drainage, as well as soil and surface waters affected by acid rain. Our studies of the properties of organic compounds in high temperature water continued with determinations of the acid dissociation constants of morpholinium and dimethylammonium ions to 250°C in dilute to concentrated NaCl and NaTrifluoromethanesulfonate solutions. Finally, as a complement to the potentiometric methods for determining metal ion speciation and solubility in hydrothermal solutions, we have developed chemically-inert, extremely-low-flow-rate, packed-column reactors, and have used these to study the solubilities of gibbsite, zinc and nickel oxides, and ferrite/chromite spinels over a wide range of temperatures, salinities and pH's.

### **Mechanisms and Rates of Isotope Exchange in Mineral-Fluid Systems**

*D. R. Cole, 865-574-5473, fax 865-574-4961, coledr@ornl.gov; L. R. Riciputi; J. Horita*

**Objective:** The major objective of this research is to measure the rates of isotopic exchange between mineral and fluids controlled by one of two general mechanisms: surface reactions leading to recrystallization and volume diffusion.

**Project Description:** Equilibrium isotope fractionation factors and rates of isotopic exchange (via diffusion or mineral transformation mechanisms) form the cornerstones for interpretation of stable isotope data from natural systems. Microscale studies (high precision of small sample sizes or *in situ* spot analysis) of mineral-fluid interaction in natural systems indicate that: (a) isotopic heterogeneity and disequilibrium may be more widespread than previously realized, (b) isotopic disequilibrium can occur at high as well as low temperatures, (c) different minerals exhibit varying susceptibilities to retrograde fractionation and re-equilibration, and (d) the mechanisms of isotopic exchange are varied depending on the prevailing geochemical conditions (*e.g.*, temperature, pressure, fluid chemistry, fluid/solid ratio, *etc.*). Because of the recent advances in analytical techniques, the need for accurate, reliable fractionation factors and rate constants has never been greater. Realizing this need, we have focused our BES research on the experimental determination of rates and equilibrium fractionations for a variety of geologically relevant mineral-fluid (gas) systems for which data are either lacking, limited or, in some cases, controversial.

**Results:** We are conducting a study in collaboration with Dr. Ted Labotka (UTK) on the self-diffusion of C and O in calcite in the system calcite-CO<sub>2</sub> in the temperature range 600-800°C and different pressures (0.1 to 200 Mpa). This effort takes advantage of our capability to do depth profiling with the Cameca 4f ion microprobe. At 800°C we observe a pronounced decrease in the C diffusivity with increasing pressure from 0.1 to 10 MPA, the a more or less leveling off of the diffusion out to pressures of 200 MPa. This is the first time this kind of behavior has been documented for carbon in calcite in an anhydrous system. Oxygen diffusion, on the other hand, exhibits no real pressure dependency from 0.1 to 200 MPa at 800°C.

Recently, we used the ion microprobe to measure D/H profiles parallel to the  $b$  crystallographic orientation (faster direction) in epidote reacted with D<sub>2</sub>O between 200 and 600°C at 200 MPa. Similarly, we measured the D/H profiles in pargasite (calcic amphibole) reacted with D<sub>2</sub>O at 300-500°C and 200 MPa, but parallel to the faster  $c$  crystallographic direction. Preliminary activation energies for both of these experimental systems are ~16 kcal/mol. The diffusion coefficient at 500°C and 200 MPa for epidote ( $\log D = 3.98 \times 10^{-15} \text{ cm}^2/\text{sec}$ ) is 5 orders of magnitude slower than that determined from bulk exchange experiments (Graham et al., 1980). The diffusion coefficients for epidote between 200-600°C are slower than those estimated from either a plate or cylinder model using bulk exchange data (Graham et al., 1980). The diffusion coefficient at 400°C and 200 MPa for pargasite ( $6.51 \times 10^{-16} \text{ cm}^2/\text{sec}$ ) is 2 orders of magnitude slower than diffusion coefficients measured from bulk exchange experiments for amphiboles (Graham 1984). This work is being conducted in collaboration with Suman De, PhD student visiting from the University of Alberta, and his adviser, Dr. Tom Chacko.

There are numerous examples of the coupling of chemical reactions and diffusion in nature. In hydrothermally altered intermediate volcanics such as the Rico system, CO<sub>2</sub> formation of albitic/sericitic rims on plagioclase (200-1000 microns in diameter) has been observed where original grain habit (size and shape) and twinning are still preserved. These rims are well defined zones that follow closely the outline of the grain edge, or exhibit more irregular patterns that include altered areas developed on cracks that cross-cut the feldspar. Detailed microscopic and SEM observations indicate the altered zones consist of a mosaic of sub-grains generally < 10 microns in diameter. The key observation in many systems is that the rim thickness increases at the expense of the unaltered, residual grain whose effective radius decreases. Clearly, the conversion of one phase to another (plagioclase to albite) involves chemical reaction at the phase boundary with diffusion through a "porous" reaction layer. A shrinking-core model was used to estimate the amount of time needed to develop different magnitudes of rim formation, assuming spherical grain geometry. Chemical reaction rates ( $k$ ) were fixed by T, P and fluid composition (*e.g.*, pH; salinity), whereas diffusivities ( $D$ ) were fixed by P and T. Unrealistically long or short times were estimated if either rate parameter was assumed to be rate limiting. Simulation of conditions at Rico ( $T = 150\text{-}300^\circ\text{C}$ ;  $P = 100 \text{ MPa}$ ; salinity = 1 m NaCl) indicates that narrow rims (10-100's micron) formed at low T's (150-200°C) took 100,000 to 1 million yrs to develop, whereas thicker rims (up to 1 mm) formed at higher T's (250-300°C) took only 50,000 to 100,000 yrs to develop. These times represent integrated values, and do not account for cessation of fluid-rock interaction due to episodic sealing of the flow system.

### **Nanoscale Complexity at the Oxide-Water Interface**

*D.J. Wesolowski, 865-574-6903, fax 865-574-4961, wesolowskid@ornl.gov; A.A. Chialvo, D.A. Palmer, P. Bénézech, L. Liyang, W. Hamilton*

**Objective:** The objective of this project is to combine a wide range of unique capabilities and expertise at Oak Ridge and Argonne National Laboratories (P. Fenter, N.C., Sturchio), Penn State University (S. Lvov, J. Kubicki), The University of Illinois (M.L. Machesky), The University of Tennessee (P. Cummings), and Northwestern University (M. Bedzyk) in a detailed study of the molecular-level structure and properties of the mineral-water interface.

**Project Description:** The pH- and temperature-dependent charging of oxide surfaces by reaction with water, and the association of solution counterions with the charged surface, form an interfacial feature termed the electrical double layer (EDL), which results from a complex interplay of electrostatic and van der Waals forces, quantum effects, lattice strain, ion hydration and hydrogen bonding in solution, and specific binding of solute ions with the surface and one another. The nature of the EDL controls many processes at many scales, such as nanoparticle assembly and alteration, crystal growth rates and morphologies, bacterial attachment and nutrient uptake, colloid transport and flocculation, corrosion and fouling in the power, chemical and materials industries, and contaminant transport and adsorption in aquifers. It is only within the last few years that X-ray and neutron sources are becoming available that have sufficient energies and intensities to unambiguously measure the geometries and bonding environments of surface species, solution ions and solvent structures within the EDL *in situ*. To date, almost nothing quantitative is known about EDL phenomena at temperatures above 25°C. Furthermore, there have been very few truly integrated efforts to achieve a greater understanding of this critical interfacial phenomenon, combining expertise in aqueous, electrochemical, materials, X-ray, neutron and computational sciences.

**Results:** This is a new project with only limited results to date. This team proposes the following unique experimental and modeling studies, applied to a selected set of oxide phases ( $\text{TiO}_2$ ,  $\text{Al}_2\text{O}_3$ , *etc.*) and aqueous solution components (Na-Rb-Sr-Y-Sm-Cl-Br- $\text{SeO}_3$ -organic anions, *etc.*), chosen to optimize the attainment of unambiguous, quantitative information on the EDL structure and properties:

- Specific ion adsorption, pH-titration, electrokinetic, and atomic force microscopy studies on oxide powders and single-crystals (25-350°C) using unique pH and electrochemical measurement capabilities at ORNL and Penn State;
- X-ray standing wave, reflection and absorption studies on single crystal surfaces to high temperature at Argonne's Advanced Photon Source;
- Neutron reflection and small angle scattering from single crystal surfaces and colloidal suspensions to high temperature several DOE and NIST facilities, ORNL's upgraded High Flux Isotope Reactor, and ultimately the Spallation Neutron Source under construction at ORNL ;
- Quantum mechanical calculations of surface species and interactions, and large-scale molecular simulations at ORNL and Penn State, fully integrated with the experimental approaches above and recently developed temperature extrapolations of classical multisite surface complexation models.

Success in the proposed research will yield new conceptual models for, and fundamental understanding of, interfacial phenomena critical to a variety of disciplines and technologies. Integration of macroscopic and microscopic experimental results with molecular theory and simulation will permit scaling and transfer to an even wider range of systems and applications.

## **CONTRACTOR: PACIFIC NORTHWEST LABORATORY**

Battelle, PNNL  
Richland, WA

**CONTRACT:** DE-AC06-76RLO 1830

**CATEGORY:** Geochemistry

**PERSON IN CHARGE:** A. Felmy

### **Local Reactions on Carbonate Surfaces: Structure, Reactivity, and Solution**

*D.R. Baer, 509-376-1609, fax 509-376-5106, don.baer@pnl.gov; J.E. Amonette 509-376-5565, fax 509-376-3650, jim.amonette@pnl.gov*

**Objectives:** The purpose of this program is to develop a fundamental, microscopic understanding of the structure and chemistry of carbonate surfaces, including the interactions with adsorbate.

**Project Description:** This project involves an interdisciplinary theoretical and experimental effort designed to gain a fundamental, molecular level understanding of carbonate mineral surface structure and chemistry. Carbonate minerals are particularly important in the global carbon dioxide cycle and in subsurface contaminant migration processes. The availability of large single crystals allows fundamental measurements to be made on well-defined surfaces. By linking experimental studies of geochemical reactions on single-crystal surfaces with first-principles quantum-mechanical model calculations to describe the surface and interfacial structure and chemistry, a systematic study of the factors controlling the surface chemistry of carbonate minerals can be made. In particular, the effects of substitutional impurities and other point-chemical defects on the structure and geochemical reactivity of carbonate mineral surfaces and interfaces can be isolated and quantified. Moreover, this improved microscopic understanding will eventually provide insights into the behavior of these materials in natural systems.

The approach to meeting program goals involves three interdependent efforts: 1) developing *ab initio* and mechanistic models for interpreting experimental observations regarding the structure and chemistry of the calcite cleavage surfaces; 2) studying the structure and chemistry of the cleavage surface in solution and vacuum; and 3) measuring the reaction kinetics and local nano-scale surface topology during calcite dissolution using scanning probe microscopy and optical microscopy methods.

**Results:** During the past year a terrace ledge kink model was applied to measurements of the influence of various cations on calcite dissolution. The aqueous dissolution of the (10 $\bar{1}$ 4) surface of calcite had been observed at pH near 9 using an atomic force microscope (AFM) equipped with a fluid cell. The influences of carbonate (CO<sub>3</sub><sup>2-</sup>), strontium (Sr<sup>2+</sup>), and manganese (Mn<sup>2+</sup>) ion concentrations on the rates of step motion were measured. Carbonate ions were shown to have a step-specific effect on calcite dissolution. At low levels (<1  $\mu$ M) of CO<sub>3</sub><sup>2-</sup>, the retreat rate of the more structurally open [441]<sub>+</sub> steps was faster than the retreat rate of the structurally confined [441]<sub>-</sub> steps, leading to anisotropic dissolution. Increasing the CO<sub>3</sub><sup>2-</sup> level to as high as 900  $\mu$ M decreased the rate of retreat of both steps, but the [441]<sub>+</sub> step was slowed to a much greater extent changing the degree of dissolution anisotropy.

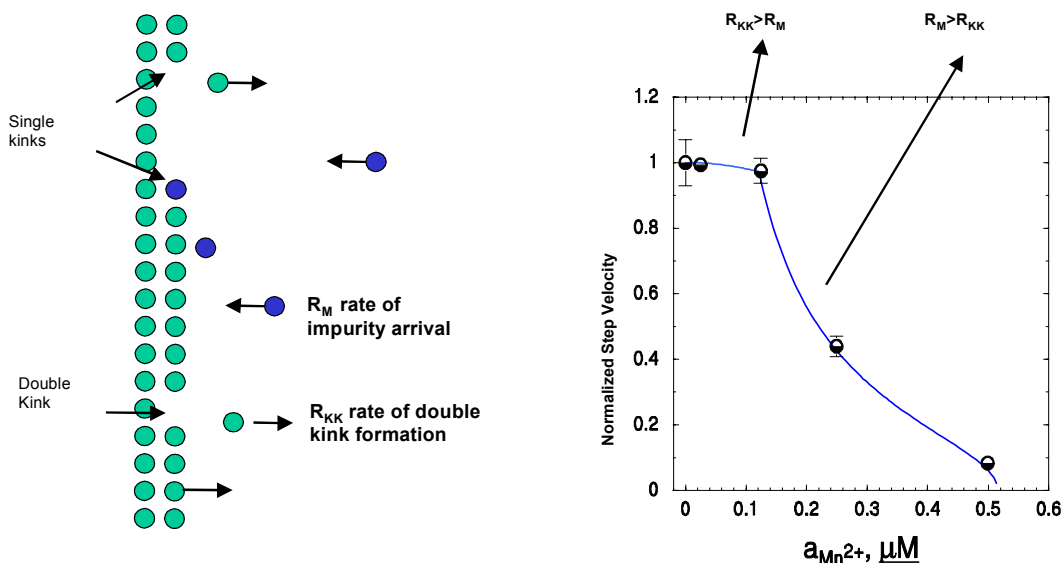
This decrease in step velocity at high  $\text{CO}_3^{2-}$  levels was attributed to a corresponding increase in the back reaction (*i.e.*, precipitation) as the solution approached saturation with respect to calcite. Strontium cations were also shown to have a step-specific effect on calcite dissolution similar to that of  $\text{CO}_3^{2-}$ . Manganese cations, on the other hand, slowed the rate of retreat of the [441]- step to a greater extent than  $\text{Sr}^{2+}$ .

The dissolution rate and etch-pit morphology are highly dependent on the presence of cationic impurities and  $\text{CO}_3^{2-}$  ions in solution. While we cannot directly determine the exact mechanisms or species involved, solution reactions and the observed concentration behaviors indicate that the changes in dissolution rate and etch-pit morphology are kinetically driven by the arrival rates of ions or ion pairs at the calcite surface. Kink propagation is retarded by adsorption of the ions or ion pairs along steps and at single-kink sites.

All of our observations can be understood by considering how “impurity” ions sorbed on kink and step sites “block” dissolution. Although there are many assumptions and approximations in the model, the essence is that the adsorbing species can both influence the formation of double-kink sites and block (or at least inhibit) the dissolution of single-kink sites. At low concentrations, retardation of double-kink formation is the dominant process. At higher concentrations, retardation of single-kink dissolution along the step is dominant. A sharp change in step-edge migration velocities is predicted at the threshold concentration where rate control shifts from double-kink formation to single-kink dissolution. This change is clearly shown in the AFM measurements of step movement [Fig. 1].

### Impurity Blocking of Dissolution at Steps on a Surface

*The major impact of impurities occurs when the rate of impurity arrival is faster than the rate of the generation of new kink sites. This is a dynamic process where impurity arrival perturbs or blocks normal dissolution events.*



The structure of the calcite water interface was studied using synchrotron based x-ray diffraction by graduate student Phillip Geissbuhler and Professor Larry Sorensen at the University of Washington and

Neil Sturchio of Argonne National Laboratory (now at Univ. of Illinois, Chicago). This work found that the surface-carbonate groups of calcite are rotated into the surface relative to the bulk structure and that water above the surface is ordered into an apparent "epitaxial" structure.

In a new series of experiments conducted in collaboration with Professor Andreas Lutge and postdoc Rolf Arvidson at Rice University, phase contrast vertical-scanning interferometry experiments were made of calcite dissolution and pit formation. Our scanning-probe measurements and the optical interferometry observations provide a complementary picture of the surface processes. While the optical measurements offer a wider field of view, the AFM observations allow higher spatial resolution and a more detailed look at the surface.

A summary of this program and other mineral and oxide related research can be found at <http://www.emsl.pnl.gov:2080/capabs/oxides/> under the heading "Program Summaries".

### **Structure and Reactivity of Iron Oxide and Oxyhydroxide Surface**

*J.R. Rustad, 509-376-3979, fax 509-376-3650; james.rustad@pnl.gov, A.R. Felmy, 509-376-4079, fax 509-376-3650; ar.felmy@pnl.gov; D.A. Dixon 509-372-4999, fax 509-376-3650, david.dixon@pnl.gov; M. Dupuis 509-376-4921, fax 509-376-0420, michel.dupuis@pnl.gov*

**Objectives:** This project is focused on developing large-scale molecular dynamics simulation methods to better understand chemical speciation at oxide-water interfaces.

**Project Description:** Through assimilation of the results of diverse experiments in surface science, aqueous chemistry, crystal chemistry and accurate *ab initio* electronic structure calculations, we are constructing a comprehensive simulation capability for oxide-water interfaces. Components of these simulations include reactive surface functional groups, sorbing anions and metals, and explicit calculation of the influences of solvent and the electric double layer. Massively parallel computer codes using this simulation model are being applied to problems having length scales of 5-10 nanometers.

**Results:** Molecular dynamics simulation of sodium perchlorate solutions (0.5-7 molal) in contact with hydroxylated magnetite (001), goethite (110) and (021), and hematite (012) have been carried out. All surfaces are basic, and accept protons from solvating water molecules resulting in a positive surface charge on the order of 100 mC/m<sup>2</sup>, leaving hydroxide ions in solution. These reactions occur very quickly within the first 10-20 picoseconds of the simulation. There is significant surface specificity: goethite (021) is protonated to approximately 50 mC/m<sup>2</sup> while goethite (110) is protonated to approximately 150 mC/m<sup>2</sup>. Singly coordinated FeOH<sub>2</sub> groups participate actively in acid-base equilibria on the surface. Despite having gas-phase acidities similar to FeOH<sub>2</sub> functional groups, Fe<sub>3</sub>OH functional groups do not undergo deprotonation reactions in solution. Their inertness results from their tendency to be "buried" more deeply into the oxide, which sterically inhibits solvent relaxation after deprotonation. Specific electrolyte binding is significant on magnetite (001), but is less well developed in the other systems. The simulation results underscore the complex behavior of the surface proton balance and suggest that surface functional groups are not simple, well-defined FeOH groups but might be better described as FeOH<sub>2</sub>...OH, with the solvated, bound hydroxide ion extending 5-10 angstroms into the double layer.

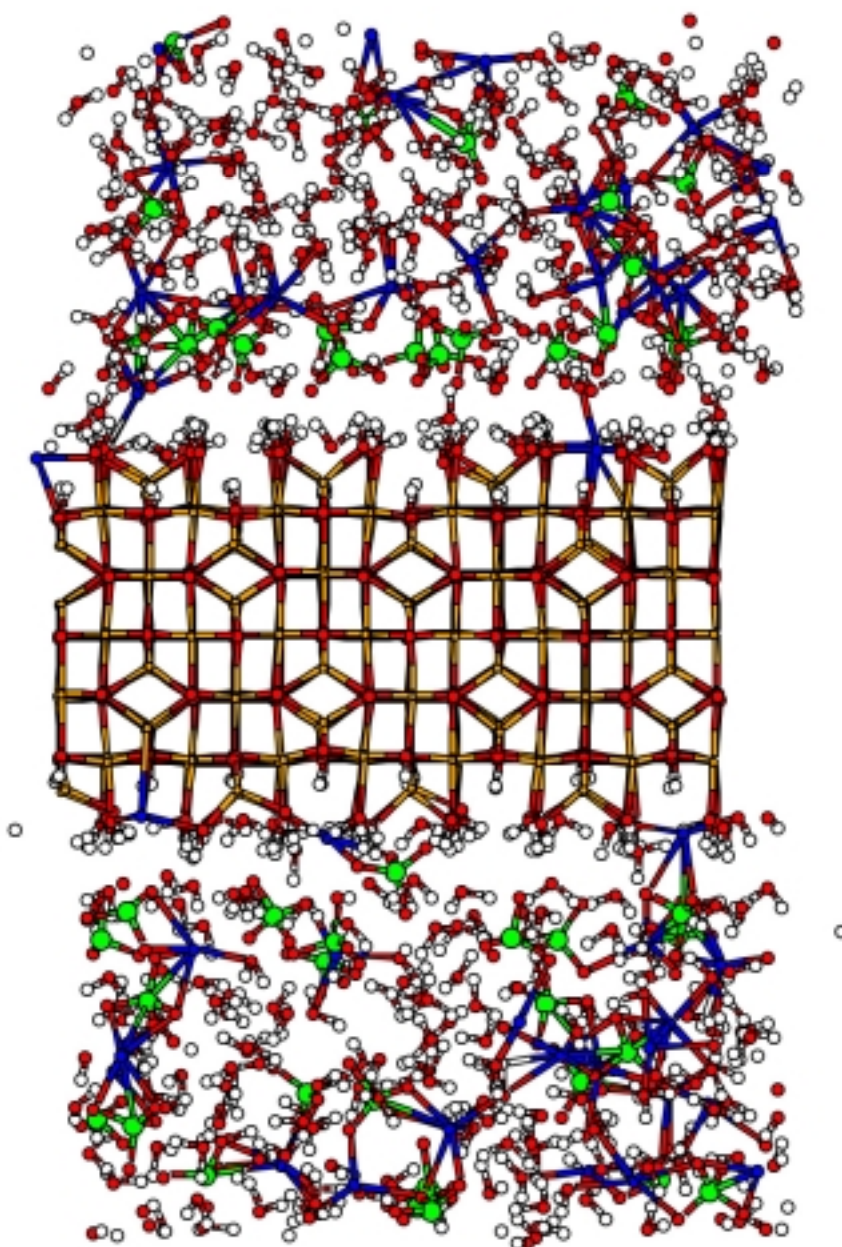


**Figure 1.** Simulated magnetite (001) surface solvated in 7 molal sodium perchlorate. Brown atoms are Fe, blue atoms are Na, green atoms are Cl, red atoms are O, and white atoms are H.

## Molecular Basis for Microbial Adhesion and Geochemical Surface Reactions in Fe-Reducing Bacteria

T.P. Straatsma 509-375-2802, fax 509-375-6631, [tp\\_straatsma@pnl.gov](mailto:tp_straatsma@pnl.gov); A.R. Felmy 509-376-4079, fax 509-376-3650, [ar.felmy@pnl.gov](mailto:ar.felmy@pnl.gov); D.A. Dixon 509-372-4999, fax 509-375-6631, [david.Dixon@pnl.gov](mailto:david.Dixon@pnl.gov); J.R. Rustad 509-376-3979; fax 509-376-3650; [james.rustad@pnl.gov](mailto:james.rustad@pnl.gov); R.D. Lins Neto 509-372-4712; fax 509-375-6631; [roberto.linsneto@pnl.gov](mailto:roberto.linsneto@pnl.gov)

**Website:** [http://www.emsl.pnl.gov:2080/docs/mssg/www\\_bio/geo.html](http://www.emsl.pnl.gov:2080/docs/mssg/www_bio/geo.html)

**Objectives:** The overall goal of this project is the development of a computational modeling capability for the study of environmentally important geochemical reactions at the outer bacterial envelope of gram-negative bacteria. Using highly scalable implementations and new advances in molecular theory and simulation this effort represents a pioneering study in complex and collective phenomena.

**Project Description:** Molecular and thermodynamic modeling methods are designed and applied to study the molecular processes that govern microbial metal binding, microbial adsorption to mineral surfaces, and microbe mediated oxidation/reduction reactions at the bacterial exterior surface. The understanding of these mechanisms is crucial in the development of successful bioremediation strategies, in particular in dealing with the technological difficulties in the transport of bacteria to the subsurface locations where they are needed.

**Results:** Lipopolysaccharides form the major constituent of the outer membrane of gram-negative bacteria, and are a key factor in microbial adhesion and metal binding. A molecular model has been developed for the rough LPS of *Pseudomonas aeruginosa*, based on Hartree-Fock SCF calculations of the complete molecule at the 6-31g\* level, followed by a restrained electrostatic potential (RESP) fitting procedure to obtain partial atomic charges. This charge model has been used in molecular dynamics (MD) simulations of the bacterial membrane, composed of a periodic layer of 16 LPS molecules exposed to the exterior aqueous environment and a phospholipid layer exposed to the periplasmic space.

The LPS membrane is held together by strong electrostatic interactions between the negatively charged phosphate and carboxylate groups and the  $\text{Ca}^{2+}$  counterions. Analysis of the MD trajectory reveals that the  $\text{Ca}^{2+}$  ions are primarily confined to a thin area (ca. 2 nm) in the inner core region of the LPS membrane (ca. 10 nm) and interact mainly with the phosphorylated sugars. The distribution of phosphate groups is split into two regions, but the  $\text{Ca}^{2+}$  distribution is fairly uniform, due to the positioning of the carboxyl groups filling the gap between the phosphate distributions. The phosphate groups bound to N-acetyl-glucosamine (NAG) sugars form the inner region and are characterized by two  $\text{PO}_4^{2-}$  groups per LPS. The second, outer phosphate-rich region is formed by heptose monomers, each contributing three  $\text{PO}_4^{2-}$  groups. Significant structural differences are found for these two regions. In the inner region, clusters of four phosphate groups are held together by  $\text{Ca}^{2+}$  ions, in which each contributing phosphate group is from a different NAG residue. In the outer region such a distinct pattern is not observed. The  $\text{Ca}^{2+}$  ion arrangement leads to a well-defined structural lower region, which correlates with the reduced mobility found for this region.

Gram-negative bacteria, such as *P. aeruginosa*, have the ability to adsorb to mineral surfaces through electrostatic interactions with the outer membrane. Electrostatic potentials calculated for the MD trajectory show well-defined regions of negative and positive charge in the membrane. The figure shows the large, negatively charged patches on the membrane surface and the positive region found in the LPS inner core. This charge distribution is a result of the distribution across the membrane of the charged groups and the  $\text{Ca}^{2+}$  ions. This finding agrees well with experimentally reported negative potential of the

rough LPS membrane surface. The MD trajectory shows these negatively charged surface patches to change shape in the fs time scale, suggesting that the membrane has a high adaptability for interactions with the environment.

### **Electron Transfer at the Fe(III) Oxide-Microbe Interface**

*J. M. Zachara, 509-376-3254; fax 509-376-3650; john.zachara.pnl.gov, J. K. Fredrickson 509-376-7063; fax 509-376-1321; jim.fredrickson@pnl.gov, Y. A. Gorby 509-373-6177; fax 509-376-1321; yuri.gorby@pnl.gov; T. Beveridge 519-824-4120; fax 519-837-1802; tjb@micro.uoguelph.ca*

**Objectives:** The project objectives are to 1.) develop an improved understanding of the interfacial mechanisms of electron transfer between dissimilatory Fe(III)-reducing bacteria and Fe(III) oxides (DIRB); and 2.) define the structural, thermodynamic, and kinetic factors that control the rate and extent of bacterial Fe(III) oxide reduction and the nature of biomineralization products formed.

**Project Description:** Research is investigating microscopic aspects of bacterial iron (III) oxide reduction using spatially-resolved synchrotron based spectroscopies, high resolution electron and scanning probe microscopies, and transmission and conversion electron Mössbauer spectroscopies. Laboratory experiments using a well studied bacterium (*Shewanella putrefaciens*), abiotic reductants (anthraquinone disulfonate, AQDS), and Fe(III) oxide films and crystallites of known face exposure and variable defect densities (ferrihydrite, hematite, magnetite) are used to investigate fundamental hypotheses related to electron transfer and biomineralization at the oxide-organism interface. Focal points of the research include: 1.) the influence of Fe(III) oxide surface structure and energy on microbiologic reduction and the nature/spatial distribution of geochemical products formed; and 2.) delineating surface and structural features of bio-reduced Fe(III) oxides that are indicative of the electron transfer process.

**Results:** Research over the past year has addressed three subjects: 1.) developing a thermodynamic model for the bio-reduction/bio-dissolution of goethite, 2.) determining the influence of electron donor to acceptor ratios on the biomineralization of 2-line ferrihydrite by DIRB, and 3.) characterizing microscopic bio-dissolution features on the surface of hematite. Results of the latter experimental campaign are described below.

We performed a series of *ex-situ* AFM experiments to probe well-characterized basal surfaces of hematite for dissolution features arising from controlled exposure to DIRB, in the presence and absence of the electron shuttle AQDS. Tabular single crystals of hematite were synthesized that exhibited well developed planar basal surfaces with layer growth features similar to those observed on natural hematites. Hematite samples were incubated with *Shewanella putrefaciens* CN32, with and without AQDS, under anoxic conditions in bicarbonate buffered medium (pH = 6.8) using lactate as the electron donor.

Using AFM, two distinct types of dissolution features were frequently observed on the basal surfaces: 1.) uniformly distributed etch pits < 500 nanometers in size, and 2.) prominent bulk defect controlled micron-scale etch pits (Fig. 1). The former were randomly distributed across atomically flat terraces and were often triangular in shape; the latter were localized at the apices of crystal growth hillocks and often

radiated outward along structurally controlled directions. Neither of these features was associated with the starting material or in abiotic controls run in parallel.

Although our results cannot categorically rule out the current cell-oxide contact model, they suggest an alternative electron transfer mechanism. The observed dissolution features on the bio-reduced tabular hematite are consistent with a surface-controlled chemical dissolution mechanism promoted by solutes rather than direct cellular contact. Electron transducing solutes of cellular origin would attack energetically unstable surface sites such as step edges or areas of localized structural strain. For the tabular hematite morphology, concentrations of the latter defects are directly related to locations of growth hillocks on the basal plane, and misfit boundaries have been shown to radiate outward along pseudo-hexagonal directions. The smaller scale random etch pits, in contrast, are consistent with point defect attack. The AFM observations clearly suggest that the microorganisms do not discriminate these types of features during surface attachment and subsequent dissimilatory Fe(III) reduction.

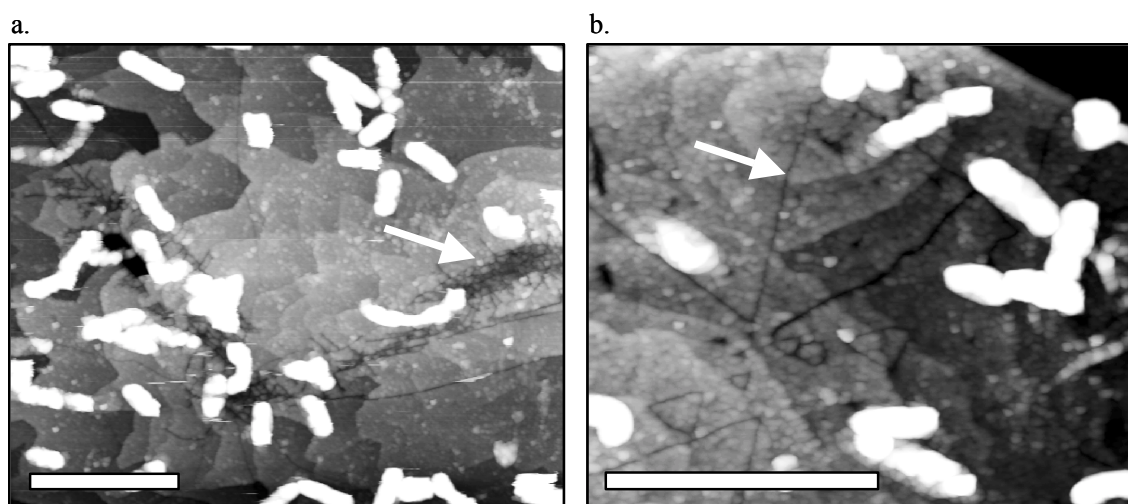


**Figure 1.** Topographic AFM images of hematite grains reduced by DIRB (Scale bars represent 4  $\mu\text{m}$ ). Cell distributions (white) did not correlate with surface microtopography. As indicated by the arrows, micron-scale etching localized at the (a) apices of growth hillocks were routinely found and (b) structurally controlled etch channels often radiating outward along what are likely misfit boundaries in the bulk structure.

**CONTRACTOR: SANDIA NATIONAL LABORATORIES**

Lockheed Martin  
Albuquerque, New Mexico 87185

**CONTRACT:** DE-AC04-94AL85000

**CATEGORY:** Geophysics

PERSON IN CHARGE: H. R. Westrich

**Forward modeling and inversion of seismic data in 3D isotropic elastic media**

*D. F. Aldridge, 505-284-2823, fax 505-844-7354, dfaldri@sandia.gov; N. P. Symons*

**Objectives:** Develop numerical algorithms for simulating seismic wave propagation within three-dimensional (3D) isotropic elastic media. Utilize these algorithms for modeling borehole seismic data acquired at Bayou Choctaw Salt Dome, Louisiana. Develop full waveform inversion algorithms for estimating subsurface 3D isotropic elastic parameter distributions from observed seismic data.

**Description:** Inversion of full waveform seismic data is a large-scale, nonlinear, geophysical inverse problem. A successful attack on this problem requires robust computational tools for simulating realistic seismic data from a prescribed earth model. The general inversion procedure entails iteratively refining a candidate earth model until an acceptable match is obtained between predicted (*i.e.*, computed) and observed seismic data. In the case where the earth is adequately approximated as an isotropic elastic medium, updates to the mass density  $\rho$  and Lamé parameters  $\lambda, \mu$  (alternately, elastic wavespeeds  $\alpha, \beta$ ) are calculated on a 3D spatial grid on each iteration. Imposition of model regularization constraints (*e.g.*, smoothness) restricts the non-uniqueness associated with the problem, and allows noisy data to be examined.

**Results:** A seismic wave propagation algorithm appropriate for 3D isotropic elastic media has been developed and is undergoing continual improvement. The algorithm is based on the velocity-stress equations of linear elastodynamics, a system of nine, coupled, first-order partial differential equations. An explicit, time-domain, finite-difference numerical scheme solves this system for the three components of the particle velocity vector and the six independent components of the stress tensor on a 3D spatial grid.

Significant computational resources are required to execute this algorithm. In order to treat realistic-sized earth models (*e.g.*, tens of millions of spatial gridpoints) and trace durations (*e.g.*, tens of thousands of timesteps) within reasonable execution times, parallel versions of the algorithm have been developed and sited on appropriate computational platforms.

Synthetic seismograms replicating borehole seismic data acquisition experiments conducted at Bayou Choctaw Salt Dome in Louisiana have been computed. These are a reasonable match to the field recorded data, although with reduced spectral bandwidth. Computational modeling yields greater understanding of the various geological and geophysical factors influencing the strength, character, and even existence, of salt flank reflections. In particular, accurate modeling of amplitudes and waveforms

of shear reflections requires the introduction of anelastic attenuation/dispersion into the synthetic seismogram algorithm.

Linear algebraic equations for the iterative updates to an isotropic elastic earth model (*i.e.*,  $\delta\rho$ ,  $\delta\lambda$ ,  $\delta\mu$ ) have been derived from the reciprocity principle of continuum mechanics. Computational implementation of these updating equations, via both serial and parallel algorithms, is currently underway.

### **Three Dimensional Transient Electromagnetic Inversion**

*G. A. Newman, 505-844-8158, fax 505-844-7354, ganewma@sandia.gov; D. L. Alumbaugh, University of Wisconsin-Madison*

**Objectives:** This project seeks to develop a three-dimensional imaging capability for transient electromagnetic fields in a manner similarly developed for seismic wavefields for high resolution imaging of the subsurface. Specific applications considered include the characterization of DOE hazardous waste sites and nuclear waste repositories and monitoring of sequestered CO<sub>2</sub> in gas depleted reservoirs.

**Project Description:** The objective of this project is to develop a full 3D inversion capability for transient electromagnetic fields. Although the development of practical multidimensional TEM inversion methods are just beginning, seismic imaging techniques have advanced the idea of back propagating or migrating the wavefield into the earth in order to image the subsurface. By applying a similar concept for electromagnetic fields, an imaging algorithm will be developed, which employs a conjugate gradient search for an optimal solution. This algorithm will be governed by the diffusive Maxwell's equations and is efficiently implemented by back propagating the data residuals into the model. To achieve realistic model complexity, the algorithm will use finite difference methods for computing predicted data and cost functional gradients. Parallel computing platforms will also be utilized for reasonable computation times. Finally, the algorithm will be tested on TEM data acquired over hazardous waste sites and nuclear waste repositories. It will also be used in an experiment design to determine its resolving power for monitoring the sequestration of CO<sub>2</sub> in gas-depleted reservoirs.

**Results:** Implementation of the 3D finite difference modeling code on single processor workstations is now completed. This code solves the diffusive Maxwell equations, in the presence of the air-earth interface, using explicit time stepping scheme and has been checked for a range of simple earth models. A borehole version of the code, which neglects that air-earth interface condition, is also available. This later code is now being employed in an experiment design study to access the applicability of TEM method for monitoring sequestered CO<sub>2</sub>. A non-linear conjugate gradient solution, using the finite difference code, is also under development and will employ back propagation to efficiently compute functional gradients. Parallelization of this code and of the finite difference solution mentioned earlier remains to be implemented.

For high-resolution TEM imaging, monitoring of the transmitter waveform is a necessity. Because the nature of current system induced in the ground depends on the transmitter turn-off time, and because an accurate inversion scheme requires a detailed knowledge of the current distribution at all times, having an accurate knowledge of the transmitter waveform will be crucial to the success of the project. To

address the question of transmitter stability and waveform monitoring, we have been employing a Zonge nanoTEM system at the University of Wisconsin to test a computer controlled ‘virtual oscilloscope’ acquisition system produced by Pico-systems. The oscilloscope has a minimum sampling interval of 20ns which is fast enough for TEM systems that would be employed in a sequestration monitoring scenario, and it allows for the ‘captured’ waveform to be written directly to lap-top computer memory. Initial testing has yielded interesting results as preliminary surveys have shown that the transmitter waveform can change significantly depending on the subsurface characteristics of the site under investigation. In this case we tested the system over two different locations, one of which is known from a magnetometer survey to have significant amounts of metal present. The transmitter at this second site was shown to produce a significant negative side lobe in the waveform in its effort to turn off the source-current when compared to the first site. Thus, it appears that transmitter monitoring will be required for accurate 3D inversion.

### **Micromechanical Processes in Porous Geomaterials**

*J. T. Fredrich, 505-844-2096, fax 505-844-7354; fredrich@sandia.gov; Teng-fong Wong, State University of New York at Stony Brook*

**Objectives:** This project focuses on the systematic investigation of the microscale characteristics of natural earth materials, and how these micro-scale characteristics control the macroscopic deformation and transport behavior. The research uses an integrated approach consisting of experimental rock mechanics testing, quantitative 2D and 3D microscopy and statistical microgeometric characterization, and theoretical and numerical analyses. The objective is to enhance fundamental understanding of failure and transport processes in geologic materials, and thereby strengthen the theoretical basis for the application of laboratory results to various technological operations of importance.

**Project Description:** Knowledge of the microscale characteristics and behavior of rocks is important for several energy-related applications, including global climate change and carbon management; oil field geoscience; geotechnical engineering efforts such as design and assessment of geologic nuclear waste repositories; and environmental remediation efforts at contaminated DOE and/or DoD installations. We use an integrated approach consisting of experimental rock mechanics testing, quantitative microscopy, and theoretical and numerical analyses. The experimental investigation provides a detailed understanding of the microstructure of geologic materials and how the microscale characteristics affect macroscale behavior including brittle failure and fluid transport. Detailed and quantitative microstructural studies complement laboratory rock mechanics experiments. The results are used to formulate and evaluate theoretical and numerical models of rock deformation and fluid flow.

**Results:** (1) The sensitivity of numerical lattice Boltzmann pore-scale fluid flow simulations to image segmentation was assessed quantitatively. The 3d confocal image data are gathered at 8-bit resolution and typically 10-15% of the voxels contain a mixture of solid and void phase. We compared two global and one local segmentation scheme. Additionally, a numerical framework was developed to allow the raw unsegmented image data to be mapped directly onto the LB flow simulation using a new formulation that we term the method of partially saturated computational cells. (2) In collaboration with Prof. Kohlstedt at the Univ. of Minnesota, we are performing 3d lattice Boltzmann flow simulations to

calculate the permeability of partially molten mantle rocks using binarized image data from serial sectioning. This is a unique application of our modeling capability as the permeability of the system of interest can only be assessed through numerical simulation. (3) Microscopy studies were performed to elucidate the micromechanics of compaction in an analogue reservoir sandstone. The microscopy, that included quantitative stereological measurements, suggested that compaction of this weakly cemented sandstone under a triaxial load path was accommodated in two distinct stages. The first stage of compaction was associated with breakage of the minimal cement bonding the framework grains and subsequent rotation of the intact framework grains to yield a more compact grain packing. This stage reduced the macroporosity by an estimated 27%. The second stage of compaction was associated with intense grain comminution and subsequent rotation of the grain fragments and resulted in substantial additional reduction in porosity and bulk volume. (4) Laboratory data for the reservoir formations at the Lost Hills Oil Field, California were analyzed using a new cap plasticity model that captures the transition from compaction to dilatation that occurs as the load path moves through the cap yield surface and approaches the shear failure surface. (5) Synchrotron microtomographic experiments were performed at the APS on pristine and deformed samples of Castlegate sandstone. Several data sets were acquired at 1.7 and 3.4 micron resolution that included both multiple data sets acquired from a single sample, as well as multiple data sets from a single volume but at different resolutions. Data are being analyzed quantitatively to characterize the microgeometry.

### **The Role of Fracture Intersections in the Flow and Transport Properties of Rock**

*H. Stockman, 702-363-5822, fax 702-363-5822, stockman3@earthlink.net; S. Brown of New England Research; A. Caprihan of New Mexico Resonance*

**Objectives:** The purpose of the modeling is to extend the range of the experiments, by varying conditions (*e.g.*, fracture junction offset) that are difficult or impossible to vary in the laboratory. In addition, by providing detailed maps of concentration and velocity variations, the modeling elucidates the causes of enhanced mixing (*i.e.*, deviations from predictions of planar fracture models), and determines experimental times necessary to achieve steady-state conditions.

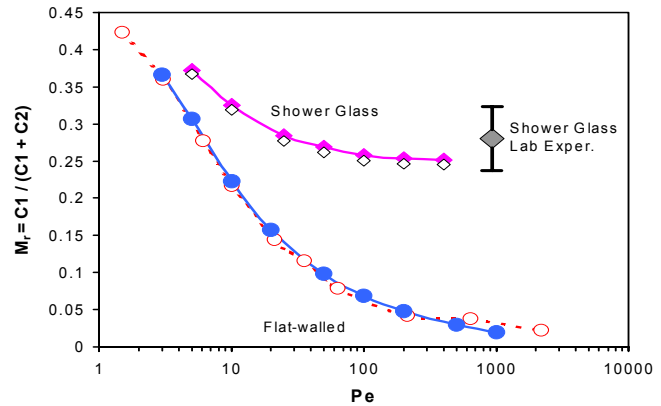
**Project Description:** In the 8 months since the previous report, a much better match to experimental results has been achieved, in part by using experiments with well-known geometries. The new experiments are constructed with panes of textured glass, much like the rippled glass in a shower door. In addition, the efficiency and flexibility of the codes has been greatly improved, and to date, several hundred mixing calculations have been completed. Three new computer systems were added to the network, to cut calculation time, including a 1.4 GHz Pentium 4 system with 1 GB RAM.

**Results:** The mixing ratio  $Mr = C1/(C1 + C2)$ , where  $C1$  and  $C2$  are the concentrations at the outlets of flow at the intersection of right-angled fractures. We have recently focussed on the effects of Peclet and Reynolds number ( $Pe$  and  $Re$ ). A recent paper by Kosakowski and Berkowitz (Geophysical Research Letters, 1999) proved that inertial effects could significantly alter flow patterns at intersections. In addition, these authors speculated that the inlet conditions, and the size of the inlet channels for numerical models, had strong effects on the apparent  $Mr$ . Typically, experiments use  $Pe$  and  $Re$  that are much higher than those observed in the field, and numerical models must be of finite size and must approximate experimental inlet conditions, so the accuracy of the extrapolation to field conditions is of

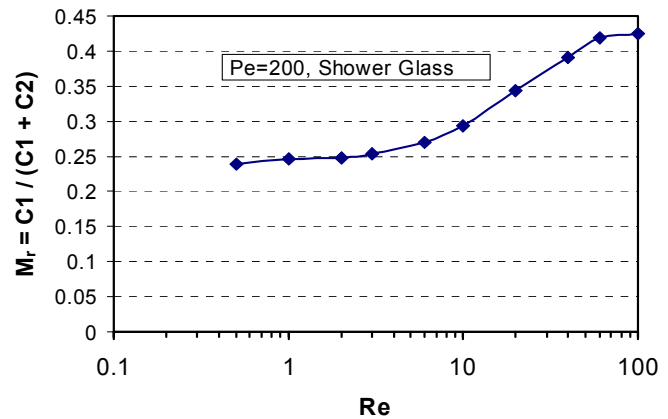
great concern. The study by Stockman *et al.* in 1997 (Geophysical Research Letters) showed that the dependence of  $M_r$  on  $Pe$  could be quite significant for flat-walled fracture intersections. However, the significance for the rough intersections, found in nature, was unknown.

The dependencies of the  $M_r$  on  $Pe$ , for both rough (shower glass) and flat-walled intersections, are compared in Figure 1a. The dashed line represents previous LB calculations (Stockman *et al.*, 1997) for a 2D LB code and the simple wrap boundary condition. Variation with  $Pe$  is much less dramatic for the rough, shower-glass geometry; furthermore, the variation becomes small at  $Pe > 50$ , suggesting lower  $Pe$  are adequate to model experimental results obtained  $Pe \sim 10^3$ . Agreement with the experimentally determined  $M_r$  is reasonably good. The  $M_r$  for a model with no bounding side walls (open diamonds) is  $\sim 98\%$  of  $M_r$  for the default geometry (filled diamonds), suggesting that the presence of sidewalls has little effect for such rough fractures. For the flat-walled fracture, agreement with results from the previous 9-vector, 2D code is quite good, with the small discrepancies at higher  $Pe$  attributable to the differences in inlet conditions and  $Re$ .

1 a



1 b



1 c

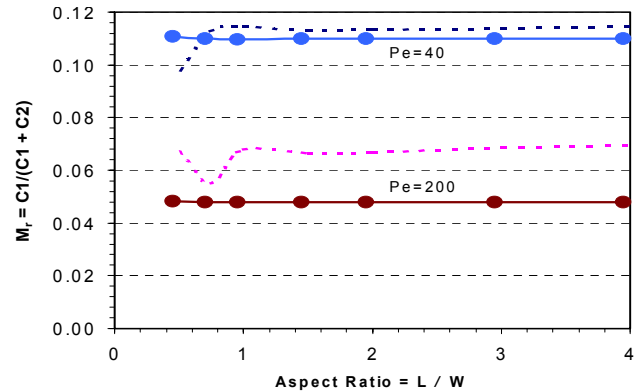


Figure 1b shows the calculated effect of  $Re$  on the  $M_r$ , for the "shower glass" intersection models. For the highest  $Re$  used in our experiments ( $\sim 10$ ), the effect is not that significant. The calculated effects of using different inlet conditions, and different inlet channel lengths, for a flat-walled intersection are shown in Figure 1c. The aspect ratio  $L/W$  is the length/width of the inlet and outlet channels for the simulation; the dashed lines represent the simple wrap boundary condition described by Stockman *et al.* (1997), and the solid lines represent the more realistic mass-flow condition we currently use. For both inlet conditions, the effects of the  $L/W$  are quite small, provided  $L/W > 1$ , and for the mass-flow condition, the effects are completely insignificant. Overall, our current results support the accuracy and

appropriateness of the LB models, as well as the extrapolation of experimental results to lower Pe and Re.

### **Continuum and Particle Level Modeling of Concentrated Suspension Flows**

*L. Mondy 505-844-1755; fax 505-844-8251, lamondy@sandia.gov; A. Graham, Texas Tech University; M. Ingber, University of New Mexico*

**Objectives:** The purpose of this program is to combine experiments, computations, and theory to make fundamental advances in our ability to predict transport phenomena in concentrated, multiphase, disperse systems, particularly when flowing through geologic media.

**Project Description:** The proposed research will elucidate the underlying physical principles that govern concentrated multiphase systems in areas essential to continued progress in geosciences. In order to be of use in real world applications, significant enhancements to currently available continuum-level suspension flow models will be required. We will use both experimentation and high performance computing to obtain microstructural information that is necessary to the development and refinement of the continuum models. For example, we expect to use this microstructural information to gain insight into the physics of particle interactions and particle sedimentation, which are particularly important in sand control issues found in petroleum production. Further, we expect that continuum-level modeling could eventually be directly implemented in codes currently used to predict hydraulic fracturing operations in the petroleum industry. The understanding gained about the physics of multiphase flows will, however, have much broader application in geosciences.

**Results:** The continuum models originally developed by Phillips *et al.*(1992) and Nott and Brady (1994) have been extended to account for normal stress contributions in general three-dimensional flows. The Phillips-type model currently also allows for non-neutrally buoyant particles and non-Newtonian suspending liquids. However, we have found that without the enhancement of the suspension flow model with an anisotropic flow tensor, the results for the non-Newtonian suspending fluid are qualitatively incorrect in some cases. Experimental measurements based on nuclear magnetic resonance (NMR) imaging were taken to test our theory that effects of a shear-thinning suspending fluid are also influenced by the particle-induced normal stress contributions. For Newtonian suspending liquids, we have concentrated on modeling viscous resuspension of a settled bed of particles -- a phenomenon important in many geologic flows. Although the model works extremely well for most flows influenced by gravity, numerical instabilities appear when the particle concentration, and hence the viscosity, changes abruptly. A porous Brinkman source term that will slow the flow depending on the particle volume fraction is known to be a more robust approach to phase-change than that of solely ramping the viscosity. Therefore, such a source term was implemented in our model. Preliminary results showed promise in minimizing numerical instabilities.

In addition, massively parallel computing has allowed particle level simulations, based on the boundary element method (BEM), with up to a thousand particles. These simulations were used to determine the magnitude of the normal stresses developing from particle interactions. They are continuing to be used, as well, to develop more accurate hindered settling functions for particles interacting with other types of particles or in a porous medium. These simulations lead to detailed information on individual particle and fluid motion that is unobtainable through experiments. In addition, a multipole-accelerated boundary element method (BEM) has been developed to simulate many thousands of individual interacting particles. Three-dimensional simulations are now possible for dynamically interacting particles.

## **Transport Visualization for Studying Mass Transfer and Solute Transport in Permeable Media**

*L. Meigs, 505-844-2375, fax 505-844-4426, lcmeigs@sandia.gov, R. Haggerty, Oregon State University and C. Harvey, Massachusetts Institute of Technology*

**Objectives:** This research seeks: (1) to determine when the small-scale permeability structure causes solute spreading to be dominated by classical dispersion and when it causes solute spreading to be dominated by mass transfer; and (2) to understand how time-scales of mass transfer depend on physical, quantifiable characteristics of the geologic medium.

**Project Description:** Theoretical work is being conducted to define regimes of transport based on quantifiable measures such as dimensionless numbers. A portion of this theoretical work (and associated experiments) is focused on determining the conditions under which physical mass transfer (*i.e.*, diffusion into immobile zones) is significant, and to developing models for predicting the effects of mass transfer over long time scales. The numerical simulations are coupled with laboratory experiments using transmitted light, x-ray absorption, and conventional breakthrough curves to test and further understand the regimes of transport. Within the mass transfer regime, the geometries of flow and transport parameters that lead to multiple rates of mass transfer and scaling of transport processes are being evaluated.

**Results:** In order to map the regimes of transport, a method was developed for generating random hydraulic conductivity ( $K$ ) fields that have highly connected flow paths or barriers, which have been found to be critical to understanding the regimes of transport. These fields share the same low-order statistics as multigaussian fields (mean, variance and covariance function), but have very different flow and transport characteristics because they are highly connected. Specifically, the results show that 2D hydraulic conductivity fields with the same basic spatial statistics, but different degrees of connectedness, may produce: (1) effective conductivities that are significantly above or below the geometric mean, (2) solute transport behavior that is best modeled through Fickian dispersion or behavior that is better modeled as rate-limited mass transfer, and (3) mass transfer that is driven that by either diffusion or advection. This work demonstrates that standard characterizations of heterogeneity may not capture the flow and transport characteristics of all aquifers.

A series of laboratory experiments are being designed to allow us to evaluate our understanding and predictions about the regimes of transport. These transport experiments are being conducted on thin chambers filled with glass beads using transmitted light to spatially map solute concentrations. Breakthrough concentrations are also being measured. Prototype experiments conducted within the mass transfer regime have enabled us to refine our experimental design.

## Effects of fluid flow on inelastic deformation and failure in dilating and compacting rock

W. A. Olsson, 505-844-7344, fax 505-844-7345; [waolss@sandia.gov](mailto:waolss@sandia.gov); D. J. Holcomb

**Objectives:** One of the proposed strategies for mitigation of carbon dioxide emissions is the sequestration of CO<sub>2</sub> in depleted oil or gas reservoirs. For the implementation of this strategy, it is critically important to understand how production of the original contents of the reservoir has changed the stress and deformation states and the properties of the rocks making up the reservoir trap. For example, certain low-permeability deformation structures, such as shear and compaction bands, may compartmentalize a hydrocarbon reservoir before or during production. Thus, inelastic deformation resulting from tectonic stress or stresses created during production of oil or gas, or reinflation with CO<sub>2</sub>, may produce structures that interfere with fluid migration and make the reservoir unattractive as a potential producer of oil and gas or repository of CO<sub>2</sub>.

**Project Description:** We are applying coordinated experimental, theoretical, and numerical techniques to the problem through an existing university-national laboratory collaboration. J. W. Rudnicki at Northwestern University, is addressing the theoretical and numerical aspects; and W. A. Olsson and D. J. Holcomb at Sandia National Laboratories are designing and carrying out the experimental part of the program. Deformation experiments are being performed on porous sandstone characteristic of oil and gas reservoirs. There are three main objectives of this work: (1) Illuminate the phenomenology of dilatant/compactive rock containing pore fluid in the drained and the undrained response, and test predictions of current theory. Triaxial compression experiments on Castlegate sandstone (porosity = 28%) under certain conditions lead to nonuniform compaction. We wish to better understand the dynamics of the compaction process in these experiments and to determine the parameter space over which nonuniform compaction occurs. (2) Collect the appropriate constitutive data constrained and suggested by developing theoretical models. Because porous rock is known to have a cap on the yield surface, this is being addressed especially with regard to its relation to nonuniform compaction. (3) Design well-posed experiments that can be used as validation tests against a numerical implementation of the theory to be developed as part of this research, for example, a new theoretical analytical model, developed in this project, concerning conditions for nonuniform compaction (Issen and Rudnicki, *JGR*, 105, 21,529-21,536, 2000) will be compared to results from our experimental program.

**Results:** We instrument cylinders of Castlegate with 14 acoustic transducers and subject them to triaxial loading at 20 to 80 MPa initial confining pressure and deform them along constant mean stress or constant shear stress paths. These stress paths allow the separation of the effects of inelastic volume strain from inelastic shear strain. More accurate determination of the shear failure curve and the failure cap is achieved this way. Acoustic emissions (AE) are monitored continuously throughout the experiments, and then locations of the events are determined. During triaxial loading, near peak stress, one or two narrow tabular zone(s) of AE events, perpendicular to the the maximum compression direction, invariably appear near one or both ends of the cylinder. These zone(s) move toward the center of the specimen with increasing applied axial strain, and can be forced to coalesce by continuing to shorten the specimen. Detailed microscopy on several scales shows that the rock behind the AE zones is highly compacted by severe and extensive grain breakage. We interpret these moving zones of AE events to be the boundaries between compacted and uncompact material. Therefore, compaction of the specimens occurs nonuniformly by the initiation and slow propagation of compaction fronts into the uncompact material. This led to an analysis of the dynamics of nonuniform compaction in terms of very slow moving shocks.

Fluid flow measurements have been made axially across the specimens during several experiments. The apparent permeability dropped dramatically upon formation of the band(s), and then continued to decrease steadily with propagation of the band(s). Total change in apparent permeability as the AE zones traverse the specimen is about 2 orders of magnitude. Complicating the analysis of this type of experiment is the addition to the applied flow rate of water being squeezed from the compacting regions.

### **Investigation of Permeability Upscaling**

*V. Tidwell 505-844-6025, fax 505-844-6023, vctidwe@sandia.gov; J. Wilson, New Mexico Institute of Mining and Technology*

**Objectives:** Experimentally investigate permeability upscaling for a variety of geologic materials, interpreting the measured permeability upscaling in light of the physical characteristics of the porous medium and the measurement characteristics of the sampling instrument. Specific objectives during this period are to (1) investigate and model the effects of non-uniform flow, local-scale anisotropy/heterogeneity, and non-Gaussian permeability distributions on permeability upscaling, (2) quantify measurement characteristics of the minipermeameter and incorporate them into models of permeability upscaling, and (3) extend physical investigations of permeability upscaling by testing rock types not well represented in current data base.

**Project Description:** Porous media flow and transport data is collected at a variety of scales, and then integrated into models at an even different and larger scale. Upscaling is used to translate the data to model effective media properties. A laboratory investigation of permeability upscaling is being conducted with the use of a novel minipermeameter test system. It allows precise, rapid, non-destructive measurement of permeability over a range of different sample supports (*i.e.*, sample volumes). By varying the size of the minipermeameter tip seal, measurements spanning five orders of magnitude on a per-volume basis are made subject to consistent boundary conditions and flow geometry. Thousands of measurements on multiple faces of meter-scale blocks of rock are collected with each of five different tip seals (0.31 - 5.08 cm ID) plus a single large tip seal (15.24 cm ID) designed to integrate over the entire sampling domain. This process is repeated on multiple rock samples, each of which exhibit different textural and structural characteristics. Key summary statistics are calculated from the data sets and analyzed with reference to their corresponding sample support. The measured data are then interpreted with the assistance of theory and simulation.

**Results:** Over 200,000 permeability measurements, associated with six different sample supports, have been collected from four rock samples: a planar bedded sandstone, a sandstone exhibiting nested scales of cross-stratification, a densely-welded tuff and a poorly-welded tuff. For each rock sample and each summary statistic investigated (*e.g.*, mean, semivariogram), distinct and consistent upscaling trends were measured. Rocks of similar genetic origin (*e.g.*, tuffs) were found to exhibit similar statistical and upscaling characteristics, while rocks of differing origin (*e.g.*, tuffs *vs.* sandstones) exhibited distinct differences. The noted differences can largely be attributed to variations in the physical attributes (*i.e.*, spatial patterns, correlation length scales) characterizing the individual rock samples. Quantitative interpretations were pursued through comparisons drawn with theoretical upscaling models, each differing according to key fundamental assumptions. Results indicate that the non-uniform flow geometry imposed by the minipermeameter and the local-scale (*i.e.*, at or below the smallest scale of

measurement) heterogeneity are key processes influencing the measured permeability upscaling. Using image analysis we compared the permeability measurements and a wide variety of objective textural measures drawn from the corresponding digital (visual) images. There was no significant direct correlation despite the obvious resemblance of the permeability maps and visual images for each rock. This may have implications for geophysical characterization methods. Linear filter analysis was employed to characterize instrument sample support (*i.e.*, effective size of the sample support and the spatial weighting of heterogeneities comprising that support) associated with each measurement. We continue to collect and analyze additional data on new and old samples, including eolian sandstones and carbonates.

To better interpret upscaling results we studied the details of the gas minipermeameter measurement method using numerical and analytical mathematical models. We derived solutions for the flow field under various conditions of media heterogeneity, and developed an adjoint state method for theoretically determining the instrument's spatial filter function. The function shows great sensitivity to the permeability just below the inner tip seal radius, and a lower but still significant sensitivity to the permeability just below the outer tip seal radius. The function is proportional to the square of fluid velocity, a previously unreported observation for any instrument. In a recent collaboration with Fred Molz of Clemson University, we offer a simple explanation for this observation. We also calculated Green's Functions for the flow field, which are being used to derive stochastic perturbation solutions for minipermeameter flow in a stochastically heterogeneous rock sample.

We took a 30 by 30 by 2.5-cm thick slab of cross-stratified Massillon sandstone, characterized it with detailed permeability measurements with different tip seal sizes, x-ray measurements of porosity, and visual image analysis. We then saturated the slab with water and ran sodium-iodide tracer through the slab longitudinally. Break-through curves (BTCs) were constructed from effluent sampling, and two-dimensional digital images of the solute concentration fields at selected times during the tracer experiment were acquired using X-ray absorption. The tracer behavior was strongly influenced by the nested scales of heterogeneity in this rock sample, exhibiting even the influence of individual lamina in the cross-beds.

### **The Physics of Two-Phase Immiscible Fluid Flow in Single Fractures and Fractured Rock**

*R. J. Glass, 505-844-5606, fax 505-844-6023, rjglass@sandia.gov; H. Rajaram at University of Colorado, Boulder; M. J. Nicholl, Oklahoma State University*

**Objectives:** Employ detailed physical experiments and high-resolution numerical simulations to develop a quantitative understanding of the critical processes controlling two-phase flow and transport in fractures. Fundamental understanding may subsequently be abstracted for application to large-scale problems in petroleum extraction, isolation of hazardous or radioactive waste, remediation of subsurface contaminants, and CO<sub>2</sub> sequestration.

**Project Description:** Under two-phase immiscible flow conditions, fluid flow and solute transport characteristics of the fracture are controlled by the geometry of the respective phases. In turn, phase geometry is determined by a combination of aperture variability, phase accessibility, capillary and viscous effects associated with the two-phase flow processes themselves, and external forces such as

gravity. In addition, if one of the fluids is slightly soluble in the other, mass transfer between the phases will influence phase geometry.

In this collaborative project between Sandia National Laboratories, Oklahoma State University, and the University of Colorado at Boulder, systematic physical experimentation is coupled with concurrent numerical simulation to explore the factors controlling phase geometry, flow, transport, and inter-phase mass transfer in rough-walled fractures. A high-resolution light-transmission technique has been developed to allow accurate experimental measurements (aperture, phase geometry, solute concentration) in transparent analog fractures. Use of this technique will lead to data of unprecedented accuracy for evaluating current understanding of fundamental processes, and motivate refinement of theoretical concepts.

**Results:** Evaluation of data from a previous field experiment in which infiltration was followed by excavation of the rock mass shows complicated behavior in an unsaturated fracture network that is consistent with recent laboratory investigations in single fractures. Short term ponded infiltration (36 minutes) into the dry network (impermeable matrix) produced viscous dominated flow near the infiltration surface, with a transition to unsaturated conditions at shallow depth (~2-3 m); phase geometry within the excavated rock mass changed from pervasive to complicated, exhibiting evidence of fragmentation, preferential flow, fingers, irregular wetting patterns, and varied behavior at fracture intersections. Electromagnetic Resistance Tomography performed during infiltration confirms rapid penetration, followed by equally rapid drainage of the network following infiltration. Estimates suggest that ~85 to 99% of the fluid slug escaped the excavated area; hence the actual penetration depth could have been quite large.

The occurrence of random and non-unique behavior during measurement of two-phase constitutive properties in fractures or porous media was investigated by visualizing micro-scale phase displacement processes during equilibrium retention and transient outflow experiments. In both cases, the drainage process is shown to be a mixture of fast gas fingering, and slower gas back filling. Each of these micro-scale processes is controlled by: the size and the speed of the applied boundary step, the initial saturation and phase geometry, and small-scale heterogeneities. Because the micro-scale processes combine to yield macro-scale behavior, the same controls will influence measured effective properties, thereby calling into question current definitions for constitutive properties.

Detailed numerical exploration of the continuum-scale Richards equation with standard monotonic constitutive relations shows it to be inadequate for simulation of unsaturated flow in initially dry, highly nonlinear, and hysteretic media (such as fractures) where gravity-driven fingers occur. Recent published reports of finger-like numerical solutions with nonmonotonic profiles are found to be artifacts of the downwind averaging method that are generated by the combined effects of a truncation error induced oscillation at the wetting front and capillary hysteresis.

Micro-scale phenomena were observed to control macroscopic behavior during surfactant flood mobilization and solubilization of nonaqueous phase liquids (NAPLs) within a fracture. At relatively low capillary numbers ( $N_{ca} < 10^{-3}$ ), surfactant mobilization floods resulted in higher NAPL saturations than for similar  $N_{ca}$  pure water floods. These differences in macroscopic saturations are explained by differences in micro-scale mobilization processes. Solubilization of the residual NAPL remaining after the mobilization stage of the surfactant flood was dominated by the formation of micro-scale dissolution fingers, which produced nonequilibrium macro-scale NAPL solubilization. A macroemulsion phase also was observed to form spontaneously and persist during the solubilization stage of the experiments.

Dissolution of NAPLs in variable-aperture fractures couples fluid flow, transport of the dissolved NAPL, interphase mass transfer, and the corresponding NAPL-water-interface movement. Each of these fundamental processes is controlled by the variability of the fracture aperture and the geometry of the entrapped NAPL. Development of a depth-averaged computational model of dissolution that incorporates the small-scale processes controlling dissolution precludes the need for empirical mass-transfer coefficients. Implementation of an efficient algebraic multigrid algorithm for solving the flow and transport equations allows dissolution simulations at scales ( $> 2 \times 10^6$  nodes) much larger than the scale of the largest regions of entrapped NAPL. Direct comparison of a dissolution experiment to a simulation suggests that this coupled depth-averaged approach to modeling dissolution accurately predicts the evolution of NAPL-mass and NAPL-distribution within the fracture.

## **CATEGORY: Geochemistry**

PERSON IN CHARGE: H. R. Westrich

### **Atomistic Simulations of Clay Minerals and Their Interaction with Hazardous Wastes: Molecular Orbital and Empirical Methods**

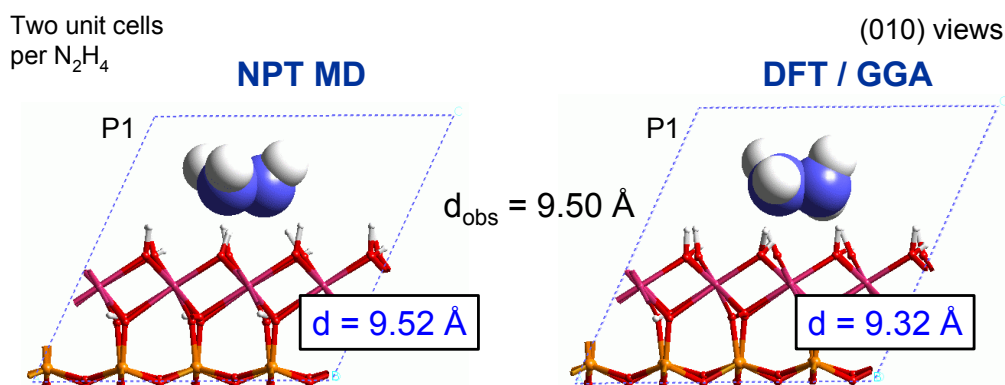
*R. T. Cygan, 505-844-7216, fax 505-844-7216, rtcygan@sandia.gov*

**Objectives:** Examine the interaction of selected metal ions, anions, and organic contaminants on the external and interlayer surfaces of clay minerals using molecular orbital and empirical simulation methods. The computer simulations will improve our understanding of the fundamental mechanisms of adsorption processes and may help to predict and optimize environmental approaches for the mitigation of hazardous waste.

**Project Description:** Modeling of clay and clay-fluid systems combine energy minimization and molecular dynamics methods using both molecular cluster and periodic system representations of the bulk clay minerals, their external and interlayer surfaces, and the interacting fluids. One set of modeling techniques uses an empirically derived forcefield to describe the energy of all atomic interactions. Bulk structures, relaxed surface structures, and intercalation processes are evaluated and compared to experimental and spectroscopic findings for validation. More sophisticated calculations incorporate state-of-the-art quantum methods that complement the empirical models. *Ab initio* approaches based on density functional theory (DFT) are used to examine the electronic structure of various clay minerals. Massively parallel computers provide the capability to obtain fully optimized periodic structures for large unit cell structures typical for clay minerals. Electron density distributions, deformation maps, HOMO/LUMO extents, and electrostatic potentials are used to evaluate the crystallographic control and mechanisms for contaminant sorption. This project is being performed in collaboration with Andrey G. Kalinichev (University of Illinois), R. James Kirkpatrick (University of Illinois), Jian-Jie Liang (Molecular Simulations Inc., San Diego), and Kate Wright (Royal Institution of Great Britain).

**Results:** A molecular mechanics forcefield that was developed for modeling hydrous phases was used to simulate the bulk structure of various clay phases, and to examine the swelling behavior of two

smectite clays (montmorillonite and beidellite). In addition, simulations of the intercalation of hydrazine ( $N_2H_4$ ) in kaolinite ( $Al_2Si_2O_5(OH)_4$ ) were performed to better assess the experimental and spectroscopic data from Los Alamos National Laboratory (David Bish) and Purdue University (Cliff Johnston). Results indicate the occurrence of strong hydrogen bonding between the hydrazine and the interlayer surfaces of kaolinite (see Figure). Rather than having one of the hydrazine hydrogens penetrate the siloxane hexagonal cavity as originally proposed, the intercalated kaolinite can comfortably situate the hydrazine with the N-N bond sub-parallel to the clay layers. Molecular dynamics results are in excellent agreement with observation, and with the more costly quantum approach based on density functional theory using the generalized gradient approximation. The quantum approach provides theoretical structures that are also in excellent agreement with known refinements. Related modeling efforts have determined the surface structure and energetics for the primary cleavage surface of calcite, magnesite, and dolomite, under both dry and fully saturated surfaces. These simulations provide a surface and interface model that agrees with the synchrotron results obtained by Neil Sturchio at the University of Illinois at Chicago.



## PART II: OFF-SITE

### GRANTEE: AMERICAN MUSEUM OF NATURAL HISTORY

Department of Earth and Planetary Sciences  
New York, NY 10024

**Grant :** DE-FG02-92ER14265

#### **The Influence of Carbon on the Electrical Properties of Crustal Rocks**

*E.A. Mathez, 212-769-5379, fax 212-769-5339, mathez@amnh.org ; A. G. Duba, LLNL, 510-422-7306, fax 510-423-1057; alduba@llnl.gov, T. J. Shankland, 505-667-4907, fax 505-667-8487, shankland@lanl.gov*

**Objectives:** The intent of this work is to comprehend the electrical conduction mechanisms in carbon-bearing rocks and in mantle minerals to relate electrical conductivity ( $\sigma$ ) measured in the field to the nature and origin of carbon in crustal rocks and to temperature in the mantle.

**Project Description:** Electrical conductivity depends strongly on temperature and on the presence of other phases such carbon, fluids, or ore minerals at the lower temperatures of the crust and basins. One research approach is to measure  $\sigma$  of mantle minerals as functions of temperature, orientation, oxygen fugacity  $fO_2$ , and iron content. These data supply the best models for "electrogeotherms" yet available. Another approach is to document textures of carbon in crustal rocks from basins and metamorphic zones and relate them to rock conductivity. In this case, the nature of the carbon is determined by time-of-flight mass spectroscopy and its distribution determined by electron microbeam techniques in the same samples used for conductivity measurement.

**Results:** Amphibolites from 4.6 and 9.1 km depth in the KTB borehole have developed extensive, interconnected networks of carbonaceous films on cracks and grain boundaries as determined by electron probe and time-of-flight secondary ion mass spectrometry. In the sample from 9.1 km depth, the carbon is almost completely elemental. In contrast, the carbonaceous matter in the samples from 4.6 km depth is a mixture of elemental carbon and simple hydrocarbons such as alkanes, and possibly C-O-H compounds. The microcracks in the 4.6 km sample also contain a retrograde micro-assemblage consisting of ferri-oxy-hydroxide, calcite, and possibly clay minerals, suggesting that the carbonaceous matter and retrograde minerals formed together at relatively high crustal levels and at a time much later than peak metamorphism. Because the carbon films likely influence the electrical conductivity of the rocks *in situ*, it is proposed that production of hydrocarbons (which are insulating materials) during retrograde metamorphism of grain boundary and microcrack carbon tends to increase the resistivity of the rocks. This chemical destruction of the interconnectivity of electrical pathways may contribute to the observed diminished electrical conductivity of the shallow crust relative to the deep crust. The paper may be seen at:

<http://146.201.254.53/publicationsfinal/articles/2000GC000081/article2000GC000081.pdf>.

## **GRANTEE: ARIZONA STATE UNIVERSITY**

Center for Solid State Science  
Box 871704  
Tempe AZ 85287-1704

**Grant:** De-FG03-94ER14414

### **A Sims Study of the Chemical Dynamics of Organic/Inorganic Interactions in Sedimentary Basins**

*Richard L. Hervig 602-965-3107; fax 602-965-9004; richard.hervig@asu.edu; Lynda Williams 602-965-5081, fax 602-965-8102, lynda.williams@asu.edu*

**Objectives:** Microanalyses of oxygen and boron isotopes in authigenic silicates are being obtained to determine their variation in hydrocarbon-producing sedimentary basins. These analyses can be used to constrain mass transport processes occurring during diagenesis and hydrocarbon migration.

**Project Description:** Our research for the last project period focussed on understanding the B-isotope systematics of clay minerals, specifically illite/smectite (I/S), during burial diagenesis, and how it related to changes in O-isotopes. Experiments to measure equilibrium isotope fractionation during the reaction of smectite to illite were lengthy (4-5 months each). The fractionation results determined between the I/S and water were found to be co-linear with high temperature experiments that measured silicate melt/hydrous fluid boron isotope fractionation. These data were used to construct a new B-isotope fractionation curve for silicates. The B-isotope fractionation curve was applied to hydrocarbon reservoirs in the U.S. Gulf Coast and Alberta basins, and in the Cretaceous Pierre shale of Colorado where contact metamorphism induced mineralogical reactions comparable to diagenesis. These applications revealed that the new fractionation data successfully predicts the B-isotopes of clays in a wide range of geologic settings. This allows estimates of paleofluid chemistry to be made.

**Results:** The newest results come from a re-interpretation of the illite-forming experiments reported last year. We had initially found that boron isotope equilibrium was not approached until 4-5 months after the start of the experiment. However, we found that we could re-expand the experimental run products by glycolating them (similar to earlier illite synthesis experiments). The expanded clays were then washed in a mannitol solution. This process removed boron from the expanded interlayer, and the resulting clay was analyzed by SIMS for B and boron isotopes. With the interlayer boron removed, we analyzed only boron substituting in the tetrahedral layer. The results show that the boron content and isotopic composition of clays reach equilibrium in a matter of days (Fig 1). During the experiments, partial collapse of the clay trapped boron in the interlayer, generating artificially high B contents and a boron isotope ratio strongly influenced by the fluid. Only during R3 ordering was the interlayer B excluded from the mineral.

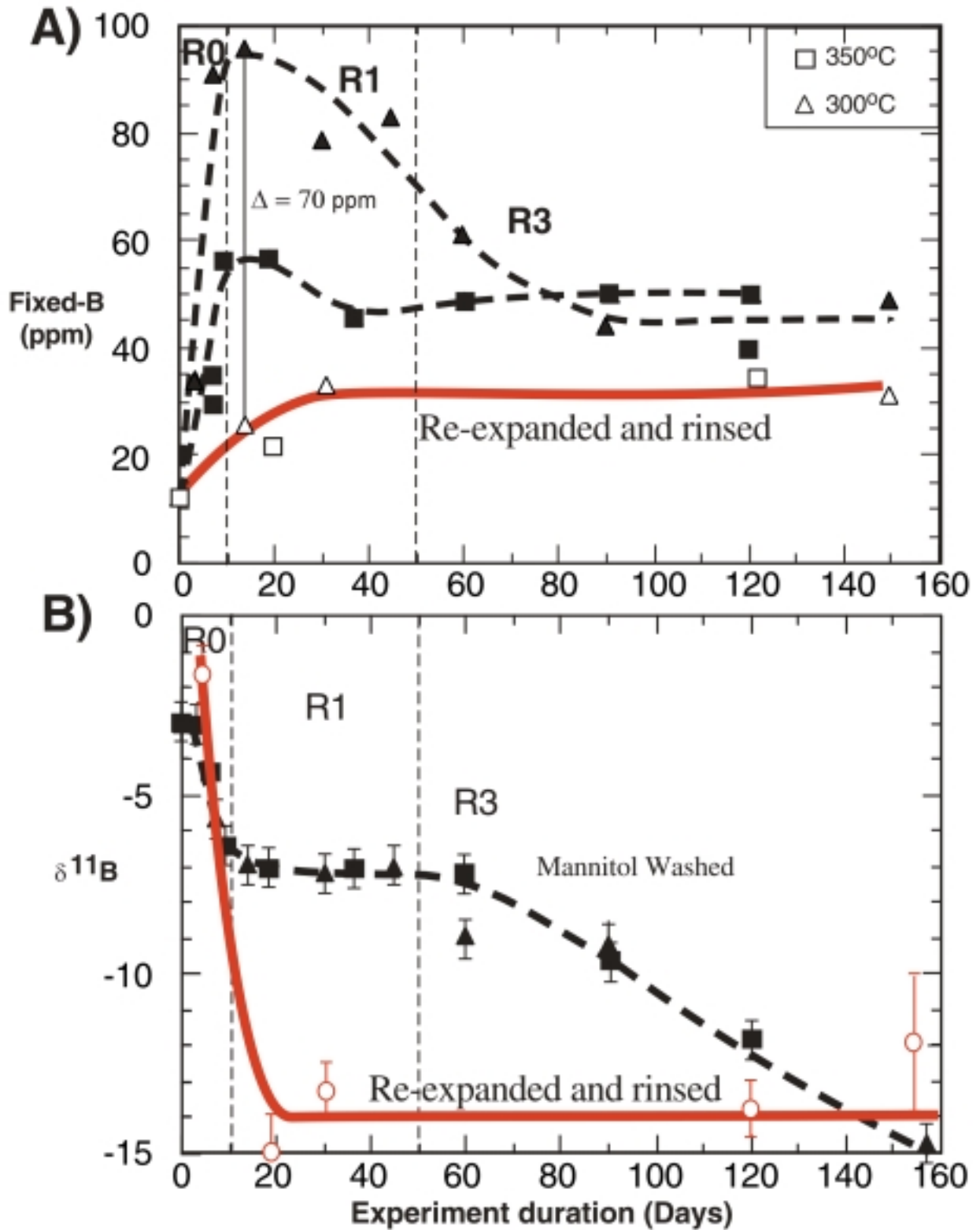


Figure 1 Experimental results showing trends in B-content (A) and  $\delta^{11}\text{B}$  (B) before (dashed) and after (solid line) re-expansion of the I/E interlayers to remove trapped boron.

## **GRANTEE: BOSTON UNIVERSITY**

Department of Physics and  
Center for Computational Science  
590 Commonwealth Ave.  
Boston MA 02215

**Grant:** DE-FG02-95ER14498

### **Analysis and Interpretation of Multi-Scale Phenomena in Crustal Deformation Processes: Using Numerical Simulations of Complex Nonlinear Earth Systems**

*W. Klein, 617-353-2188, fax 617-353-9393, klein@buphy.bu.edu; John B. Rundle, Univ. of Colorado, 303-492-5642, fax 303-492-5070, rundle@cires.colorado.edu*

**Objectives:** To develop a physical understanding of the origins of geodetic crustal strains in non-linear geomechanical systems, to examine the patterns and correlations that occur in these systems and to use these patterns to forecast the future activity that may produce disasters that affect a wide variety of critical energy facilities.

**Project Description:** The complex earth system generates a variety of phenomena that are highly non-linear and operate over a broad range of spatial and temporal scales. Signatures of these processes include scaling (fractal distributions), global and local self-organization, intermittancy, chaos and the emergence of coherent space-time structures and patterns. We are using massively parallel simulations to model geodynamical effects observed in earthquake systems in order to determine the origin of these phenomena. These investigations and the theoretical efforts done in parallel are particularly aimed at quantifying the limits of predictability for disasters such as earthquakes that occur within the earth system. We are currently continuing our development of the theoretical and computational tools that allow us to both obtain sufficient data on realistic models and to analyze the data we obtain. From these simulations, we will then predict geodetic and other deformation associated with impending earthquakes to be tested against Global Positioning System, Synthetic Aperture Radar, seismicity and other field data.

**Results:** We have made significant advances in several areas. These include: 1) The application of the theoretical model we have developed to derive and or calculate known properties of fault systems. This includes the calculation of the power law increase of Benioff strain observed prior to characteristic earthquakes and the derivations from our model of the rate and state friction laws. 2) We have made additional advances in understanding long-lived patterns that are exhibited by fault systems. Analysis of these patterns has led to a greater understanding of the relation between events on connected faults and how this impacts forecasting. It has also provided additional support for the critical point model of main events in a shock sequence. 3) We have extended our understanding of earthquake fault models. This has taken two forms. First we have analyzed the moment scaling and found a richer structure than was initially suspected and we have extended our investigations to a wide range of models and have identified several variables which when varied strongly modify the observed phenomena.

## GRANTEE: CALIFORNIA INSTITUTE OF TECHNOLOGY

Division of Geological and Planetary Sciences  
Pasadena, California 91125

**Grant :** DE-FG03-85ER13445

### **Infrared Spectroscopy and Stable Isotope Geochemistry of Hydrous Silicate Glasses**

*E. Stolper 626-395-6504, fax 626-568-0935, ems@expet.gps.caltech.edu; S. Epstein 626-395-6100, epstein@gps.caltech.edu*

**Objectives:** The focus of this project is the application of experimental petrology, infrared spectroscopy, and stable isotope geochemistry to problems in petrology and geochemistry, with particular emphasis on the behavior of magmatic systems and variations of CO<sub>2</sub> content and isotopic composition in the atmosphere.

**Project Description:** *Part 1* of this project has as its focus the determination of oxygen isotope fractionations between CO<sub>2</sub> gas, olivine mineral, and silicate melts. It involves experimental determinations of oxygen isotope fractionation in CO<sub>2</sub> vapor-silicate melt systems and in olivine-silicate melt systems. *Part 2* is the study of the isotopic compositions and concentrations of CO<sub>2</sub> and H<sub>2</sub>O in the air in the Los Angeles area. One-liter samples have been collected in evacuated glass bulbs every one to two days, purified by vacuum extraction techniques, analyzed for concentration by manometry, and analyzed for isotopic composition by conventional gas-source mass spectrometry. The data are compared with a set collected here in 1972-73, as well as with the NOAA-CMDL network data, and with air pollutant data from the South Coast Air Quality Management District.

**Results:** *Part 1:* During the last year, we have used the technique developed the previous year to perform experiments at 1250 and 1400°C on a Na-melilite melt, which is an analogue for basaltic melt. The experiments have been performed in a vertical tube furnace, through which flows a continuous stream of CO<sub>2</sub> having a known isotopic composition. Using starting Na-melilite with different oxygen isotope compositions, we have achieved reversal experiments supporting the interpretation of our results as equilibrium fractionations. The results of reversal experiments at 1250°C show convergent time-variation fractionation between CO<sub>2</sub> gas and Na-melilite melt to a constant plateau reached after ~1 day and likely equal to the equilibrium fractionation. A constant value is also observed after 7 hours of exchange at 1400°C. Using starting Na-melilite with different Na content (8 to 17 wt.% of Na<sub>2</sub>O), we have been able to demonstrate that the Na content of the soda-melilite glass does not have a significant effect on oxygen isotope partitioning. Consequently, the oxygen isotope fractionation between CO<sub>2</sub> and Na-rich melilite melt ranging from 8 to 17 wt.% of Na<sub>2</sub>O is 2.7±0.3‰ and 2.3±0.3‰ (±2σ) at 1250 and 1400°C, respectively. These results are in agreement with, but more precise than the range expected for CO<sub>2</sub>-basalt based on extrapolations of experimental data and empirical calculations in the literature.

*Part 2:* We have collected 1-liter samples every one to two days for over two years on the Caltech campus and compared our results for CO<sub>2</sub> concentrations and isotopic compositions with a set of data collected during 1972-73 in a similar location. Excellent correlations between concentration and δ<sup>13</sup>C confirm that the area has had an increase in CO<sub>2</sub> concentration accompanied by a lightening of the heavy endmember (clean air). Both of these observations reflect the increased amount of fossil fuel combustion products that have been added to the atmosphere in the past 26 years. Unlike the seasonal variations in CO<sub>2</sub> concentrations that have been observed at sites at our latitude dominated only by

oceanic influences, the data for the Caltech campus show very little seasonal variation, perhaps because the pollution effects overwhelm it. Indeed, we observe significantly higher overall concentrations and lighter isotopic compositions than the oceanic sites, consistent with this model. Candidates for the “pollutant” end member include automobile exhaust, exhaust from burning natural gas, and human breath exhalation. The trend for the air samples in Pasadena very closely corresponds to automobile exhaust. The temporal pattern of the CO<sub>2</sub> data for the Caltech campus show very good correlation with NO<sub>2</sub> data from Los Angeles County’s Air Quality Management District for sites ranging from Hawthorne, near the ocean, to Pomona, well inland of Pasadena, demonstrating that we are not observing local conditions. We have found that collecting samples close to the ground introduces scatter due to the respiration and photosynthesis of ground vegetation. Much less scatter is observed when samples are collected on the roof of a three-story building.

We have obtained an infrared CO<sub>2</sub>-H<sub>2</sub>O analyzer, which is continuously collecting concentration data, allowing us to address more questions, such as diurnal variations and variations with location, since the analyzer is portable. We have started to study effects of different weather patterns, such as Santa Ana winds and the common marine layer. The marine layer creates a unique pattern in the diurnal variations observed, virtually eliminating the overnight increase in CO<sub>2</sub> concentration observed on clear nights. This change could be due to the dissolution of the CO<sub>2</sub> in the fog, removing it from the air, or the dilution of the CO<sub>2</sub> produced on the land, by the respiration of the plants, by clean, marine air.

## GRANTEE: CALIFORNIA INSTITUTE OF TECHNOLOGY

Division of Geological and Planetary Sciences  
Pasadena, CA 91125

**Grant:** DE-FG03-88ER13851

### Isotope Tracer Studies of Diffusion in Silicates and of Geological Transport Processes Using Actinide Elements

*G. J. Wasserburg 626-395-6139, fax 626-796-9823, isotopes@gps.caltech.edu*

**Objectives:** The initial aims of this project have not been modified.

**Results:** Over the past year we have completed two studies of Os concentration and isotopic composition in rivers from the Himalayan uplift and in hydrothermal fluids from the Juan de Fuca Ridge. Both of these studies have been published. We have completed a study of paleo-climate in Soreq Cave, Israel, and have expanded our studies of the transport of U-Th through riverine and estuarine environments. We are completing two studies of weathering and transport in the vadose in two very different environments—one a tropical regime with a deep laterite profile and the other a northern arboreal forest with only a thin weathering zone. We have begun a new study of U-Th in aquifers with low water velocity.

- 1) The first of the Os papers (Sharma *et al.* 1999) demonstrated that the major rivers draining the Himalayan uplift cannot be responsible for the increase in  $^{187}\text{Os}/^{188}\text{Os}$  over the past 20 Ma. It was also argued that a Himalayan source for the  $^{87}\text{Sr}/^{88}\text{Sr}$  increase with time over this period. These results are in strong contrast with the claims that the principle cause of shift in seawater has been due to weathering from the Himalayas. Instead, it is argued that global changes in climate and weathering (possibly associated with the Himalayan uplift) are the cause of the increase in  $^{187}\text{Os}/^{188}\text{Os}$  and  $^{87}\text{Sr}/^{88}\text{Sr}$  with time. This challenge to the much-exercised Himalayan weathering model now must be subject to other tests.
- 2) The study of hydrothermal springs represent the first set of Os measurements on mantle sources contributing non-radiogenic Os to the oceans. This work unambiguously shows that there is mantle-type Os injected into seawater at spreading centers, but that the amounts are orders of magnitude too small to account for the low  $^{187}\text{Os}/^{188}\text{Os}$  value in seawater. It is argued that low-temperature, off-ridge fluids are responsible for the input of mantle Os and Sr. (Sharma *et al.*, 2000).
- 3) A study of paleo-climate in the Eastern Mediterranean was led by M. Bar-Matthews. This was a most complete and informative study of C and O isotopic variation as a function of time during the last 60,000 years. This study completes the work that we have been doing on the Soreq cave. Further studies will be carried out on other caves by other groups in Israel to pursue the climate problem more extensively. (Bar-Matthews *et al.* 1999)
- 4) A study was made by Andersson *et al.* (2001) on the transport of uranium isotopes into the marine environment. This work has been most successful and clearly identifies the role of particles and colloids in the removal of U from riverine input, and the exchange with the large U reservoir in seawater. The study is accepted for publication and will appear shortly.
- 5) The investigation of both long-lived and short-lived nuclei in the U-Th series (including  $^{230}\text{Th}$ ) was carried out in rivers, bogs and the estuarine environment. This study focused on the transport from a

continental source region, through bogs, to rivers and finally to the estuarine environment. Surprisingly, it was found that bogs with extremely high U concentrations did not have a major role in the chemistry and radioisotope concentration in run-off or in rivers.

6) Two studies on weathering and transport in the vadose zone were carried out. The first of these was in a tropical regime (Cameroon) with a very deep laterite profile and the other was in a northern arboreal forest (Sweden) with only a thin weathering zone. The first study was sufficiently complete (Viers et al.) and a draft manuscript has already been prepared. It should be completed in the next four months. This is unfortunately slow because the study scientist has returned to a professorial position in France.

7) A new project has been initiated with Dr. Ben Reynolds, who has recently joined the group. This project involves a study of U-Th series nuclides in aquifers with low water velocity. A first study has begun on an aquifer in northern New Mexico that had previously been studied for  $^{14}\text{C}$  and He. Reynolds is now in the field collecting samples.

## **GRANTEE: UNIVERSITY OF CALIFORNIA AT BERKELEY**

Department of Earth and Planetary Science  
Berkeley, California 94720

**Grant:** DE-FG03-85ER13419

### **Advective-Diffusive/Dispersive Transport of Chemically Reacting Species in Hydrothermal System**

*Harold C. Helgeson 510-642-1251, fax 510-643-9980, brogie@socrates.berkeley.edu*

**Objectives:** The overall research objective of this project is to quantify the reaction process responsible for the generation of petroleum in sedimentary basins using thermodynamic calculations and compositional information to characterize metastable equilibrium states (Shock, 1988; Helgeson et al, 1993; Seewald, 1994) and the causes and consequences of irreversible reactions in hydrocarbon source rocks and reservoirs.

**Project Description:** The formation and evolution of petroleum in sedimentary basins is generally attributed to the thermal catagenesis of kerogen; *i.e.* kinetically controlled irreversible generation from kerogen of high molecular weight liquid hydrocarbons in bitumen and their progressive conversion to the lighter species that predominate in petroleum because of increasing time and temperature with increasing depth of burial. This widely accepted time/temperature paradigm is based largely on extrapolation of the results of laboratory pyrolysis experiments to the natural process of petroleum generation by correlating the products of the experiments with observed changes in kerogen composition with depth in sedimentary basins. However, high-temperature pyrolysis experiments are by design irreversible, and the extent to which the results of these experiments represent, or can even be reliably extrapolated to account for petroleum generation in nature has never been adequately documented.

Although the phenomenological association of petroleum generation and maturation with increasing temperature and time during burial is self-evident, the causal implications of this association are highly questionable. In fact, it has been shown that in closed systems, source rocks with hydrogen-rich organic matter may retain their petroleum generating potential at temperatures far greater than those normally associated with the formation of crude oils. It can be demonstrated that degradation of organic matter with increasing depth is an oxidation/reduction process that requires the presence of H<sub>2</sub>O.

Theoretical considerations and thermodynamic calculations have led to the hypothesis that hydrolytic disproportionation of hydrocarbons plays a crucial role in the diagenetic deoxygenation of immature kerogen, as well as the generation and maturation of crude oil in hydrocarbon source rocks. Recent field and laboratory evidence supporting this hypothesis indicates that hydrolytic disproportionation of organic matter is not only a dominant process in petroleum source rocks and reservoir systems, but that it plays a widespread and important role in ore deposition and high-temperature metasomatism of sedimentary, granitic, and mantle-derived rocks.

**Results:** Research carried out in the current budget period has been primarily concerned with characterizing the mass transfer accompanying diagenetic deoxygenation of immature kerogen in sedimentary basins. Ample evidence indicates that large amounts of CO<sub>2</sub> are produced during diagenetic deoxygenation and hydrogenation of kerogen as it reacts with H<sub>2</sub>O during burial of source



## **GRANTEE: UNIVERSITY OF CALIFORNIA AT BERKELEY**

Space Sciences Laboratory  
Berkeley, California 94720-7450

**Grant:** DE-FG03-96ER14676

### **Collaborative Research: Studies for Surface Exposure Dating in Geomorphology**

*K. Nishiizumi 510-643-9361, fax 510-643-7629, kuni@ssl.berkeley.edu; W. E. Dietrich 510-642-2633, bill@seismo.berkeley.edu; M. W. Caffee, R. C. Finkel, Lawrence Livermore National Laboratory; R. C. Reedy, Los Alamos National Laboratory*

**Objective:** An experimental and theoretical program to fully develop the systematics of *in situ* produced cosmogenic nuclides in terrestrial surface samples and their application to the dating of surface features and processes.

**Project Description:** Surface exposure dating utilizing cosmogenic nuclides is now acknowledged as a successful means with which to date many terrestrial surfaces. It is also recognized that there are many new applications for these techniques. Although the method rests on a firm physical and geochemical foundation, there are examples of conflicting results. This project includes determination of precise production rates and production depth profiles, studies of altitude and latitude effects, intercalibration with other methods, isolation of *in situ* produced nuclides from other lithologies. The effort will focus on chemical isolation of cosmogenic nuclides of geologic and artificially exposed samples, on implementation of surface exposure dating methods using new radionuclides such as *in situ*  $^{14}\text{C}$  and pure spallation  $^{36}\text{Cl}$ , measurements of proton and neutron cross sections and development of theoretical production rate calculation.

**Results:** We continue to work on development of a method for determining *in-situ*  $^{14}\text{C}$  in geologic samples by developing a step-wise heating technique to separate *in-situ*  $^{14}\text{C}$  from meteoric  $^{14}\text{C}$ . The extraction line consists of three sub-systems: carrier and flow gas measurement and aliquotting, sample heating, and  $\text{CO}_2$  purification. Blank tests on samples spiked with dead carbon have shown that we can now melt 20 g of quartz and extract carbon with a blank of approximately  $2-3 \times 10^6$  atoms of  $^{14}\text{C}$ . The next series of tests will be performed on heavily shielded samples collected from deep in the Homestake mine in South Dakota. These samples will allow us to test the effectiveness with which we can remove meteoric  $^{14}\text{C}$  and to determine the blank levels of our extraction line when it is heated with actual samples.

Although quartz is the best mineral for studies of cosmogenic nuclide surface exposure dating, quartz is rare in many geological settings. We developed a method for separating *in-situ* produced  $^{10}\text{Be}$  from meteoric  $^{10}\text{Be}$  using stepwise leaching methods. We have measured cosmogenic  $^{10}\text{Be}$  in Hawaiian and Icelandic volcanic samples and in a sample of olivine that has been exposed for  $10^4$  years. This sample has been used for intercalibration with noble gas measurements.

## **GRANTEE: UNIVERSITY OF CALIFORNIA AT BERKELEY**

Institute of Environmental Science and Engineering  
Berkeley, California 94720-1766

**Grant:** E-FG03-96ER14667

### **Dissolution of Fe(III)(hydr)Oxides by Aerobic Microorganisms**

*Garrison Sposito 510-643-8297, fax 510-643-2940, sposito@ce.berkeley.edu; L.E. Hersman, Los Alamos National Laboratory; P.A. Maurice, University of Notre Dame*

**Objectives:** The overall objective of our ongoing DOE-BES sponsored research is to determine the rates and mechanisms whereby bacteria dissolve Fe(III)(hydr)oxides in aerobic soil environments, where Fe is insoluble. Information about the rates and mechanisms of Fe(III)(hydr)oxide dissolution is fundamental for a wide range of hydrobiogeochemical soil, surface-water, and aquifer processes, yet little is known about dissolution promoted by aerobic bacteria. Fe(III)(hydr)oxides sorb radionuclides and organic contaminants; thus, their dissolution may cause remobilization of these sorbed pollutants. Our current studies focus on the effect of Al-for-Fe substitution in goethite on the kinetics of its dissolution by the hydroxamate siderophore, desferrioxamine-B (DFO), and the competing bioligand, oxalate. The Al-for-Fe substitution alters crystal size, texture, multidomainicity, surface area, structural strain and, therefore, could influence the rate and mechanism of goethite dissolution.

**Project Description:** The Al content of the four samples of Al-goethite (S1-S4) used was determined from surface area determinations, acid digestion experiments, and unit-cell parameters. The Al content (100 x in  $\text{Fe}_{1-x}\text{Al}_x\text{OOH}$ ) determined was:  $1.92 \pm 1.6$  (S1),  $4.15 \pm 2.2$  (S2),  $5.82 \pm 2.1$  (S3), and  $6.62 \pm 1.3$  (S4). Continuous-flow stirred-tank reactors were used with the Al-goethite samples at pH 5 in the presence of DFO and oxalate. The composition of the influent solution was: 0.01 M  $\text{NaClO}_4$ , 5mM MES buffer, DFO (0-1000  $\mu\text{M}$ ). The system was covered with aluminum foil at  $20 \pm 2^\circ\text{C}$ . The Fe concentration in the effluent solution was determined using ICP-AES at emission wavelength 259.9 nm.

**Results:** DFO and oxalate both increased the steady-state dissolution rate of the Al-goethites relative to the proton-promoted rate at pH 5 (see the table below).

Oxalate enhanced the steady-state dissolution rate over that observed in the presence of DFO alone, regardless of Al content.

The dissolution rate of Al-goethite observed in the presence of both DFO and oxalate was significantly different from the sum of the dissolution rates measured in the presence of DFO only or oxalate only. For S1 and S2, the observed rate was higher than the sum, whereas for S3 and S4 it was lower.

### Effect of DFO and oxalate ligands on the dissolution of Al-goethite

Sample (mole fraction Al)	[DFO] ( $\mu\text{M}$ )	[Oxalate] ( $\mu\text{M}$ )	Rate of Dissolution ( $\text{nmol Fe g}^{-1}\text{h}^{-1}$ )
–	–	–	$2.4 \pm 0.3$ *
S1 ( $x = 0.02$ )			
40	–	–	$11.1 \pm 0.8$
–	100	–	$0.02 \pm 0.01$
40	100	–	$134 \pm 28$ †
40	1000	–	$60 \pm 7$
–	–	–	$2.6 \pm 0.2$ *
S2 ( $x = 0.04$ )			
40	–	–	$9.2 \pm 0.3$
–	100	–	$0.07 \pm 0.01$
40	100	–	$111 \pm 14$ †
40	1000	–	$153 \pm 24$
–	–	–	$0.003 \pm 0.003$ *
S3 ( $x = 0.06$ )			
40	–	–	$33 \pm 3$
–	100	–	$140 \pm 18$
40	100	–	$52 \pm 8$
40	1000	–	$167 \pm 9$
–	–	–	$0.11 \pm 0.04$ *
S4 ( $x = 0.07$ )			
40	–	–	$92 \pm 17$
–	100	–	$3.0 \pm 0.2$
40	100	–	$84 \pm 6$
40	1000	–	$92 \pm 30$

\* proton-promoted rate

† exceeds sum of two rates immediately above

Aluminum-goethite dissolution occurred nonstoichiometrically; *i.e.*, the Fe release rate was much higher than the Al release rate, regardless of Al content or the presence of ligands

These results point toward a complex relationship between the structure of Al-goethite at low Al content and the rates of Fe and Al release in the presence of DFO and/or oxalate. Experiments to elucidate Al-goethite structure are in progress.

## GRANTEE: UNIVERSITY OF CALIFORNIA AT DAVIS

Department of Land, Air and Water Resources  
Davis, CA 95616

**Grant:** DE-FG-0396ER14629

### **The Kinetics of Dissociation of Aluminum-Oxygen Bonds in Aqueous Complexes: An NMR Study**

*William H. Casey, 916-752-3211, fax 916-752-1552, whcasey@ucdavis.edu; Brian L. Phillips  
Chem., Eng. and Material Science, 916-752-0940, fax 916-752-8995; blphillips@ucdavis.edu*

**Objectives:** We measure rates and mechanisms of bond rupture at the elementary scale in dissolved aluminum complexes and compare them to calculations of the molecular properties.

**Project Description:** At a molecular scale, most reactions of geochemical importance involve a bonded atom or molecule that is replaced with another. The rates of bond cleavage depend very sensitively on the other ligands that are also in the inner-coordination sphere of the metal. We probe these effects at the most fundamental level by coupling NMR spectroscopy to aqueous experiments and *ab initio* calculations of electronic structures of the molecules

#### **Results:**

##### *Rates of Elementary Reactions*

We continue our research into rates of Al-O bond dissociation in dissolved aluminum complexes as a function of ligands substituted into the inner-coordination sphere and we compare these elementary rates with computer simulations of the molecular properties, such as electronic charges on the bound oxygens. The essential idea is that stable ligands in the inner-coordination sphere of Al(III) modify the reactivity of other bonds to oxygens that are also in the inner-coordination sphere. Table 1 presents a summary of the existing rate data; most are from our research group. These results are important because they provide simple molecular models to test predictive models for bond rupture in more complicated settings, such as the surface of a mineral.

##### *Surface Chemistry of (Hydr)oxide Minerals*

We complement these measurements with studies of the aqueous-mineral interface and recently employed  $^{19}\text{F}$ -NMR spectroscopy to detect the selective replacement of bridging hydroxyl groups and terminal bound water molecules at the surface of colloidal bayerite and boehmite.

##### *High-Pressure NMR Probe for Reaction Mechanisms*

We are nearly finished building a titanium NMR probe to measure reaction rates at up to 4-5 kbar in pressure. We tested the probe at pressure and finished the RF circuit for  $^{17}\text{O}$ . Our initial experiments are underway.

Table 1: Rate coefficients and activation parameters for exchange of water molecules from the inner-coordination sphere of Al(III) complexes to the bulk solution, as determined from  $^{17}\text{O}$ -NMR. The datum for  $\text{Al}^{3+}$  is from Hugi-Cleary *et al.*(1985), a Swiss group, but all other rate coefficients are from our research. Data for the  $\text{Al}_{13}$  and  $\text{GaAl}_{12}$  complexes derived from NSF-supported research.

Species	$k_{ex}^{298}$ ( $\pm \ln(\sigma)$ )	$\Delta H^\ddagger$	$\Delta S^\ddagger$
( $\text{s}^{-1}$ )	( $\text{kJ}\cdot\text{mol}^{-1}$ )	( $\text{J}\cdot\text{K}^{-1}\cdot\text{mol}^{-1}$ )	
$\text{Al}^{3+}$	1.29	84.7( $\pm 3$ )	41.6( $\pm 9$ )
$\text{Al}(\text{ssal})^+$	3000	37( $\pm 3$ )	-54( $\pm 9$ )
$\text{Al}(\text{sal})^+$	4900	35( $\pm 3$ )	-57( $\pm 11$ )
$\text{Al}(\text{mMal})^+$	660	66( $\pm 1$ )	31( $\pm 2$ )
$\text{Al}(\text{mMal})_2^-$	6900	55( $\pm 3$ )	13( $\pm 11$ )
$\text{Al}(\text{ox})^+$	109	68.9( $\pm 2$ )	25.3( $\pm 6.7$ )
$\text{AlF}^{2+}$	111	79( $\pm 3$ )	60( $\pm 8$ )
$\text{AlF}_2^+$	19600	69( $\pm 5$ )	70( $\pm 17$ )
$\text{AlOH}^{2+}$	31000	36.4( $\pm 5$ )	-36.4( $\pm 15$ )
$\text{Al}_{13}$	1100	53( $\pm 12$ )	-7( $\pm 25$ )
$\text{GaAl}_{12}$	227	63( $\pm 7$ )	29( $\pm 21$ )

ox=oxalate; ssal=sulfosalicylate; sal=salicylate; mMal=methylmalonate;  $\text{Al}_{13} = \text{AlO}_4\text{Al}_{12}(\text{OH})_{24}(\text{H}_2\text{O})_{12}^{7+}$ ;  $\text{GaAl}_{12} = \text{GaO}_4\text{Al}_{12}(\text{OH})_{24}(\text{H}_2\text{O})_{12}^{7+}$ .

## **GRANTEE: UNIVERSITY OF CALIFORNIA AT DAVIS**

Thermochemistry Facility  
Department of Chemical Engineering and Materials Sciences  
One Shields Ave.  
Davis, California 95616-8779

**Grant:** DE-FG03-97ER14749

### **Thermodynamics of Minerals Stable near the Earth's Surface**

*Alexandra Navrotsky, 530-752-9289, fax 530-752-9307, anavrotsky@ucdavis.edu*

**Website:** <http://navrotsky.engr.ucdavis.edu/>

**Objectives:** The goals of the project are to increase both the data base and the fundamental understanding of the thermodynamics of volatile-bearing mineral phases (amphiboles, micas, clays, zeolites, carbonates, sulfates) important to surficial, sedimentary, and shallow crustal processes.

**Project Description:** Using high temperature solution calorimetry, this research determines the enthalpies of formation of hydrous silicate, carbonates, and sulfates. Systematics in energetics of ionic substitutions are sought in order to predict the thermodynamics of complex multicomponent minerals. Mixing properties of mica, amphibole, clay, zeolite, sulfate, and carbonate solid solutions are also studied.

**Results:** *Hydration energetics:* Using data for manganese oxide minerals and for zeolites, a model is being developed in which the cation hydration (described by the number of water molecules per extra-framework cation) is the major factor influencing enthalpies of formation relative to anhydrous stable phases. This concept unifies, explains, and predicts enthalpies of formation of a large number of hydrated frameworks. Negative (exothermic) enthalpies of formation of hydrated open frameworks from anhydrous dense ones plus liquid water correlate linearly with negative entropies of formation. This implies that the "structuring" of water around alkali and alkaline earth cations is the major driving force for the stability of low temperature open framework minerals such as zeolites. The systematics of hydration enthalpies and entropies are further correlated.

*Sulfates:* Molten  $3\text{Na}_2\text{O} \cdot 4\text{MoO}_3$  has been shown to be a satisfactory calorimetric solvent for sulfate minerals. Work on the sulfates of Ca, Sr, Ba, and Pb and their solid solutions is in progress.

*Hydroxalicates:* A systematic calorimetric study of the energetics of mixed metal hydroxides (M = Mg, Co, Ni, Fe) with charge balancing anions is initiated. These materials are important in issues of contaminant transport and corrosion.

## GRANTEE: UNIVERSITY OF CALIFORNIA AT DAVIS

Departments of Chemistry and Land, Air and Water Resources  
One Shields Avenue, Davis, CA 95616

**Grant:** DE-FG03-92ER14307

### Electrochemical Measurements of Thermodynamics Properties of Minerals and the Processes of Reconstruction at Mineral Surfaces

*Peter A. Rock, 530- 754-8919, fax 530-754-9057, rock@lsdo.ucdavis.edu; William H. Casey 530 752-3211, fax 530-752-1552, whcasey@ucdavis.edu*

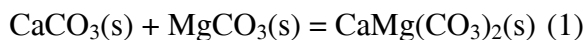
**Objectives:** To determine thermodynamic properties of carbonates, hydroxycarbonates and oxides of relevance to DOE objectives and goals for CO<sub>2</sub> sequestration and the removal of toxic metal ions from waste water streams and aquifers.

**Project Description:** We are: (1) measuring thermodynamic properties for carbonates, hydroxy carbonates and oxide solid-solution minerals that are important in soils and aquifers and in the abatement and remediation of radioactive waters; (2) devising new theoretical approaches to the calculation of the energetics of metal carbonates, hydroxy carbonates and oxides in pure and binary phases; (3) and, using AFM to explore the processes of reconstruction at mineral surfaces.

**Results:** We have extended our new theoretical method for calculating lattice energies of calcite-structure metal carbonates (G. Mandell and P.A. Rock, *J. Phys. Chem. Solids* 59, 95-702 and 703-712, 1998) to metal carbonate solid solutions. Theoretical excess energies for solid solutions (Ca,M)CO<sub>3</sub>(ss) [where M, Mn or Fe] have been calculated (G. Mandell, et. al., *J. Phys. Chem. Solids* 60, 651-661 (1999)). A comparison between our theoretical results and experimental results is encouraging, especially for the Ca<sub>x</sub>Cd<sub>1-x</sub>CO<sub>3</sub>(ss) and Ca<sub>x</sub>Mn<sub>1-x</sub>CO<sub>3</sub>(ss) systems.

Recently, we have discovered how to extend the theory to carbonates with the aragonite structure. This advance enables us to explore the energetics of the calcite ↔ aragonite phase transition, as well as metal carbonate solid solutions with the aragonite structure; for example, Ca<sub>x</sub>Sr<sub>1-x</sub>CO<sub>3</sub>(ss) for which we have independently obtained experimental excess Gibbs energy data. The method has also been applied to metal oxides with the hematite structure.

We have used our electrochemical cell technique (Rock, et. al), *Geochim. Cosmochim. Acta* 58, 4281-4291, 1994) to determine  $\Delta G_f^\circ$  for dolomite (manuscript accepted subject to minor revision by Amer. J. Sci.). Our value of  $\Delta G_f^\circ$  of  $-2147.82 \pm 2.20 \text{ kJ} \cdot \text{mol}^{-1}$  for dolomite, together with new  $\Delta G_f^\circ$  data for MgCO<sub>3</sub>(s) (determined in our lab) and literature data for CaCO<sub>3</sub>(s) yield for the equation



$$\Delta G_f^\circ = -11.56 \pm 2.20 \text{ kJ}$$

whereas the calorimetric data of Capobianco and Navrotsky (1987) yield a value of  $\Delta H_f^\circ = -11.48 \pm 0.50 \text{ kJ}$  for reaction (1). Because, as Navrotsky has pointed out,  $\Delta S_{rxn}^\circ(11) = 0$ , the agreement of the independent electrochemical and thermochemical method is remarkable. We also have used our lattice

energy theory to calculate the value  $\Delta G_{rxn}^o$  (1); the result obtained was -12.64kJ which is in excellent agreement with the experimental data.

We have completed an electrochemical determination of  $\Delta G_{rxn}^o$  for the Goethite-Hematite conversion  
 $\text{Fe}_2\text{O}_3(\text{s}) + \text{H}_2\text{O}(\text{l}) = 2\text{FeOOH}(\text{s})$

A theoretical analysis of the energetics of this reaction is in progress.

## GRANTEE: UNIVERSITY OF CALIFORNIA AT LOS ANGELES

Department of Earth and Space Sciences  
Los Angeles, CA 90095-1567

**Grant:** DE-FG-03-89ER14049

### **Application of $^{40}\text{Ar}/^{39}\text{Ar}$ Thermochronometry and Ion Microprobe Stable Isotope Geochemistry to the Evolution of Petroleum Reservoirs and Hydrothermal Systems**

*T.M. Harrison 310-825-7970, fax 310-825-4396, tmh@argon.ess.ucla.edu*

**Website:** <http://oro.ess.ucla.edu/doe.html>

**Objectives:** Understanding the rates and mechanisms involved in the formation of exploitable geological energy sources, including fossil fuel, geothermal, and fissionable materials, requires knowledge of the age of origin and subsequent thermal history of the system over geological time. The objective of this research is to assess the utility of micro-scale isotopic techniques in deriving both fluid evolution and thermal history results for crustal environments that bear upon energy exploration and reservoir assessment.

**Project Description:** We are using coupled application of the ion microprobe and  $^{40}\text{Ar}/^{39}\text{Ar}$  thermochronometry to: (1) assess the thermal and diagenetic histories of sedimentary basins (southern San Joaquin basin, central California); (2) study the intrusion history and thermal evolution of a young geothermal system (Geysers steam field, northern California) to resolve fundamental questions regarding its origin; and (3) develop tools to investigate the stability of uraninite in the presence of fluid and radiation effects to better understand the nature of unconformity-type uranium deposits (Athabasca Basin). Some of these efforts require significant developmental work to make meaningful progress. In particular we have found it necessary to develop a robust ion microprobe calibration for isotope ratio analysis of oxygen and carbon isotopes of complex carbonate compositions to in order to investigate rock-fluid interactions. Similar developments have been required to study the U-Pb and oxygen isotopic systematics of uraninites and associated phases.

**Results:** 1) Thermal and diagenetic histories of sedimentary basins. The ability to perform in situ, micron-scale, carbon and oxygen isotopic analyses of carbonate minerals and cements opens up the possibility of assessing long term ( $10^6$ - $10^7$  year) permeability histories of hydrocarbon reservoirs and obtaining paleoclimate histories with ultra high (annual to decadal) temporal resolution. Ion microprobe techniques for determining carbon and oxygen isotopic ratios with sub-‰ precision are now routine, but have thus far been restricted to end member carbonates because of significant compositional matrix effects on measured isotopic ratios. This represents a significant limitation for cements in sedimentary basin environments where carbonates exhibit an extensive solid solution. We synthesized a suite of complex carbonate compositions across the  $\text{CaCO}_3$ - $\text{MgCO}_3$ - $\text{FeCO}_3$  ternary using both hydrothermal and piston-cylinder approaches. Natural specimens were used for endmember compositions and those along the dolomite-ankerite join. The oxygen and carbon isotopic compositions of mg-sized aliquots of these materials were characterized using conventional gas source mass spectrometry. Matrix effects were then obtained by comparing these data with results from ion microprobe analyses. Our results yield the following instrumental mass fractionation (imf) relationships (in ‰): calcite-siderite  $\text{imf} = -25.90 x_{\text{Fe}}^2 + 16.20 x_{\text{Fe}} - 29.19$ ; calcite-magnesite  $\text{imf} = -37.75 x_{\text{Mg}}^2 + 4.291 x_{\text{Mg}} - 30.13$  (valid for  $x_{\text{Mg}} < 0.5$ ); dolomite-ankerite  $\text{imf} = -21.98 x_{\text{Fe}}^2 + 29.17 x_{\text{Fe}} - 34.43$ ; siderite-magnesite  $\text{imf} = -172.8 x_{\text{Fe}}^3 + 325.0$

$x_{\text{Fe}}^2 - 168.7 x_{\text{Fe}} - 22.26$ . Replicate measurements show that the form of these functions is preserved, although relative shifts between analytical sessions are observed.

2) Thermal energy potential of active magmatic-hydrothermal systems. The known extent and emplacement history of granitoids (1.13-1.25 Ma) within the Geysers Magmatic Complex, Sonoma County, California, cannot explain its protracted geothermal activity. Significant thermal inputs from younger sources appear to be required; the size of the system scaling with age (i.e., younger smaller bodies or older larger bodies). We have begun a systematic search for this source by: obtaining new samples from both archived sources (cuttings from over 22 bore holes penetrating the felsite) and field sampling of volcanic equivalents of intrusive granitoids; U-Pb zircon dating of these rocks; examination of melt inclusions in zircon to better constrain the initial isotopic disequilibrium in the U-Pb system in order to refine dating estimates.

3) High temporal resolution paleoclimatology from in situ oxygen and carbon isotopes of speleothem. Oxygen and carbon isotopic variations in speleothems (i.e., cave deposits) provide one of the best records of climate variations during the Pleistocene. Current methods involving gas-source measurement of  $\delta^{18}\text{O}$  and  $\delta^{13}\text{C}$  and U-series dating are restricted to providing data averaged over ca. 100 years and thus limit temporal resolution of the onset of regional and global climate change at the century level. Tests of hypotheses involving more rapid timescales require higher temporal, and thus spatial, resolution. Ion microprobe measurements of oxygen and carbon isotopes across a sectioned stalactite from the Soreq Cave, Israel, that had been previously dated by U-series methods yields an ultra high temporal paleoclimate record that encompasses the last glacial maximum (18 to 8.5 ka B.P.). While the ion microprobe  $\delta^{18}\text{O}$  results are characterized by somewhat lower precision than conventional methods (typically 0.5‰ versus 0.1‰), they reproduce the previously defined trend with a temporal resolution that is 50 times higher. Under favorable conditions, annual resolution is feasible using the ion microprobe approach. The new data reveal well-resolved climate oscillations with a period of  $\sim 10^2$  years that are not evident in the bulk analyses and suggest greater instability of glacial climate than previously appreciated.

## **GRANTEE: UNIVERSITY OF CALIFORNIA AT SANTA BARBARA**

Department of Geological Sciences  
Santa Barbara, CA 93106

**Grant :** DE-FG02-96ER14619

### **Fluid Flow in Faults: Estimating Permeability and Diagenetic Effects in a Transpressional Setting, Southern California**

*James R. Boles, 805-893-3719, fax 805-893-2314, boles@magic.geol.ucsb.edu; Grant Garven 410-516-8689, fax 410-516-7933, garven@jhu.edu*

**Objectives:** This is a collaborative effort to determine the magnitude of fluid mass transfer and diagenetic effects along faults that have developed in a transpressional setting. The study will contribute a fundamental understanding of the hydraulic effects of faults on sediment diagenesis, petroleum migration and groundwater flow.

**Project Description:** We have targeted three major faults and petroleum fields in southern California for study: Wheeler Ridge and Elks Hills in the San Joaquin Basin and the Refugio Fault in the Transverse Ranges near Santa Barbara. Subsurface core samples, outcrop samples, well logs, reservoir properties and published structural-seismic sections are being collected to characterize the tectonic history and diagenetic evolution for the known fault networks. These data provide constraints for finite element flow and transport models that are being developed to predict fluid pressures, flow patterns, rates of deformation, temperatures, and diagenetic patterns in the fault systems during thrusting and normal faulting.

**Results:** Jim Boles and his Ph.D. student have studied cores from 340 wells in the San Joaquin Basin: twenty-seven of these cores stored at the Wheeler Ridge Oil Field have been sampled in addition to cores stored at the California Core Repository in Bakersfield. Our sampling strategy is to document diagenesis in reservoir strata at Wheeler Ridge and then compare this to cores close to the Wheeler Ridge Thrust Fault. We are conducting petrographic analyses of thin sections, isotopic analyses of carbonate cements, and analyzing geothermal indicators in these samples such as plagioclase and smectite/illite composition. We also have constructed time-temperature burial histories for each of these wells using ARCO's Genesis software. Permeability-depth trends indicate several orders of magnitude decrease in permeability within 100 meters of the hanging wall of the fault, suggesting that either mechanical crushing and/or cementation has occurred above the fault. The nature of the mineral changes will constrain fluid volume, temperature, and if datable the potential timing of fluid movement. Grant Garven and his Ph.D. student have been busy preparing finite element simulations that complement the petrologic fieldwork. In FY2000, they prepared 2-D simulations that compared effects of faults. The models consider cases in which the thrust faults are considered to act as conduits and barriers. We are also comparing the hydrologic effects of both topography and deformation as driving forces for fluid flow across the Wheeler Ridge thrust sheet.

**GRANTEE: UNIVERSITY OF CALIFORNIA AT SANTA BARBARA**

Department of Mechanical and Environmental Engineering  
Santa Barbara, CA

**Grant:** DE-FG03-00ER15114

**Three-Dimensional Miscible Porous Media Flows with Viscosity Contrasts and Gravity Override**

*Eckart Meiburg, tel and fax 805-893-5278, meiburg@engineering.ucsb.edu*

**Objectives:** To gain an understanding of the dynamics of miscible, variable density and viscosity flows in porous media, by means of detailed high fidelity numerical simulations. A main objective is to investigate the interaction among the effects of heterogeneity, density and viscosity fluctuations in the practically relevant quarter five-spot configuration.

**Project Description:** The project involves a three-dimensional computational investigation into the spatio-temporal dynamics of miscible porous media flows under the coupled effects of permeability heterogeneities, mobility contrast, and gravitational segregation. To this end, we employ high-accuracy numerical simulations based on a combination of compact finite difference and spectral methods. Our own recent two-dimensional simulations of plane, neutrally buoyant displacements and of flows with gravity override show that heterogeneities play a fundamentally different role in those flows. As a result, their role in three-dimensional displacements with buoyancy effects cannot be extrapolated by combining results of different two-dimensional analyses, and a fully three-dimensional investigation is needed to obtain the necessary, qualitatively new understanding of the role of heterogeneities. Overall, the investigation aims to outline the borders between the various parameter regimes in which the displacement will be dominated by different physical mechanisms.

**Results:** Initial three-dimensional direct numerical simulations have been performed in order to investigate miscible porous media flows with mobility and density contrasts in the quarter five-spot configuration. Both homogeneous and heterogeneous environments are currently being considered. The dynamics of the displacement processes are analyzed in terms of the interaction mechanisms among the three vorticity components related to viscosity, density and permeability variations. Depending on the aspect ratio, the initially vertical front has been seen to break up into several horizontal layers, which subsequently give rise to individual fingers. Even a moderate density difference leads to a considerable reduction in the breakthrough efficiency, as it redirects the fluid along one of the horizontal boundaries and thereby increases the local effective Peclet number, thus enhancing the fingering instability. For certain parameter combinations, a secondary instability is seen to emerge as a result of vertical density stratification.

## UNIVERSITY OF CALIFORNIA AT SANTA BARBARA

Institute for Crustal Studies  
Santa Barbara, California 93106-1100

**Grant:** DE-FG03-91ER14211

### **Magma Rheology, Mixing of Rheological Fluids, Molecular Dynamics Simulation, and Lithospheric Dynamics**

*F. J. Spera 805-893-4880, fax 805-893-8649, spera@magma.geol.ucsb.edu*

**Website:** <http://magma.geol.ucsb.edu/>

#### **Objectives:**

- Laboratory measurements of magma rheological properties on magma
- Determination of the structure and properties of multicomponent silicate melts and glasses at elevated temperature and pressure.
- Numerical modeling of porous media thermohaline convection
- Geochemical material balance modeling of assimilation and fractional crystallization subject to energy constraints.

**Project Description:** This collaborative project with D. A. Yuen at the University of Minnesota will improve our understanding of the thermal, chemical, dynamical and mechanical state of the continental crust and subcrustal lithosphere with particular focus on the interactions between the various subsystems. The work-plan includes: (1) new rheological laboratory measurements on melts and magmatic suspensions (2) Determination of the thermodynamical and transport properties of molten silicates by MD simulations (3) Mixing processes of rheological fluids in convection and visualization of complex processes (4) Coupling between mantle convection with temperature-dependent and non-Newtonian rheology and mantle diapirs on the thermal regime and subsidence curves of rift-related basins (5) The dynamical influences of lithospheric phase transitions on the thermal-mechanical evolution of sedimentary basins (6) The development of stress fields and criteria for faulting in the crust and finally (7) Modeling of heat and mass transport driven by thermal and compositional heterogeneities in porous media (8) Open system Geochemical modeling of magmatic systems.

**Results:** Results cited below are for the UCSB part of this project. Additional results are given in the summary of activities by the University of Minnesota team. Molecular dynamics (MD) simulation provides a unique window into the microscopic processes controlling the properties of amorphous silicates of geochemical importance. Seventeen simulations for composition  $\text{CaAl}_2\text{Si}_2\text{O}_8$  in a microcanonical ensemble of 1300 particles (O+Si+Al+Ca) were conducted at temperatures 1700-5000 K and 1 GPa. The computer glass transition was detected at  $T_g \approx 2800$  K by study of thermodynamic properties, speciation equilibria and tracer diffusivity as a function of temperature.  $T_g$  is observed as a change in slope of enthalpy (H) *versus* temperature at  $T = T_g \approx 2800$  K. The configurational isobaric heat capacity of supercooled melt relative to the glass is 53.3 J/K mol, within a factor of two of the experimental value. The 'computer' isobaric heat capacity for equilibrium liquid at 3000 K, is  $457 \pm 35$  J/K mol *versus* the calorimetric value of 461 J/K mol. In equilibrium liquid, speciation defined by

equilibria such as  $^{11}\text{O} + ^{13}\text{O} = 2 ^{12}\text{O}$  and  $\text{TO}_4 + \text{TO}_6 = 2 \text{TO}_5$  are temperature-dependant with  $\Delta H$  and  $\Delta S$  approximately equal to -39 kJ/mol and 19 J/mol K and -10 kJ/mol and 12 J/mol, respectively in excellent agreement with laboratory values. The static structure factor for oxygen-oxygen shows that the glass transition is not associated with significant changes in the static structure. Self-diffusivity orders at fixed temperature according to  $D_{\text{Ca}} > D_{\text{O}} > D_{\text{Al}} > D_{\text{Si}}$  with  $D_{\text{Ca}} \sim 20\%$  larger than  $D_{\text{O}}$  and  $D_{\text{O}} \approx 2 D_{\text{Si}}$ . Activation energies for diffusion for all atoms lie in the range 170–190 kJ/mol. The small range in tracer diffusivity and activation energy ( $E_a$ ) found for different atoms suggests cooperative motion is important. The Eyring viscosity, computed from oxygen self-diffusivity, is 0.42 Pa s at 2800 K is in good agreement with the Maxwell estimate ( $\eta = G_{\infty} \tau$ ) and MD-computed relaxation times. The picture is that a given particle and its neighbors remain trapped for a finite *waiting* or *residence* time before undergoing a cooperative thermally activated rearrangement. The waiting time distribution is strongly temperature-dependent and related to the dramatic increase in structural relaxation time as temperature approaches  $T_g$ . At  $T < T_g$  the van Hove function for oxygen and calcium exhibits a double-peaked structure characteristic of hopping diffusion through correlated jumps involving neighboring particles to nearest neighbor sites in an otherwise ‘frozen’ structure. The MD simulations are consistent with a picture of ‘dynamic heterogeneity’ as the ultimate cause of the sluggish dynamics as an equilibrium (ergodic) liquid becomes deeply supercooled. At some temperature above the Kauzmann temperature ( $T_K$ ) where the extrapolated entropy of deeply supercooled liquid equals that of crystalline solid, long lived, highly cooperative, collective particle motions take place in restricted regions of three-dimensional space.

In experimental rheological work, measurements of the viscosity of bubble-bearing rhyolite emulsions have been completed. We show that for Capillary numbers in the range 1-100 the relative viscosity is a monotonically decreasing function of porosity (volume bubble-fraction) and that at 50 vol. % bubbles, the shear viscosity is smaller, by a factor of ten, relative to the single-phase (zero porosity) melt at the same pressure and temperature.

The final piece of research completed this year involves development of a geochemical model (EC-RAFC) for describing the geochemical evolution of open magmatic systems subject to simultaneous assimilation, recharge and fractional crystallization. This work is currently in press at the *Journal of Petrology*. We present an algorithm for modeling the trace element evolution of a magmatic system treated as an open system subject to exchange of mass and energy with its surroundings. The code to perform EC-RAFC calculations on a PC or a Mac is available at the web site listed above.

## **GRANTEE: UNIVERSITY OF CALIFORNIA AT SANTA CRUZ**

Institute of Physics and Planetary Physics  
Santa Cruz, CA 95064

**Grant:** DE-FG03-98ER14845

### **Fast 3D Modeling and Prestack Depth Migration Using Generalized Screen Methods**

*R.S. Wu 831-459-5135, fax 831-459-2423, wrs@es.ucsc.edu; X.B. Xie; T. Lay; E. Silver; X.Y. u*

**Website:** <http://www.es.ucsc.edu/~acti>

**Objectives:** Develop high accuracy and high efficiency numerical methods for seismic modeling/imaging in three-dimensional complex structures. The methods are based on the generalized screen propagator following one-way wave equation approximation.

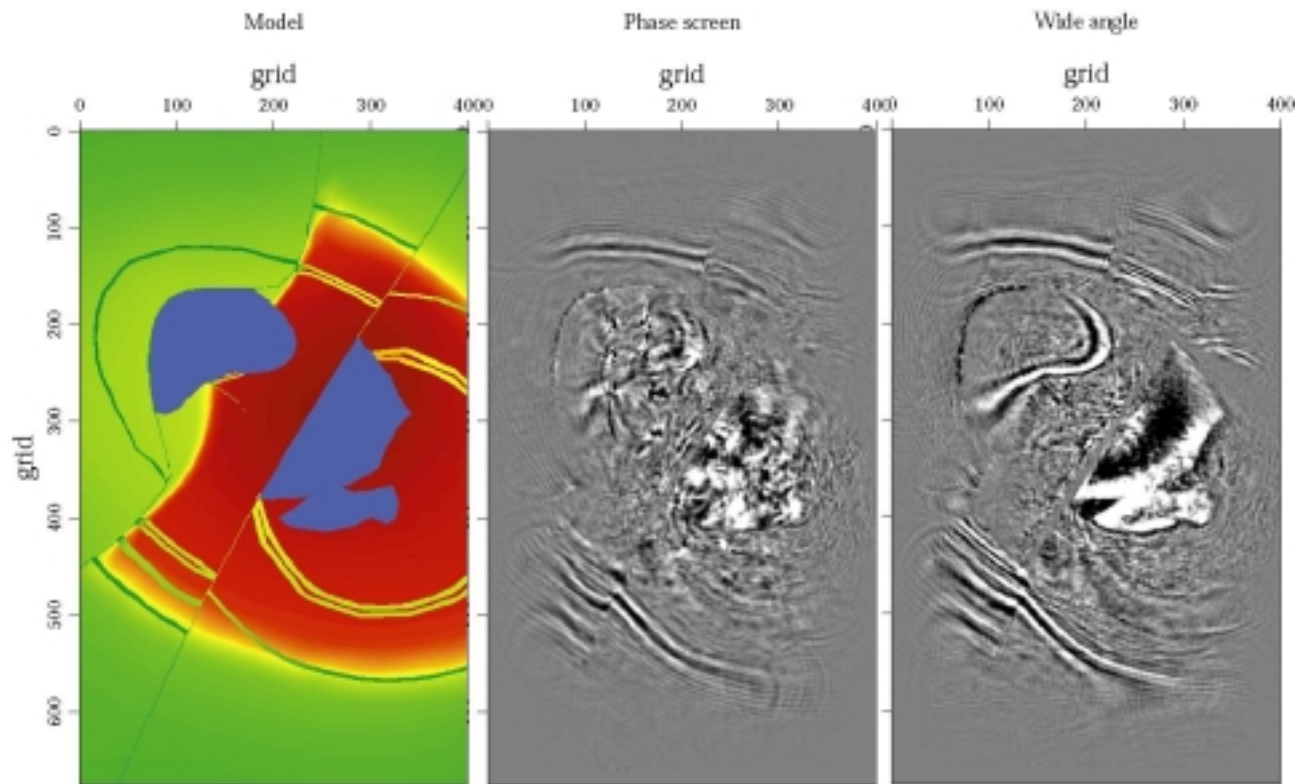
**Project Description:** The project is a collaborative effort of three institutions, LANL, MIT, and UCSC. The research is implemented at the Modeling and Imaging Laboratory, Institute of Geophysics and Planetary Physics, at UCSC. The purpose of this project is to develop new theories and methods for efficient modeling and imaging in 3D complex environments. The basic approach is based on the fast one-way propagation methods, which bridge the gap between high-frequency asymptotic methods and full-wave equation methods. This wave-equation-based method can generate excellent modeling/imaging results compared with the current ray-based methods, while still keep high efficiency.

**Results:** The 3D poststack and prestack migration for the SEG/EAGE salt model are conducted with the pseudo-screen method and a wide-angle Pade screen propagator (Wu, Jin, Xie and Mosher, 2000). For land type data sets, Xie, Mosher and Wu (2000) gave a shot gather version of the wide angle Pade depth migration method, and tested it on the 45 shot SEG/EAGE 3D data set. Jin, Mosher and Wu, (2000) gave an offset domain migration method for marine type data sets, and tested the new method with the SEG/EAGE C3 narrow azimuth data set. Both methods gave very good image qualities. The offset domain method is also a very efficient method. For large marine data set, its speed is comparable or even faster than the commonly used Kirchhoff method.

A method based on wave-equation and finite-difference algorithms is introduced (Guan, Wu and Fu, 2000) to remove scattering effects of rugged topography. A simple conformal method is used in the finite-difference algorithm for a better simulation of scatterings due to the irregular surface. Numerical tests are conducted to show the effectiveness of the method.

The modeling of AVO requires efficient algorithms that can handle both thin-bed effects and lateral heterogeneities. Existing algorithms can hardly meet these requirements. Wu and Wu (2001) tested the thin-slab method as a propagator to handle thin-bed effects as well as lateral variations in lithology.

Pilot investigations on elastic wave migration (Xie and Wu, 2001) and converted wave migration (Wu, Guan and Wu, 2001) were also conducted during this period.



Comparison of migration images for 3D SEG/EAGE model using different methods. The depth profile is located at  $Z = 2100\text{m}$ . From left to right are velocity model, image using phase screen method, and image using wide angle P wave method, respectively. The image from wide angle method is much better than that from phase screen method.

## GRANTEE: THE UNIVERSITY OF CHICAGO

Department of the Geophysical Sciences  
Chicago, IL 60637

**Grant:** DE-FG02-97ER14773

### Kinetic Isotope Fractionation

*Frank M. Richter 773-702-8118, fax 773-702-9505, richter@geosci.uchicag.edu*

**Objectives:** The main theme of our present research is to better understand fluid-mineral chemical exchange mechanisms and associated transport mechanisms. The specific focus is on kinetic isotope fractionations associated with transport by diffusion.

**Project Description:** The research project has evolved from measuring the mass dependence of isotope mobility (self diffusion coefficients) in doped, isochemical, and isothermal diffusion couples to studies of kinetic isotope fractionation by chemical diffusion between natural fluids. The systems being investigated include molten rhyolite-basalt, supercritical water with dissolved silica, and water at near room temperature conditions with dissolved Ca salts. The Ca experiments are preliminary to studies involving dissolution and transport of  $\text{CaCO}_3$ . In the case of dissolved  $\text{Ca}^{2+}$  we need to resolve the effect, if any, of codiffusers on the kinetic isotope fractionation in aqueous solutions. Electrical neutrality requires that  $\text{Ca}^{2+}$  have codiffusing anions, for which we can explore a range of masses by using  $\text{Cl}^-$ ,  $\text{Br}^-$ , and  $\text{I}^-$ .

**Results:** We have completed a series of basalt-rhyolite diffusion couples using natural starting materials run in a piston cylinder apparatus for various lengths of time at  $T \approx 1400^\circ\text{C}$  and  $P \approx 10$  kbars. The starting materials were mid ocean ridge basalt and a natural low Ca rhyolite. We have measured the Ca and Li isotopic fractionation associated with the diffusion of Ca and Li, between basalt and rhyolite. The results are in excellent agreement with our earlier predictions (see Fig. 8, GCA, Vol. 63, No. 18, pp. 2853-2861, 1999):  $\sim 6\%$  change in  $\delta^{44}\text{Ca}$  and  $\sim 30\%$  in  $\delta^7\text{Li}$ . Thus, we have clear evidence that diffusion in silicate liquids can produce kinetic isotope fractionations that are more than an order of magnitude larger than present analytical precision (*e.g.*  $\pm 0.2\%$  for  $\delta^{44}\text{Ca}$ ).

We recently measured D/H fractionation associated with the diffusion of water in rhyolite melt. The diffusion couple juxtaposes a rhyolite melt with 0.18 wt% water to the same melt but rehydrated to about 7 wt% water. The water diffusing into the low water side of the couple produces a local negative D/H anomaly of about 50‰. This suggests that the dominant effect is the faster diffusion of  $\text{H}_2\text{O}$  relative to HDO rather than equilibrium D/H fractionation such that the mobile molecular water is heavy relative to the immobile hydroxyl. The key result is that diffusion of water in silicate melt produces measurable D/H fractionation.

## **GRANTEE: THE UNIVERSITY OF CHICAGO**

Center for Advanced Radiation Sources  
5640 S. Ellis Avenue  
Chicago, IL 60637

**Grant:** DE-FG02-94ER14466

### **GeoSoilEnviroCARS: A National Resource for Earth, Planetary, Soil and Environmental Science Research at the Advanced Photon Source**

*Stephen R. Sutton 630-252-0426, fax 630-252-0436, sutton@cars.uchicago.edu; Mark L. Rivers 630-252-0422, fax 630-252-0436, rivers@cars.uchicago.edu*

**Website:** <http://gsecars.uchicago.edu>

**Objectives:** GeoSoilEnviroCARS is a national consortium of earth scientists whose goal is to design, construct and operate, as a national user facility, synchrotron radiation beamlines at the Advanced Photon Source, Argonne National Laboratory.

**Project Description:** Instrumentation for the following techniques is provided: (1) x-ray absorption fine structure spectroscopy; (2) fluorescence microprobe analysis and microtomography; (3) powder, microcrystal and surface diffraction; (4) high-pressure crystallography with diamond anvil cells and multi-anvil presses, and (5) radiography at high pressure in the multi-anvil press. The availability of these facilities, dedicated to earth science, allows extension of synchrotron-based research to higher temperature and pressure, much lower elemental concentration levels, low atomic number elements, low dimensionality materials (surfaces and interfaces), small volume samples, and transient phenomena. Major areas that greatly benefit include phase transitions in mantle minerals, the properties of the Earth's core, migration and remediation of toxic metals and radioisotopes in contaminated sediments, redox chemistry of transition metals at the root-soil interface and its role in agriculturally-relevant plant diseases, the chemical nature of hydrothermal fluids, chemical reactions on mineral surfaces, and petrogenesis of strategic elements.

**Results:** GeoSoilEnviroCARS is currently making beam time available through a web-based proposal system at <http://gsecars.uchicago.edu>. In FY2000, fifty-seven beam time proposals were received and forty-four new users conducted experiments. Forty undulator experiments were performed and thirty-one experiments were done on the bending magnet beam line, for a total of seventy one experiments for the year.

Results in low temperature geochemistry and crustal processes include (lead investigator in parentheses):

*Europium sorption at iron-chromium oxide/water interfaces* (S. Traina, Ohio State University): To decontaminate iron and steel surfaces, it is necessary to identify the local structure and coordination chemistry of sorbed species at the mineral-water interface. Such information is required in order to develop molecular scale predictions of the efficacy of remediation approaches. MicroXAFS studies of europium, a common fission product, sorbed to iron oxides showed Eu is more loosely bonded to the surface of Cr-substituted hematite compared to that of pure hematite or eskolaite.

*Diffusion-limited biotransformation of chromium in soils* (T. Tokunaga, Lawrence Berkeley National Laboratory): The distribution of metal contaminants such as chromium can be strongly localized by

transport limitations and redox gradients within soil aggregates. MicroXAFS depth profiling revealed shallow diffusion depths (mms) and very sharply terminated diffusion fronts in soils amended with organic carbon reflecting rapid increases in Cr reduction kinetics over very short distances. Chromium contamination in soil aggregates is restricted to the exteriors due to these localized transport and rapid reduction effects.

*Iron and lead sequestration at the soil-root interface* (S. Fendorf, Stanford University): Formation of plant-induced heterogeneous redox microenvironments results in an effective metal sequestration mechanism involving development of ferric hydroxide plaque on root surfaces and subsequent precipitation of carbonate nodules. Fluorescence microtomography images showed lead to be sequestered in the plaque and manganese and zinc in the nodules. This accumulation of metal ion contaminants retards translocation of the metals within plants and their introduction to animals, yet promotes lethal exposure of waterfowl that feed preferentially on the roots.

*Speciation and solubility of ore metal ions from studies of synthetic fluid inclusions at temperatures >350 °C* (J. Mavrogenes, Australian National University): In order to understand the formation of hydrothermal ore deposits, it is necessary to determine both the solubility and speciation of ore-metal ions in supercritical solutions. High temperature microXAFS spectra of copper-bearing fluid inclusions from ore deposits showed predominantly oxygen coordination with a bond length dependence on temperature and brine content.

*Chemical speciation of gold in arsenopyrite* (L. Cabri, Canada Centre for Mineral and Energy Technology): “Invisible” gold in arsenopyrite occurs in two apparently mutually exclusive chemical forms: chemically bound and elemental. In some arsenopyrite crystals, the gold concentration is closely related to growth zoning but there is no clear correlation with the chemical form. The finding of two types of invisible gold in arsenopyrite from different deposits has beneficial implications for extractive metallurgy.

*Chlorine/Bromine ratios in microscopic fluid inclusions in natural quartz*: (D. Vanko, Georgia State University): The Cl/Br ratio of Archean seawater is hypothesized to have been significantly different from that of today suggesting that the global biogeochemical processes that govern seawater halide chemistry have changed between the Archean and the present. Preliminary Cl/Br results on fluid inclusion showed lower values for Archean compared to modern specimens, consistent with previous “crush-leach” experimental results.

*Strontium heterogeneity and speciation in coral aragonite* (N. Allison, University of Brighton): Sea surface temperatures (SSTs) have been inferred previously from the Sr/Ca ratios of coral aragonite, however, Sr in some coral skeletons is more heterogeneously distributed than expected from SST data. Ion and x-ray microprobe imaging showed strontium heterogeneity correlates with the crystalline fabric of the coral skeleton suggesting non-equilibrium calcification processes. This heterogeneity has major ramifications for the reliability of Sr-based palaeothermometry at high temporal resolution. Strontium may exist as Sr-substituted for Ca in aragonite and as separate SrCO<sub>3</sub> (strontianite) domains. MicroEXAFS results on *Porites lobata* skeleton material showed Sr predominately in aragonite.

*Microscale imaging of pore structure in hydrothermal sulfide chimneys* (P. O’Day, Arizona State University): Research on seafloor vent systems provide insights into geochemical cycling in the ocean as well as microbial metabolism and survivability. The laboratory study of such systems requires knowledge of the relationships among pore structure, permeability, fluid flow, and mineralogy within natural chimneys. Microtomography results showed porosities and permeabilities of “smoker” products

depend on age and temperature of formation, younger and cooler samples exhibiting greater porosity, with important implications for porous flow transport of metals and sustainability of microbial communities.

*Pore geometry changes associated with the development of compaction bands in an analogue reservoir rock* (J. Fredrich, Sandia National Laboratories): Important physical properties of rocks, such as elastic moduli, seismic velocity, and compressability, depend strongly on porosity. Microtomographic imaging of previously compressed rock cores was used to characterize the change in pore geometry associated with compactive deformation. The images revealed the details of load-induced compaction, from porosity reduction without grain fracturing to severe fracturing. These results provide critical information for flow simulations.

## **GRANTEE: THE UNIVERSITY OF CHICAGO**

Center for Advanced Radiation Sources  
5640 S. Ellis Avenue  
Chicago, IL 60637

**Grant:** DE-FG02-92ER14244

### **Synchrotron X-ray Microprobe and Microspectroscopy Research in Low Temperature Geochemistry**

*Stephen R. Sutton 630-252-0426, fax 630-252-0436, [sutton@cars.uchicago.edu](mailto:sutton@cars.uchicago.edu)*

**Website:** <http://x26a-cars.nsls.bnl.gov>

**Objectives:** The objectives are to develop and apply a synchrotron-based x-ray microprobe that can be used to determine the composition, structure, oxidation state, and bonding characteristics of earth materials with trace element sensitivity and micrometer spatial resolution.

**Project Description:** The project focuses on development and application of the x-ray fluorescence microprobe on Beam Line X26A at the National Synchrotron Light Source (NSLS), Brookhaven National Laboratory. Geochemical problems that are under investigation include the nature of hydrothermal fluid inclusions, toxic metal and radioisotope speciation in contaminated sediments, determinations of the chemical histories of contaminated sites through microanalytical studies of indigenous organisms, and redox chemistry of metals at the root-soil interface.

**Results:** Examples of research results include the following (collaborators in parentheses)

*Arsenic Solid State Speciation in Industrially Contaminated Soils* (D. L. Sparks, University of Delaware): Arsenic speciation was determined in industrially arsenic contaminated materials using microXANES and microXRF. While As(V) is predominant in the samples where Fe, Ca and Ba are rich, mixtures of As(III and V) were detected where Ba, Ca, Fe are not concentrated. As(V) becomes more pronounced in oxidized samples and is associated with Fe and Ba, indicating an As(V) adsorption complex and/or Ba-As(V) precipitates. The As(III) spectra were similar to those of As(III)-sulfide minerals, such as orpiment and realgar and dissimilar to spectra for As(III) adsorption complexes on metal hydroxides.

*Identification and Speciation of As-bearing Solids in Mine Tailings* (H. Jamieson, Queen's University): Arsenic-bearing solids are present in tailings from the Giant Mine, Yellowknife, Canada, and weathering reactions may lead to attenuation or release of As to the environment. MicroXANES results on mill products and tailings showed that the former contains arsenic in mixed oxidation state whereas the tailings contained only sulfide-bound As. These data will be used to evaluate the risk to human and ecosystem health from mine waste and contaminated soil.

*Uranium Speciation in Jurassic Fish Coprolites* (G. Hanson, SUNY-Stony Brook): Uranium-enriched coprolites were studied to better understand mechanisms of uranium mobility and speciation in sediments. The samples derived from a single black shale horizon in the Shuttle Meadow Formation of the Hartford Basin in southern Connecticut. Microdiffraction showed the material to be dominated by dolomite, fluorapatite and pyrite. Uranium, predominately U(VI), showed a zoning profile inverse to that of divalent and trivalent cations. The oxidized state of U calls into question assumptions regarding

the reducing conditions under which such sediments are thought to have been deposited and the role of organic matter in localizing U in sediments.

*Chemical Heterogeneities in Brazilian Oxisols* (J. J. Marques, Purdue University): Oxisols, the old, highly weathered soils common on stable land surfaces in tropical regions, are widespread in Brazil. The clay fraction consists predominately of the end products of chemical weathering, kaolinite, gibbsite, goethite, and hematite. Aggregates (1,000 to 50  $\mu\text{m}$ ) were studied to determine geochemical surface depletions due to plant uptake and leaching in an attempt to understand nutrient cycling. No geochemical gradients were observed in the aggregates indicating that such depletions are minimal.

*Surface Constraints on Hexavalent Chromium Incorporation in Calcite* (R. Reeder, SUNY, Stony Brook): Hexavalent chromium, a serious environmental contaminant, is characterized by high mobility in soils and aquifers partly because of its weak interaction with mineral surfaces. Recent studies have shown that uptake of chromate by coprecipitation with calcite may be enhanced significantly by rapid crystallization, such as may be found during wetting/drying or evaporative conditions. Micro-XRF analyses demonstrated that chromate is preferentially incorporated into vicinal region A, in contrast with previous results on  $\text{SO}_4^{2-}$  and  $\text{SeO}_4^{2-}$  which were preferentially incorporated into vicinal face B. The results demonstrate that the presence of multiple, structurally distinct surface sites influences Cr(VI) uptake behavior by calcite.

*Metal Sorption on Soil Manganese Oxides* (D. Ross, University of Vermont): Soil manganese oxides contain reactive sites that affect the behavior of many contaminant metals through sorption and, in some cases, oxidation. These oxides are more reactive than synthetic Mn oxides. MicroXAFS coupled with metal adsorption experiments were used to study the surface reactivity of native soil Mn oxides from Vermont's Champlain Valley. Surface reactivity was assessed by the Cr oxidation test (the quantity of Cr(VI) formed from added Cr(III)Cl<sub>3</sub>). The combination of these techniques provided insights on the nature of the reactive sites. Addition of Mn(II), Co(II), Cu(II), and Pb(II) all significantly decreased the soils ability to oxidize added Cr(III), usually in the order Mn>Co>Pb>Cu. Sorption of these added metals appeared to occur primarily in regions of high Mn oxide concentration.

*Ferric and Ferrous Iron Diffusion in Silicate Melts* (D. Baker, McGill University): The differing rates of diffusion between ferrous and ferric iron can act as a fractionation mechanism during crystal growth, crystal dissolution, separation of a fluid phase from the melt, and the mixing of two melts. This fractionation can ultimately affect the stability and distribution of minerals during crystallization. In particular, the stability of magnetite is critically dependent upon the concentration of ferric iron. MicroXAFS measurements of ferrous/ferric ratios support the hypothesis that oxidation state exerts a significant effect on the diffusion of a cation. At 1315C in air, the diffusion coefficient for ferrous iron in this system is  $7.2 \times 10^{-12} \text{ m}^2 \text{ s}^{-1}$  and for ferric iron is  $2.5 \times 10^{-12} \text{ m}^2 \text{ s}^{-1}$ .

*Uranium (VI) Incorporation in Iron Oxide Minerals* (J. Coughlin, University of Georgia): The incorporation of uranium (U) into the structures of naturally occurring mineral phases may be one method by which the aqueous transport of U in the environment can be retarded. In the absence of high levels of complexing ligands such as carbonate, dissolved U species have a high affinity for Fe oxide minerals including hematite and goethite. MicroXAFS results suggest uranium can be incorporated into Fe oxides as a uranate species until a point of saturation is reached, and that beyond this excess precipitating U(VI) forms discrete crystalline uranyl phases that resemble schoepite. These results provide compelling evidence that U can be incorporated within Fe oxides.

*Heavy Metal Species in Sediments of Lake Süßer See, Germany* (M. Duff, University of Georgia): Almost all streams in the Mansfeld (eastern Germany) mining region feed into Lake Süßer See where the lake sediments have accumulated heavy metals. The sediment metal speciation was studied to determine their hazard potential with regard to remobilization and to discover the geochemical processes of heavy metal accumulation. Spectroscopic studies on sediment samples indicate that most of the heavy metals are bound in sulfides (ZnS, CuS, Cu<sub>2</sub>S, CuFeS<sub>2</sub>). For Zn, other phases are present, such as Zn(II)-carbonate or Zn(II)-hydroxycarbonate and possibly trace amounts of ZnO. The micro-XRF elemental imaging showed that some of the Pb was co-associated with Zn (possibly as a solid solution with ZnS). The micro-XANES spectra for Pb at these Zn-enriched regions and at Zn-depleted regions resembled that of PbS.

## **GRANTEE: THE CITY COLLEGE OF THE CITY UNIVERSITY OF NEW YORK**

Benjamin Levich Institute & Department of Physics  
New York, New York 10031

**Grant:** DE-FG02-93-ER14327

### **Particulate Dynamics in Filtration and Granular Flow**

*Joel Koplik 212-650-8162, fax 212-650-6835, koplik@sci.ccny.cuny.edu*

**Objectives:** We propose to seek a better understanding of the dynamics of collective particulate motion in deep-bed filtration processes, in flows in geological fracture systems, and in gravity-driven granular flows.

**Project Description:** Three general topics will be considered. First, the results of our previous studies of the motion of particles suspended in a fluid flowing in a porous medium will be used in network-model simulations of deep-bed filtration processes. Secondly, we will study transport processes (fluid flow, passive tracer dynamics, and suspended particle dynamics) in geological fractures, where the rock surface is a self-affine fractal. Here we will use scaling arguments and lattice Boltzmann numerical simulations, and collaborate with an experimental group at Orsay. Third, we will consider several topics in granular flows, specifically segregation and mixing processes, simple models of the effects of surrounding fluid in granular flows, and the structure of the wake of an obstacle placed in a gravity-driven flow.

**Results:** This year's progress on the topics listed above is as follows.

(1) We have concluded our simulational studies of deep-bed filtration in network models of statistically homogeneous porous media. In this work a fully dynamical evolving pore space is studied, leading to rather extensive computations. The general features of these simulations are quite consistent with experiment, and also show the same trends as found with more simplified modeling, but show quantitative agreement only if the pore size distribution is "just right".

(2) We have developed relatively simple theoretical estimates for the single-phase permeability and the effective hydrodynamic dispersivity of two-dimensional self-affine rough fractures, and confirmed them by numerical simulations using the lattice Boltzmann method. The more realistic three-dimensional problem is much harder, and we are first using the numerical simulations to gain some insight into how to model the transport coefficients. Experimental work at Orsay is in progress.

(3) We have been using an event-driven particle dynamics calculation to study the granular analog of the classical fluid mechanics problem of the wake of a sphere in a uniform flow. Here, a large fixed disk is placed in the path of a uniform flow of smaller inelastic disks, and the flow field is studied. Some effort was needed to produce an incident steady flow, due to losses from intergranular friction and simulation end-region effects. Preliminary results indicate that compressibility of the granular fluid is crucial, and that there exist different regimes of behavior as a function of mean velocity.

## **GRANTEE: UNIVERSITY OF COLORADO**

Cooperative Institute for Research in Environmental Sciences  
Colorado Center for Chaos & Complexity  
Department of Physics  
Campus Box 216, Boulder, CO 80309

**Grant:** DE-FG03-95ER14499

### **Analysis and Interpretation of Multi-Scale Phenomena in Crustal Deformation Processes: Using Numerical Simulations of Complex Nonlinear Earth Systems**

*John B. Rundle 303-492-5642, fax 303-492-5070, rundle@cires.colorado.edu; W. Klein, Boston University*

**Objectives:** To develop a physical understanding of the origins of geodetic crustal strains in nonlinear geomechanical systems, to examine the space-time patterns and correlations that occur in these systems, and to use these patterns to forecast the future activity that may produce disasters affecting a wide variety of critical energy facilities.

**Project Description:** The complex earth system generates a variety of phenomena that are highly non-linear and operate over a broad range of spatial and temporal scales. Signatures of these processes include scaling (fractal distributions), global and local self-organization, intermittency, chaos and the emergence of coherent space-time structures and patterns. We are using massively parallel simulations to model geodynamical effects observed in earthquake systems in order to determine the origin of these phenomena. These investigations and the theoretical efforts done in parallel are particularly aimed at quantifying the limits of predictability for disasters such as earthquakes that occur within the earth system. We are currently continuing our development of the theoretical and computational tools that allow us to both obtain sufficient data on realistic models and to analyze the data we obtain. From these simulations, we will then predict geodetic and other deformation associated with impending earthquakes to be tested against Global Positioning System, Synthetic Aperture Radar, seismicity and other field data. We have made significant advances in several areas. These include: 1) the application of the theoretical model we have developed to derive and or calculate known properties of fault systems. This includes the calculation of the power law increase of Benioff strain observed prior to characteristic earthquakes and the derivations from our model of the rate and state friction laws. 2) We have made additional advances in understanding long-lived patterns that are exhibited by fault systems. Analysis of these patterns has led to a greater understanding of the relation between events on connected faults and how this impacts forecasting. It has also provided additional support for the critical point model of main events in a shock sequence. 3) We have extended our understanding of earthquake fault models. This has taken two forms. First we have analyzed the moment scaling and found a richer structure than was initially suspected and we have extended our investigations to a wide range of models and have identified several variables which when varied strongly modify the observed phenomena.

## **GRANTEE: UNIVERSITY OF COLORADO**

Department of Geological Sciences  
Boulder, CO 80309-0399

**Grant:** DE-FG03-95ER14518

### **Evolution of Rock Fracture Permeability During Shearing**

*Shemin Ge 303-492-8323, fax 303-492-2606, ges@spot.colorado.edu; Hartmut Spetzler*

**Objectives:** To investigate the evolution of fracture apertures from the initial crack to a state with a certain amount of slip displacement under shearing.

**Project Description:** Significant progress has been made in understanding how fracture permeability relates to geometric factors of fracture surfaces and stress conditions. However, the history of the earth reveals a dynamic environment in which small fractures dislocate after their initial separation and large faults slip over observable distances. Yet, limited effort has been made to study the evolution of fracture permeability under varying stress and deformation conditions. Understanding how apertures change dynamically during shearing would help interpret how fracture permeability varied in the past and thereby enhance our ability to infer paleo-systems of fluid flow and mineral or energy transport. This project aims at studying the evolution of fracture permeability in a shear deformation environment.

**Results:** The main effort in the past year has focused on the theoretical and numerical study of the effects of non-Darcian flow on solute transport in rock fractures. Studies have been conducted to understand the relationship between the dispersion coefficient and the fluid velocity, or Peclet number,  $Pe$ , in rough-walled fractures. The relationship between the dispersion coefficient  $D_L$  and the average fluid velocity,  $U$ , is often assumed to be linear. It is also reported that the dispersion coefficient is proportional to the velocity raised to the power of  $n$ , where  $n$  is 2 for parallel-plate fractures and 1.3 for rough fractures. Recent studies have shown that the relationship between the dispersion coefficient and Peclet number can be fitted by a quadratic equation, which combines two dispersion mechanisms: Taylor dispersion proportional to  $Pe^2$  and macro dispersion proportional to  $Pe$ . Experiments were conducted at Reynolds number,  $Re$ , less than 1 in order for flow to stay in the Darcian flow regime. In practice, hydraulic gradients much higher than natural gradient are often used to clean up contaminated groundwater, where non-Darcian flow is expected to occur. Under these circumstances, the solute dispersion mechanism needs to be evaluated for the full range of flow domains from Darcian to non-Darcian flows. In addition, only single solute has been used in existing studies to derive the  $D_L$ - $Pe$  relationship. In the field, different solutes with different molecular diffusion coefficients may transport together through rock fractures. It has not yet been studied whether the relationship derived from one solute is applicable to situations with multi-solutes, especially in the non-Darcian flow domain.

We explored the applicability of the  $D_L$ - $Pe$  relationship derived from a one-solute system under a full range of flow regimes from Darcian to non-Darcian flows. We adopted the Lattice Boltzmann (LB) method to simulate solute transport in rough fractures. Fluid flow simulations at various fluid velocities were conducted to find the  $Re$  at which non-Darcian flow starts (Figure 1a). At  $Re$  around 15 to 20, the relationship between the applied body force in flow direction and the average fluid velocity deviates from a linear pattern. Body force times particle density is equivalent to pressure gradient. We used two solutes, one of which (Solute 2) has a molecular diffusion coefficient two times higher than the other (Solute 1). Hence, to keep the  $Pe$  the same for both solutes, the fluid velocity of Solute 2 should be two

times as high as that of Solute 1. Figure 1b confirms that the relationship between  $D_L/D_m$  and  $Pe$  is well described by a quadratic equation. For Solutes 1 and 2, at  $Re$  of 15 to 20, non-Darcian flow starts, which corresponds to the  $Pe$  of 300 to 400 and  $Pe$  of 150 to 200, respectively. Most data points on the Solute 1 curve are within the Darcian flow regime. The solute 2 curve, on the other hand, covers the range from Darcian and non-Darcian flows. For  $Pe$  less than 150 and 200, *i.e.*, within Darcian flow regimes, the relationship of both solutes agrees well. But for  $Pe$  higher than 150 to 200, the Solute 2 curve deviates from the Solute 1 curve, which is mainly due to the effects of non-Darcian flow. This result implies that within the Darcian flow domain, the solute dispersion to diffusion coefficient ratio depends mainly on the  $Pe$ . As flow goes to the non-Darcian flow regime,  $Re$  also becomes a factor to find solute dispersion in addition to the  $Pe$ . Therefore, the relationship between dispersion and  $Pe$  needs to be thoroughly evaluated for every solute, when the flow is in non-Darcian flow.

(a)

(b)

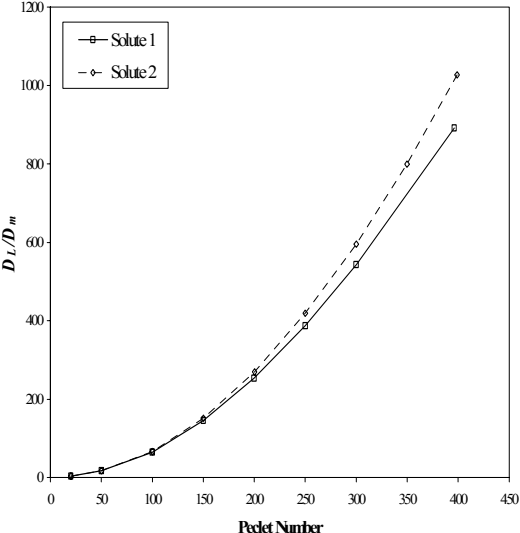
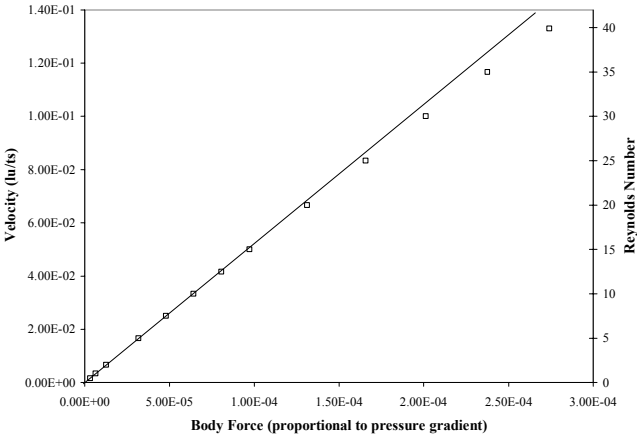


Figure 1. The relationship between  $D_L/D_m$  and  $Pe$  is affected by non-Darcian flow which starts around  $Re=15$  to  $20$  corresponding to  $Pe=150-200$  in Solute 2. Diffusion coefficients of Solute 1 and 2 are  $0.005$  and  $0.01$   $lu^2/ts$ , where  $lu$  and  $ts$  are lattice unit and time step. Body force times density is equivalent to pressure gradient.

## **GRANTEE: UNIVERSITY OF COLORADO**

Department of Geological Sciences  
Boulder, Colorado 80309-0399

**Grant :** DE-FG03-99ER14979

### **Nucleation and Growth Kinetics of Clays and Carbonates on Mineral Substrates**

*Kathryn L. Nagy 303-492-6187, fax 303-492-2606, kathryn.nagy@colorado.edu*

**Objectives:** To investigate the kinetics of nucleation and growth of clays and carbonates on mineral substrates. Data are needed to model reactive fluid flow in porous media as applied to the natural processes of soil formation and sediment diagenesis, and to engineered processes such as subsurface CO<sub>2</sub> sequestration.

**Project Description:** Secondary mineral nucleation and growth controls global cycling of elements during weathering, sequestration of contaminant metals in the environment, and fluid flow pathways in sedimentary basins. Although simulations of fluid flow now include complex reactions with minerals they still cannot reproduce natural systems because kinetic data are lacking, especially data describing heterogeneous nucleation and growth. Experiments are conducted to nucleate and grow clays and carbonate on mica, quartz, and feldspar as a function of solution composition and temperature. Substrate characteristics that control nucleation such as surface charge and molecular-scale structure are being evaluated. Rates are determined from solution changes and atomic force microscopy (AFM) images of precipitate volume. Synchrotron X-ray reflectivity and Extended X-ray Absorption Fine Structure spectroscopy (with P. Fenter and N. Sturchio at Argonne National Laboratory and A. Manceau at the University of Grenoble) are used to assess nucleation mechanisms. Quantitative rate laws will be constructed.

**Results:** We have determined the structure of the muscovite mica-water interface using X-ray reflectivity at sector 12 on the bending magnet beamline (BESSRC-CAT) of the Advanced Photon Source (APS). The data show that the surface of muscovite relaxes slightly in the presence of water to a depth of no greater than one unit cell, and that the overlying water is structured to within one monolayer. The structure of this interface has also been determined reproducibly to ~ 1 Angstrom-scale resolution in the presence of 0.01 M CaCl<sub>2</sub> and 0.01 M BaCl<sub>2</sub> solutions with the goal of determining the nature of the sorbing cation (divalent vs. monovalent metal-chloride; inner vs. outer sphere) and structure of the associated water molecules. The data also provide information on surface roughness which is compared to roughness determined from AFM images. Reversibility of the structural data has been demonstrated by simple cation exchange experiments. Parallel experiments designed to nucleate and grow calcite under controlled compositional conditions on the muscovite basal surface are in progress using steady-state flow experiments in the fluid cell of an atomic force microscope. The structure of the orthoclase feldspar-water interface was also determined at the APS in collaboration with P. Fenter.

## **GRANTEE: UNIVERSITY OF COLORADO**

Department of Civil, Environmental and Architectural Engineering  
Boulder CO 80309-0428

**Grant:** DE-FG03-96ER14590

### **Two-Phase Immiscible Fluid Flow in Fractured Rock: The Physics of Two-Phase Flow Processes in Single Fractures**

*H. Rajaram, 303-492-6604, fax 303-492-7317, hari@colorado.edu; R. J. Glass, Sandia National Laboratories, M. J. Nicholl, Oklahoma State University*

**Objectives:** Employ detailed physical experiments and high-resolution numerical simulations to develop a quantitative understanding of the critical processes controlling two-phase flow and transport in fractures. Fundamental understanding may subsequently be abstracted for application to large-scale problems in petroleum extraction, isolation of hazardous or radioactive waste, remediation of subsurface contaminants, and CO<sub>2</sub> sequestration.

**Project Description:** Under two-phase immiscible flow conditions, fluid flow and solute transport characteristics of the fracture are controlled by the geometry of the respective phases. In turn, phase geometry is determined by a combination of aperture variability, phase accessibility, capillary and viscous effects associated with the two-phase flow processes themselves, and external forces such as gravity. In addition, if one of the fluids is slightly soluble in the other, mass transfer between the phases will influence phase geometry.

In this collaborative project between Sandia National Laboratories, Oklahoma State University, and the University of Colorado at Boulder, systematic physical experimentation is coupled with concurrent numerical simulation to explore the factors controlling phase geometry, flow, transport, and inter-phase mass transfer in rough-walled fractures. A high-resolution light-transmission technique has been developed to allow accurate experimental measurements (aperture, phase geometry, solute concentration) in transparent analog fractures. Use of this technique will lead to data of unprecedented accuracy for evaluating current understanding of fundamental processes, and motivate refinement of theoretical concepts.

**Results:** Evaluation of data from a previous field experiment in which infiltration was followed by excavation of the rock mass shows complicated behavior in an unsaturated fracture network that is consistent with recent laboratory investigations in single fractures. Short term ponded infiltration (36 minutes) into the dry network (impermeable matrix) produced viscous dominated flow near the infiltration surface, with a transition to unsaturated conditions at shallow depth (~2-3 m); phase geometry within the excavated rock mass changed from pervasive to complicated, exhibiting evidence of fragmentation, preferential flow, fingers, irregular wetting patterns, and varied behavior at fracture intersections. Electromagnetic Resistance Tomography performed during infiltration confirms rapid penetration, followed by equally rapid drainage of the network following infiltration. Estimates suggest that ~85 to 99% of the fluid slug escaped the excavated area; hence the actual penetration depth could have been quite large.

The occurrence of random and non-unique behavior during measurement of two-phase constitutive properties in fractures or porous media was investigated by visualizing micro-scale phase displacement

processes during equilibrium retention and transient outflow experiments. In both cases, the drainage process is shown to be a mixture of fast gas fingering, and slower gas back-filling. Each of these micro-scale processes is controlled by: the size and the speed of the applied boundary step, the initial saturation and phase geometry, and small-scale heterogeneities. Because the micro-scale processes combine to yield macro-scale behavior, the same controls will influence measured effective properties, thereby calling into question current definitions for constitutive properties.

Detailed numerical exploration of the continuum-scale Richards equation with standard monotonic constitutive relations shows it to be inadequate for simulation of unsaturated flow in initially dry, highly nonlinear, and hysteretic media (such as fractures) where gravity-driven fingers occur. Recent published reports of finger-like numerical solutions with nonmonotonic profiles are found to be artifacts of the downwind averaging method that are generated by the combined effects of a truncation error induced oscillation at the wetting front and capillary hysteresis.

Micro-scale phenomena were observed to control macroscopic behavior during surfactant flood mobilization and solubilization of nonaqueous phase liquids (NAPLs) within a fracture. At relatively low capillary numbers ( $N_{ca} < 10^{-3}$ ), surfactant mobilization floods resulted in higher NAPL saturations than for similar  $N_{ca}$  pure water floods. These differences in macroscopic saturations are explained by differences in micro-scale mobilization processes. Solubilization of the residual NAPL remaining after the mobilization stage of the surfactant flood was dominated by the formation of micro-scale dissolution fingers, which produced nonequilibrium macro-scale NAPL solubilization. A macroemulsion phase also was observed to form spontaneously and persist during the solubilization stage of the experiments.

Dissolution of NAPLs in variable-aperture fractures couples fluid flow, transport of the dissolved NAPL, interphase mass transfer, and the corresponding NAPL-water-interface movement. Each of these fundamental processes is controlled by the variability of the fracture aperture and the geometry of the entrapped NAPL. Development of a depth-averaged computational model of dissolution that incorporates the small-scale processes controlling dissolution precludes the need for empirical mass-transfer coefficients. Implementation of an efficient algebraic multigrid algorithm for solving the flow and transport equations allows dissolution simulations at scales ( $> 2 \times 10^6$  nodes) much larger than the scale of the largest regions of entrapped NAPL. Direct comparison of a dissolution experiment to a simulation suggests that this coupled depth-averaged approach to modeling dissolution accurately predicts the evolution of NAPL-mass and NAPL-distribution within the fracture.

## **GRANTEE: UNIVERSITY OF COLORADO**

Cooperative Institute for Research in Environmental Sciences  
Dept. of Geological Sciences  
Boulder, Colorado 80309

**Grant:** DE-FG03-94ER14419

### **Seismic Absorption and Modulus Measurements in Single Cracks and Porous Rocks: Physical and Chemical Effects of Fluids**

*Hartmut Spetzler, 303-492-6715, fax 303-492-1149, spetzler@spot.colorado.edu*

**Objective:** We are studying the effects of small amounts of organic substances (*e.g.*, alcohols, chlorinated hydrocarbons) on the mechanical properties of partially saturated porous rocks. The eventual goal is the development of a tool for monitoring changes in organic contaminant levels near waste sites.

**Project Description:** Small amounts of adsorbed organic substances on a surface significantly change the physical behavior (*e.g.*, wettability) of that surface. In porous rocks, this changed wettability can inhibit fluid flow, and thus change the bulk mechanical properties of the rock. An apparatus has been developed that measures Young's modulus and attenuation ( $1/Q$ ) of both real rocks and artificial samples. Measurements of attenuation in partially saturated, contaminated sandstones are being made in parallel with the development of a three-dimensional model that incorporates new understanding of physicochemical surface relaxation mechanisms.

**Results:** A new relaxation mechanism that can produce attenuation in rocks has been observed and described. This mechanism is seen to be sensitive to surface chemistry (presence of organic contaminants). Attenuation measurements of a single crack contaminated with n-propanol and partially saturated with distilled water show a large increase in attenuation at frequencies of 0.001-1 Hz. This increase is attributed to surface relaxation and its effect on contact angle hysteresis. These inhibit fluid flow at certain frequencies due to time-dependent surface wettability. Imbibition of fluids into clean and into contaminated Hele-Shaw cells confirm the data collected under dynamic conditions in single cracks. Theory and observations in single cracks predict that a chlorinated solvent (TCE) should produce a measurable attenuation signature in partially saturated sandstones, but attenuation measurement results of these rocks have been inconclusive, possibly due to incomplete contamination of the pore walls. We are now developing a method of producing repeatable contamination states by forced injection of contaminant and/or saturant. This avenue of research is expected to yield a more complete understanding of the combination of saturation and contamination conditions that lead to the attenuation mechanism of interest.

## **GRANTEE: COLORADO SCHOOL OF MINES**

Department of Chemistry and Geochemistry  
Golden, Colorado 80401

**Grant:** DE-FG03-00ER15090

### **Possible Vertical Migration of CO<sub>2</sub> Associated with Large-Scale Injection into Subsurface Geologic Formations**

*Ronald W. Klusman, 303-273-3617, fax 303- 273-3629, rklusman@mines.edu*

**Objective:** Determine if detectable gas leakage to the surface occurs, and its magnitude, at the CO<sub>2</sub> overpressured Rangely, Colorado oil field. Carbon dioxide-enhanced oil recovery has been in operation at Rangely since 1986.

**Project Description:** One of the proposals for large-scale sequestration of fossil fuel CO<sub>2</sub> is deep geologic disposal in depleted oil/gas reservoirs or deep aquifers. The literature generally ignores the possibility of vertical migration of gases caused by overpressure. Over-pressuring a reservoir or aquifer will be necessary in order to have acceptable rates of dispersal of injected CO<sub>2</sub>.

This research will investigate the possibility of loss of gases from a CO<sub>2</sub> overpressured reservoir. Carbon dioxide has been used for enhanced oil recovery (EOR) at the large Rangely oil field, northwest Colorado since 1986. The research will evaluate the soil gas compositions and fluxes to the atmosphere for evidence of microseepage of either CH<sub>4</sub> and/or CO<sub>2</sub> that originated in the reservoir at a depth of 2000 m. These data will also be supported by measurement of stable carbon isotopes and <sup>14</sup>C to ascertain possible source(s) of the gases. The slowing of microbiological processes in the cold, semiarid climate at Rangely will aid in separating the possible microseepage signal from shallow methanotrophic consumption of CH<sub>4</sub>, and from soil respiration-produced CO<sub>2</sub> in soil gases.

**Results:** Funding became available in mid-October, 2000, when equipment and supplies were ordered. Two reconnaissance field trips for purposes of methodology testing were carried out from December 13-31, 2000. These initial measurements demonstrated small rates of CH<sub>4</sub> exchange across the soil atmosphere interface (+/- 5 mg CH<sub>4</sub> m<sup>-2</sup>day<sup>-1</sup>) over the oil field. Carbon dioxide fluxes were positive (flow from the soil to the atmosphere) and generally <2 g CO<sub>2</sub> m<sup>-2</sup>day<sup>-1</sup> (<0.5 micro moles CO<sub>2</sub> m<sup>-2</sup> sec<sup>-1</sup>). These values are typical for wintertime ranges previously observed in background regions in the Intermountain West. Soil gas concentrations at 30-100 cm depths ranged from <1 ppmv to 12 ppmv CH<sub>4</sub>, and 365 ppmv to >2000 ppmv CO<sub>2</sub>. Samples for stable carbon isotopic determinations on CH<sub>4</sub> and CO<sub>2</sub> were also collected at the same time, but are not yet analyzed. Samples of the injection-and produced-gases were also collected from wellheads for carbon isotope ratio determination.

Some modification of field procedures are being tested now, and at least one more field trip will be made this season, while still under winter conditions. The research will continue in the summer of 2001 to assess the magnitude of the CH<sub>4</sub> and CO<sub>2</sub> exchange rates under summer conditions. It is expected that summer CH<sub>4</sub> exchange rates will be more negative (flow from the atmosphere into the soil) and the flow of CO<sub>2</sub> into the atmosphere will be greater, due to increased soil respiration. Isotopic measurements will continue to assess any potential change in sources of the measured gases.

## **GRANTEE: COLORADO SCHOOL OF MINES**

Center for Wave Phenomena  
Green Center, Golden, CO 80401-1887

**Grant :** DE-FG03-98ER14908

### **Three-dimensional Analysis of Seismic Signatures and Characterization of Fluids and Fractures in Anisotropic Formations**

*Ilya Tsvankin, 303-273-3060, fax 303-273-3478, ilya@dix.mines.edu; Vladimir Grechka;  
Kenneth L. Larner*

**Objectives:** The main goal of the project is to develop efficient velocity analysis and parameter estimation methods for azimuthally anisotropic reservoirs using the 3-D (azimuthal) variation in seismic signatures. The anisotropic parameters can then be related to the reservoir properties that control the flow of hydrocarbons.

**Project Description:** The CSM group is working on the inversion of azimuthally dependent reflection traveltimes and prestack amplitudes for the effective parameters of azimuthally anisotropic media. The combination of  $P$ -waves and converted  $PS$ -waves helps to estimate a representative set of the anisotropic parameters for models containing subvertical fracture systems or tilted transversely isotropic layers. The project includes theoretical studies, development of inversion and processing algorithms and their application to 3-D seismic field data. The inverted anisotropic model is used to evaluate the physical parameters of fracture networks and the lithologic properties of source and reservoir rocks; the rock-physics part of the project is largely addressed by the groups from LLNL and Stanford University. The project results should provide a foundation for high-resolution characterization of heterogeneous anisotropic reservoirs using wide-azimuth multicomponent seismic surveys.

#### **Results:**

*3-D description of dip moveout of  $PS$ -waves and application to parameter estimation for vertical transverse isotropy (VTI media).* An efficient 2-D and 3-D parametric description of reflection moveout of mode-converted waves was developed for arbitrary anisotropic media and applied to the joint inversion of  $P$ -wave and  $PS$ -wave moveout data in VTI media.

*Velocity analysis of converted waves based on the hyperbolic moveout equation.* A special resorting procedure that we call “resorting to the travelttime minimum” (RTM) removes the asymmetry of converted-wave moveout and makes conventional velocity-analysis methods originally developed for pure modes suitable for  $PS$ -waves.

*Feasibility of depth-domain velocity analysis for VTI media using surface  $P$ -wave data.* Anisotropic reflection tomography and analytic approximations for normal-moveout velocity demonstrate that  $P$ -wave reflection data can be inverted for the vertical velocity and key anisotropic parameters  $\epsilon$  and  $\delta$  if the model contains non-horizontal intermediate interfaces.

*Inversion of normal moveout for monoclinic media.* The combination of the NMO ellipses and vertical velocities of  $P$ -waves and two split  $S$ - or  $PS$ -waves is inverted for the anisotropic parameters of monoclinic media formed by two or more vertical fracture sets.

*Estimation of fracture parameters for models with orthorhombic symmetry from reflection seismic data.* Compliance formalism for the effective anisotropic parameters of fractured reservoirs with orthorhombic symmetry is used to devise practical fracture-characterization algorithms based on the reflection signatures of  $P$ - and  $PS$ -waves.

*Estimation of fracture parameters for models with monoclinic symmetry from reflection seismic data* A complete fracture-characterization procedure is developed for two monoclinic reservoir models, one containing orthogonal vertical fracture sets and the other formed by a single set of microcorrugated fractures.

**GRANTEE: COLUMBIA UNIVERSITY**

Lamont-Doherty Earth Observatory  
Palisades, New York 10964-8000

**Grant :** DE-FG02-95ER14572

**Rock Varnish Record of Holocene Climate Variations in the Great Basin of Western US**

*Tanzhuo Liu, 845-365-8441, fax 845-365-8155, tanzhuo@ldeo.columbia.edu; Wallace Smith Broecker, 845-365-8413, fax 845-365-8169, broecker@ldeo.columbia.edu*

**Objectives:** The objective of this research is to document Holocene climate variations recorded in rock varnish from the Great Basin of western US.

**Project Description:** Rock varnish is a very slowly accreting (<1 to 40  $\mu\text{m}$  /ky) patina on subaerially exposed rock surfaces in arid to semi-arid deserts. Due to its sedimentary origin, rock varnish displays layered stratigraphy. Our previous work funded by the DOE indicates that the chemical composition of varnish stratigraphy changes markedly with climate. During dry periods it is manganese-poor and during wet periods manganese-rich. Such climate-related stratigraphy in varnish can be correlated across a given geographic region, suggesting that the climate signals recorded in varnish are of regional extent. In the Great Basin of western US, manganese-poor varnish layers formed during interglacials when the Great Basin was unusually dry, and manganese-rich layers were deposited during periods of glaciation when the Great Basin was wetter than at present. Therefore, rock varnish can be used as a recording media to study the climate, in particular moisture history of the world's deserts.

Varnish samples will be collected from a number of independently and radiometrically dated geomorphic features of latest Pleistocene and Holocene age in the entire Great Basin. These samples will then be thin-sectioned to uncover the distinct lamination patterns in rock varnish that recorded Holocene climate variations. Microchemical analyses with electron probe will be used to quantitatively characterize the varnish lamination patterns. The ages of the sampled geomorphic features will be utilized to provide radiometric time constraints for calibration of the Holocene lamination sequence. In addition, relative thickness of rock varnish will be used to interpolate ages for the internal layers within the varnish stratigraphy.

**Results:** Based on examinations of hundreds of varnish samples from the radiometrically dated geomorphic features in the Great Basin of western US, we have established the Holocene lamination sequence. This sequence consists of twelve evenly spaced weak dark layers interfingering with thirteen orange layers. Age calibration of varnish samples from Fish Lake Valley, eastern California and Las Vegas Valley, southern Nevada indicates that the six dark layers in the upper portion of the sequence deposited over the last ~6000  $^{14}\text{C}$  years, and the five dark layers in the lower portion of the sequence deposited slightly after the termination of the Pleistocene, in response to the late and early Holocene relatively wet climate in the Great Basin, respectively. The nearly evenly spaced twelve dark layers in the Holocene varnish record suggest millennial-scale climate cycles that appear to be tied to the Holocene millennial-scale cold events recorded in the deep sea sediments of the subpolar North Atlantic. Also, varnish data collected over the last five years from the entire Great Basin of western US and three other desert regions of the world indicate a positive correlation between Mn content in Holocene varnishes and present-day rate of precipitation, suggesting the potential use of rock varnish as a

paleowetness recorder in the world's deserts. Future work will be focused on radiometric calibration of the varnish record and building its thickness-based numerical chronology.

## GRANTEE: UNIVERSITY OF CONNECTICUT

Department of Marine Sciences  
1084 Shennecossett Road  
Groton, CT 06340-6097

**Grant :** DE-FG02-95ER14528

### Geochemical and Isotopic Constraints on Processes in Oil Hydrogeology

*T. Torgersen, 860-405-9094, fax 860-405-9153, Thomas.Torgersen@Uconn.edu; B.M. Kennedy, Lawrence Berkeley National Laboratory, 510-486-6451, fax 510-486-5496, bmkennedy@lbl.gov*

**Objectives:** This research project (with Lawrence Berkeley National Laboratory) evaluates the processes that produce, dissolve and distribute noble gases and noble gas isotopes among liquid hydrocarbon, gaseous hydrocarbon and aqueous phases. This project also uses the abundances and isotopic composition of noble gases in hydrocarbon systems to evaluate hydrocarbon sources and characteristics, groundwater end-members, and migration processes, mechanisms, and time scales.

**Project Description:** The mechanisms, processes, and time scales of fluid flow in sedimentary basins represent fundamental questions in the Earth Sciences with direct application to exploration and exploitation strategies for energy and mineral resources. This project investigates the noble gas composition of hydrocarbon samples on a basin and field scale where adequate commercial production and ancillary information are available, to provide a test of the use and applicability of noble gases to delineate end members, migration mechanism and migration paths for hydrocarbons. Samples are analyzed for the five stable noble gases (He, Ne, Ar, Kr, Xe) and their isotopes.

**Results:** (1) *Sources of Air-Like Noble Gases in Hydrocarbon Reservoirs:* The atmospheric component is identified primarily by isotopic composition and by relative gas abundances (*e.g.* Ne/Kr/Xe/Ar), determined from the abundances of non-radiogenic isotopes, typically  $^{20,22}\text{Ne}$ ,  $^{36}\text{Ar}$ ,  $^{84}\text{Kr}$ , and  $^{130}\text{Xe}$ . It is generally assumed that the source for all atmospheric noble gases in subsurface fluids is air-saturated sea, meteoric or connate water. Evidence for water-derived noble gases in hydrocarbon systems is extensive and provides strong support that water plays an important role in hydrocarbon systems. However, evidence has surfaced suggesting that the hydrocarbons themselves are also a source of atmospheric derived noble gases (Torgersen and Kennedy, 1999) with a relative abundance pattern that is highly enriched in the heavy noble gases (Kr and Xe).  $^{130}\text{Xe}/^{36}\text{Ar}$  enrichment factors up to ~600 relative to air have been observed. This component cannot be derived from air-saturated water by distillation and/or solubility driven equilibration with oil, gas, or oil-gas systems. Instead, we believe this fractionated air component is derived from the petroleum source rock. Support for this hypothesis is provided by laboratory studies of noble gases in carbon-rich and petroleum source rocks.

We now have evidence for a third air-like noble gas component, identified by an unusual Ne/Kr/Xe/Ar relative abundance pattern that is unlike air saturated water or the highly fractionated source rock component. Systematic field-wide trends in noble gas compositions suggest that this third air-like

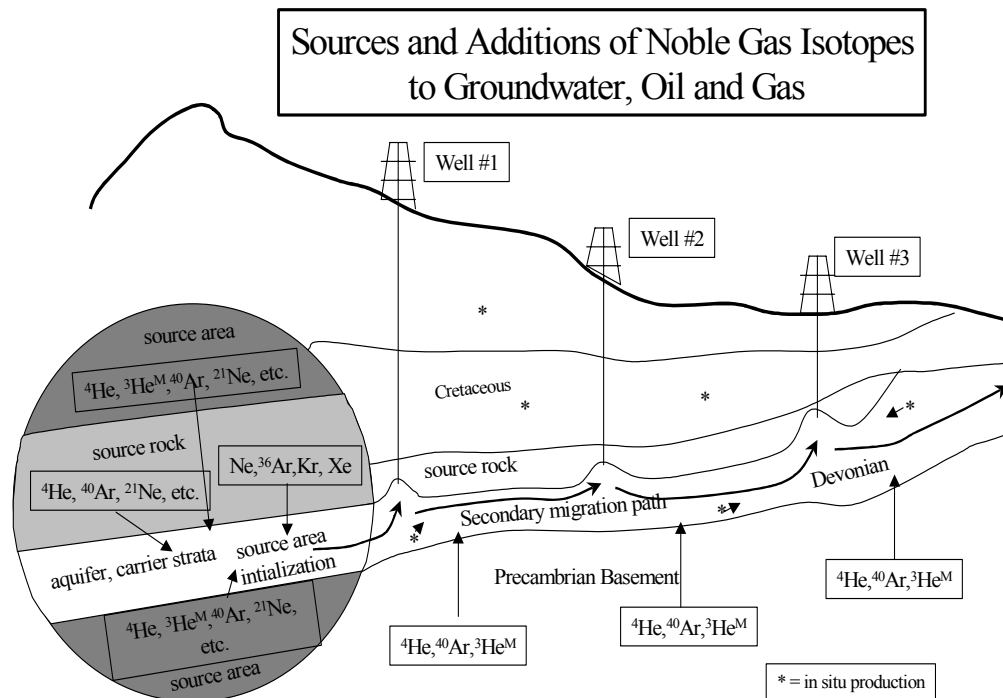


Figure 1: A diagrammatic illustration of Alberta hydrocarbon system showing the sources and additions of noble gas isotopes to the groundwater, groundwater/oil and oil/gas systems. Note that the source rock most likely contributes to the enriched F[Xe] and F[Kr] initial condition but that both the source rock and the source area can contribute radiogenic and nucleogenic noble gas isotopes as well as mantle ( $^3\text{He}$ ) to the initial system. Along the flow path,  $^4\text{He}$ ,  $^{40}\text{Ar}$  and (possibly) mantle ( $^3\text{He}$ ) can be added to the groundwater and are exchanged via solubility into the oil and then gas hydrocarbon phases. The integrated measure of the hydrocarbon interaction with the ASW groundwater is quantified by the  $^{36}\text{Ar}$  concentration in the hydrocarbon. Kennedy and Torgersen (2000) have also shown the addition of an enriched F[Ne] from the groundwater along the flow path. Its source is as yet undetermined.

component may be derived from the reservoir sediments. Understanding the formation and occurrence of these atmospheric noble gas sources and their interaction with oil and natural gas systems will lead to a better understanding of the processes and scales related to primary and secondary migration, basin scale fluid movement, gain or loss of secondary porosity, and biodegradation.

(2) *Noble Gas Evolution in Hydrocarbon Fields: Secondary Migration Processes and End-member Characterization:* Hydrocarbons carry an indigenous noble gas component acquired from the hydrocarbon source area. Typically, this component contains radiogenic noble gases (e.g.  $^4\text{He}$  and  $^{40}\text{Ar}$ ) and an air-like component characterized by highly fractionated abundance patterns ( $^{130}\text{Xe}/^{36}\text{Ar}$  ratios > 600 times the ratio in air have been observed). The solubility of noble gases in hydrocarbons and water dictate that noble gases will be stripped from groundwater (air saturated water, ASW) during secondary migration and will dilute the indigenous noble gas signature in the hydrocarbon. The composition of ASW is also modified in the carrier strata by basal fluxes and *in situ* production. The degree of dilution by the modified ASW component is a function of the total amount of water with which the hydrocarbon interacts during secondary migration (water/hydrocarbon interaction ratio). Systematic

trends in noble gas composition ( $F[\text{Ng}]$  and isotopic compositions vs.  $1/[^{36}\text{Ar}]$ ) identify wells which produce hydrocarbons originating from common source areas and that interact with a common groundwater. Zeroth order interpretation of noble gas evolution as simple mixing can characterize noble gas composition of the source area (slope of the line) and modified groundwater with which it interacts (the intercept at  $1/[^{36}\text{Ar}] \sim 0$ ). Application of the concept to multiple data sets (published and unpublished) provides proof of concept and identifies distinct and readable noble gas evolution trends that are interpretable as secondary migration paths.

In the gas fields of Alberta, Canada, evolution trends defined by noble gas compositions support the hydrologically defined secondary migration flow paths of Garven (1989) and Hitchon (1984). Two groups of wells have source areas (distinct from source rock) that are characterized by very large but different enrichment factors of radiogenic  $^4\text{He}$  and  $^{40}\text{Ar}$  (as well as  $^{21}\text{Ne}$ ,  $^{136}\text{Xe}$ ) that could not have been derived solely from the source rock. These large enrichments suggest that Tertiary orogeny, preceding secondary migration, degassed large volumes of old crust into the source areas. This noble gas evolution defined scenario supports a role for tectonics in the accumulation of hydrocarbons (Oliver, 1986, 1989). Noble gas evolution analysis can thus provide a fundamental constraint on models of hydrocarbon migration and emplacement.

## GRANTEE: UNIVERSITY OF DELAWARE

Department of Chemistry and Biochemistry  
Newark, Delaware 19716

**Grant:** DE-FG02-89ER14080.A003

### **Development of an Experimental Database and Theories For Prediction of Thermodynamic Properties of Aqueous Electrolytes and Nonelectrolytes of Geochemical Significance at Supercritical Temperatures and Pressures**

*R. H. Wood 302-831-2941, fax 302-831-6335, rwood@udel.edu; Everett L. Shock 314-726-4258, fax 314-935-7361, shock@zonvark.wustl.edu*

**Website:** <http://dogstar.duch.udel.edu/wood/research.html>

**Objectives:** The objectives of this research are to combine new experimental measurements on heat capacities, volumes, and association constants of key compounds with theoretical equations of state and with first principals quantum mechanical predictions to generate predictions of thermodynamic data which in turn allow quantitative models of geochemical processes at high temperatures and pressures.

**Project Description:** This project is part of ongoing collaboration between Prof. Everett Shock of Washington University and Prof. Robert Wood of the University of Delaware, which involves 1) experimental measurements on key compounds 2) making substantial improvements in theoretical equations of state for aqueous nonelectrolytes and electrolytes based largely on these experimental measurements 3) pursuing novel applications of these equations of state to the study of high temperature/pressure geochemical processes involving aqueous fluids, and 4) Developing and using *ab initio* quantum calculations with Molecular Dynamics simulations to predict chemical potentials of aqueous solutes where experimental measurements are impossible or not available. The experimental work is conducted at the University of Delaware. Geochemical applications of the data are done at Washington University. Efforts to improve the equations of state and develop predictive methods are shared between the two labs, because this task in particular requires close collaboration between the two Principle Investigators.

**Results:** We have developed equations for the conductance of mixtures of electrolytes because this combined with our high temperature and pressure conductance apparatus allows measurements of a very wide variety of aqueous equilibria. The equations were tested on aqueous sodium sulfate and an association constant of sodium with sulfate was derived which agrees well with literature data. Measurements on mixtures of sodium acetate and acetic acid have allowed new association constants for sodium with acetate ion and new measurements of the dissociation constant of acetic acid. Our conductance apparatus has been rebuilt with a diamond shield so we can measure acids and bases.

We have developed semi-empirical equations of state that allow predictions at high temperatures and pressures of the properties of almost all solutes in water given little or no experimental data. Two different approaches are used depending on the kind and amount of data available. The more accurate approach is useful for nonelectrolytes only and needs estimates of the gas-phase, water-solute second virial coefficient. The other method gives useful predictions of ions and does not need gas phase virial coefficients but is not as accurate at high temperatures and low water densities. Parameters for this equation for a wide variety of functional groups have been derived allowing predictions of all organic

species composed of the groups C(hydrocarbon), H(hydrocarbon), COOH, CONH<sub>2</sub>, NH<sub>2</sub>, OH, COO<sup>-</sup>, NH<sub>3</sub><sup>+</sup>, from 25 to 300°C thus we can predict the properties of literally millions of compounds by this approach. New experimental data has been used to derive new parameters for the revised Helgson-Kirkham-Flowers (HKF) equation of state. Correlation of these parameters with other properties were developed and used to make predictions for a variety of aqueous non-electrolytes.

We have been developing a molecular dynamic plus quantum chemistry method of predicting (within about 5 kJ) the chemical potential of virtually any solute in water at essentially any temperature and pressure. Tests of this method on water virtually at high temperature show that it worked very well. We have used this method to predict the properties of water at temperatures of up to 2000°C and densities of up to 1.8 gms/cm<sup>3</sup>. We have also made predictions of the sodium chloride ion pair and its ionization constant at high temperatures. We have started calculations of the gas phase properties of H<sub>4</sub>SiO<sub>4</sub> so we can test our method with this solute and make predictions at higher pressures and temperature than are available experimentally.

We have made measurements on the volumetric properties of acetic acid and used them to assess the accuracy of our various predictive methods.

**GRANTEE: UNIVERSITY OF FLORIDA**

Chemical Engineering Department  
Gainesville, Florida 32611-6005

**Grant:** DE-FG02-98ER14853

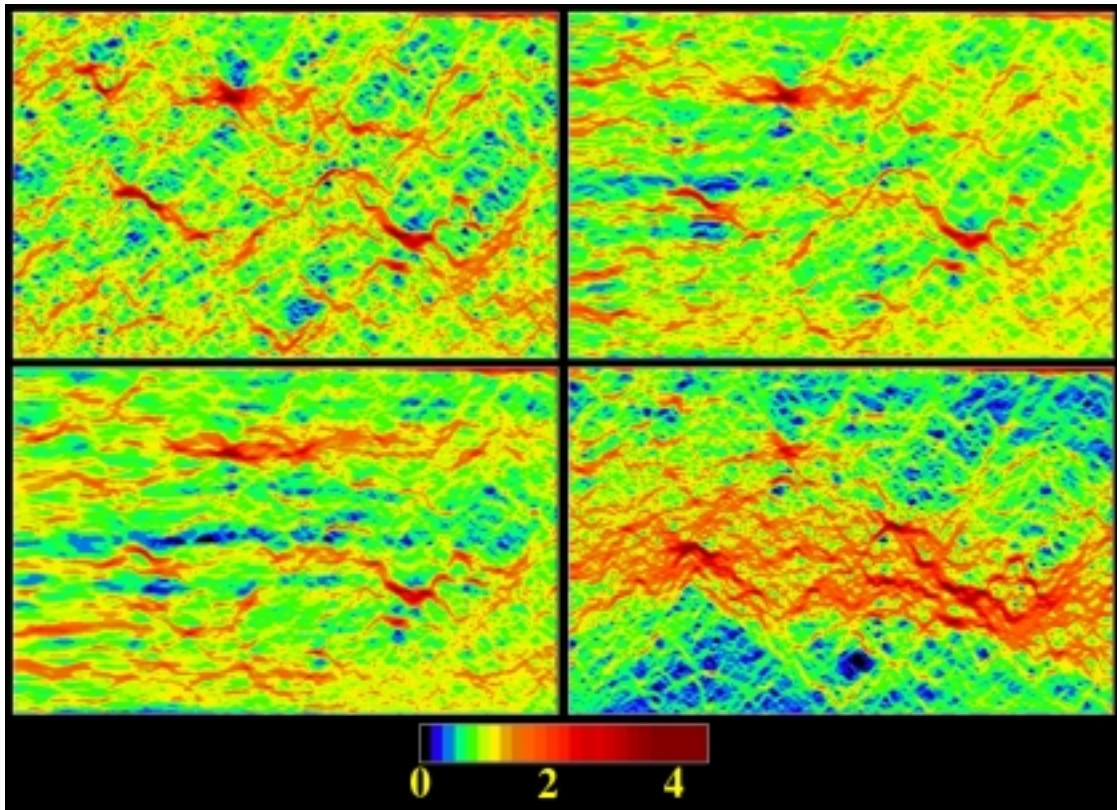
**Pore Scale Simulations of Rock Deformation, Fracture, and Fluid Flow in Three Dimensions**

*Anthony JC Ladd, 352-392-6509, fax 352-392-9513, ladd@che.ufl.edu*

**Objectives:** The overall research objective of this project is to develop micro-mechanical models for the dissolution of porous rocks by a chemically reacting fluid. The aim of the work is an improved understanding of how the coupling between chemical reactions, hydrostatic pressure, and fluid flow produces morphological changes in the sample.

**Project Description:** Numerical simulation techniques are being developed to model the flow of a chemically reacting fluid through a porous matrix. These simulations will combine a very fast fluid flow code with a stochastic simulation of the transport of chemical reactants and products. The code iterates between fluid-flow simulations and cycles of chemical transport and reaction, to predict the changes in morphology arising from the coupling between chemical reactions at the solid-fluid surfaces and the flow of fluid through the pore spaces. The motivation for this work is to explain the observations of Dr. William Durham (Lawrence Livermore National Laboratory), who found that chemical erosion tends to reduce the small-scale spatial heterogeneity in narrow fractures, while enhancing it on larger scales.

**Results:** A new boundary condition for the lattice-Boltzmann model has been developed, which allows a no-slip condition to be specified at scales less than the resolution of the grid (R. Verberg and A.J.C. Ladd, *Phys. Rev. Lett.* 84:2148-2151, 2000). This makes a significant advance in the application of the lattice-Boltzmann method, since it allows for the subtle changes in the shape of the rock matrix as the surfaces erode. Recently, we have simulated acid erosion in a fractured specimen of Carrara marble, using an initial fracture topography that was obtained from Dr. W.B. Durham. The simulations consist of three separate calculations that are iterated to determine the time-evolution of the velocity field and surface morphology. From the initial fracture topography, the velocity field is calculated by means of our new lattice-Boltzmann model, which allows for a continuous variation in the position of the solid surfaces. Next, the steady-state distribution of reactants, and the flux of reactants across each fracture surface are determined by a stochastic solution of the convection-diffusion equation in the presence of this velocity field. Finally, a new structure is determined by eroding material from each fracture surface; the amount of material is proportional to the local flux of tracer particles across that surface. A new three-dimensional image of the fracture was then generated and used in the next iteration. Results from these simulations are illustrated below.



Flow in a narrow fracture undergoing chemical erosion. Contour plots indicating the local volumetric flow relative to the mean flow velocity are shown, using a spatial resolution of 125 microns to discretize the height profile. The topography of the initial (top left) and eroded (top right) fracture surfaces were measured by Dr. William Durham (Lawrence Livermore National Laboratory), using a mechanical profilometer with a spatial resolution of 0.25mm and a height resolution of about 5 microns. The simulation results (bottom left and bottom right) were determined by cycles of erosion from the initial topography. The experimental result is shown after erosion of 1.3 grams of calcite (top right) and the simulation results after erosion of 0.51 (20 iterations, bottom left) and 1.1 grams of calcite (40 iterations, bottom right).

The experimental topography shows a single large flow channel in the center of the specimen, while the simulation shows a few main channels distributed across the fracture. Furthermore, the simulation exhibited more pronounced erosion near the inlet than the laboratory experiment. These discrepancies are most likely a result of the rather crude models for the chemical kinetics and fracture closure.

## GRANTEE: GEORGIA INSTITUTE OF TECHNOLOGY

School of Earth and Atmospheric Sciences  
Atlanta, Georgia 30332-0340

**Grant:** DE-FOG5-95ER14517

### **Biom mineralization: Organic-Directed Controls on Carbonate Growth Structures and Kinetics Determined by *In situ* Atomic Force Microscopy**

*P. M. Dove, 540-231-2444, fax 540-231-3386, dove@vt.edu*

**Objectives:** To determine the kinetics and mechanisms by which amino acids interact with carbonate mineral surface complexes and how key inorganic impurities mediate calcite crystal growth to govern the polymorphs and the structures that form. The long-term goal is to develop a mechanistic understanding of the physical basis for biom mineralization and roles of solutes in governing carbonate precipitation and growth in natural and engineered Earth systems.

**Project Description:** Primary biom minerals form through biologically mediated activities of marine and freshwater organisms. They result from organic-directed crystal nucleation and growth processes acting in concert to yield chemically and morphologically complex structures. When combined with a macromolecular matrix of proteins, polysaccharides, and lipids, these structures fulfill specific physiological functions such as providing stiffness and strength to mineralized skeletal tissues. An understanding of organic-mineral surface interactions also has applications for 1) developing avoidance strategies for cementation/scaling in oil/gas fields; 2) understanding roles of organics in the long-term behavior of carbonates in waste repositories; 3) developing new biomaterial technologies in the synthesis of lightweight mineral composites. This project combines *in situ* Atomic Force Microscopy (AFM) investigations with kinetic measurements and surface chemical modeling to determine the rates and mechanisms by which amino acids and inorganic impurities modify the crystallization of calcium carbonate minerals.

**Results:** Kinetics of Calcite Growth: Surface Processes and Relationships to Macroscopic Rate Laws (Geochim. Cosmochim. Acta, 2000, p 2255-2266). Classical crystal growth theory is linked with observations of microscopic surface processes to quantify the dependence of calcite growth on supersaturation,  $\Omega$ , and show relationships to the same dependencies often approximated by affinity-based expressions. The dependence of overall growth rate upon dislocation source structure was also analyzed using fundamentals of crystal growth theory. The resulting surface process-based rate expressions for spiral growth show the relationships between  $R_m$  and the distribution and structures of dislocation sources. These theoretical relations are upheld by the process-based experimental rate data reported in this study. The dependence of growth rate on dislocation source structures is essential for properly representing growth because most growth sources are complex with multiple dislocations. Expressions resulting from this analysis show where popular affinity-based rate laws hold or break down. Our findings demonstrate that the widely used second order chemical affinity-based rate laws are physically meaningful only under special conditions. Observations of various types of surface defects that give rise to step formation suggest that popular 'rate laws' are composites of contributions from each type of dislocation structure.

Resolving the Controversial Role of  $Mg^{2+}$  in Calcite Biom mineral Formation. Science (submitted). Magnesium is a key determinant in  $CaCO_3$  biom mineral formation and has emerged as an important

paleotemperature proxy. However, macroscopic observations have failed to provide a clear physical understanding of how  $\text{Mg}^{2+}$  modifies carbonate growth. Atomic force microscopy was used to directly resolve the controversial mechanism of calcite inhibition by  $\text{Mg}^{2+}$  through molecular-scale determination of the thermodynamic and kinetic controls of  $\text{Mg}^{2+}$  on calcite morphology and growth. Comparison of directly observed monomolecular step velocities to standard impurity models demonstrated that calcite growth inhibition was due to enhanced mineral solubility through  $\text{Mg}^{2+}$  incorporation. Terrace width measurements on calcite growth spirals showed that step-edge energies were unaffected by  $\text{Mg}^{2+}$  incorporation according to the Gibbs-Thomson relation. Finally, solubilities determined from microscopic observations of step dynamics are linked to macroscopic measurements of the  $\text{Ca}_{1-x}\text{Mg}_x\text{CO}_3$  system.

Selective Binding of Amino Acids to Atomic Steps of Calcite Creates Chiral Structures. *Nature* (in prep.). The conventional paradigm that defines current views on biomineralization is commonly described by the term “stereochemical recognition”, a concept that emphasizes geometrical and chemical incentives to binding. However, this view of the organic-inorganic interactions at the mineral surface seems incompatible with the mechanistic picture of crystallization given by the terrace-step-kink model of Burton, Cabrera and Frank. Indeed, this traditional model of growth emphasizes the inhibiting effect of modifiers on step motion through step pinning at kink sites, rather than stereochemical matching to newly expressed facets. We reconcile these two divergent views. By using the chiral structure of the amino acids as a probe, we show both qualitatively and quantitatively that macroscopic shape modification results from changes to the calcite step-edge free energies in response to enantiomer-specific binding of the amino acids to individual step risers. In essence, the amino acid acts like a surfactant, and the concept of stereochemical recognition merges smoothly with that of the terrace-step-kink model.

## **GRANTEE: UNIVERSITY OF HAWAII**

Department of Geology and Geophysics  
Honolulu, Hawaii 96822

**Grant :** DE-FG03-95ER14525 A004

### **Growth of Faults, Scaling of Fault Structure, and Hydrologic Implications**

*Stephen Martel, 808-956-7797; fax 808-956-5512, martel@soest.hawaii.edu; Kevin Hestir, Utah State University; 801-797-2826, fax 801-797-1822, hestir@sunfs.math.usu.edu; James P. Evans, Utah State University, 801-797-2826, fax 801-797-1588, jpevans@cc.usu.edu; Jane C.S. Long, University of Nevada at Reno, 702- 784-6987, fax 702-784-1766; JCSLONG@mines.unr.edu*

**Website:** <http://www.soest.hawaii.edu/martel/Stevem.html>

**Objectives:** The main research objectives are: (a) to determine how faults grow in three dimensions in brittle crystalline rocks (granites and basalts), and (b) to further develop physically based stochastic models for predicting geometric and hydrologic properties of such faults.

**Project Description:** We are investigating how faults of different scale grow in granite and basalt in three-dimensions. We are systematically examining the geometries, structure, and mechanics of faults with trace lengths of a few meters to several kilometers, and using this knowledge to develop physically based stochastic models for predicting the geometry of faults over a wide range of scale and for analyzing their hydraulic behavior.

**Results:** In the granitic rock of the Sierra Nevada, California, a strike-slip fault with a trace length of several kilometers has been mapped in Sequoia National Park, and slip distribution data have been collected along it. Observations from the Sierra also show two new ways that pre-existing igneous dikes have influenced how faults develop. First, the aforementioned fault apparently developed, at least in part, by brittle fracturing along pre-existing igneous dikes. Second, some faults developed from joints clustered around igneous dikes. This suggests that the joints, and hence the faults, reflect processes associated with the intrusion (and perhaps cooling) of the dikes. For normal faults in Hawaiian basalts, approximately one hundred new profiles have been surveyed across faults of the Koae fault system to determine the distributions of slip and secondary fractures. Two-dimensional boundary element analyses motivated by our prior mapping accounts for the main geologic features along those faults: gaping vertical fissures on the uplifted footwall; monoclinical flexures and steeply inclined cavities along the scarps; and buckles on the footwall. The fissures and cavities must strongly influence the hydrologic properties of the normal faults; these findings should be relevant to several DOE sites in the western United States.

## GRANTEE: UNIVERSITY OF ILLINOIS AT URBANA-CHAMPAIGN

Department of Geology  
245 Natural History Building  
1301 W. Green St., Urbana, IL, 61801

**Grant:** DE-FG02-00ER15028

### Computational and Spectroscopic Investigations of Water-Carbon Dioxide Fluids and Surface Sorption Processes

*R. James Kirkpatrick 217-333-7414, fax 217-333-9142, kirkpat@uiuc.edu*

**Website:** <http://www.geology.uiuc.edu/~kirkpat/index.html>

**Objectives:** To understand on the molecular scale 1) the chemical interaction of dissolved anionic species with mineral surfaces and 2) the properties of geochemically relevant water-carbon dioxide-salt fluids at elevated pressures and temperatures.

**Project Description:** 1) Investigation of the structural environments and dynamical behavior of surface and interlayer exchanged anions in mineral-fluid systems is being undertaken using a combination of *in situ* NMR spectroscopy, sorption isotherm experiments and molecular dynamics (MD) computational modeling. This combination of techniques provides otherwise unobtainable, species-specific information and allows integration of molecular and macroscopic perspectives. Initial focus is on the carbonate species  $\text{CO}_3^{2-}$  and  $\text{HCO}_3^-$ , but a wide range of species, including  $\text{Cl}^-$ ,  $\text{ClO}_4^-$ ,  $\text{SeO}_3^{2-}$ ,  $\text{SeO}_4^{2-}$ ,  $\text{NO}_3^-$ ,  $\text{HPO}_4^{2-}$ , and  $\text{PO}_4^{3-}$ , are also being investigated. Initial solid substrate phases include single-metal and mixed-metal hydroxides. MD modeling of both neat solutions and solution-mineral interfaces is central.

2) Investigation of the structure and properties ( $P$ - $V$ - $T$  relations, diffusion, solute hydration and hydrogen bonding) of water-carbon dioxide fluids with and without dissolved salts is being undertaken using molecular dynamics computational modeling. Work is focused on supercritical  $\text{CO}_2$  and  $\text{H}_2\text{O}$ - $\text{CO}_2$  and  $\text{H}_2\text{O}$ - $\text{CO}_2$ - $\text{NaCl}$  mixtures at crustal temperature and pressures.

#### Results:

##### *Surface and Interlayer Structure and Dynamics*

Combined sorption isotherm and  $^{13}\text{C}$  NMR  $T_1$  studies of  $\text{CO}_3^{2-}$  sorption on amorphous aluminum hydroxide have greatly advanced the use of NMR techniques to study sorption/exchange in aqueous systems. In contrast to our previous studies using  $^{35}\text{Cl}$ , here the sorption densities from NMR are comparable to those from isotherms at low solution concentrations but are lower at higher concentrations due to surface precipitation. NMR provides important insight into the surface precipitate structure.

Multinuclear NMR and IR spectroscopy, XRD, and water sorption experiments have provided a comprehensive understanding of the structural and chemical controls of interlayer structure and dynamics and the swelling behavior of Mg,Al and Li,Al layered double hydroxides containing a wide range of inorganic anions. The Mg,Al and Li,Al systems have quite different dynamical and swelling behaviors, and although the ionic charge/anion radius ratio is an important parameter, the behavior of the different anions is complex.

Computational efforts provide important insight into the interlayer and surface behavior. Energy minimization calculations have provided significant structural and thermodynamic insight into the swelling behavior of layered double hydroxides. Molecular dynamics modeling is providing key information about the surface lifetimes and surface diffusion coefficients of water and anionic species on a variety of oxide and hydroxide surfaces. In both cases, the computational results are in good agreement with experiment and yield important structural and dynamical insight and guidance.

#### *Fluid Structure and Dynamics*

MD modeling of CO<sub>2</sub> and H<sub>2</sub>O-CO<sub>2</sub> and H<sub>2</sub>O-CO<sub>2</sub>-NaCl solutions has advanced significantly. For CO<sub>2</sub> at temperatures up to 380K and 0.1Gpa modified interaction parameters give self-diffusion coefficients in excellent agreement with known values and a structure in reasonable agreement with the limited neutron diffraction data available. For H<sub>2</sub>O-CO<sub>2</sub> solutions containing small amounts of the second component, results show that up to 573K show that the solvent structure is not substantially affected by the presence of the second component within the solubility limits. Solute water molecules in liquid and supercritical CO<sub>2</sub> form hydrogen-bonded clusters, and H<sub>2</sub>O transport rates are comparable to those in pure water. In contrast, CO<sub>2</sub> dissolved in H<sub>2</sub>O occurs in clathrate-like cages formed by hydrogen bonded water molecules, reducing CO<sub>2</sub> diffusion coefficients by about an order of magnitude relative to pure CO<sub>2</sub> under similar thermodynamic conditions. This unexpected result is experimentally testable. Preliminary calculations for H<sub>2</sub>O-CO<sub>2</sub>-NaCl solutions are being analyzed.

MD modeling of aqueous solutions containing Na<sub>2</sub>CO<sub>3</sub> and NaHCO<sub>3</sub> show substantial ion association (stronger for carbonate than for bicarbonate). These results may explain results of ongoing sorption isotherm experiments. Surprisingly, aqueous CaCl<sub>2</sub> shows little inner sphere ion cluster formation due to strong hydration of Ca<sup>+2</sup>.

## **GRANTEE: INDIANA UNIVERSITY**

Laboratory for Computational Geodynamics  
Department of Chemistry  
Bloomington, Indiana 47405

**Grant:** DE-FG29-1ER14175

### **Self-Organized Mega-Structures in Sedimentary Basins**

*Peter J. Ortoleva, 812-855-2717, fax 812-855-8300, ortoleva@indiana.edu*

**Website:** <http://www.indiana.edu/~lcg>

**Objectives:** A deeper understanding of the sedimentary basin is sought to improve our ability to predict the location and characteristics of natural resources, and in the process, identify new phenomena. The approach is based on the identification of fundamental reaction, transport and mechanical (RTM) processes, and the development of rate laws based on them, to solve the equations of mass, momentum and energy conservation.

**Project Description:** Our central postulate is that as a result of the basin RTM processes, the sedimentary basin displays a richness of oscillatory, self-organization and other nonlinear phenomena. In order to test this, we are developing new models of the dynamics of fracture network statistics, diagenesis, gouge, faulting, multi-phase flow and other fundamental processes. We are developing finite element algorithms for solving the conservation equations on moving, deforming, hexahedral grids. In the process of simulating various basin scenarios, we find that the spatial or temporal distribution of descriptive variables (ranging from grain shape and other millimeter-scale factors to gouge, fracture zones and salt diapirs), organizes itself into repetitive patterns. These patterns are not the result of prior depositional or other external factors. They emerge spontaneously due to the nonlinearity of the conservation equations, the coupling between processes, and that the basin system is driven sufficiently far from equilibrium by the overall tectonic, hydrologic and thermal influences affecting the basin at its boundaries.

**Results:** An important aspect of developing improved rock rheologic multi-phase flow and other laws is to delineate the relation between the molecular scale and the larger scales. In particular, we have focused on the mesoscopic scale of oil/water and gas/water interfaces, wetting, droplets and other aspects of the multi-phase reaction-transport problem to develop the phenomenological laws needed for basin and reservoir simulation. Our results are summarized in a monograph, *Mesosopic Chemical Physics*, that contains many of the mathematical, statistical, mechanical, homogenization, and other techniques needed to formulate and determine these rate laws. A new information theory method was developed for automatically formulating and calibrating multi-phase flow laws. The method was used to calibrate capillary pressure and relative permeability dependencies on oil vs. water pore volume fraction.

Our probability functional method was also used to develop a method for predicting the most probable state of the subsurface given well log surface or other remote data. A physically-motivated regularization method was used that allowed for stable and efficient solution of inverse problems, such as reservoir history matching or the determination of the geological timescale-history of tectonic or other overall basin factors required for basin simulation. This provides a method for automating the basin

modeling process and thereby, determining geological history of the basin interior and predicting the configuration of present day reservoirs and other features.

## **GRANTEE: INDIANA UNIVERSITY**

Department of Geological Sciences  
Bloomington, Indiana 47405-1405

**Grant:** DE-FG02-00ER 15032

### **Isotopically Labile Organic Hydrogen in Thermal Maturation of Organic Matter**

*A. Schimmelmann, 812-855-7645, fax 812-855-7961, aschimme@indiana.edu; M. Mastalerz, 812-855-9416, fax 812-855-2862, mmastale@indiana.edu*

**Website:** <http://php.indiana.edu/~aschimme/hydronit.html>

**Objectives:** Explore the geochemical conditions and mechanisms that contribute to changes in the abundance of isotopically labile organic hydrogen in sedimentary organic matter during thermal maturation. Evaluate the diagenetic and/or paleoenvironmental significance of D/H ratios in different types of kerogen, oil, and fractions of oil.

**Project Description:** Isotopically labile organic hydrogen in organic matter occupies chemical positions that participate in isotopic exchange and in chemical reactions during thermal maturation. We quantify the extent of isotopic transfer of hydrogen and nitrogen between organic matter and (i) ambient water and (ii) dissolved ammonia in long-term laboratory experiments. Natural kerogens of different type and maturity, and a large matrix of oils, fractions of these oils, and associated formation waters are isotopically characterized to assess the extent of natural hydrogen isotopic transfer during maturation and storage over geologic time. FTIR and NMR spectroscopic and petrographic methods assist in the interpretation of isotopic data. We also investigate the paleoenvironmental significance of an apparent correlation between hydrogen exchangeability and the  $^{15}\text{N}/^{14}\text{N}$  ratio in stratigraphic sequences of kerogens.

**Results:** Laboratory heating experiments (hydrous pyrolysis) have shown that organic hydrogen in thermally maturing kerogen is receiving up to 80 % of its hydrogen atoms from ambient water hydrogen. During the same experiments, slightly less hydrogen transfer is observed in the artificial generation of oils. Simple heating of oils with water in the laboratory does not result in significant hydrogen isotopic exchange. Our working hypothesis is that hydrogen transfer from inorganic sources into the organic aliphatic hydrogen pool occurs only when activation energy is available during chemical reactions, for example during the breaking of carbon-carbon bonds. Once formed, aliphatic compounds with little chemical reactivity retain their D/H ratios over geologic time and in the presence of formation water with different D/H ratios. Support for this hypothesis derives from our collaboration with the Australian Geological Survey. We are determining the D/H ratios of ca. 50 Australian oils and their associated formation waters (i.e. waters that are present today in contact with oils), in addition to D/H ratios of the aromatic, polar, and saturated fractions of the oils. The lack of strong correlation between organic and water D/H ratios (Fig. 1) suggests that oil and water hydrogen do not equilibrate isotopically, even over geologic time under pressure and temperature conditions of oil reservoirs. Extrapolating from laboratory experiments to natural thermal maturation, the preserved organic D/H ratios are thus likely reflecting two influences, namely (i) an original biogenic/paleoenvironmental signal and (ii) the D/H ratio of the water that was present within the source rock when oil was formed from kerogens.

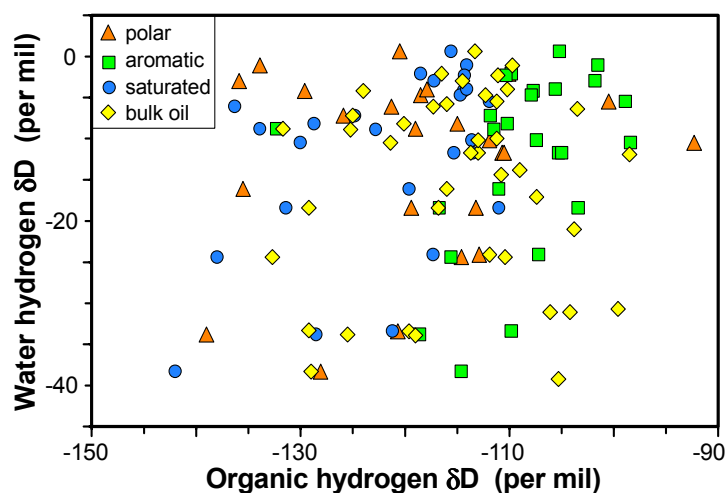


**Figure 1:** Lack of correlation between organic D/H ratios in oil (and in fractions of oil) and formation water D/H ratios in Australian petroleum reservoirs indicates that carbon-bound hydrogen in oil does not isotopically exchange with water hydrogen, even over prolonged periods.

The isotopic, geochemical, FTIR-spectroscopic, and petrographic effects of increasing natural thermal maturity on various types of kerogens are being studied using a variety of samples. Two sets are mentioned here. Vitrinites were handpicked from six coals from the Illinois and Appalachian Basins having vitrinite reflectance values of 0.55 to 5.15 %. Rising thermal maturity causes an increase in aromaticity, and reduces the abundances of O, S, N, exchangeable hydrogen, and organic deuterium. Seven kerogens from New Albany Shale having maturities equivalent to vitrinite reflectance values of 0.29 to 1.5 % were characterized by FTIR and hydrogen stable isotope mass-spectrometry. The lowest maturity samples (vitrinite reflectance 0.29 and 0.35 %) are characterized by lowest aromaticity, relatively high concentrations of oxygenated groups (carboxyl in particular), and highest abundance of exchangeable hydrogen. Kerogens with vitrinite reflectance values of 0.57 and 0.61 % show greatly reduced carboxyl abundance, higher aromaticity, and less exchangeable hydrogen. In kerogens with a vitrinite reflectance of 0.63 % carboxyl is hardly detectable, aromaticity is increased, hydrogen exchangeability is low, aromatic carbon bands are shifted towards lower wave numbers, and bands assigned to aryl rings with isolated C-H groups become dominant in the out-of-plane region. Kerogens with a vitrinite reflectance of 1.5 % show a much higher contribution of aromatic bands, both in the aromatic stretching region and in the out-of-plane region.

**GRANTEE: THE JOHNS HOPKINS UNIVERSITY**

Department of Earth and Planetary Sciences  
Baltimore, Maryland 21218-2687

**Grant:** DE-FG02-96ER14619

**Fluid Flow in Faults: Estimating Permeability and Diagenetic Effects in a Transpressional Setting, Southern California**

*Grant Garven, 410-516-8689, fax 410-516-7933, garven@jhu.edu; James R. Boles, UC-Santa Barbara; 805-893-3719, fax 805-893-2314, boles@magic.geol.ucsb.edu*

**Objectives:** This is a collaborative effort to determine the magnitude of fluid mass transfer and diagenetic effects along faults that have developed in a transpressional setting. The study will contribute a fundamental understanding of the hydraulic effects of faults on sediment diagenesis, petroleum migration and groundwater flow.

**Project Description:** We have targeted three major faults and petroleum fields in southern California for study: Wheeler Ridge and Elks Hills in the San Joaquin Basin and the Refugio Fault in the Transverse Ranges near Santa Barbara. Subsurface core samples, outcrop samples, well logs, reservoir properties and published structural-seismic sections are being collected to characterize the tectonic history and diagenetic evolution for the known fault networks. These data provide constraints for finite element flow and transport models that are being developed to predict fluid pressures, flow patterns, rates of deformation, temperatures, and diagenetic patterns in the fault systems during thrusting and normal faulting.

**Results:** Jim Boles and his Ph.D. student have studied cores from 340 wells in the San Joaquin Basin: twenty-seven of these cores stored at the Wheeler Ridge Oil Field have been sampled in addition to cores stored at the California Core Repository in Bakersfield. Our sampling strategy is to document diagenesis in reservoir strata at Wheeler Ridge and then compare this to cores close to the Wheeler Ridge Thrust Fault. We are conducting petrographic analyses of thin sections, isotopic analyses of carbonate cements, and analyzing geothermal indicators in these samples such as plagioclase and smectite/illite composition. We also have constructed time-temperature burial histories for each of these wells using ARCO's Genesis software. Permeability-depth trends indicate several orders of magnitude decrease in permeability within 100 meters of the hanging wall of the fault, suggesting that either mechanical crushing and/or cementation has occurred above the fault. The nature of the mineral changes will constrain fluid volume, temperature, and if datable the potential timing of fluid movement. Grant Garven and his Ph.D. student have been busy preparing finite element simulations that complement the petrologic fieldwork. In FY2000, they prepared 2-D simulations that compared effects of faults. The models consider cases in which the thrust faults are considered to act as conduits and barriers. We are also comparing the hydrologic effects of both topography and deformation as driving forces for fluid flow across the Wheeler Ridge thrust sheet.

## **GRANTEE: THE JOHNS HOPKINS UNIVERSITY**

Dept. of Earth and Planetary Sciences  
Baltimore, MD 21218.

**Grant:** DE-FG02-96ER-14616

### **Predictive Single-Site Protonation and Cation Adsorption Modeling**

*Dimitri A. Sverjensky 410-516-8568, fax 410-516-7933, sver@jhu.edu*

**Objectives:** The overall goal of this research is to develop a predictive model of adsorption processes at the mineral-water interface that can be applied to a fundamental understanding of the role of adsorption in geochemical processes such as weathering, diagenesis, the chemical evolution of shallow and deep groundwaters and ore-forming fluids, and the fate of contaminants in groundwaters.

**Project Description:** The research is aimed at generating a comprehensive, internally consistent, quantitative description of proton and cation adsorption on oxides and silicates using an extended triple layer model. The model will be developed to integrate the available experimental information on proton and cation adsorption based on internally consistent assumptions. By so doing, it will considerably facilitate the comparison of experimental data from different investigators. In addition, the model will permit predictions of surface speciation to supplement the lack of experimental adsorption data for many systems of geochemical interest. In addition, it will provide a basis for extending applications of the concept of surface complexation to oxide and silicate dissolution kinetics. The proposed extended triple layer model will include: (1) Internally consistent assumptions and methods of estimating site densities and capacitances; (2) Explicit recognition of ion solvation; (3) Explicit recognition of proton attraction-repulsion; (4) Inclusion of the extended Debye-Huckel model for aqueous ionic activity coefficients; and (5) Inclusion of a geochemical thermodynamic data file for aqueous species and minerals.

**Results:** For the prediction of surface charge and metal adsorption, the capacitance at the solid-water interface is a critical parameter because it gives us a relationship between surface charge, which is measurable, and surface potential, which is not measurable. By analysing surface charge measurements for a wide variety of electrolytes and oxides using a consistent model, I have shown that the capacitances have systematic trends that reveal important information about the nature of the oxide-electrolyte-water interface. For example, on rutile surfaces, ions such as sodium and potassium adsorb as inner-sphere complexes, close to the surface. In contrast, on quartz surfaces, sodium and potassium adsorb as outer-sphere complexes, much further from the surface. The specific distances are consistent with independently measured X-ray studies. This greatly improves the predictive capabilities of the extended triple-layer model.

In addition, an analysis of the adsorption of alkaline earth metals on oxides revealed that the same surface complexes apply for very different minerals. The combination of this study with the results of the capacitance study described above also suggests that the bonding on different mineral surfaces can differ greatly. For example, on rutile, it is suggested that calcium forms inner-sphere complexes, whereas on quartz, the same stoichiometry forms an outer-sphere complex. Qualitatively, these results appear to be consistent with available X-ray studies of rutile and silica surfaces. In addition, the equilibrium constants of these complexes can be related by crystal chemical and Born solvation theory. This means that the adsorption of calcium can be predicted on many other oxides and under conditions that have yet to be investigated experimentally.

## GRANTEE: THE JOHNS HOPKINS UNIVERSITY

Department of Earth and Planetary Sciences  
3400 N. Charles St.  
Baltimore MD 21218

**Grant:** DE-FGO2-97ER 14074

### Reactions and Transport of Toxic Metals in Rock-Forming Silicates at 25°C

*David R. Veblen, 410-516-8487, fax 410-516-7933, DVeblen@JHU.edu; Eugene Ilton, Lehigh Univ.*

**Objectives:** This project is an investigation of reactions between silicate minerals and toxic metal-bearing aqueous fluids. We are specifically exploring the mechanisms of oxidation-reduction reactions at the mineral-fluid interface and transport of reactive components along the grain-boundary interface in rocks.

**Project Description:** The project has three main components: experimental investigation of Cr and U reduction and sorption by micas; high-resolution transmission electron microscopy (HRTEM) characterization of grain boundaries; and experimental investigation of transport and sorption of heavy metals along grain boundaries. The first component includes development of X-ray photoelectron spectroscopy (XPS) methodologies to probe sorption behavior. The second component includes molecular-dynamical modeling of grain-boundary structures to provide insight into their transport properties. This second component also includes development of near-atomic-resolution analysis and imaging methodologies of electron-energy-loss spectroscopy (EELS), high-angle-annular-dark-field imaging (HAADF) and energy-filtered-transmission-electron-microscopy (EFTEM) in mineralogical systems. The third component combines the geochemical and mineralogical studies to elucidate transport properties and mechanisms important in Earth materials.

**Results:** During this third year of the three-year cycle, the geochemical work has focused on the sorption and reduction of uranium on biotite and the effect of alkali cations (Na, K, and Cs) on biotite dissolution. These objectives were pursued through a series of systematic, batch sorption experiments, X-ray photoelectron spectroscopy (XPS) analyses of run products, and initial attempts to use HRTEM to image single atoms of U and Cs sorbed to biotite. Electron transfer from Fe(II) in biotite to sorbed U(VI) occurs at edge sites, is blocked by the siloxane layer and by K in solution and, as expected, is dependent on the Fe and Fe(II) concentration in biotite. Over the course of this year, we developed and refined XPS methodologies to minimize artifacts arising from charge broadening and beam damage. We also developed a curve fitting procedure to extract peak parameters for U4f(7/2), despite severe overlaps with Mg auger lines and K1s. HRTEM imaging of single U atoms sorbed to biotite was stymied by experimental difficulties. However, we are developing new approaches to alleviate these difficulties, such as using pre-ionmilled specimens oriented in a manner that dampens sample vibrations.

In the course of our experiments, we reacted single crystal mica surfaces with Cr(III)-bearing solutions containing 25 mM of either Na, K, or Cs ions at pH = 4 under air. We then investigated the leaching of octahedral cations from those micas using XPS analysis. Leaching was greater in Na and Cs solutions than in K solutions. To verify that this was completely an alkali cation effect, we repeated the experiments without Cr(III) and found the same results. We then varied the pH, water/rock ratio and ambient atmosphere (air/argon) and found that Na facilitated leaching, relative to K, regardless of

experimental conditions. However, the strength with which Cs facilitated leaching, relative to K, diminished at  $\text{pH} > 4$ , under argon, and at low water/rock ratios. We then did a 44-hour, bulk dissolution experiment with biotite powders at  $\text{pH} = 4$ ,  $T = 25^\circ\text{C}$ , an argon atmosphere, and solutions containing 25 mM Na, K, or Cs. In these experiments, we monitored the chemistry of the solutions to track octahedral-layer dissolution. Leaching was greater in the Na solutions than in the Cs and K solutions, and nearly identical for the Cs and K experiments. At present, the only unifying observation among all the experimental conditions is that leaching is strongly correlated with loss of K from the interlayer region of biotite.

The mineralogical component of the project has centered on HRTEM imaging and modeling of a range of silicate-silicate and silicate-oxide grain boundaries. The work continues to show that boundaries between minerals are tight and semi-coherent. These boundaries contain defects that create through-going channels (nanopores) that form a rapid network for chemical transport. Over the course of our TEM studies on grain boundaries this year, we have (1) demonstrated sub-nanometer analytical resolution using energy filtered TEM (EFTEM) and (2) developed a tilting procedure to enhance compositional contrast and reduce residual diffraction contrast in EFTEM imaging. We have also begun to implement exit wavefunction reconstruction techniques and are in the beginning stages of developing a valence image technique.

## GRANTEE: KENT STATE UNIVERSITY

Department of Geology  
Kent, Ohio 44242

**Grant:** DE-FG02-96ER14668

### Dissolution of Fe(III)(hydr)oxides by Aerobic Microorganisms

*Patricia A. Maurice 330-672-2680, pmaurice@Maurice.kent.edu; L. Hersman, G. Sposito*

**Objectives :** The overall objective of this research is to determine the mechanisms whereby aerobic microorganisms acquire Fe from Fe(III)(hydr) oxides. Specific objectives are to characterize the types of attachment features used by the microorganisms, and to determine how dissolution varies with mineral surface properties.

**Results:** During this project year, we completed a study of microbially mediated dissolution of Al-substituted goethites and made significant progress on a study of microbially mediated dissolution of kaolinite. This research resulted in 1 published paper (Maurice et al., *GCA*, 2000), 2 invited papers submitted for review (in *Chemical Geology* and *Geomicrobiology*), and 2 completed M.S. theses in the Dept. of Geology at Kent State University (Lee, 1999 and Vierkorn, 2000). In addition, we completed with L. Hersman a study of microbial dissolution of hematite, goethite, and ferrihydrite, and submitted a manuscript to *Applied Environmental Microbiology*. We also began a study of siderophore-promoted dissolution of kaolinite. Although the original proposal called for a postdoctoral associate to begin work in Spring 2000, we delayed this because of P. Maurice's 7/00 move to the University of Notre Dame. The new postdoctoral associate will begin work Sept. 1, 2000 and will focus on microbial effects on mineral aggregation kinetics.

*Microbially mediated dissolution of Al-substituted goethites*, Maurice P.A., Lee Y.-J., and Hersman L.E. (2000) *Geochimica et Cosmochimica Acta*, 64: 1363-1374

Goethite particles in soil environments often contain Al<sup>3+</sup> substituted for Fe<sup>3+</sup> in octahedrally coordinated sites. Al substitution has been shown to alter mineral stability and abiotic dissolution rates. This study focused on the effects of Al substitution (to 8.8 mol%) on synthetic goethite dissolution by an aerobic *Pseudomonas mendocina* var. bacteria. In contrast to dissimilatory iron reducing bacteria (DIRB), this bacterium is not capable of using Fe as a terminal electron acceptor for oxidative phosphorylation, and hence only requires mM concentrations of Fe for metabolism.

Pure and substituted goethites were reacted with microorganisms in Fe-limited growth media wherein the only source of Fe was the solid phase, so that microbial populations could only grow by obtaining Fe through mineral dissolution. Because at least some Fe was taken up by the bacteria, we could not measure Fe release rates directly from dissolved Fe concentrations. Rather, we relied upon microbial growth measurements as indirect indicators of mineral dissolution.

Increasing Al substitution resulted in particles with progressively decreasing mean particle length and aspect ratios, as well as fewer domains, as measured by atomic-force microscopy (AFM); but with increasing structural order as determined by XRD line widths. Experiments conducted in the dark at 22°C, exposed to the atmosphere, showed that maximum microbial population did not correlate with particle specific surface area, which is in contrast with previous studies using DIRB. Maximum microbial population increased a small amount with increasing Al content of the goethites, in contrast

with several previous investigations of abiotic dissolution. Because dense biofilms formed, we were unable to use AFM to observe mineral dissolution features.

AFM imaging suggested that more highly substituted goethites formed denser aggregates, and previous investigations have shown that aggregate structure is important for microbial attachment, which is prerequisite for dissolution. Hence, effects of Al substitution on aggregate structure is a focus of ongoing research.

*Microbially mediated kaolinite dissolution, Maurice P.A., Vierkorn M.A., Hersman L.E., and Fulghum J.E. (Submitted to Chemical Geology.) Maurice P.A., Vierkorn M.A., Hersman L.E., Fulghum J.E., and Ferryman A. (Submitted to Geomicrobiology.)*

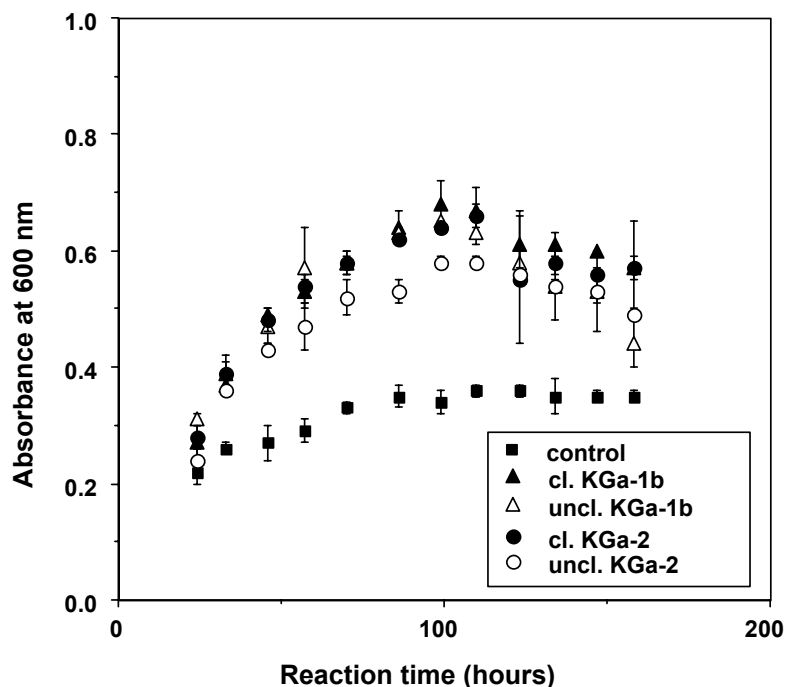


Figure 1. Results of microbial dissolution experiment comparing strongly and weakly cleaned kaolinites KGa-1b and KGa-2. In this and subsequent figures, the control contains only bacteria in growth media with no kaolinite present. Each data point represents the mean of 3 individual samples. This figure shows that in the presence of all four kaolinite samples, the bacteria are able to grow to population sizes (measured by absorbance at 600 nm) greater than those of non-kaolinite-containing controls. Because microbial growth is Fe-limited in these experiments, the bacteria must be able to obtain Fe from the solid phase. The weak cleaning procedure for the kaolinite is seen to have little or no effect on the microbial growth.

This research investigated the effects of an aerobic *Pseudomonas mendocina* bacterium on dissolution of well and poorly ordered Clay Minerals Society Source Clay kaolinites KGa-1b and KGa-2 under Fe-limited conditions. When the only source of Fe was uncleaned or weakly cleaned kaolinite, the bacteria were able to grow to population sizes greater than non-kaolinite-containing controls, indicating that they acquired Fe from the solid phase. Rates of Al release from kaolinite were greatly enhanced in the

presence of the bacteria (Figure 1); the mechanism(s) of this enhancement could include pH increases and/or production of Al chelating agents such as siderophores.

Strong cleaning of the kaolinites in HCl at 85°C removed some surface Fe, as measured by X-ray photoelectron spectroscopy, and also resulted in a Si-enriched surface precipitate that could be observed by atomic force microscopy (Figure 2). Substantial etch pits were also observed on some particles. The bacteria were able to grow well on strongly cleaned KGa-2 but not on strongly cleaned KGa-1b.

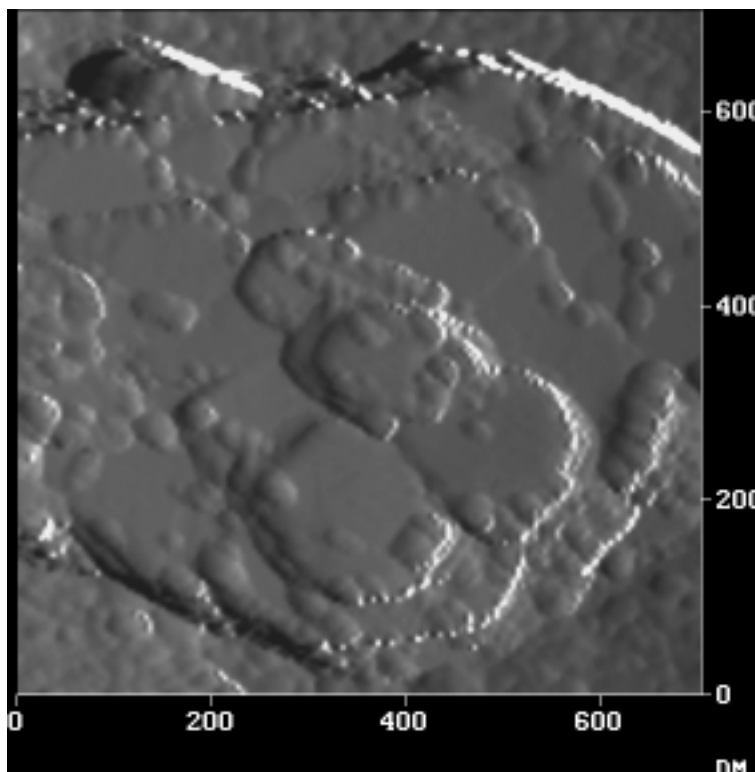


Figure 2. A TMAFM image in air of poorly ordered kaolinite following cleaning in HCl at 85°C. A Si-enriched secondary phase (composition determined by X-ray photoelectron spectroscopy) is present on the particle surfaces, particularly along particle and step edges.

Dissolution in 0.001 M oxalate was used as a means of comparing amounts of Fe that could be easily removed from the kaolinites by a complexing ligand. Significant Fe was released from weakly cleaned and uncleaned KGa-1b and KGa-2 as well as from strongly cleaned KGa-2, but very little was released from strongly cleaned KGa-1b. We therefore suggest that the bacteria are most able to access kaolinite-associated Fe that is readily available to complexation by organic ligands. Overall, our results demonstrate that clay minerals such as kaolinite may be important sources of Fe to microbial systems and also that bacteria may have significant effects on clay mineral dissolution in aerobic environments. During the summer and fall of 2000, we plan to focus on determining the mechanism(s) of microbial enhancement of kaolinite dissolution and to conduct a series of kaolinite dissolution experiments in the presence of microbial siderophores.

## **GRANTEE: LEHIGH UNIVERSITY**

Department of Earth and Environ. Sciences  
31 Williams Drive  
Bethlehem, PA 18015

**Grant :** DE-FGO2-97ER 14507

### **Reactions and Transport of Toxic Metals in Rock-Forming Silicates at 25°C**

*Eugene S. Ilton, 610-758-5834, fax 610-758-3677, esi2@Lehigh.edu; David Veblen, 410-516-8487, fax 410-516-7933, Dveblen@JHU.edu*

**Objectives:** This project is an investigation of reactions between silicate minerals and toxic metal-bearing aqueous fluids. We are specifically exploring the mechanisms of oxidation-reduction reactions at the mineral-fluid interface and transport of reactive components along the grain-boundary interface in rocks.

**Project Description:** The project has three main components: experimental investigation of Cr and U reduction and sorption by micas; high-resolution transmission electron microscopy (HRTEM) characterization of grain boundaries; and experimental investigation of transport and sorption of heavy metals along grain boundaries. The first component includes development of X-ray photoelectron spectroscopy (XPS) methodologies to probe sorption behavior. The second component includes molecular-dynamical modeling of grain-boundary structures to provide insight into their transport properties. This second component also includes development of near-atomic-resolution analysis and imaging methodologies of electron-energy-loss spectroscopy (EELS), high-angle-annular-dark-field imaging (HAADF) and energy-filtered-transmission-electron-microscopy (EFTEM) in mineralogical systems. The third component combines the geochemical and mineralogical studies to elucidate transport properties and mechanisms important in Earth materials.

**Results:** During this third year of the three-year cycle, the geochemical work has focused on the sorption and reduction of uranium on biotite and the effect of alkali cations (Na, K, and Cs) on biotite dissolution. These objectives were pursued through a series of systematic, batch sorption experiments, X-ray photoelectron spectroscopy (XPS) analyses of run products, and initial attempts to use HRTEM to image single atoms of U and Cs sorbed to biotite. Electron transfer from Fe(II) in biotite to sorbed U(VI) occurs at edge sites, is blocked by the siloxane layer and by K in solution and, as expected, is dependent on the Fe and Fe(II) concentration in biotite. Over the course of this year, we developed and refined XPS methodologies to minimize artifacts arising from charge broadening and beam damage. We also developed a curve fitting procedure to extract peak parameters for U4f(7/2), despite severe overlaps with Mg auger lines and K1s. HRTEM imaging of single U atoms sorbed to biotite was stymied by experimental difficulties. However, we are developing new approaches to alleviate these difficulties, such as using pre-ionmilled specimens oriented in a manner that dampens sample vibrations.

In the course of our experiments, we reacted single crystal mica surfaces with Cr(III)-bearing solutions containing 25 mM of either Na, K, or Cs ions at pH = 4 under air. We then investigated the leaching of octahedral cations from those micas using XPS analysis. Leaching was greater in Na and Cs solutions than in K solutions. To verify that this was completely an alkali cation effect, we repeated the experiments without Cr(III) and found the same results. We then varied the pH, water/rock ratio and ambient atmosphere (air/argon) and found that Na facilitated leaching, relative to K, regardless of

experimental conditions. However, the strength with which Cs facilitated leaching, relative to K, diminished at  $\text{pH} > 4$ , under argon, and at low water/rock ratios. We then did a 44-hour, bulk dissolution experiment with biotite powders at  $\text{pH} = 4$ ,  $T = 25^\circ\text{C}$ , an argon atmosphere, and solutions containing 25 mM Na, K, or Cs. In these experiments, we monitored the chemistry of the solutions to track octahedral-layer dissolution. Leaching was greater in the Na solutions than in the Cs and K solutions, and nearly identical for the Cs and K experiments. At present, the only unifying observation among all the experimental conditions is that leaching is strongly correlated with loss of K from the interlayer region of biotite.

The mineralogical component of the project has centered on HRTEM imaging and modeling of a range of silicate-silicate and silicate-oxide grain boundaries. The work continues to show that boundaries between minerals are tight and semi-coherent. These boundaries contain defects that create through-going channels (nanopores) that form a rapid network for chemical transport. Over the course of our TEM studies on grain boundaries this year, we have (1) demonstrated sub-nanometer analytical resolution using energy filtered TEM (EFTEM) and (2) developed a tilting procedure to enhance compositional contrast and reduce residual diffraction contrast in EFTEM imaging. We have also begun to implement exit wavefunction reconstruction techniques and are in the beginning stages of developing a valence image technique.

## GRANTEE: UNIVERSITY OF MARYLAND

Department of Chemistry and Biochemistry  
College Park, Maryland 20742

**Grant:** DE-FG02-94ER14467

### Theoretical Studies on Metal Species in Solution and on Mineral Surfaces

*J. A. Tossell, 301-405-1868, fax 301-314-9121, tossell@chem.umd.edu*

**Objectives:** This study utilizes the techniques of computational quantum chemistry to study the structures, energetics and properties of various metal species in solution, in mineral glasses, or absorbed on mineral surfaces. The focus in the past year has been on complexes of heavy transition metals with thioarsenites in sulfidic solutions, on calculation of the acidities of oxyacid species in solution and on surfaces, on determination of electric field gradients at “tricluster” O atoms in aluminosilicate glasses and on silicon-serine complexes involved in biomineralization.

**Project Description:** To understand the mechanisms of dissolution of minerals and formation of ore deposits one must understand the structures and properties of metallic species in aqueous solution. We have studied the interaction of the transition metals of the  $\text{Cu}^+$  and  $\text{Zn}^{2+}$  families with a number of different thiometallate ligands, such as  $\text{AsS}(\text{SH})(\text{OH})^-$ . We have also analyzed the acidities of oxyacid molecules in solution, as models for mineral surfaces. To understand the nature of possible “tricluster” species in aluminosilicate glasses we have calculated their structural, energetic and spectral properties, focusing upon some unusual edge-sharing species observed both in the inorganic chemistry literature and in minerals like the  $\text{Al}_2\text{SiO}_5$  polymorphs. We have also studied complexes between serine and silicic acid, to determine the intermediates in silica biomineralization.

**Results:** To obtain an atomistic understanding of the structure and stability of the copper thioarsenite complex,  $\text{CuH}_2\text{AsO}_2$ , characterized experimentally by Clark and Helz (Environ. Sci Tech., 34, 1477, 2000) in their study of the solubility in sulfidic solution of covellite,  $\text{CuS}$ , digenite,  $\text{Cu}_{1.8}\text{S}$ , and arsenosulvanite,  $\text{Cu}_3\text{AsS}_4$ , we earlier carried out quantum mechanical calculations on several isomers of the Cu-thioarsenite complex, a number of related complexes and the corresponding uncomplexed ligands. Using an *ab initio* molecular orbital approach which includes electron correlation (2<sup>nd</sup> order Moller-Plesset perturbation theory using a polarized double zeta valence orbital basis and effective core potentials) we calculate the lowest energy isomer to be  $\text{CuS}(\text{SH})\text{As}(\text{OH})^-$  (with bonds from Cu to S, SH and As), which has a calculated enthalpy of formation (from  $\text{Cu}^+(\text{aq})$  and  $\text{AsS}(\text{SH})(\text{OH})^-(\text{aq})$ ) of about -110 kJ/mol. If entropic effects are ignored, this gives a log K value of about 19.1 for the formation constant, (fortuitously) close to the value of 19.8 determined by Clark and Helz. More significantly, our method reproduces the experimental trend in log K values for the formation of the simpler complexes  $\text{CuCl}_2^-$ ,  $\text{Cu}(\text{SH})_2^-$  and  $\text{Cu}(\text{CN})_2^-$ , and allows us to understand why the  $\text{CuS}(\text{SH})\text{As}(\text{OH})^-$  complex is so stable. We find that the complexes of  $\text{Cu}^+$  with  $\text{AsS}(\text{SH})_2^-$ ,  $\text{AsS}(\text{SH})(\text{NH}_2)^-$  and  $\text{AsS}(\text{SH})(\text{CH}_3)^-$  are also very stable, while the complexes with related As(V), P(III) and P(V) S-containing ligands are considerably less. The determining chemical characteristic of the strongly complexing ligands is the presence of two coordinating S atoms (one -S and one -SH) and an electron-rich As center. Electron

withdrawing substituents such as F on the As greatly reduce the stability of the complex, breaking the Cu-As bond (Tossell, *Environ. Sci. Tech.*, 34, 1483, 2000).

We have since extended these studies by calculating the structures and stabilities of a number of complexes of the  $\text{Cu}^+$  and  $\text{Zn}^{2+}$  family transition metal ions with thioarsenites and thioantimonides. We find that the  $\text{Au}^+$ ,  $\text{Hg}^{2+}$  and  $\text{Pb}^{2+}$  complexes of  $\text{AsS}(\text{SH})(\text{OH})^-$  are particularly stable. The existence of a direct M-As bond is not necessary to the stability of the complex. XANES and vibrational spectra have been calculated to help in the identification of such complexes. Complexes of  $\text{AsS}(\text{SH})(\text{OH})^-$  with  $\text{Au}^+$  and  $\text{AuSH}$  may be implicated in “invisible gold” in arsenian pyrites. The other stable complexes identified may provide an explanation for the strong correlations commonly observed between the concentrations of heavy transition metals like  $\text{Hg}^{+2}$  and metalloids like As and Sb. The importance of such ternary complexes in the origin of element associations has been previously ignored.

We have also undertaken a systematic study of the acidities in aqueous solution of  $\text{Si}(\text{OH})_4$  and its oligomers (including a silica surface model,  $\text{Si}_7\text{O}_{19}\text{H}_{10}$ ) and related molecules, like  $\text{H}_3\text{PO}_4$ . Our goal is to calculate gas-phase deprotonation energies at the quantum mechanical state-of-the-art, accurate to better than 2 kcal/mol, and to evaluate hydration enthalpies at as high a level of accuracy as possible. This will allow us to determine the physics and chemistry behind the differing pKa's of  $\text{Si}(\text{OH})_4$  and the silica surface. We have found that gas-phase deprotonation energies, evaluated at a quantum mechanical level as low as 6-31G\* Hartree-Fock, correlate well with experimental solution pKa's. The correlation becomes even better if we use better methodology for the gas-phase calculations and if we incorporate approximate hydration energies. The gas-phase deprotonation energies also correlate well with underbondings at the O in the anion, evaluated using Brown's bond-length based approach, and with electrostatic energies from some charge models. For the oligomers the deprotonation energies are systematically lower than that for the monomer, consistent with the higher acidity of silica compared to  $\text{Si}(\text{OH})_4(\text{aq})$ . The difference may be somewhat exaggerated by specific H-bonding interactions, particularly in the flexible dimer, which may be partially counteracted by reduced stabilization by the aqueous solvent.

The nature and existence of so-called “tricluster” O's in aluminosilicate glasses (O's with three nearest neighbour tetrahedral atoms like Al or Si) is a continuing topic of debate. Quantum mechanical studies on conventional planar tricluster geometries have given electric field gradients (EFG's) at the O too large to match the peaks assigned to such triclusters by  $^{17}\text{O}$  NMR. We have systematically explored other tricluster species, using our knowledge of the inorganic chemistry literature to identify double 3-ring geometries in alumoxanes and O-O edge sharing geometries in aluminosiloxanes, using a cluster MO approach and the Hartree-Fock method. The O-O edge sharing geometries have O EFG's and NMR shifts close to the range observed in the NMR of Ca aluminosilicate glasses. In collaboration with Dr. R. E. Cohen (Geophysical Lab) we have also carried out FLAPW density functional band calculations on the O EFG's in the andalusite and sillimanite polymorphs of  $\text{Al}_2\text{SiO}_5$ . One of the sites (O(C) in andalusite) has an edge-sharing geometry and a small calculated EFG, even smaller than those from the cluster calculations. Such a site may be a candidate for the “tricluster” species.

We have examined the structures, stabilities and NMR shieldings of possible complexes between serine (an amino acid with a -OH functional group) and monomeric silicic acid. We find that near neutral pH, where the silicic acid is fully protonated, the most stable complex has a direct Si-O-C bond, not just a H-bonding interaction with the  $\text{Si}(\text{OH})_4$ . At higher pH, where the silicic acid is deprotonated, Si-O-C complexes of five-coordinate Si become stable. Calculated  $^{29}\text{Si}$  shifts for these five-coordinate species are in the range -117 to -120 ppm, making it possible to distinguish them from  $\text{Q}^3$  and  $\text{Q}^4$  inorganic

polymeric Si. Such five coordinate complexes also show very large shielding anisotropies (80 – 100 ppm), compared to much smaller values for four-coordinate Si, which may provide a better means for their identification.

## **GRANTEE: MASSACHUSETTS INSTITUTE OF TECHNOLOGY**

Department of Earth, Atmospheric and Planetary Sciences  
Cambridge, MA 02139-4307

**Grant :** DE-FG02-00ER14

### **Evolution of Pore Structure and Permeability of Rocks under Hydrothermal Conditions**

*J. Brian Evans, 617-253-2856, fax 617-258-0620, brievans@mit.edu; Yves Bernabé; Wenlu Zhu; Ulrich Mok*

**Objectives:** The pore structure and transport properties of rocks, including fluid permeability and electrical conductivity, can be altered by a wide variety of diagenetic, metamorphic, and tectonic processes. We are studying the interrelationships among permeability, mechanical properties, and the pore shape, under hydrothermal conditions, in mineral aggregates, with and without reactions.

**Project Description:** We are conducting three suites of experiments: 1.) Measurements of permeability and electrokinetic properties of synthetic sandstones with varying surface roughness. 2.) Measurements of evolution of permeability during the compaction of granular aggregates of quartz with varying grain size and pore-fluid chemistry at temperatures from 450-800°C, in stagnant fluids, at pore pressures up to 200MPa, and at confining pressures between 200-400 MPa. 3.) Measurements of permeability in granular aggregates under similar conditions with slowly flowing pore fluids. Current results indicate that the measurements of macroscopic transport properties can be rationalized by considering the evolution of the pore space. As the mineral aggregates react and lithify, a larger fraction of porosity becomes ineffective for fluid or electrical transport. In the new work, observations to quantify changes in surface roughness, porosity, and pore dimensions will be made using standard optical, scanning electron, and laser confocal scanning optical microscopes. The image data will then be used in network models to predict the permeability. A better understanding of the processes that change porosity in the Earth is important for improving resource recovery, predicting rates of metamorphism, understanding fault mechanics and fault stability, and estimating rates of deformation by pressure solution.

**Results:** We measured the relationship between permeability and porosity during diagenetic alteration of a suite of synthetic sandstone samples (porous glass) with initial porosity from 5% to 35%. Experiments were conducted at 150-250°C and at 20 MPa pore pressure with pure water as pore fluid over several days. We measured in-situ permeability, porosity, and electrical streaming potential using a newly designed hydrothermal alteration vessel. The relation between permeability and porosity in the sintered, unaltered glass packs is similar to that of Fontainebleau sandstone, but the evolution of permeability during chemical alteration is much different and is comparable to that of shale or Rotliegend sandstone (see Figure 1). The path of evolution of the relationship between porosity and permeability (EPPR) depends critically on the mechanisms of the alteration of the porosity. By comparing data from a variety of natural and synthetic samples, it is possible to identify classes of EPPR curves that depend on the geometry of the original material and the process of porosity reduction (*e.g.*, diagenetic reaction, brittle compaction, and plastic deformation). To complete the investigation on synthetic glass we redesigned the apparatus for constant flow-through experiments, allowing us to examine EPPR and streaming potential of higher porosity samples (>15%) in more detail and to consider the alteration kinetics and fluid chemistry. We also prepared our measurement system for examining natural sandstones and synthetic quartz-feldspar mixtures.

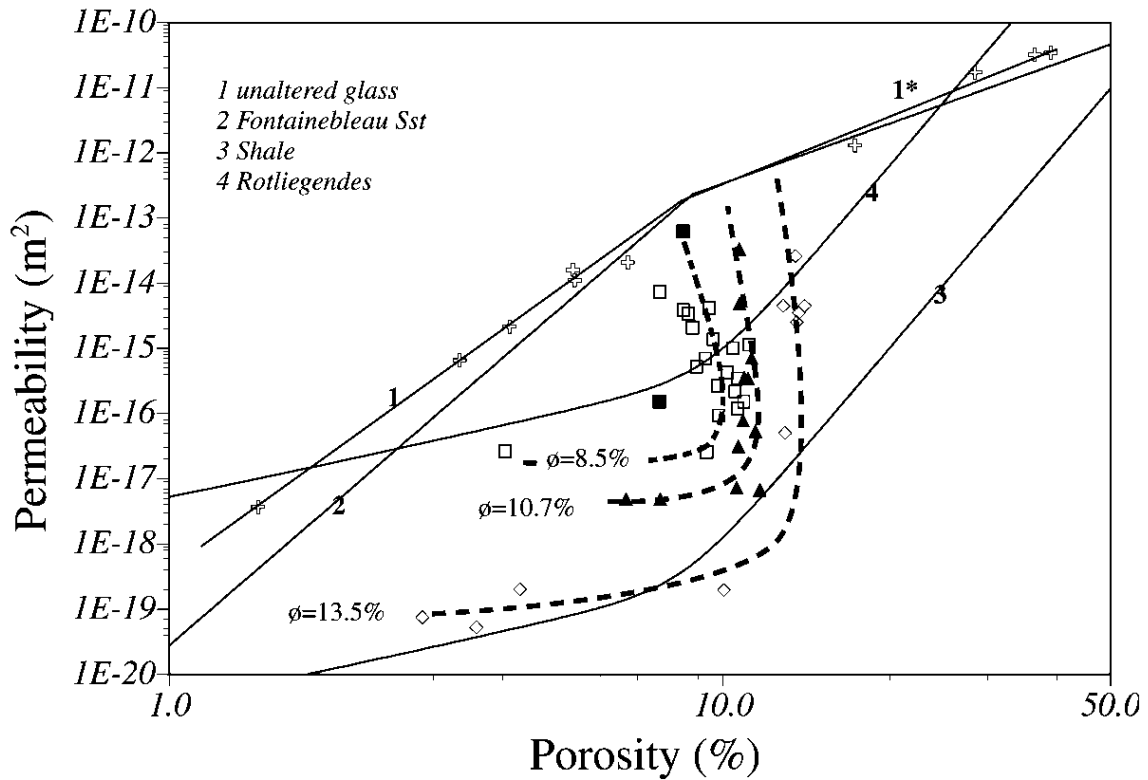


Figure 1: Permeability versus porosity measured during alteration in log-log scale for three samples with different initial porosities (trends are shown in dashed shaded lines). In addition, we plotted results on unaltered glass (crosses, line 1) including data from *Blair et al.*[1996] (line \*1). For comparison we also plot natural rock models [*Pape et al.*; 1999] (lines 3 and 4). The behavior of unaltered glass is quite similar to that of Fontainebleau sandstone (line 2) [*Pape et al.*, 1999].

## **GRANTEE: MASSACHUSETTS INSTITUTE OF TECHNOLOGY**

Department of Civil and Environmental Engineering  
Cambridge, Massachusetts 02139

**Grant :** DE-FG02-00ER15029

### **Transport Visualization for Studying Mass Transfer and Solute Transport in Permeable Media**

*Charles Harvey, 617-258-0392, fax 617-258-8850; charvey@mit.edu; Lucy Meigs, lcmeigs@sandia.gov; Roy Haggerty, haggert@geo.orst.edu*

**Objectives:** This research seeks: (1) to determine when the small-scale permeability structure causes solute spreading to be dominated by classical dispersion and when it causes solute spreading to be dominated by mass transfer; and (2) to understand how time-scales of mass transfer depend on physical, quantifiable characteristics of the geologic medium.

**Project Description:** Theoretical work is being conducted to define regimes of transport based on quantifiable measures such as dimensionless numbers. A portion of this theoretical work (and associated experiments) is focused on determining the conditions under which physical mass transfer (*i.e.*, diffusion into immobile zones) is significant, and to developing models for predicting the effects of mass transfer over long time scales. The numerical simulations are coupled with laboratory experiments using transmitted light, x-ray absorption, and conventional breakthrough curves to test and further understand the regimes of transport. Within the mass transfer regime, the geometries of flow and transport parameters that lead to multiple rates of mass transfer and scaling of transport processes are being evaluated.

**Results:** In order to map the regimes of transport, a method was developed for generating random hydraulic conductivity ( $K$ ) fields that have highly connected flow paths or barriers, which have been found to be critical to understanding the regimes of transport. These fields share the same low-order statistics as multigaussian fields (mean, variance and covariance function), but have very different flow and transport characteristics because they are highly connected. Specifically, the results show that 2D hydraulic conductivity fields with the same basic spatial statistics, but different degrees of connectedness, may produce: (1) effective conductivities that are significantly above or below the geometric mean, (2) solute transport behavior that is best modeled through Fickian dispersion or behavior that is better modeled as rate-limited mass transfer, and (3) mass transfer that is driven that by either diffusion or advection. This work demonstrates that standard characterizations of heterogeneity may not capture the flow and transport characteristics of all aquifers.

A series of laboratory experiments are being designed to allow us to evaluate our understanding and predictions about the regimes of transport. These transport experiments are being conducted on thin chambers filled with glass beads using transmitted light to spatially map solute concentrations. Breakthrough concentrations are also being measured. Prototype experiments conducted within the mass transfer regime have enabled us to refine our experimental design.

## **GRANTEE: MASSACHUSETTS INSTITUTE OF TECHNOLOGY**

Department of Earth, Atmospheric, and Planetary Sciences  
Cambridge, MA 02139

**Grant :** FG02-99ER15004

### **Theoretical Studies of Landscape Erosion**

*Daniel H. Rothman, 617-253-7861, dan@segovia.mit.edu*

**Website:** <http://segovia.mit.edu/>

**Objectives:** To formulate quantitative theories for processes that erode landscapes and create river networks, to determine unique topographic signatures of such processes, and to test predictions using digital elevation data.

**Project Description:** Whereas the results of large-scale landscape erosion are nearly obvious to the eye, they are notoriously difficult to predict by quantitative physical theories. Moreover, when predictions can be made, they often show that real landscapes differ only slightly from random landscapes. Therefore a better understanding of the processes that shape landscapes requires not only well-defined quantitative measures but also theories that specify the physical and geological significance of these quantities.

We study two aspects of landscapes: the geometry of river networks, and the statistical features of the surfaces in which they are embedded. The former are characterized by scaling laws that reflect the structure of the networks, while the latter are described in terms of spatial correlations between drainage basins and the slopes they form. We study both the foundation of these relations in addition to the extent to which real landscapes exhibit them.

**Results:** Our studies of river-network scaling laws have focused primarily on Hack's law, an approximate power-law relation between basin area and stream length. We find that Hack's law contains systematic deviations at all scales. At the largest scales, these deviations result from the overall shape of the geologically imposed boundaries that form the river basin. Specifically, elongate basins yield large Hack exponents. We therefore conclude that the observed distribution of Hack exponents is due in part to the requirement that a river network drain an area of a geologically predefined shape. We have also studied the statistical fluctuations of river-network scaling laws. We find that the spatial distribution of stream segments is random, suggesting that this is the most fundamental description of river-network architecture.

Last, we have begun studies of the relation between slope and drainage area so that we may better specify the forces and fluxes associated with erosion. We have shown that a power-law relation between slope and area, long thought to be a fundamental indicator of erosive mechanisms, can instead result from purely geometric considerations. Because this result holds under general, but not universally applicable, conditions, it usefully specifies the class of physically significant slope-area relations. In a related study, the computation of a novel correlation function has shown that the orientation of small-scale channel-like features is coupled to large-scale structure. A key finding is that this two-scale interaction is scale dependent, suggesting that a commonly applied effective equation for erosion can itself depend on scale.

## **GRANTEE: MASSACHUSETTS INSTITUTE OF TECHNOLOGY**

Earth Resources Laboratory  
Department of Earth, Atmospheric, and Planetary Sciences  
Cambridge, Massachusetts 02139

**Grant:** DE-FG02-00ER15041

### **Fluid Mobility Estimation From Electro seismic Measurements: Laboratory, Field, and Theoretical Study**

*M. Nafi Toksöz, 617-253-7852, fax 617-253-6385, toksoz@erl.mit.edu; Daniel R. Burns*

**Objectives:** The objective of this project is to develop an improved theoretical model and obtain higher quality laboratory and field data of the electro seismic phenomena in order to use electro seismic data to estimate *in-situ* permeability values.

**Project Description:** Permeability is a parameter of critical importance for the simulation of and prediction of hydrocarbon production, groundwater contaminant transport, and the viability of underground sequestration of CO<sub>2</sub>. Recent field and laboratory measurements suggest that electro seismic signals can be used to estimate *in-situ* permeability values. In this application, a propagating seismic wave initiates fluid motion in a permeable formation. This fluid flow causes a charge separation due to fluid ion adsorption on grain surfaces of the rock, resulting in an excess charge in the moving fluid. This charge separation induces an electrical field that can be measured. This project consists of three major tasks: 1) to investigate the basic physics of fluid flow in porous media through the use of nuclear magnetic resonance (NMR) imaging of pore-scale fluid flow and numerical simulation of such flow using cellular automaton lattice gas models; 2) to perform a series of laboratory experiments to measure electro seismic effects on a range of samples as functions of frequency; and 3) to refine the theoretical models of electro seismic signal generation based on imaging and lab measurements and use this model to analyze existing field data acquired in a borehole in a VSP and logging geometry by MIT's Earth Resources Laboratory.

**Results:** During this first nine months of the project we have focused our efforts on the first two tasks: NMR imaging and laboratory measurements. In the area of NMR imaging, we completed a study of the effect of image resolution on permeability estimates. In this study, we used a high-resolution 3-D image (7.5 micron) of a sandstone sample and estimated the permeability based on fluid flow simulation through the imaged pore structure. We then coarsened the image and re-ran the simulation. The results show that the permeability estimates are proportional to the image resolution, but the largest size flow paths control the flow properties of the sample. We have also completed a study, partially supported by this grant, on the frequency dependence of streaming potential coupling coefficients. Streaming potential measurements were acquired in the frequency range of 5-200Hz on a capillary tube and two glass filters with different pore diameters. The resulting data were compared to predictions using the Packard and Pride models. Although both models fit the data well, Pride's model is more complete. Pride's model has also been used to analyze electro seismic data acquired over the frequency range of 100-2000Hz in a borehole drilled into fractured granite, but the model predictions do not fit the data particularly well. The theoretical models will be studied in more detail in the coming year.

## **GRANTEE: UNIVERSITY OF MINNESOTA, TWIN CITIES**

Dept. of Geology and Geophysics and Minnesota  
Supercomputer Institute  
Minneapolis, MN, 55415-1227

**Grant:** DE-FG03-91ER14212

### **Magma Rheology, Mixing of Rheological Fluids, Molecular Dynamics Simulation , and Lithospheric Dynamics**

*D.A. Yuen, 612-624-1868, fax 612-624-8861, davey@krissy.mni.umn.edu; F. J. Spera, University of CA, Santa Cruz*

**Website:** <http://banzai.msi.umn.edu>

**Objectives:** Mixing efficiency in complex rheology, molecular dynamics of complex fluids and micro-scale Rayleigh-Taylor instabilities, effects of complex rheology in lithospheric dynamics.

**Project Description:** This project will improve our understanding of the thermal, chemical, dynamical and mechanical state of the continental crust and subcrustal lithosphere with particular focus on the interactions between the various subsystems. The work plan includes: (1) rheological laboratory measurements on melts and magmatic suspensions; (2) Determination of the thermodynamical and transport properties of molten silicates by MD simulations; (3) Mixing processes of rheological fluids in convection and visualization of complex processes; (4) Coupling between mantle convection with temperature-dependent and non-Newtonian rheology and mantle diapirs on the thermal regime and subsidence curves of rift-related basins; (5) The dynamical influences of lithospheric phase transitions on the thermal-mechanical evolution of sedimentary basins; (6) The development of stress fields and criteria for faulting in the crust; (7) Modeling of heat and mass transport driven by thermal and compositional heterogeneities in porous media; and (8) Open system geochemical modeling of magmatic systems.

**Results:** The results described below are for the U of Minnesota part of this project. Additional results are given in the summary of activities can be found in the summary of activities by the University of California team led by F.J. Spera. We have studied with 2-D molecular dynamics the mixing phenomenon in the microscale, between 500 and 10 000 Å. We have employed up to 3 million particles interacting with a two-body potential and up to one million time-steps were integrated. We have focused on the temporal evolution of the mixing layer between two superimposed particle systems in a gravitational field directed from the heavier to the lighter particle ensemble. We have compared the micro properties with those observed in the macroworld. We found that the bubble-and spikes stage of mixing process is similar in both the micro (molecular-scale) and macro worlds. The mixing layer growth constant  $A$ , which can be obtained from molecular dynamics, is approximately the same as that obtained for 2-D simulations in the macroscale. The occurrence of Rayleigh-Taylor instability in the microscale, and its similarity to the same process in the macroscale, can also expand the concept of turbulence to microscaled flows on the nanoscale. This work has been published in *Physica D*, 137, 157-171, 2000.

We have studied the mixing properties and differences between Newtonian and non-Newtonian convection. Both the line and field methods were employed. The line-method is based on monitoring of

passive particles linked into lines, while the field method relies on the advection of a passive scalar field by solving a partial differential equation with a hyperbolic character. Both visual and quantitative estimates revealed that the efficiency of the Newtonian mixing is greater than that for non-Newtonian (power-law) rheology. A chemical heterogeneity placed in the non-Newtonian convection forms preferentially horizontal structures, which may persist for at least 1 Ga in the upper-mantle. In addition, the non-Newtonian medium reveals a lesser amount of stretching of the lines than the Newtonian material. The rate of the Newtonian stretching fits well with an exponential time-dependence, while the non-Newtonian rheology shows the stretching rate close to a power-law dependence with time. Due to the non-linear character of the power-law rheology, the non-Newtonian fluid offers a natural scale-dependent resistance to deformation, which prevents efficient mixing at the intermediate length scales. This paper has several movies and can be found in *Electronic Geosciences*, 4:1, 1999.

We have studied the effects of low-temperature plasticity on the formation of shear zones. A thermal-mechanical model has been developed for describing the shear deformation of Maxwell viscoelastic material with a rheology close to dry olivine. In addition to diffusion and dislocation creep, we have included deformation by low-temperature plasticity, called the Peierls mechanism, which is significant at low temperatures and has a strong exponential dependence on the shear stress. When a sufficient magnitude of heat is produced by the rapid conversion of the elastically stored energy into viscous dissipation, thermal instability takes place and the deformation localizes in a narrow zone. For dry olivine and realistic values of the strain-rate, the effect of low-temperature plasticity is influential for temperatures between around 800 and 1000 K. This finding suggests that low-temperature plasticity may be crucial in regulating thermal-mechanical stability in the shallow portion of subducting slabs. This work has appeared in *Earth Planet Sci. Lett.*, 168, 159-172, 1999.

We have studied the effects of non-Newtonian rheology in producing ultra-fast plumes, which can spread out rapidly in horizontal direction upon impacting the lithosphere. These plumes can move at upward velocities in excess of meters / year and are considerably faster than the Newtonian plumes. These results show a direct separation of timescales between the rapidly rising non-Newtonian plumes and the ambient mantle circulation. This work has come out in *Tectonophysics*, Vol. 311, 31-43, 1999.

We have also studied mantled inclusions, commonly encountered in mylonites, which can record the deformation history. We have carried out two-dimensional numerical studies of time-dependent deformation behavior of inclusion and its dependence on rheology under simple shear. The inclusion is taken to be deformable and having its own intrinsic rheological properties. The results of numerical modeling shows that a key factor of structural appearance is the effective viscosity contrast between the inclusion and the matrix material. A high viscosity contrast from non-Newtonian rheology inhibits the stretching of the inclusion, preserving its round shape. This result is similar to our results in mixing. Wings or tails can only be developed in mineralogic systems with a high effective viscosity contrasts. This work has been published in *Earth Planet. Sci. Lett.*, 165, 25-35, 1999.

## **GRANTEE: NATIONAL ACADEMY OF SCIENCES, BOARD ON EARTH SCIENCES AND RESOURCES**

2101 Constitution Ave. NW  
Washington D.C. 20418

**Grant:** DE-FG02-97ER14810

### **Board on Earth Sciences and Resources and Its Activities**

*Anthony R. de Souza, 202-334-2744, fax 202-334-1377, adesouza@nas.edu*

**Website:** <http://www4.nationalacademies.org/cger/besr.nsf>

**Objectives:** The purpose of the Board on Earth Sciences and its committees is to provide a focal point for National Research Council activities related to earth science policy.

**Project Description:** The Board addresses the following strategic earth science issues: identifying the frontiers of basic and applied research in the Earth sciences; strengthening multidisciplinary programs and integrated approaches to research; assessing mineral and energy resources; investigating human interactions with the Earth; understanding environmental change; improving access to and use of scientific and geospatial data and information; evaluating breakthrough technologies for mitigating environmental problems; and enhancing Earth science education.

**Results:** During FY 2000, the Board on Earth Sciences and Resources produced 6 reports:

- *Review of Scientific Aspects of the NASA Triana Mission*
- *Seeing into the Earth: Noninvasive Characterization Of the Shallow Subsurface for Environmental and Engineering Applications*
- *Review of the Volcano Hazards Program of the U.S. Geological Survey*
- *Future Roles, Challenges, and Opportunities for the U.S. Geological Survey*
- *Research Opportunities in the Earth Sciences for the National Science Foundation*
- *Review of NASA's Earth Science Enterprise Research Strategy for 2000-2010*

In addition to producing reports, the board and its standing committees in 2000 had about 40 projects under development or in the funding stage and over 10 studies under way. During the year, the Board and its standing committees convened or facilitated meetings to exchange information among scientists, engineers, and policy makers from government, university, and industry. Examples include: a public symposium in June 1999 on the topic of hazards and resources in the new century; a fall 2000 10-day conference entitled Twentieth Conference of the U.S. Board on Geographic Names; and a 3-day meeting, NASA Solid Earth Science Working Group Meeting.

## **GRANTEE: UNIVERSITY OF NEVADA AT RENO**

Department of Geological Sciences  
Reno, Nevada 89512

**Grant:** DE-FG03-98ER14885

### **Growth of Faults, Scaling of Fault Structure, and Hydrologic Implications**

*Jane C.S. 702-784-6987, fax 702-784-1766, JCSLONG@mines.unr.edu; Stephen Martel 808-956-7797, fax 808-956-5512, martel@soest.hawaii.edu; Kevin Hestir, Utah State University, 801-797-2826, fax 801-797-1822, hestir@sunfs.math.usu.edu; James P. Evans, Utah State University, 801-797-2826, fax 801-797-1588, jpevans@cc.usu.edu*

**Website:** <http://www.soest.hawaii.edu/martel/SteveM.html>

**Objectives:** The main research objectives are: (a) to determine how faults grow in three dimensions in brittle crystalline rocks (granites and basalts), and (b) to further develop physically based stochastic models for predicting geometric and hydrologic properties of such faults.

**Project Description:** We are investigating how faults of different scale grow in granite and basalt in three-dimensions. We are systematically examining the geometries, structure, and mechanics of faults with trace lengths of a few meters to several kilometers, and using this knowledge to develop physically based stochastic models for predicting the geometry of faults over a wide range of scale and for analyzing their hydraulic behavior.

**Results:** In the granitic rock of the Sierra Nevada, California, a strike-slip fault with a trace length of several kilometers has been mapped in Sequoia National Park, and slip distribution data have been collected along it. Observations from the Sierra also show two new ways that pre-existing igneous dikes have influenced how faults develop. First, the aforementioned fault apparently developed, at least in part, by brittle fracturing along pre-existing igneous dikes. Second, some faults developed from joints clustered around igneous dikes. This suggests that the joints, and hence the faults, reflect processes associated with the intrusion (and perhaps cooling) of the dikes. For normal faults in Hawaiian basalts, approximately one hundred new profiles have been surveyed across faults of the Koaie fault system to determine the distributions of slip and secondary fractures. Two-dimensional boundary element analyses motivated by our prior mapping accounts for the main geologic features along those faults: gaping vertical fissures on the uplifted footwall; monoclinial flexures and steeply inclined cavities along the scarps; and buckles on the footwall. The fissures and cavities must strongly influence the hydrologic properties of the normal faults; these findings should be relevant to several DOE sites in the western United States.

**GRANTEE: NEW ENGLAND RESEARCH**

331 Olcott Drive, Ste L1  
White River Junction, Vermont 05001-9263

**Grant:** DE-FG02-98ER14906

**The Role of Fracture Intersections in the Flow and Transport Properties of Rock**

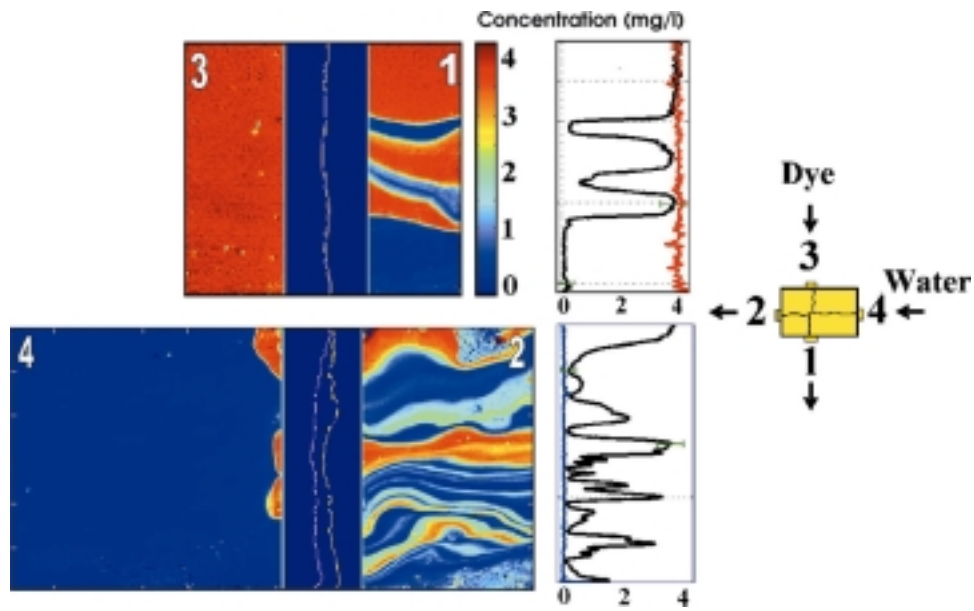
*Stephen R. Brown 802-296-2401, fax 802-296-8333, sbrown@ner.com; Harlan W. Stockman, Sandia National Laboratories; Arvind Caprihan, New Mexico Resonance*

**Objectives:** Flow and solute mixing behavior at fracture intersections is a complex function of surface roughness and channeling. The objective of this project is to gain a more complete understanding of flow channeling in fracture networks by physically modeling and analyzing several configurations of flow and transport through fracture intersections.

**Project Description:** We are addressing several problems concerning flow and transport through fracture intersections using a combination of numerical modeling, quantitative measurements, and visual observation of processes in real rough-walled fractures. Our observations include: channeling in single fractures, channeling within and through single fracture intersections, and channeling through fracture networks. These studies consider bulk flow, transport of solutes, and transport of multiple immiscible phases. For this work we use a combination of quantitative measurements, digital video imaging and magnetic resonance imaging (MRI) observations of flow through real rough-walled fractures, and numerical modeling via lattice Boltzmann (LB) methods. These observations will ultimately be used to develop quantitative models describing the channeling and mixing behavior in 3-D intersections of rough-walled fractures.

**Results:** Several natural fracture intersections were replicated in transparent epoxy, while a synthetic intersection was made from textured glass. Laboratory experiments of single-phase mixing of solutes were performed by flowing water and dye solutions through the specimens. We find that in intersecting natural fractures the degree of average mixing is greater than predicted by parallel plate streamline routing. Apertures at the intersection vary spatially, resulting in highly variable flow rates around the intersection. This leads to multiple pure fingers of each solution both bending around and crossing straight through an intersection. While the outlet fluids are heterogeneous (not mixed locally), the average degree of mixing is higher than expected for hydraulically equivalent parallel plates.

We are comparing the experimental flow and mixing results to two different numerical methods using the experimentally-observed intersection geometry. First, the lattice Boltzmann method is used to solve the Navier-Stokes equations for 3-dimensional flow. Second, the Reynolds equation for 2-dimensional flow is solved simultaneously for flow in both variable aperture fractures, with source/sink terms creating an intersection between the two fractures. Numerical simulations for the textured glass laboratory specimen agree well with the laboratory experiments, both in the amount of average mixing and in the spatial distribution of dye streamlines.



Example experiment for a natural fracture intersection. Digital video cameras are used to monitor the experiment and the location and concentration of dye in the fractures is derived by image analysis. Pure water (blue) flows into one inlet and dyed water (red, concentration=4mg/l) flows into the other inlet. The images and graphs of dye concentration show that the outlet legs of the intersection contain heterogeneous fingers of pure water and pure dye.

## **GRANTEE: UNIVERSITY OF NEW MEXICO**

Department of Geosciences  
Albuquerque, New Mexico

**Grant:** DE FG03-97ER14778

### **Continuum and Particle Level Modeling of Concentrated Suspension Flows**

*M. Ingber, University of New Mexico; L. Mondy, 505- 844-1755, fax 505-844-8251, lamondy@sandia.gov; A. Graham, Texas Tech University*

**Objectives:** The purpose of this program is to combine experiments, computations, and theory to make fundamental advances in our ability to predict transport phenomena in concentrated, multiphase, disperse systems, particularly when flowing through geologic media.

**Project Description:** The proposed research will elucidate the underlying physical principles that govern concentrated multiphase systems in areas essential to continued progress in geosciences. In order to be of use in real world applications, significant enhancements to currently available continuum-level suspension flow models will be required. We will use both experimentation and high performance computing to obtain microstructural information that is necessary to the development and refinement of the continuum models. For example, we expect to use this microstructural information to gain insight into the physics of particle interactions and particle sedimentation, which are particularly important in sand control issues found in petroleum production. Further, we expect that continuum-level modeling could eventually be directly implemented in codes currently used to predict hydraulic fracturing operations in the petroleum industry. The understanding gained about the physics of multiphase flows will, however, have much broader application in geosciences.

**Results:** The continuum models originally developed by Phillips *et al.*(1992) and Nott and Brady (1994) have been extended to account for normal stress contributions in general three-dimensional flows. The Phillips-type model currently also allows for non-neutrally buoyant particles and non-Newtonian suspending liquids. However, we have found that without the enhancement of the suspension flow model with an anisotropic flow tensor, the results for the non-Newtonian suspending fluid are qualitatively incorrect in some cases. Experimental measurements based on nuclear magnetic resonance (NMR) imaging were taken to test our theory that effects of a shear-thinning suspending fluid are also influenced by the particle-induced normal stress contributions. For Newtonian suspending liquids, we have concentrated on modeling viscous resuspension of a settled bed of particles -- a phenomenon important in many geologic flows. Although the model works extremely well for most flows influenced by gravity, numerical instabilities appear when the particle concentration, and hence the viscosity, changes abruptly. A porous Brinkman source term that will slow the flow depending on the particle volume fraction is known to be a more robust approach to phase-change than that of solely ramping the viscosity. Therefore, such a source term was implemented in our model. Preliminary results showed promise in minimizing numerical instabilities.

In addition, massively parallel computing has allowed particle level simulations, based on the boundary element method (BEM), with up to a thousand particles. These simulations were used to determine the magnitude of the normal stresses developing from particle interactions. They are continuing to be used, as well, to develop more accurate hindered settling functions for particles interacting with other types of particles or in a porous medium. These simulations lead to detailed information on individual particle

and fluid motion that is unobtainable through experiments. In addition, a multipole-accelerated boundary element method (BEM) has been developed to simulate many thousands of individual interacting particles. Three-dimensional simulations are now possible for dynamically interacting particles.

## **GRANTEE: NEW MEXICO INSTITUTE OF MINING AND TECHNOLOGY**

Department of Earth & Environmental Science  
Socorro, New Mexico 87801

**Grant:** DE-FG03-96ER14589

### **Investigation of Permeability Upscaling**

*John L. Wilson, 505-835-5308, fax 505-83506436, jwilson@nmt.edu; Vincent C. Tidwell, Sandia National Laboratories, 505-844-6025, fax 505-844-6023, vctidwe@sandia.gov*

**Objectives:** Experimentally investigate permeability upscaling for a variety of geologic materials, interpreting the measured permeability upscaling in light of the physical characteristics of the porous medium and the measurement characteristics of the sampling instrument. Specific objectives during this period are to (1) investigate and model the effects of non-uniform flow, local-scale anisotropy/heterogeneity, and non-Gaussian permeability distributions on permeability upscaling, (2) quantify measurement characteristics of the minipermeameter and incorporate them into models of permeability upscaling, and (3) extend physical investigations of permeability upscaling by testing rock types not well represented in current data base.

**Project Description:** Porous media flow and transport data are collected at a variety of scales, and then integrated into models at an even different and larger scale. Upscaling is used to translate the data to model effective media properties. A laboratory investigation of permeability upscaling is being conducted with the use of a novel minipermeameter test system. It allows precise, rapid, non-destructive measurement of permeability over a range of different sample supports (*i.e.*, sample volumes). By varying the size of the minipermeameter tip seal, measurements spanning five orders of magnitude on a per-volume basis are made subject to consistent boundary conditions and flow geometry. Thousands of measurements on multiple faces of meter-scale blocks of rock are collected with each of five different tip seals (0.31 - 5.08 cm ID) plus a single large tip seal (15.24 cm ID) designed to integrate over the entire sampling domain. This process is repeated on multiple rock samples, each of which exhibits different textural and structural characteristics. Key summary statistics are calculated from the data sets and analyzed with reference to their corresponding sample support. The measured data are then interpreted with the assistance of theory and simulation.

**Results:** Over 200,000 permeability measurements, associated with six different sample supports, have been collected from four rock samples: a planar bedded sandstone, a sandstone exhibiting nested scales of cross-stratification, a densely-welded tuff and a poorly-welded tuff. For each rock sample and each summary statistic investigated (*e.g.*, mean, semivariogram), distinct and consistent upscaling trends were measured. Rocks of similar genetic origin (*e.g.*, tuffs) were found to exhibit similar statistical and upscaling characteristics, while rocks of differing origin (*e.g.*, tuffs *vs.* sandstones) exhibited distinct differences. The noted differences can largely be attributed to variations in the physical attributes (*i.e.*, spatial patterns, correlation length scales) characterizing the individual rock samples. Quantitative interpretations were pursued through comparisons drawn with theoretical upscaling models, each differing according to key fundamental assumptions. Results indicate that the non-uniform flow geometry imposed by the minipermeameter and the local-scale (*i.e.*, at or below the smallest scale of measurement) heterogeneity is a key process influencing the measured permeability upscaling. Using image analysis, we compared the permeability measurements and a wide variety of objective textural

measures drawn from the corresponding digital (visual) images. There was no significant direct correlation despite the obvious resemblance of the permeability maps and visual images for each rock. This may have implications for geophysical characterization methods. Linear filter analysis was employed to characterize instrument sample support (*i.e.*, effective size of the sample support and the spatial weighting of heterogeneities comprising that support) associated with each measurement. We continue to collect and analyze additional data on new and old samples, including eolian sandstones and carbonates.

To better interpret upscaling results we studied the details of the gas minipermeameter measurement method using numerical and analytical mathematical models. We derived solutions for the flow field under various conditions of media heterogeneity, and developed an adjoint state method for theoretically determining the instrument's spatial filter function. The function shows great sensitivity to the permeability just below the inner tip seal radius, and a lower but still significant sensitivity to the permeability just below the outer tip seal radius. The function is proportional to the square of fluid velocity, a previously unreported observation for any instrument. In a recent collaboration with Fred Molz of Clemson University, we offer a simple explanation for this observation. We also calculated Green's Functions for the flow field, which are being used to derive stochastic perturbation solutions for minipermeameter flow in a stochastically heterogeneous rock sample.

We took a 30 by 30 by 2.5-cm thick slab of cross-stratified Massilon sandstone, characterized it with detailed permeability measurements with different tip seal sizes, x-ray measurements of porosity, and visual image analysis. We then saturated the slab with water and ran sodium-iodide tracer through the slab longitudinally. Break-through curves (BTCs) were constructed from effluent sampling, and two-dimensional digital images of the solute concentration fields at selected times during the tracer experiment were acquired using X-ray absorption. The tracer behavior was strongly influenced by the nested scales of heterogeneity in this rock sample, exhibiting even the influence of individual lamina in the cross-beds.

**GRANTEE: STATE UNIVERSITY OF NEW YORK AT STONY BROOK**

Department of Geosciences  
Stony Brook, New York 11794-2100

**Grant:** DE-FG02-94ER14449

**High Precision Radiometric Dating of Sedimentary Materials**

*G.N. Hanson, 631-632-8210, fax 631 632 8240, gilbert.hanson@sunysb.edu; W.J. Meyers*

**Objectives:** To develop field, petrographic and geochemical criteria to allow high precision U-Pb dating of sedimentary minerals within rapidly deposited sequences of carbonate and clastic rocks.

**Project Description:** The original goal was to obtain radiometric ages for sedimentary material with uncertainties of three million years or less to date the times of sedimentation. We have since shown that it is possible in some circumstances to obtain uncertainties of 1 Ma or less.

We started with the dating of soil calcite and have since shown the potential of U-Pb dating of sedimentary -lake, swamp, evaporitic and spring calcite. The most obvious applications for precise ages for times of sedimentation are:

1. providing more precise duration's for unconformity bound genetic packages in sequence stratigraphy,
2. more precisely calibrating the geologic time scale,
3. correlation between marine and terrestrial stratigraphic sections and
4. correlation between fossil-rich and fossil-poor stratigraphic sections.

**Results:**

**Pennsylvanian-Permian Boundary in Central Appalachian Basin**

The dominantly terrestrial sediments of the Appalachian Basin in southeastern Ohio and western Pennsylvania are considered Pennsylvanian based on controversial plant fossil correlations and characteristic cyclicality of sedimentation. These sedimentary groups in stratigraphic order and our concordant U-Pb ages for syn-sedimentary calcite within these groups are:

<b>Group</b>	<b>U-Pb Age (2σ)</b>
Monongahela	275 ± 6 Ma
Conemaugh	294 ± 6 Ma
Allegheny	302 ± 4 Ma
Pottsville	

The Pennsylvanian – Permian boundary is traditionally placed at the top of the Monongahela Group. The Pennsylvanian - Permian boundary is 302.4 ± 2.4 Ma reported by Rasbury *et al.*(1998) for a biostratigraphically well constrained marine sequence. Our ages place the boundary near the top of the Allegheny Group and places the overlying Conemaugh and Monongahela Groups in the Permian. These

data show that precise U-Pb ages can resolve problems in correlations between terrestrial and marine sequences.

*U-Pb age of Evaporitic Calcite in the Upper Permian Castile Formation*

Calcite in the uppermost Permian evaporitic Castile Formation of the Delaware Basin of Texas and New Mexico yields a concordant U/Pb age of  $251.6 \pm 2.5$  Ma. The age overlaps the currently accepted ages for the Permian-Triassic boundary based on dating of ashes from the marine section in China. This study illustrates the potential for dating calcite from biostratigraphically poorly constrained evaporitic sequences to aid in their correlation to normal marine sections.

*U-Pb ages for Calcite Derived from Relict Aragonitic Botryoids*

Relict aragonite botryoidal marine cements from the Tansil equivalent strata of the Capitan Reef of the Gaudalupe Mountains yield a concordant age of  $262 \pm 5$  Ma. This age is consistent with published zircon ages from the same section. The 10 Ma gap between the latest Capitanian and the overlying Castile Formation suggests an unconformity between these units that has not been recognized.

## **GRANTEE: STATE UNIVERSITY OF NEW YORK AT STONY BROOK**

Department of Applied Mathematics and Statistics  
Stony Brook, New York 11794-3600

**Grant:** DE-FG02-92ER14261

### **Medial Axis Analysis of Porous Media**

*W. Brent Lindquist, 631-631-8361, fax 631-632-8490, lindquis@ams.sunysb.edu*

**Website:** <http://www.ams.sunysb.edu/~lindquis>

**Objectives:** The goals of this program are to extract quantitative information on the geometry of pore structure in rock, the distribution of fluids in the pore spaces under two phase flow regimes, and the relationship between the pore structure and fluid distribution.

**Project Description:** High resolution (3 to 10 micron), three-dimensional images of rock samples, either dry or containing fluids, are obtained using X-ray computed microtomography. For two-phase flow studies, fluid contrast is achieved by doping one phase with a higher X-ray absorbing agent. For pore structure studies using dry or single-phase flooded rock, the void space is segmented and its structure (coordination numbers, channel lengths, pore volumes, throat sizes) determined using computational geometry algorithms. For fluid distribution studies, images of two-phase fluid distribution are differenced against single-phase fluid distribution in the same rock volume to identify the position of individual fluids. Distributions of each phase are numerically mapped in the pore space and correlations with pore properties computed.

**Results:** An extensive analysis of the void structure (imaged at 5.7 micron resolution) of a suite of Fontainebleau sandstones ranging from 7.5 to 22% porosity was completed. In FY '00, three projects are being pursued. In collaboration with S.-R. Song (Taiwan National Univ.) the characterization of the void structure in a suite of vesiculated basalts is nearing completion. Vesiculated basalts present a challenge due to the extreme range of vesicle sizes, and are of interest due to their presence in potential nuclear waste storage facilities. In collaboration with R. Seright (Petroleum Recovery Research Center, New Mexico Tech.), the effect of water- and oil-soluble polymerizing gels on the distribution of oil and water phases in Berea sandstone is being determined. Such gels appear to enhance oil recovery, though the exact mechanism is not well understood. The goal of this study is to elucidate this mechanism. In collaboration with M. Knackstedt (Australian National University), network flow models are being used to determine the impact of the various measured properties of the void space on two-phase fluid flow. Our results indicate that including the correct quantification of spatial correlation between properties (*e.g.* pore-pore size correlations) is necessary in obtaining physically accurate computations of fluid motion.

## **GRANTEE: STATE UNIVERSITY OF NEW YORK AT STONY BROOK**

Department of Geosciences  
Stony Brook, NY

**Grant:** DE-FG02-96ER14633

### **Surface Chemistry of Pyrite: An Interdisciplinary Approach**

*Martin A.A. Schoonen, 631-632-8007, mschoonen@notes.cc.sunysb.edu; Daniel R. Strongin, 215-204-7119, fax 215-204-1532, dstrongin@nimbus.ocis.temple.edu*

**Website:** <http://sbmp97.ess.sunysb.edu>

**Objective:** The primary goal of this research program is to understand the microscopic aspects of pyrite oxidation. Characterization of the reaction sites that control this chemistry is one of the immediate goals. Our continuing research strategy is to understand macroscopic observations of pyrite reactivity with an atomic/molecular level view. The results of this research will lead to a better understanding how pyrite reacts in a range of chemical environments.

**Project Description:** The reactivity of pyrite in anoxic and oxic environments is being investigated by integrating aqueous geochemical and modern surface science techniques. In addition the effect of visible light illumination of the pyrite surface during oxidation has been investigated (see below). The surface science techniques have generally operated in the ultra-high vacuum environment, but a recent emphasis has been to develop in-situ techniques to study the mineral surface on a microscopic level in the presence of an aqueous or gaseous phase. Research concentrates on well characterized and clean "as-grown" and powdered samples of pyrite. Electron spectroscopies in UHV and vibrational spectroscopy at real pressures are used to understand the atomic composition and the nature of the functional groups on pyrite after exposure to oxidizing aqueous and gaseous environments. In FY2000, two primary studies have investigated the effect of adsorbed phosphate and light on pyrite oxidation.

#### **Results:**

Modification of the pyrite surface with phosphate and the effect on oxidation

The effect of phosphate on the oxidation of crushed and {100} pyrite was investigated with aqueous geochemical and surface science techniques. Phosphate in solution significantly suppressed pyrite (crushed) oxidation for pH>4. At pH of 3 or less, phosphate expressed no experimentally discernable effect on pyrite oxidation. The use of surface science techniques, specifically, X-ray photoelectron spectroscopy (XPS), showed that at pH>4, phosphate became bound to Fe<sup>3+</sup> sites on {100} pyrite during the oxidation process. Phosphate bound in this way showed a significant inhibition on pyrite oxidation (based on XPS determinations of sulfur and iron oxide product concentrations) under our experimental conditions. These results suggested that the rate of pyrite oxidation in the absence of phosphate was facilitated near or at Fe<sup>3+</sup> bearing oxidation phases on the surface. Phosphate bound on Fe<sup>3+</sup> oxide product either prevents O<sub>2</sub> adsorption on this phase or electronically modifies these surface regions, but in either case inhibits electron transfer from pyrite-Fe<sup>2+</sup> sites to molecular O<sub>2</sub>.

Thermal and photochemical oxidation of pyrite

The thermal and photon-induced (visible light) oxidation of pyrite in solutions between pH 2 and 6 with dissolved oxygen was investigated by integrating surface science experiments and bath aqueous

geochemical oxidation experiments. Pyrite oxidation was experimentally determined to be strongly dependent on temperature. Interestingly, however, it was not possible to cast the temperature dependence in a simple Arrhenius equation, since the activation energy measured depended on the progress variable. For example, activation energies based on proton release rate, sulfate release rate, and total iron release rate vary by as much as  $40 \text{ kJ mol}^{-1}$ . It was inferred from this data that sulfur and iron oxidation and their subsequent release into solution followed different pathways. Exposure of pyrite to visible light (provided by a Xenon lamp) led to an acceleration of the oxidation rate, but the increase was typically less than a factor of two. X-ray photoelectron spectroscopy experiments showed within our experimental resolution that the chemical composition of the pyrite surface was unaffected by visible light illumination. Batch sorption experiments, however, showed that the reaction stoichiometry of the oxidation process was altered, suggesting that there was a change in reaction mechanism due to the exposure to visible light.

## **GRANTEE: STATE UNIVERSITY OF NEW YORK AT STONEY BROOK**

Department of Geosciences  
Stony Brook, New York 11794-2100

**Grant:** DE-FG02-99ER14996

### **Micromechanical Processes in Porous Geomaterials**

*Teng-fong Wong, 631-632-8212, fax 631-632-8240, Teng-fong.Wong@sunysb.edu; Joanne T. Fredrich, Sandia National Laboratories*

**Objectives:** This project focuses on the systematic investigation of the micro-scale characteristics of natural earth materials, and how these micro-scale characteristics control the macroscopic deformation and transport behavior. The research uses an integrated approach consisting of experimental rock mechanics testing, quantitative 2D and 3D microscopy and statistical microgeometric characterization, and theoretical and numerical analyses. The objective is to enhance fundamental understanding of failure and transport processes in geologic materials, and thereby strengthen the theoretical basis for the application of laboratory results to various technological operations of importance.

**Project Description:** Knowledge of the micro-scale characteristics and behavior of rocks is important for several energy-related applications, including global climate change and carbon management; oil field geoscience; geotechnical engineering efforts such as design and assessment of geologic nuclear waste repositories; and environmental remediation efforts at contaminated DOE and/or DoD installations. The experimental investigation provides a detailed understanding of the microstructure of geologic materials and how the micro-scale characteristics affect macro-scale behavior including brittle failure and fluid transport. Detailed and quantitative microstructural studies complement laboratory rock mechanics experiments. The results are used to formulate and evaluate theoretical and numerical models of rock deformation and fluid flow.

**Results:** (1) Investigation of water-weakening effect on the strength of porous sandstones. Our comprehensive data on the weakening effect of water on brittle strength and ductile compaction of several porous sandstones has allowed us to formulate a micromechanical model to consistently interpret the dilatant and compactive failure behaviors due to presence of water and initial damage in a fracture mechanics framework. Current research focuses on such behavior in carbonate rocks, including Solnhofen and Indiana limestones. (2) Triaxial compression experiments on 2 limestones (of initial porosities of ~3% and 14%) and detailed characterization of the failure envelopes in both the brittle and cataclastic flow regimes. The mechanical and microstructural data show that inelastic and failure behaviors in the Indiana limestone are qualitatively similar to those in porous clastic rocks. A manuscript describing this study is being prepared. We have also published a study on the relatively compact Solnhofen limestone. For the first time, a fairly complete set of data on porosity change and the brittle-ductile transition in the Solnhofen limestone have been acquired. The failure modes are associated with complex interplay of dilatancy, pore collapse and crystal plasticity processes, and several micromechanical models have successfully been employed to interpret the phenomena. (3) Quantitative characterization of the pore geometry of 4 Fontainebleau sandstone samples using synchrotron x-ray tomography. The data elucidate the 3-dimensional geometry and connectivity of the pore space in a suite of Fontainebleau sandstone with porosities ranging from 7.5% to 22%. Algorithms were developed to quantify the distributions of coordination number, channel length, throat size and

pore volume. This unique set of computed synchrotron X-ray tomographic data provide important constraints on geometric attributes of importance in the realistic modeling of permeability and fluid transport. (4) Damage evolution during the formation of a compaction band. Preliminary data show that localization mode in the form of compaction bands orthogonal to the maximum compressive stress is widely observed in porous sandstones in the transition from brittle faulting to cataclastic flow. We are systematically investigating the inelastic and compactive behaviors that promote such localization features. (5) Development of dilatancy and strength anisotropy in foliated rock. Mechanical tests were conducted on the Four-mile gneiss, and damage mechanics model was developed to analyze the anisotropic mechanical behavior in this and other foliated rocks, underscoring the critical role of mica in controlling the evolution of dilatancy and brittle failure.

**GRANTEE: NORTHWESTERN UNIVERSITY**

Department of Civil Engineering  
Evanston, IL 60208-3109

**Grant:** DE-FG02-93ER14344

**Interactions of Pore Fluid Pressure and Inelastic Deformation of Dilating and Compacting Rock**

*J.W.Rudnicki, 847-491-3411, fax 847-491-4011, jwrudn@northwestern.edu*

**Objectives:** To obtain an improved understanding of the interactions of pore fluid pressure and inelastic deformation of dilating and compacting rock for applications to the technologically common problem of storing fluids in or recovering fluids from the earth's crust.

**Project Description:** The effects of coupling between changes in fluid flow with the inelastic deformation and failure of porous rock are revealed by analysis of idealized geometries. These studies provide a framework for the interpretation of laboratory experiments and extrapolation to field applications.

**Results:** Reexamination of theoretical results for shear localization shows that solutions for compaction bands are possible in a range of parameters typical of brittle rock. Because the density of the material within the bands is increased, and, presumably, the permeability is decreased, the occurrence of these structures may be a significant factor affecting the withdrawal and injection of fluids from porous reservoirs.

An analysis of Rice (JGR, 1975) for shear of a layer of dilating material has been extended to arbitrary deformation states and the case of compacting materials. For materials that dilate with inelastic shearing, the condition for localization of deformation into narrow bands is met for the drained (constant pressure) response before it is met for undrained (constant fluid mass) conditions. For compacting materials, the undrained response is more compliant than the drained and conditions for localization are met for the undrained response before the drained. This is the case when the shear yield stress increases with normal stress, but when it decreases with normal stress, results for compacting materials are identical to those for the dilating materials.

Including the evolution of the uniform base solution introduces a length (or time) scale into the analyses. Interestingly, for compactive deformation, perturbation wavelengths smaller than a critical value are stable. This suggests that deformation of small laboratory specimens may be stable under conditions for which larger scale field processes would be unstable.

## **GRANTEE: OKLAHOMA STATE UNIVERSITY**

Department of Geosciences  
Stillwater, Okla. 74078

**Grant:** DE-FG03-99ER14944

### **The Physics of Two-Phase Immiscible Fluid Flow in Single Fractures and Fractured Rock**

*M. J. Nicholl; R. J. Glass, 505-844-5606, fax 505-844-6023, rjglass@sandia.gov; H. Rajaram, University of Colorado, Boulder*

**Objectives:** Employ detailed physical experiments and high-resolution numerical simulations to develop a quantitative understanding of the critical processes controlling two-phase flow and transport in fractures. Fundamental understanding may subsequently be abstracted for application to large-scale problems in petroleum extraction, isolation of hazardous or radioactive waste, remediation of subsurface contaminants, and CO<sub>2</sub> sequestration.

**Project Description:** Under two-phase immiscible flow conditions, fluid flow and solute transport characteristics of the fracture are controlled by the geometry of the respective phases. In turn, phase geometry is determined by a combination of aperture variability, phase accessibility, capillary and viscous effects associated with the two-phase flow processes themselves, and external forces such as gravity. In addition, if one of the fluids is slightly soluble in the other, mass transfer between the phases will influence phase geometry.

In this collaborative project between Sandia National Laboratories, Oklahoma State University, and the University of Colorado at Boulder, systematic physical experimentation is coupled with concurrent numerical simulation to explore the factors controlling phase geometry, flow, transport, and inter-phase mass transfer in rough-walled fractures. A high-resolution light-transmission technique has been developed to allow accurate experimental measurements (aperture, phase geometry, solute concentration) in transparent analog fractures. Use of this technique will lead to data of unprecedented accuracy for evaluating current understanding of fundamental processes, and motivate refinement of theoretical concepts.

**Results:** Evaluation of data from a previous field experiment in which infiltration was followed by excavation of the rock mass shows complicated behavior in an unsaturated fracture network that is consistent with recent laboratory investigations in single fractures. Short term ponded infiltration (36 minutes) into the dry network (impermeable matrix) produced viscous dominated flow near the infiltration surface, with a transition to unsaturated conditions at shallow depth (~2-3 m); phase geometry within the excavated rock mass changed from pervasive to complicated, exhibiting evidence of fragmentation, preferential flow, fingers, irregular wetting patterns, and varied behavior at fracture intersections. Electromagnetic Resistance Tomography performed during infiltration confirms rapid penetration, followed by equally rapid drainage of the network following infiltration. Estimates suggest that ~85 to 99% of the fluid slug escaped the excavated area; hence the actual penetration depth could have been quite large.

The occurrence of random and non-unique behavior during measurement of two-phase constitutive properties in fractures or porous media was investigated by visualizing micro-scale phase displacement processes during equilibrium retention and transient outflow experiments. In both cases, the drainage

process is shown to be a mixture of fast gas fingering, and slower gas back filling. Each of these micro-scale processes is controlled by: the size and the speed of the applied boundary step, the initial saturation and phase geometry, and small-scale heterogeneities. Because the micro-scale processes combine to yield macro-scale behavior, the same controls will influence measured effective properties, thereby calling into question current definitions for constitutive properties.

Detailed numerical exploration of the continuum-scale Richards equation with standard monotonic constitutive relations shows it to be inadequate for simulation of unsaturated flow in initially dry, highly nonlinear, and hysteretic media (such as fractures) where gravity-driven fingers occur. Recent published reports of finger-like numerical solutions with nonmonotonic profiles are found to be artifacts of the downwind averaging method that are generated by the combined effects of a truncation error induced oscillation at the wetting front and capillary hysteresis.

Micro-scale phenomena were observed to control macroscopic behavior during surfactant flood mobilization and solubilization of nonaqueous phase liquids (NAPLs) within a fracture. At relatively low capillary numbers ( $N_{ca} < 10^{-3}$ ), surfactant mobilization floods resulted in higher NAPL saturations than for similar  $N_{ca}$  pure water floods. These differences in macroscopic saturations are explained by differences in micro-scale mobilization processes. Solubilization of the residual NAPL remaining after the mobilization stage of the surfactant flood was dominated by the formation of micro-scale dissolution fingers, which produced nonequilibrium macro-scale NAPL solubilization. A macroemulsion phase also was observed to form spontaneously and persist during the solubilization stage of the experiments.

Dissolution of NAPLs in variable-aperture fractures couples fluid flow, transport of the dissolved NAPL, interphase mass transfer, and the corresponding NAPL-water-interface movement. Each of these fundamental processes is controlled by the variability of the fracture aperture and the geometry of the entrapped NAPL. Development of a depth-averaged computational model of dissolution that incorporates the small-scale processes controlling dissolution precludes the need for empirical mass-transfer coefficients. Implementation of an efficient algebraic multigrid algorithm for solving the flow and transport equations allows dissolution simulations at scales ( $> 2 \times 10^6$  nodes) much larger than the scale of the largest regions of entrapped NAPL. Direct comparison of a dissolution experiment to a simulation suggests that this coupled depth-averaged approach to modeling dissolution accurately predicts the evolution of NAPL-mass and NAPL-distribution within the fracture.

## **GRANTEE: UNIVERSITY OF OKLAHOMA**

School of Geology and Geophysics  
Norman, Oklahoma 73019

**Grant:** DE-FG03-96ER14643

### **Development and Application of a Paleomagnetic/Geochemical Method for Constraining the Timing of Fluid Migration and Other Diagenetic Events**

*R.D. Elmore, 405-325-3253, fax 405-325-3140, delmore@ou.edu; M.H. Engel*

**Objectives:** The goal of this project is to develop paleomagnetic methods for dating diagenetic events in sedimentary rocks. Specific objectives include testing the hypotheses that fluid flow (*e.g.* basinal fluids, hydrocarbons), clay diagenesis and organic matter maturation are viable mechanisms for the occurrence of pervasive chemical remanent magnetizations (CRMs) that are commonly observed in sedimentary systems.

**Project Description:** Investigations of diagenetic processes such as fluid migration, clay diagenesis and the maturation of organic matter commonly lack temporal control. The ability to constrain the time of *e.g.* oil migration would be of significant benefit for exploration. The paleomagnetic dating method is based on a genetic connection between diagenetic processes and the precipitation of authigenic magnetite. Isolation of the magnetization carried by the magnetite and comparison of the corresponding pole position to the apparent polar wander path allows the timing of diagenetic events to be determined. The research involves paleomagnetic field and laboratory tests to constrain appropriate chemical and physical conditions for magnetite authigenesis.

**Results:** We have previously documented the occurrence of chemical remanent magnetizations (CRMs) resulting from the precipitation of authigenic, magnetic minerals via rock/fluid interactions and the maturation of organic matter. However, the origin(s) of numerous, widespread, pervasive CRMs in sedimentary systems that have not been altered by externally derived fluids and/or the maturation of organic matter require that alternative explanations be sought. Work completed this past year has focused on field and laboratory tests of the hypothesis that clay diagenesis may be responsible for the occurrence of these pervasive CRMs. Results from Mesozoic carbonates in the Vocontian Trough in SE-France support the hypothesized acquisition of a CRM during burial diagenesis of smectite. Where smectite has been altered to other clays, the carbonates are characterized by a pre-folding, but secondary, normal polarity CRM throughout the basin based on fold, conglomerate and reversal tests. At sites with partial alteration, the CRM is absent or weakly developed, and where clays show no evidence of burial alteration, the units are characterized by a primary magnetization. The CRM intensity varies inversely with the amount of smectite. Geochemical data indicates that orogenic-type fluids are not an agent of remagnetization. Results from Jurassic sedimentary rocks on the Isle of Skye, Scotland, are also consistent with a connection between clay diagenesis and magnetite authigenesis. In north Skye, where detrital smectite is abundant, the rocks contain a weak magnetization. The same age rocks in south Skye, where the clays have been altered to illite, contain a multi-component CRM residing in magnetite and pyrrhotite. The CRM was acquired in the early Tertiary, which is consistent with the timing of heat flow via hydrothermal activity that caused the alteration. It should be noted, however, that isotopic evidence ( $^{87}\text{Sr}/^{86}\text{Sr}$ ,  $\delta^{13}\text{C}$ ,  $\delta^{18}\text{O}$ ) for rock alteration by hydrothermal fluids raises the possibility that the mechanism for the CRM in south Skye could be direct precipitation of magnetite by hydrothermal

fluids, with the smectite-to-illite transition being a coincidental by-product. If hydrothermal fluids rather than smectite diagenesis produced the CRM in magnetite, then more magnetite might be expected within the numerous veins that occur in the sedimentary rocks of south Skye. However, this is not the case, as there is no difference in CRM intensity between samples with veins and those without. Thus, although the possibility that hydrothermal fluids caused direct precipitation of magnetite cannot be entirely excluded, the case is presently stronger for an association between the CRM and the smectite-to-illite transition. Clay diagenesis, whether burial or fluid-enhanced, appears to be a viable mechanism for producing a CRM in magnetite.

The results of laboratory simulation experiments indicate an increase in magnetitic susceptibility when smectites are heated at moderate temperatures (65°C, 97°C). Although the actual mineral phases responsible for this enhanced magnetic susceptibility have yet to be characterized, the results support our field observations that clay diagenesis may play an important role in the occurrence of pervasive CRMs in sedimentary basins.

## **GRANTEE: OREGON STATE UNIVERSITY**

Department of Geosciences, 104 Wilkinson Hall  
Oregon State University,  
Corvallis, OR 97331

**Grant:** DE-FG03-00ER15030

### **Transport Visualization for Studying Mass Transfer and Solute Transport in Permeable Media**

*Roy Haggerty, haggertr@geo.orst.edu; Charles Harvey, charvey@mit.edu; Lucy Meigs, lcmeigs@sandia.gov*

**Objectives:** This research seeks: (1) to determine when the small-scale permeability structure causes solute spreading to be dominated by classical dispersion and when it causes solute spreading to be dominated by mass transfer; and (2) to understand how time-scales of mass transfer depend on physical, quantifiable characteristics of the geologic medium.

**Project Description:** Theoretical work is being conducted to define regimes of transport based on quantifiable measures such as dimensionless numbers. A portion of this theoretical work (and associated experiments) is focused on determining the conditions under which physical mass transfer (*i.e.*, diffusion into immobile zones) is significant, and to developing models for predicting the effects of mass transfer over long time scales. The numerical simulations are coupled with laboratory experiments using transmitted light, x-ray absorption, and conventional breakthrough curves to test and further understand the regimes of transport. Within the mass transfer regime, the geometries of flow and transport parameters that lead to multiple rates of mass transfer and scaling of transport processes are being evaluated.

**Results:** In order to map the regimes of transport, a method was developed for generating random hydraulic conductivity (K) fields that have highly connected flow paths or barriers, which have been found to be critical to understanding the regimes of transport. These fields share the same low-order statistics as multigaussian fields (mean, variance and covariance function), but have very different flow and transport characteristics because they are highly connected. Specifically, the results show that 2D hydraulic conductivity fields with the same basic spatial statistics, but different degrees of connectedness, may produce: (1) effective conductivities that are significantly above or below the geometric mean, (2) solute transport behavior that is best modeled through Fickian dispersion or behavior that is better modeled as rate-limited mass transfer, and (3) mass transfer that is driven that by either diffusion or advection. This work demonstrates that standard characterizations of heterogeneity may not capture the flow and transport characteristics of all aquifers.

A series of laboratory experiments are being designed to allow us to evaluate our understanding and predictions about the regimes of transport. These transport experiments are being conducted on thin chambers filled with glass beads using transmitted light to spatially map solute concentrations. Breakthrough concentrations are also being measured. Prototype experiments conducted within the mass transfer regime have enabled us to refine our experimental design.

## GRANTEE: THE PENNSYLVANIA STATE UNIVERSITY

Dept. of Geosciences  
University Park, PA 16802

**Grant:** DE-FG02-95ER14547

### Dissolution of Feldspar in the Field and Laboratory

*Susan L. Brantley, 814-863-1739 (tele or fax), Brantley@geosc.psu.edu; Carlo G. Pantano*

**Objectives:** In this project, the controls on feldspar dissolution in field and laboratory systems are being investigated. Much of the ongoing work is focused on dissolution of glass substrates as an analogue to feldspar.

**Project Description:** In this work, we are investigating alteration of feldspars and/or feldspar-like glasses in the field and laboratory. These investigations utilize nuclear magnetic resonance (NMR), x-ray photoelectron spectroscopy (XPS), secondary ion mass spectrometry (SIMS), and Fourier Transform Infrared Spectroscopy (FTIRRS) to analyze the formation of altered layers on the surface of the samples. In addition, atomic force microscopy (AFM) is used to analyze the rate of dissolution of feldspar crystal and glass. Rates of dissolution in the laboratory are compared to dissolution in field systems, including the Cape Cod aquifer, Massachusetts. In this latter work, we use Sr concentrations and isotopes as well as concentrations of rare earth elements to define dissolution in the field system.

**Results:** To investigate the effect of Al/Si on aluminosilicate dissolution without the complications of changing Na/Ca ratio or the presence of planar defects, three glasses,  $\text{NaAlSi}_3\text{O}_8$ ,  $\text{NaAlSi}_2\text{O}_6$ , and  $\text{NaAlSiO}_4$ , were synthesized and dissolved. Many similarities between plagioclase and this suite of glasses were observed. In contrast to plagioclase dissolution, however,  $\log(\text{rate})$  and  $n$ , the slope of the  $\log(\text{rate})$ -pH curve at low pH, increased smoothly with Al content. These observations are consistent with a transition state at high pH consisting of a deprotonated  $Q_3^{\text{Si}}$  hydroxyl group (where  $Q_v^x$  refers to an  $x$  atom in a tetrahedral site with  $v$  bridging oxygens) or a five-coordinate Si site after attack by  $\text{OH}$ , and, at low pH, a protonated  $Q_4^{\text{Al}}\text{O}Q_4^{\text{Si}}$ . According to this model, dissolution rate increases from albite to nepheline because hydrolysis of  $\text{AlOSi}$  bonds becomes more energetically favorable as the number of Al atoms per Si tetrahedra increases, a phenomenon documented by *ab initio* geometry optimizations (Figure 1). NMR analysis of these glasses also shows evidence in some cases for octahedral and tetrahedral aluminum at the glass surface after alteration. Combining further spectroscopic analyses with *ab initio* calculations will shed further light on dissolution mechanisms.

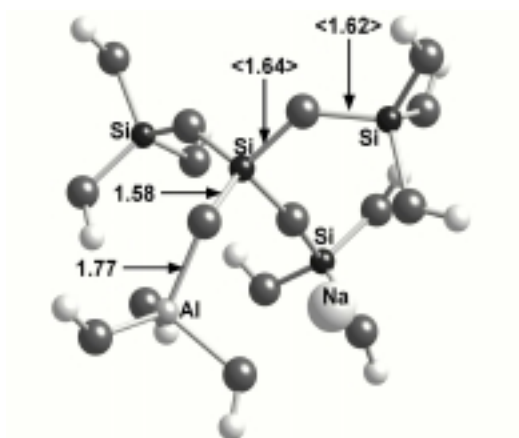


**Figure 1.** Optimized geometry (HF/3-21G\*\*) of the  $Q^4Si(AlNa)$  molecule. The bond lengths in brackets are average values. The notation refers to a central  $SiO_4$  tetrahedron bonded to 1  $AlO_4^-$  tetrahedron charge compensated by a  $Na^+$ , and 3 other  $SiO_4$  tetrahedra. The  $Q^4Si(AlNa)$  molecules represent the primary structural units present in albite glass. The  $Q^4Si(2Al,2Na)$  molecule (not shown) represents the primary structural unit present in jadeite glass and the  $Q^4Si(4Al,4Na)$  molecule (not shown) represents the primary structural units present in nepheline glass. The average Si-O bond length within  $SiOSi$  linkages ( $\sim 1.64$  Å) and the average Al-O bond length within  $AlOSi$  linkages ( $\sim 1.77$  Å) do not change as Al is added to the network. However, the average bond length of Si-O bonds within  $AlOSi$  linkages increases from  $\sim 1.58$  Å in albite glass to  $\sim 1.60$  Å in jadeite glass to  $\sim 1.62$  Å in nepheline glass. Lengthening of this bond suggests that hydrolysis of  $AlOSi$  bonds may become energetically more favorable as the number of  $AlO_4^-$  tetrahedra per  $SiO_4$  tetrahedron increases. In other words, nepheline glass (4  $AlO_4^-$  tetrahedra per  $SiO_4$  tetrahedron) should hydrolyze more rapidly than jadeite glass (2  $AlO_4^-$  tetrahedra per  $SiO_4$  tetrahedron) and albite glass (0-1  $AlO_4^-$  tetrahedra per  $SiO_4$  tetrahedron), as observed experimentally.

## **GRANTEE: THE PENNSYLVANIA STATE UNIVERSITY**

Department of Energy and Geo-Environmental Engineering  
Energy Institute  
Pennsylvania State University  
University Park, PA 16802

**Grant:** DE-FG02-00ER15111

### **Critical Chemical-Mechanical Couplings that Define Permeability Modification in Pressure-Sensitive Rock Fractures**

*Derek Elsworth, 814-863-1643, fax 814-865-3248, elsworth@psu.edu; Abraham S. Grader;  
Susan L. Brantley, Department of Geosciences*

**Objectives:** This work will examine and quantify the processes controlling changes in the permeability of natural fractures, subjected to coupled hydraulic-mechanical-chemical (HMC) effects. Specifically, it will define conditions where permeability will either increase or decrease with net dissolution in the fractures; this response is highly sensitive to the process couplings.

**Project Description:** We propose to examine the important factors controlling changes in the permeability of natural fractures that result from coupled (HMC) effects. This work seeks a consistent view of the key processes, incorporating the roles of temperature, chemistry and evolving fluid-saturation and contact-stress (shear and normal) distributions in mediating free-face and pressure-dissolution rates. We propose an extensive series of flow tests through natural fractures in sandstone and dunite cores using water and steam as the permeants. Fluid and mass balances will be recorded and correlated with in-sample saturation, porosity and fracture aperture maps, acquired in real-time by X-ray CT-imaging at a maximum spatial resolution of 15-50 microns per pixel. Post-test, the samples will be surface-profiled; at large-scale by profilometer and at small-scale by atomic force microscope, to define the characteristics of observed dissolution sites. Process-based distributed-parameter HMC models will also be developed in support of the experimental activities, and applied at fine resolution to core geometries. These models will be used to define and quantify key processes of pressure solution, free-face dissolution, and shear-dilation, and the influence of temperature, stress level, and chemistry on the rate of dissolution, its distribution in space and time, and its influence on the mechanical and transport properties of the fracture.

This experimental program will define and constrain the respective roles of temperature, local asperity-stresses, local fluid-saturations and chemistry in prescribing the relative dominance of free-face dissolution over pressure solution effects, and their respective influence over fracture permeability changes at moderate temperature and effective stress levels.

**Results:** This project has only recently been initiated.

**GRANTEE: PRINCETON UNIVERSITY**

Department of Geosciences, 151 Guyot Hall  
Princeton, NJ 08544.

**Grant:** DE-FG02-00ER15063

***In-situ* Evaluation of Soil Organic Molecules: Functional Group Chemistry, Aggregates Structures, Metal and Mineral Surface Complexation using Soft X-rays**

*Satish C. B. Myneni 609-258-5848, fax 609-258-1274, smyneni@princeton.edu*

**Objectives:**

1. The functional group chemistry and macromolecular structure of soil organic molecules, and their extracted humic substances
2. The influence of solution chemistry on the aggregate structures, protonation and metal complexation of model and natural organic molecules
3. The structure and chemistry of mineral adsorbed humic substances and soil organic molecules, and their role on ion-sorption as a function of solution chemistry and mineral surface structure

**Project Description:** The goal of this project is to examine the chemical properties of natural organic molecules in soils and aquatic systems using the in-situ synchrotron methods. In addition to the conventional laboratory methods, we are using soft X-ray spectroscopy and microscopy to examine the functional group chemistry and the macromolecular structures of humic substances. With the help of the functional group chemistry information of model organic molecules, we are trying to interpret the behavior of humic materials and their behavior in aqueous solutions and at the interfaces. This study is in collaboration with the theoreticians at Uppsala University and University of Stockholm to understand the electronic structure of different functional groups and their coordination environment in model organic molecules.

**Results:** This project was begun six months ago. In the past few months, we have examined the S-, P-, and Cl-functional groups of humic substances isolated from different sources using the soft X-ray spectroscopy. Our preliminary studies indicate that the S functional group information that we obtained is very similar to the previous studies, excepting for the identification of sulfonates. Organo-sulfates are abundant in humics, and their *1s* spectral features were misinterpreted for the sulfonates. A study is in progress to identify the concentration of sulfonates in humic materials. Studies on P-functional groups suggest that humics contain organo-phosphates as the dominant form of P with a minor concentration of phosphonates. Studies on Cl are in progress now at the Stanford Synchrotron Radiation Laboratory and the Advanced Light Source. Results of our previous research was reported in *Science* 286: 1245-1432.

## **GRANTEE: PURDUE UNIVERSITY**

Department of Earth and Atmospheric Sciences  
West Lafayette, Indiana 47907

**Grant:** DE-FG02-98ER14886

### **Mechanical Models of Fault-Related Folding**

*A.M. Johnson 765-494-0250, fax 765-496-1210, gotesson@purdue.edu*

**Objectives:** The underlying goal of the proposed research is to provide a unified, mechanical infrastructure for studies of fault-related folding and to apply that infrastructure to studies of a wide range of field examples. The mechanical theory will be presented via programs that have graphical user's interfaces (GUI) so that structural geologists may model a wide variety of folds. The proposed research will provide practical methods of predicting forms of folds and other structural traps accessory to each type of fault-related fold.

**Project Description:** The research project can be divided into four parts. The first part is to investigate the geometric characteristics that identify fault-related folds of different types. In addition to exploring existing literature and seismic profiles, field mapping of fault-related folds in central Utah and along the southwest side of the Big Horn Basin in Wyoming will be combined with borehole data and seismic profiles of the structures. This combination of data will relate the folding observed in the field to the underlying faulting. The second part of the research is to derive mechanical analogs of idealized field examples of fault-related folds as well as various geometric models of fault-related folding. The combination of boundary conditions, rheological properties and mechanisms that produce fault-related folds will be determined. The third component of the research is to explore what kinds of secondary structures occur together with primary structures, such as ramp anticlines and synclines, décollement folds, fault-arrest folds and fault-propagation folds, that would suggest new targets for petroleum exploration. The last component of the reaserch is to develop methods that will allow practitioners to generate their own examples of ideal fold forms, by specifying the conditions the practitioner suspects to be important in the tectonic environment.

**Results:** An analysis of deformation bands in the San Rafael monocline, Utah shows that the stress state reflects local folding rather than a regional compression. An explanation was developed, based on beam and fracture theory, for flexural slip during folding and localization of layer-parallel faults in the limbs of the San Rafael Swell and other monoclines. The theory indicates that the layer-parallel faults should form along relatively weak layering where change of curvature, or coil, is maximized.

Considerable progress was made on mechanical theories of four structural processes of fault-related folding: basement-cored-forced folding, sequential ramp folding, listric-fault folding, and gang-fault folding. Analysis of both fault-arrest and fault-propagation folding has been conducted. Programs with graphical user's interfaces (GUIs) have been developed for each of these theoretical processes to calculate and display the fold forms produced by the various processes. The Forced Fold program and GUI simulate the deformation of sedimentary cover over displaced rigid basement blocks. This program models the folding of a sedimentary cover with a traction-free ground surface. The sedimentary cover may be homogeneous linear or nonlinear medium, or an anisotropic medium or a layered medium. The Gang Fault Fold program and GUI model 3D folds that form over blind faults. The faults may be listric or straight in profile and curved or straight in map view.

## **GRANTEE: PURDUE UNIVERSITY**

Department of Physics  
Purdue University  
West Lafayette, Indiana 47907-1396

**Grant** DE-F602-93 ER14391

### **Seismic Monitoring of Time-Dependent, Multi-Scale Heterogeneity in Fractured Rock**

*Laura J. Pyrak-Nolte, 765-494-3027, fax 765-494-0706, ljpn@physics.purdue.edu*

**Website :** <http://www.physics.purdue.edu/rockphys>

**Objectives:** The objective of this proposal is to determine the effects of time-dependent multi-scale heterogeneity on seismic wave propagation through fractures and fractured rock. Specifically, we will address: the effects on the hydraulic -mechanical-seismic response caused by (1) heterogeneity within a fracture; (2) heterogeneity from multiple fractures and fracture networks; and (3) heterogeneity caused by geochemical interactions between pore fluids and rock, etc.

**Project Description:** A strategy for reducing carbon dioxide (CO<sub>2</sub>) emissions into the atmosphere from power plants burning fossil fuel is to capture CO<sub>2</sub> and sequester the CO<sub>2</sub> in subsurface reservoirs. Candidates for geological sequestration include depleted oil and gas reservoirs, deep saline aquifers, and underground coal beds. Though these subsurface reservoirs often differ in lithology and structure, fractures are common to all. Fractures in rock are highly conductive rapid-flow paths that can connect otherwise hydraulically isolated rock formations. The principal focus of the work is to experimentally determine the link between the seismic properties of fractures and their hydraulic permeability.

Furthermore, we will study how stress-distributions and invading fluids or gases alter the seismic signatures of fractures, with the goal of using these changes to actively monitor the changes in stress fields and the migration of fluids in a fractured reservoir. Finally, we will study how geochemical processes, such as chemical weathering or mineral deposition related to CO<sub>2</sub> chemistry, alter the seismic signatures of fractures. Achievement of the proposed research objective depends on the determination of the effect of micro-scale phenomena on macro-scale measurements through the combination of laboratory experiments and numerical analyses

**Results:** A wavefront imaging was used to measure the seismic properties of samples containing heterogeneity from multiple parallel fractures. From the acquired three-dimensional dataset, we reconstructed the complete longitudinal components of acoustic wavefronts that have propagated through a sample, and thereby obtained a direct visualization of discontinuous features in the arriving wavefronts produced by the presence of discrete fractures. This technique was applied to an intact aluminum sample and four aluminum samples containing synthetic parallel fractures. For the fracture sample, strong energy confinement of the propagating wavefront was observed inside the central waveguide, with little energy outside the first set of fractures. A theoretical analysis of wave guiding of compressional waves was performed assuming that the waveguide is formed by two fractures. Only the lowest-order guided P-wave mode was observed and the measured negative dispersion was consistent with the behavior of a guided mode. These results demonstrated that parallel fractures can guide waves in leaky waveguide modes and is therefore an important source of seismic anisotropy. The effect of a non-uniform stress field on seismic wave propagation in fractured media was also investigated. Seismic wavefront imaging was performed on intact and fractured samples subjected to a radially varying stress

field. The results show that the effect of the fractures on seismic waves is similar to the effect of lenses on optical waves. The radially varying stress field produces a radial variation in fracture specific stiffness that produces a quadratic pulse delay as a function of radial distance from the axis of symmetry. A concentration of energy occurs at a distance equal to the focal length of the “seismic lens.” These results show that knowledge of the local stress field is important when interpreting seismic data from fractured media.

## GRANTEE: RENSSELAER POLYTECHNIC INSTITUTE

Department of Earth & Environmental Sciences  
Troy, New York 12180-3590

**Grant:** FG02-94ER14432

### Transport Phenomena in Fluid-Bearing Rocks

*E.B. Watson, 518-276-8838, fax 518-276-6680, watsoe@rpi.edu*

**Objectives:** The broad goal of this project is to provide insight into fluid-assisted geochemical transport in the Earth's crust and upper mantle. There are three specific objectives: 1) to characterize *permeability* of rocks exhibiting equilibrium microstructure; 2) to obtain data on *diffusion of CO<sub>2</sub> and ionic solutes* in H<sub>2</sub>O; and 3) to characterize *transport of C-O-H species along the grain boundaries* of texturally-equilibrated rocks under fluid-absent conditions.

**Project Description:** This is a multifaceted program of experimental research on the behavior and properties of C-O-H fluids and the rocks that contain them at depths exceeding ~20 kilometers in the Earth. The objectives are pursued using solid-media, high pressure-temperature techniques developed during the initial grant period (1994-1997). The three focus areas of the project are viewed as complementary aspects of the problem of fluid-assisted mass transport that are important for different reasons: permeability controls the velocity of fluid flow in response to a given pressure gradient; solute diffusion determines the efficacy of mass transport through a stationary fluid; and grain-boundary diffusion of C-O-H species controls communication between fluid-filled that are isolated from one another (as well as transport of fluid species *in situations* where no free fluid is present). Diffusion of C-O-H species may also determine whether and how a fluid phase develops during slow, progressive devolatilization.

**Results:** During the past year, efforts related to permeability produced results in three areas: 1) "*partitioning*" of a fluid phase between rock units of differing grain size. In high P-T experiments involving either aqueous fluid or silicate melt, we showed that the fluid or melt localizes in fine-grained relative to adjacent coarser-grained regions. In some cases, this fluid localization is strong enough to impart a higher permeability to the fine-grained zones. 2) *creation of permeability via fluid infiltration* driven by interfacial energy minimization. We measured the rate of aqueous fluid penetration into initially fluid-absent quartzite at 1GPa. At 620°C and 820°C the rates are ~6 and 120 cm/year, respectively. The infiltration mechanism was shown to involve dissolution along quartz grain edges accompanied by "back-diffusion" of solute and precipitation of quartz in the fluid source reservoir. 3) *development of channel-like pores* in synthetic, fluid-bearing rocks placed in a modest temperature gradient (1-10°/mm) at high pressure. The channels develop parallel to the temperature gradient—sometimes in a matter of hours—leading to dramatically enhanced permeability in that direction.

We also made progress in determining the effect of a minor platy phase on permeability (the effect appears to be small), and in the design and implementation of an electrical conductance cell for *in situ* assessment of permeability at high pressure and temperatures.

On the diffusion front, we completed a study of H<sub>2</sub>O-CO<sub>2</sub> interdiffusion in fluids at elevated P-T conditions using the 2-chambered diffusion cell developed in the initial years of this project. Figure 1

illustrates the experimental set-up and resulting diffusion data compared with our previous results for aqueous SiO<sub>2</sub> diffusion.

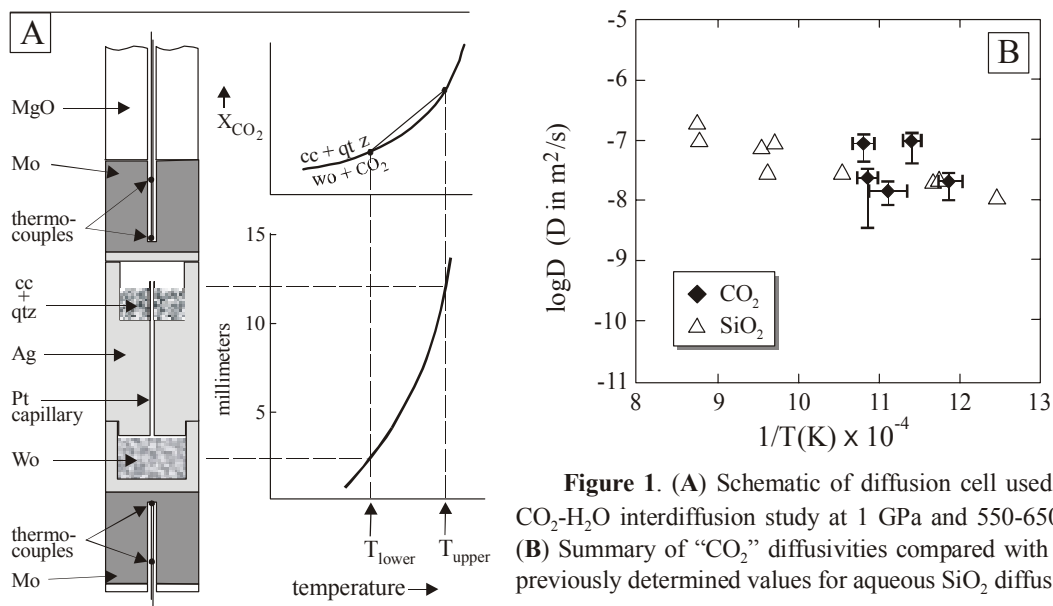


**Figure 1.** (A) Schematic of diffusion cell used for CO<sub>2</sub>-H<sub>2</sub>O interdiffusion study at 1 GPa and 550-650°C. (B) Summary of “CO<sub>2</sub>” diffusivities compared with our previously determined values for aqueous SiO<sub>2</sub> diffusion.

## GRANTEE: RICE UNIVERSITY

Chemical Engineering  
Houston, TX 77251-1892

**Grant :** DE-FG03-95ER14552

### Transition Metal Catalysis in the Generation of Petroleum and Natural Gas

*Frank D. Mango, 281-497-0384, fax 713-285-5478, f.mango@gte.net*

**Objective:** This project started on the hypothesis that the light hydrocarbons in petroleum are formed catalytically from the transition metals in carbonaceous sedimentary rocks. The conventional view that oil and gas are the products of thermal cracking was viewed as inadequate given the stability of hydrocarbons and the fact that laboratory attempts to duplicate the process had been unsuccessful. The transition metals are ubiquitous in organic sediments and could, in theory, become catalytically active during diagenesis, promoting the formation of lighter hydrocarbons and natural gas. This project's objective was to test this idea and to explore generally the catalytic properties of transition metals under realistic geologic conditions.

**Project Description:** Various natural sources of transition metals including the asphaltene fraction of petroleum, source rocks, and minerals (takovite and chlorite) are being analyzed for catalytic activity. Pure transition metal complexes (metal porphyrins, acetylacetonates, oxides and sulfides) are also under study. Reactions are being conducted in gas manifold systems under steady-state and batch-reactor conditions and products analyzed by high-resolution gas chromatography.

**Results:** Crude oil is believed to be unstable in the Earth, thermally cracking to natural gas at temperatures  $> 150^{\circ}\text{C}$ . Although the process (crude oil  $\rightarrow$  gas) is well documented geologically, it has never been demonstrated convincingly in the laboratory. Petroleum hydrocarbons are surprisingly stable and their cracking products do not resemble natural gas.

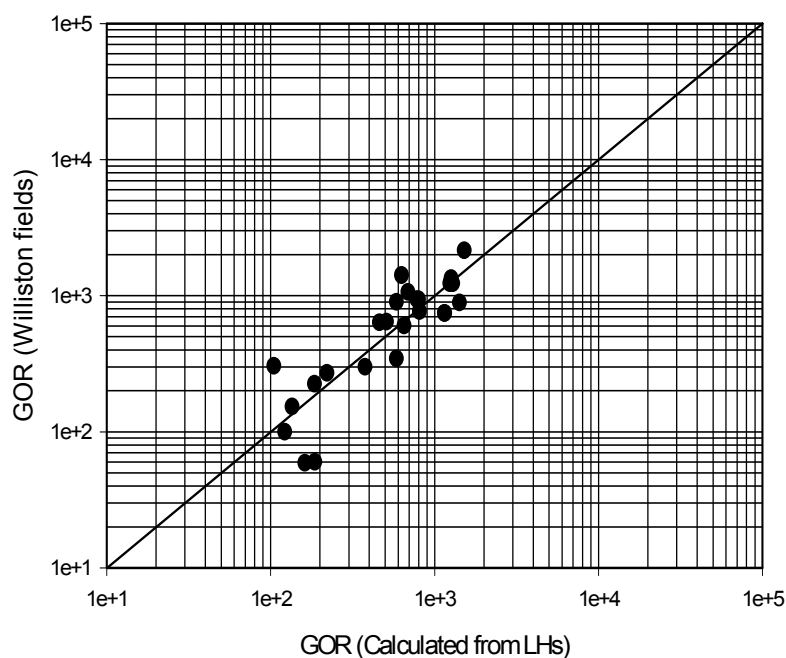
We have shown that crude oil *catalytically* decomposes to gas under mild laboratory conditions over the transition metals in carbonaceous sediments (Mango et al., *Nature*, **368**, 535, 1994; Mango, *Org. Geochem.* **24**, 977, 1996; Mango & Hightower, *Geochim. Cosmochim. Acta.* **61**, 5347, 1997). Like natural gas in deep basins, it becomes progressively enriched in methane: initially 80% (wet gas) to a final composition of 100% methane (dry gas). Catalytic gas exhibits the carbon isotopic signature of natural gas (Mango & Elrod, *Geochim. Cosmochim. Acta.* **63**, 1097, 1998) and is thus indistinguishable from natural gas.

We now report that  $\text{C}_6$  &  $\text{C}_7$  light hydrocarbons (LHs) exhibit the properties of *catalytic intermediates*, in particular a proportionality between isomers:

$$(xy_i)/(x_iy) = \alpha$$

(where  $x$  and  $x_i$  are isomers;  $y$  and  $y_i$  are isomers that are structurally similar to  $x$  and  $x_i$ ; and  $\alpha$  is a constant) (Mango, *Geochim. Cosmochim. Acta.* **64**, 1265, 2000). It holds for all oils ( $r^2 = 0.99$ ) and was duplicated experimentally. These results suggest that the LHs could be oil maturity indicators possibly correlating to other maturity functions such as GOR (gas-to-oil ratio). We have found a strong correlation between GOR and four light hydrocarbons (LHs) (2-methylpentane, 3-methylpentane, 2-

methylhexane, and 3-methylhexane). These hydrocarbon changes in relative amounts systematically as their concentrations change, approaching thermodynamic equilibrium in concert with increasing GOR, a trend attributed to oil maturity. The relationship is perhaps not surprising given the fact that all LHs (C<sub>1</sub> through C<sub>7</sub>) probably share a common catalytic genesis and thus should exhibit similar changes in concentration. Because the four hydrocarbons are major LHs, and thus easily analyzed by conventional gas chromatography, they could provide a powerful link to GOR through a simple oil analysis. An index was calibrated using 45 oils from 19 Williston basin oil fields believed to contain indigenous oil and gas. The coefficient of correlation between field GORs and oil composition is  $r^2 = 0.75$  (Figure).



## **GRANTEE: SCRIPPS INSTITUTION OF OCEANOGRAPHY**

IGPP - University of California at San Diego  
9500 Gilman Drive - Dept. 0225  
La Jolla, California 92093-0225

**Grant:** DE-FG03-97ER14757

### **Joint Inversion of Acoustic and Induction Log Data for Enhanced Resistivity Structure**

*Catherine de Groot-Hedlin, 858-534-2313, fax 858-534-5332, cdh@eos.ucsd.edu; Steven Constable*

**Objectives:** The objective of this project was to develop a robust, efficient method of inversion of induction logging data in order to enhance the resolution of geological structures. A secondary objective was to seek a connection between acoustic and electrical properties of the rock formations which would allow for a joint inversion of different data types.

**Project Description:** A problem with standard least-squares inversion algorithms is that their performance degenerates in the presence of noise, yielding increasingly physically improbable models with increasing noise levels. Since, in general, there is more than one model with responses that fit the data, regularization is used to stabilize the inversion, and to specify the type of model sought. A stable method of inverting induction-logging data was developed which constructs conductivity models with only that structure required to fit the data. This is accomplished by means of introducing a penalty term on the roughness of the model. Although the models thus constructed do not provide a formal analysis of the resolution, they give some indication of the resolving power of the induction data.

**Results:** A robust, efficient method of inversion of induction logging data for smooth 2-D models, appropriate to an environment in which mud filtrate invades flat-lying layers, was developed. The inverse problem is regularized such that the smoothest model is sought subject to the condition that the resulting computed log agrees with the field log to a given preset level. At each iteration, the Jacobian sensitivities were approximated using the distorted Born approximation. In most cases, the algorithm converges in 3-4 iterations. The resulting maximally smooth models reflect the resolving power of the induction data and are unlikely to result in over-interpretation of the data. Inversion of both synthetic and field data indicates that layer boundaries are well resolved, but radial boundaries are poorly resolved by conventional induction logging data.

The work is described in further detail in the paper entitled "Smooth inversion of induction logs for conductivity models with mud filtrate invasion", published in *Geophysics*, v65, p1468-1475.

**GRANTEE: SMITHSONIAN INSTITUTION**

National Museum of Natural History  
Department of Mineral Sciences  
Washington, DC. 20560

**Grant:** DE-FG02-00ER15070

**Low-T, Fluid-Ashflow-Tuff Interactions: How Rock Textures, Chemistry, and Mineralogy Reflect Reaction Pathways and Influence Rock Response to Heating**

*Sorena S. Sorensen, 202-357-4010, fax 202-357-2476, sorena@volcano.si.edu*

**Objectives:** The objectives are to: 1) understand the textural, mineralogical and geochemical effects of low-T K-metasomatism of felsic volcanic rocks; 2) describe and model fluid-flow mechanisms that cause low-T K-metasomatism; and 3) investigate how subsequent metamorphism could further alter K-metasomatized felsic volcanic rocks.

**Project Descripton:** We will demonstrate how textures correlate with various mineralogical and geochemical effects of low-T K-metasomatism of Tertiary volcanic rocks in three settings in the western U.S. (Socorro, NM; Creede, CO, and the Harcuvar Mtns and vicinity, AZ). We will then describe the fluid-flow mechanisms responsible for the alteration in each area. We will construct model reaction paths that predict how subsequent contact metamorphism could alter the compositions and/or textures of the rocks. We will then test these predictions against case studies of variably metamorphosed arc-volcanic rocks that had previously been variably K-metasomatized at low-T conditions. This study will integrate cathodoluminescence (CL) textural analysis with more conventional petrographic methods, along with major, minor, trace element, and oxygen isotope geochemistry of rocks and minerals. This combination of methods should both reveal grain-scale mechanisms for the metasomatic reactions, and elucidate large-scale fluid-rock processes.

**Results:** The project has only recently been initiated.

**GRANTEE: UNIVERSITY OF SOUTHERN CALIFORNIA**

Department of Aerospace and Mechanical Engineering  
854 West 36<sup>th</sup> Place  
RRB 101  
Los Angeles, CA 90089

**Grant:** DE-FG03-00ER15092

**Three-Dimensional Miscible Porous Media Flows with Viscosity Contrast and Gravity Override**

*Tony Maxworthy, 213-740-5376*

**Objectives:** To perform a three-dimensional experimental investigation into the spatio-temporal dynamics of miscible porous media flows under the coupled effects of permeability heterogeneities, mobility contrast and gravitational segregation. Comparison with numerical simulations to be carried out at UCSB.

**Project Description:** The role of heterogeneities, gravity override, and mobility contrast will be assessed in a three-dimensional, simulated porous medium in a 1/4-5 spot geometry. A rectangular parallelepiped will be filled with glass or plastic spheres and an interstitial, viscous fluid introduced to fill the box completely. The will be partially displaced by pumping a less-viscous, dyed fluid, at a known flow-rate, into one corner of the box and removing interstitial fluid at the opposite corner. The displacement will be observed by traversing the box, at various levels, with a laser light sheet and video taping the movement of the dyed front. A close index-of-refraction matching between spheres and fluid is essential for the success of this technique. The results will be compared with detailed numerical computations being performed at the University of California-Santa Barbara by a group led by Professor Eckart Meiburg.

**Results:** Since the start of the project on 9/15/00 we have tried various combinations of fluid and sphere material to find a suitable refractive index match. So far this has been of limited success due to lack of manpower at this early stage of the project. We plan to hire a post-doctoral fellow by 3 or 4/01 to carry out this and the other experimental tasks on a full-time basis. To test other aspects of the experimental technique we have run a series of experiments in a Hele Shaw cell geometry. These results will be supplemented and presented at the annual meeting of the APS-DFD in the fall of 2001.

## GRANTEE: STANFORD UNIVERSITY

Department of Geological and Environmental Sciences  
Stanford, California 94305-2115

**Grant:** DE-FG03-93ER14347-A008

### **Metal Ion Sorption at Oxide Surfaces and Oxide-Water Interfaces: Spectroscopic Studies and Modelling**

*Gordon E. Brown, Jr. 650-723-9168, fax 650-725-2199, gordon@pangea.stanford.edu; George A. Parks*

**Objectives:** This project concerns chemical interactions between metal ions in aqueous solution and oxide surfaces representative of those found in the Earth's crust. These "sorption" reactions partition the metal between fluid and solid phases and must be understood at a molecular level to develop both quantitative understanding of the geochemistry of mineral surfaces and the macroscopic models required to predict the fate of contaminants in earth surface environments. Our objectives are (1) to characterize sorption reactions by determining composition, molecular-scale structure, and bonding of the surface complexes produced using direct sorption measurements, synchrotron-based x-ray absorption fine structure (XAFS) spectroscopy and x-ray standing wave fluorescence spectroscopy, x-ray photoelectron spectroscopy (XPS), and UV/Vis/IR spectroscopy; (2) to investigate how these reactions are affected by the solid surface, the composition of the aqueous solution, the presence of simple organic ligands containing functional groups common in more complex humic and fulvic substances, the presence of microbial biofilms, and time; and (3) to develop molecular-level and macroscopic models of sorption processes. In FY 2000 we made good progress in each of these areas and continued our grazing-incidence XAFS and X-ray standing wave (XSW) studies of the interaction of heavy metals with mineral surfaces and with biofilm-coated alumina and goethite surfaces. In addition, we have used the results of our model system studies to help determine the speciation of heavy metals and metalloids in contaminated natural systems.

**Project Description and Results:** (1) *Effects of sulfate and carbonate on the interaction of Pb(II)aq with goethite surfaces:* We have used a combination of XAFS and FTIR spectroscopy to examine the possibility that the common inorganic ligands carbonate and sulfate form ternary complexes with lead on goethite surfaces. This was indeed found to be the case using molecular-level spectroscopies. In addition, uptake studies showed that the presence of sulfate in the system increased the sorption of Pb(II) by 30% and conversely that the presence of Pb(II) enhances the uptake of sulfate on the goethite by a factor of 3. Similarly, the presence of CO<sub>2</sub> caused an enhancement of Pb(II) uptake by ≈ 20%. These uptake enhancements are attributed to changes in the surface charge of goethite and a reduction in electrostatic repulsion effects.

(2) *Pb(II) sorption on biofilms on high-surface-area-minerals:* We have continued studies of the effects microbial biofilms on the uptake of Pb(II) on powdered  $\alpha$ -Al<sub>2</sub>O<sub>3</sub> and  $\gamma$ -FeOOH surfaces using XAFS and X-ray Standing Wave (XSW) methods. This project, which is jointly funded by the NSF-EGB program, has used XSW methods to show that the presence of a biofilm does not change the intrinsic properties of the surfaces at metal concentrations less than 10<sup>-6</sup> M. Our XAFS studies have shown that at higher Pb(II) concentrations, live bacteria cause precipitation of a pyromorphite-like phase.

*(3) Grazing-Incidence XAFS and XSW Studies of Pb(II) and Se(IV) Interacting with Biofilm-Coated Single Crystal Surfaces:* In FY 2000, we have continued our coupled XSW and GI-XAFS measurements of heavy metals sorbed to biofilms formed on single-crystal surfaces. For Pb(II), we find that the mineral surface sites preferentially bind Pb(II) relative to the biofilm at the lowest metal concentrations tested and that above  $\approx 10^{-6}$  M Pb by the lead binds to functional groups in the biofilms. When we add Pb(II) and Se(VI) simultaneously, with a tenfold excess of Se(VI) relative to Pb(II), we find that Pb(II) is preferentially bound to the biofilm (as expected at pH 4.5) and the Pb(II) profiles are not affected by Se(VI). However, Se(VI) uptake is enhanced by the presence of Pb(II), especially at low Se(VI) concentrations.

*(4) EXAFS Determination of the Chemical Speciation and Sorption Processes of Pb, Cr, Sr, As, and Se in Natural and Model Systems:* We have used XAFS spectroscopy, TEM, and Rietveld x-ray diffraction analysis to study the molecular-scale speciation of selected heavy metals and metalloids in contaminated mine wastes, natural sediments and soils from various localities. For example, in naturally Pb-contaminated sandstones from Largentiere, France, we found that plumbogummite is the dominant form of lead in this deposit that has formed over the past 10,000 years. Our DOE-funded XAFS work on Pb sorption on mineral surfaces in model systems proved to be invaluable in obtaining these results on complex environmental samples.

## **GRANTEE: STANFORD UNIVERSITY**

Geophysics Department  
Stanford, California 94305-2215

**Grant:** DE-FG03-99ER14933-A001

### **Seismic Signatures of Fluids in Anisotropic Rocks**

*G.M. Mavko 650-723-9438, fax 650-723-1188, gary@pangea.stanford.edu; Francis Muir; P.A. Berge 925-423-4829, fax 925-423-1057, berge@llnl.gov; Ilya Tsvankin, 303-273-3060, fax 303-273-3478, ilya@dix.mines.edu*

**Objectives:** Conduct theoretical investigations into the effects of fluids and fractures on anisotropic elastic constants, and consequent constraints on lithology that may be obtained from seismic parameters.

**Project Description:** Seismic anisotropy, now widely recognized as a common feature of most subsurface formations, may lead to significant distortions in conventional seismic processing, such as errors in velocity analysis, mispositioning of reflectors, and misinterpretation of the amplitude variation with offset (AVO) response. Furthermore, geophysical characterization of fractured reservoirs via their elastic anisotropy is an extremely important economical problem, in particular for the continental United States. In tight formations, which can include sandstones, shales, carbonates, and coal, often the only practical means to extract fluids is by exploiting the increased drainage provided by fractures. The practical difficulties that must be overcome before effectively using these fractures include: locating the fracture zones, determining the position, orientation, spatial density, and connectivity of fractures, and characterizing the spatial relationships of fractures to other reservoir heterogeneities which might enhance or inhibit the fluid flow. In this project, we are developing theoretical models to describe anisotropy in fractured media. Fluids play an important role in the anisotropy. The presence of fluids is a key interpretation problem for the oil and gas industry, in amplitude-*versus*-offset analysis and in fluid substitution modeling using Gassmann's equations.

**Results:** During this period we explored two research areas: *Fluid Substitution:* Rocks are usually at least slightly anisotropic. The anisotropy comes from alignment of grains and pores, nonhydrostatic effective stress, and aligned macrofractures. Yet, we often apply isotropic methods when analyzing seismic data, because of incomplete information about the complete elastic tensor. What is the error in fluid substitution calculations caused by ignoring anisotropy, and how valuable is the information in the full elastic tensor for estimating pore fluid signatures?

We considered a set of laboratory data from rocks that have transverse isotropic symmetry. We applied two different techniques in the fluid substitution problem; one is Gassmann's fluid substitution, which requires only one P and S velocity data as input, implying that we will ignore the anisotropy. The other approach is Brown and Korrington (B&K) fluid substitution, which is the anisotropic version of Gassmann's technique, using the complete elastic compliance tensor of the TIV material to predict the changes in the elastic tensor. In this way, by comparing both results we can evaluate the assumption of isotropy in the problem of fluid substitution for anisotropic rocks.

For these data, Gassmann fluid substitution predicts an increment of P-wave velocity of 10-15 % for brine saturation at low effective pressures, using the horizontal wave (fast direction) as input. For oil, the increment is ~5%. As the effective pressure increases the increment caused by the fluid substitution

decreases to 5% for brine and 1% for oil; that is, the rock becomes stiffer and less sensitive to the presence of different fluids because of crack closing and soft-porosity reduction. It is interesting that the change in velocity due to fluid substitution is significantly higher when using the vertical P-wave velocity (slow direction) as input, the change at the lower pressure being up to 40 % for brine saturation and 20 % for oil. This means that (as expected) the rock is more sensitive to fluid changes when using seismic data in the vertical direction, or equivalently, along the normals to the cracks and bedding planes. This result already states the importance of considering anisotropy in the problem of fluid substitution, since a different change on the elastic response of the material will be predicted depending on the orientation of the data available.

The B&K fluid substitution results show the same principal characteristics: higher velocity increment (greater fluid sensitivity) at lower effective pressures, and bigger change when propagating along the vertical propagation. In fact for brine and oil substitution, the difference between saturated and dry velocities is higher for lower pressures and becomes pressure-independent for higher values. More important is the fact that B&K approach always predicts larger velocity changes than Gassmann, for both oil and brine as saturating fluids. The discrepancy between the two predictions is slightly larger for higher effective pressures. Assuming the B&K results to represent the correct response, we can conclude then that applying Gassmann in an anisotropic medium may become a poor approximation as effective pressures increases, although the fluid effect itself decreases with increasing pressure. However, the difference in the velocity change predicted when going from a dry state to brine or oil saturation is not very high for these samples, being as much as 100m/s in the worst case.

*Dynamic Equivalent Medium Theory for Layered Media:* Previous work in this field has uniformly presupposed that the dynamics of wave propagation in a heterogeneously layered solid medium could be modeled as a homogeneous solid whose stiffness (or compliance) elements were made frequency-dependent to account for the loss of coherent energy due to scattering. A corollary to this point of view is that mass density has always been viewed as a scalar. In this project, we begin by showing that the conventional, rock-physical way of looking at Backus' result in terms of layer thickness, compliance, and mass density has an exact counterpart in an experimental acoustics parameterization involving travel-time, impedance (or admittance), and slowness. This leads to a demonstration that both impedance and slowness will usually be frequency-dependent in ways that force mass density also to be frequency-dependent and anisotropic. In turn, this suggests that acoustic measurements of layered rocks should involve both slowness and impedance.

The essence of Backus theory (Backus, 1962) is that it allows a stack of layers to be replaced by a single layer. The new homogeneous equivalent medium has elastic properties (compliance, mass density) identical in the long-wavelength limit to the heterogeneous rock under study, and under certain restrictions (uniform heterogeneity) will have the right travel-time. However, it is a kinematic theory; it is silent on the effect that scattering has on wavelet shape as it propagates through the medium.

An important consequence is that, under certain symmetry conditions, both compliance and mass density must have the same frequency-dependence as that of the slowness, which is known by simple argument to be non-zero, because scattering implies dispersion, implies frequency-dependence. By an extension of this argument, it can be shown that P and S waves will usually have different slowness frequency-dependence, in which case the mass density function must be both frequency-dependent and anisotropic.

GRANTEE: STANFORD UNIVERSITY

Geophysics Department  
Stanford, California 94305-2215

**Grant:** DE-FG03-86ER13601

### **Porous Rocks with Fluids: Seismic and Transport Properties**

*Amos Nur, 650-723-95268, fax 650-723-1188, anur@stanford.edu; Jack Dvorkin*

**Objectives:** In this study we develop techniques for simulating viscous fluid flow, electrical current flow, and elastic stresses in a realistic pore space of sedimentary rock. These algorithms are combined in a Virtual Rock Physics Laboratory (VRL) that is used to simulate rock elastic and transport properties depending on the diagenetic process that is responsible for the pore space topology (specifically, cementation and sorting). We also measure the elastic-wave speeds in methane hydrate and relate them to temperature and stress.

**Project Description:** 1. *Virtual Rock Physics Laboratory.* We combine new efficient algorithms of simulating viscous fluid flow (Lattice-Boltzmann method), electrical flow and elastic stresses (finite element method) with various pore-filling schemes to explore how various diagenetic pore-altering mechanisms affect rock elastic and transport properties. We compare the numerical results with existing empirical relations and data sets.

2. *Measuring the elastic properties of methane hydrate.* We use a new method of generating methane hydrate in the lab by filling a holder with granulated ice and then circulating methane through the system. The temperature and pressure of the system simultaneously increase to ensure the transition of the ice-methane mixture to methane hydrate. After compaction, the porosity of the granular system becomes essentially zero. Then  $V_p$  and  $V_s$  are measured in solid methane hydrate as a function of temperature and pressure. These data are required to interpret seismic and well log data in terms of methane hydrate concentration *in situ*.

**Results:** 1. *Virtual Rock Physics Laboratory.* We use two different techniques of pore filling. One is based on altering the initial Finney pack of identical spherical particles by changing their size and placing additional material (such as clay or gas hydrate) in the pore space between the particles. The other is based on randomly filling the pore space with intersecting and non-intersecting spherical particles of varying size to achieve a target porosity value. The results consistently show that the permeability of the system strongly depends on the size of the particles and their sorting. Introducing small particles in the framework of initial large grains acts to reduce permeability much more strongly than uniformly changing the size of the initial grain framework. On the other hand, the electrical conductivity (formation factor) is mostly affected by porosity and is less dependent on the sorting of the grains. The elastic rock properties strongly depend on the elasticity of the components of the framework. By introducing soft clay or gas hydrate particles into the initial quartz grain framework, we create rock that is much softer than a pure quartz and quartz and feldspar rock of comparable porosity.

## GRANTEE: STANFORD UNIVERSITY

Department of Petroleum Engineering  
Green Earth Sciences Building  
367 Panama Street, Rm. 65  
Stanford, CA 94305-2220

**Grant:** DE-FG03-99ER14983

### Diffusion of CO<sub>2</sub> during Hydrate Formation and Dissolution

*Franklin M. Orr, Jr. 650-723-2750, fax 650-725-6566, fmorr@pangea.stanford.edu*

**Objectives:** The goal of this research is to understand what factors control hydrate formation and dissolution. Specific objectives are to: (1) determine mechanisms of hydrate film growth, (2) measure the rate of hydrate growth, (4) determine solute diffusivity through hydrate, and (4) measure hydrate dissolution rates.

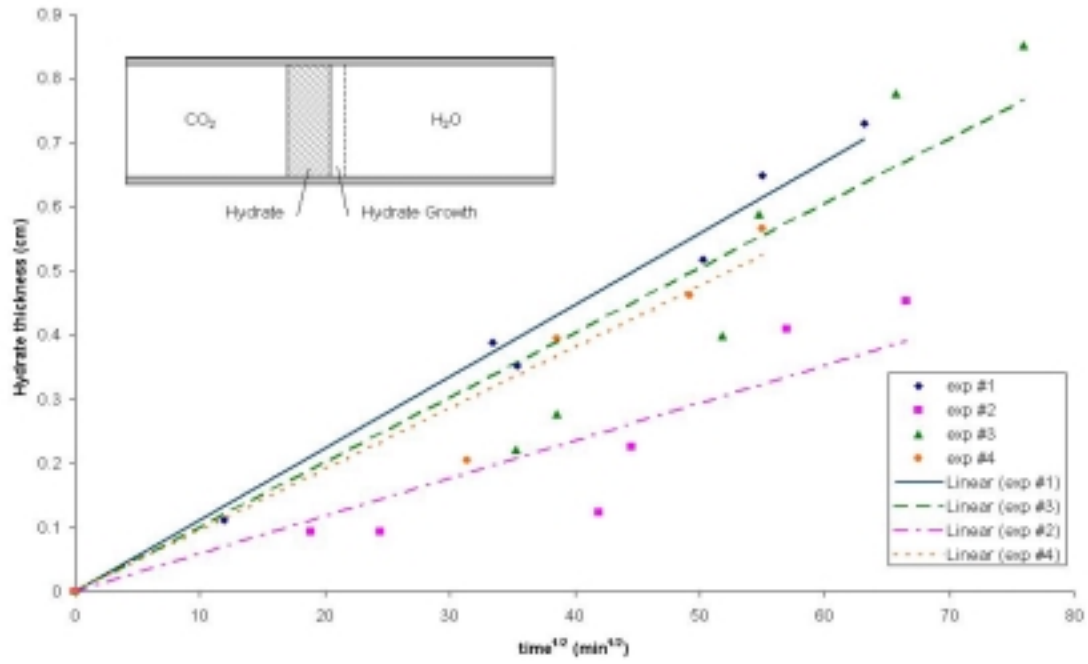
**Project Description:** Mechanisms of hydrate formation and dissolution will play key roles if direct disposal of CO<sub>2</sub> in the oceans is undertaken. When CO<sub>2</sub> is released at depths below about 400 m, hydrate forms at the interface of the CO<sub>2</sub> and water. Formation of a hydrate film reduces the rate of dissolution of the liquid CO<sub>2</sub> in the surrounding seawater. Better definition of the mechanisms and rates of hydrate formation and dissolution is needed to determine transport of released CO<sub>2</sub> and to allow design of release facilities limit environmental impact of the CO<sub>2</sub>.

Hydrate film growth is being measured in a controlled setting in a 3 mm ID capillary tube. An interface between CO<sub>2</sub> and water is positioned in the capillary, and the temperature and pressure are adjusted to conditions at which hydrate forms. The thickness of a plug of hydrate that forms between the liquid CO<sub>2</sub> and water is then measured as a function of time.

**Results:** During this year, the apparatus was assembled, and the technique for initiating hydrate formation was developed. Simply cooling the capillary tube contents at the experimental pressure did not produce hydrates in a reasonable length of time, nor did starting with ice in the capillary and warming to the experimental temperature. In the method finally adopted, the capillary tube is filled with water, and CO<sub>2</sub> at the experimental pressure and temperature is introduced into the tube, displacing the water. A very thin film of hydrate forms where water wets the capillary walls, and a plug of hydrate then forms and grows at the water/CO<sub>2</sub> interface in the center of the capillary when the interface is positioned in the tube.

An initial set of experiments was performed at a temperature of 1 C and pressure of 5.9 MPa. Results of five measurements of film growth are shown in Fig. 1. While there is some scatter, the measured film thickness is roughly linear in the square root of time. In all the experiments film growth was observed only on the water side of the hydrate plug, an observation that is consistent with much faster transport of CO<sub>2</sub> molecules through hydrate cages than transport of water molecules through the hydrate lattice. Diffusion coefficients for CO<sub>2</sub> through the hydrate are estimated to be  $3^{-6}$  to  $5^{-6}$  cm<sup>2</sup>/s, about an order of magnitude lower than the diffusion coefficient for CO<sub>2</sub> through liquid water ( $2^{-5}$  cm<sup>2</sup>/s).

Hydrate Thickness vs. Square Root of Time



## **GRANTEE: STANFORD UNIVERSITY**

Department of Geological and Environmental Sciences  
Stanford, CA 94305-2115

**Grant:** DE-FG03-94ER14462

### **Development of Fracture Networks and Clusters: Their Role in Channelized Flow in Reservoirs and Aquifers**

*D. D. Pollard, 650-723-4679, fax 650-725-0979, dpollard@pangea.stanford.edu; A. Aydin 650-725-8708, fax 650-725-0979, aydin@pangea.stanford.edu*

**Objectives:** Prediction of the spatial distribution of permeability in subsurface aquifers and reservoirs as determined by structural heterogeneities is a challenging problem for water resources and waste management in hydrogeology, and for both exploration and production in the oil and gas industry. To address this problem we are carrying out an integrated plan to map structural heterogeneities (deformation bands, joints, sheared joints, and faults) in an analogue reservoir and developing conceptual models for the evolution of these structures. We are studying the signature of the ancient chemically reactive flow systems within the Aztec Sandstone. The spatial distribution of chemical alteration formed from these reactive fluids reflects their flow pathways, and enables us to infer the *in situ* permeabilities of the structures with which the fluids interacted. This fluid flow also results in diagenetic alteration of the Aztec sandstone. The hypothesis is that the altered sandstone horizons have different fracture/fault populations. If true, an understanding of the fracture distribution in terms of the alteration pattern would be a useful knowledge base for subsurface fracture/fault prediction.

**Project Description:** We are following a methodology based on detailed field mapping of fractures and faults in the Aztec Sandstone in the Valley of Fire State Park, Nevada, and numerical analyses for permeability upscaling and fluid flow modeling using the field data.

**Results:** (1) *Distinguishing Deformation Style with Petrophysical Characterization:* It has been shown that the fundamental structural elements in sandstone bear differing influence on fluid migration. Knowledge of the presence and relative abundance of a structural element in a given sandstone body is therefore important for accurate consideration of bulk fluid flow properties. In the Valley of Fire, Nevada, we have identified two domains within the Aztec sandstone that have considerably different abundances of structural elements. The Lower domain (red sandstone) has a dominant abundance of opening mode joints; the Upper domain (buff sandstone) has a dominant abundance of deformation bands. These two domains are further distinguished with respect to their petrophysical properties. The Lower domain has lower porosity and higher bulk density and elastic moduli. Likewise, it has been found that P- and S-wave velocities are greater [by as much as 500 m/s] for the Lower domain. These observations will aid in the remote characterization of deformed sandstone bodies at depth.

(2.1) *Fluid Flow in Fractured Sandstone: Geometry and Effective Permeability of Deformation Band Sets:* Field investigations in the Aztec sandstone at the Valley of Fire State Park, southern Nevada revealed five characteristic patterns for sets of deformation bands: parallel, anastomosing parallel, conjugate, sigmoidal, and boxwork. The patterns are shown to be continuous on length scales ranging from 1 m to 100 m. Deformation bands within the patterns vary in thickness from 1 mm to 1.5 cm, and the spacing between bands varies from about 1 mm to 2 m. Within the five patterns, there exist only three orientations of deformation bands. Conceptual models for the formations of these patterns suggest

that all three sets of bands and all the patterns were formed due to compression generated by northeast vergent thrusting during the Sevier Orogeny.

Analytical methods and fine-scale finite-difference and finite-element modeling based on homogenization theory were used to calculate upscaled effective permeability tensors for the matrix rock plus the deformation bands. This method is capable of discretely representing the deformation bands. Effective permeability tensors were calculated for each of the deformation band patterns while varying the band permeability/matrix permeability ratio and while varying the thickness and spacing of the deformation bands. It was found that these patterns of deformation bands can reduce the host rock bulk permeability by 2+ orders of magnitude. Likewise, the bands can create permeability anisotropy of up to 2 orders in magnitude.

The bulk permeability reduction and anisotropy caused by the deformation band sets are of the same order of magnitude as those caused by the presence of shale lenses within sandstone. We conclude that these small-scale structural heterogeneities can have equally important effects on permeability and permeability anisotropy as large-scale structural or sedimentological heterogeneities. This result has profound implications for the design and implementation of reservoir and aquifer flow simulations.

(2.2) ) *Fluid Flow in Fractured Sandstone: Upscaling Permeability of Faults developed from shearing across pre-existing joint zones*: The structure of strike slip faults resulting from slip along pre-existing joint sets has been described by detailed geologic mapping used to determine their hydrodynamic properties. The resulting fault zone corresponds to a damage zone composed of joints, sheared joints, fault related deformation bands, and fault gouge. A permeability upscaling methodology using quantitative analog data from the faulted Aztec sandstone was used to quantify the permeability properties of blocks around 25 m<sup>2</sup> comprising parts of the fault zone. Permeability of each fault zone's features and open fracture apertures have been measured or estimated and considered for the upscaling of permeability properties of faults. A numerical procedure for the determination of equivalent grid block permeability tensors for heterogeneous porous media was used; and, in order to determine their upscaled permeability properties, the large blocks were discretized in smaller grid blocks.

Cross-plots of upscaled permeability calculated for each grid block, as well as the permeability tensor characterizing the whole studied block, indicate that faults formed by shearing of joint zones have a strongly anisotropic permeability structures. Fault-parallel permeability may be increased by up to 2 orders of magnitude relative to the host rock. Fault-normal permeability may be reduced by up to 3 orders of magnitude compared to the host rock. These properties are related to the width and continuity of the fault gouge zones as well as the density of deformations bands or small faults within and around the fault. They are also function of the aperture and distribution of orientations of splay fractures as well as the matrix permeability. Principal permeability directions of the upscaled block may correspond to an average direction between mean joint trend and mean fault core direction for a small amount of slip. At larger slip amounts, principal permeability directions get closer to the mean fault core, but can deviate noticeably from this direction.

We have also shown that fault zone permeability varies with slip magnitude. Although increased slip leads to higher density of shear induced joints, the fault-parallel permeability is not necessarily increased because of the dispersion in joint orientations. For the same reason, fault-normal permeability doesn't necessarily decrease when slip increases, although the number and density of low permeability features, such as gouge, sheared joints and deformation bands, increases. As a result, for a given size of block, principal permeability values may decrease as slip increases.

**GRANTEE: STANFORD UNIVERSITY**

Department of Geophysics  
Stanford, CA 94305-2115

**Grant:** DE-FG03-00ER14962.001

**Coupled Fluid Deformation Effects in Earthquakes and Energy Extraction**

*P. Segall 650-725-7241, fax 650-725-7344, segall@stanford.edu*

**Objectives:** A fundamental understanding of the effect of magmatic intrusions on geothermal systems.

**Project Description:** The focus of the project is Long Valley caldera, an active hydrothermal area east of the Sierra Nevada in California. Long Valley is the site of anomalous seismic activity and ground deformation. One aspect of the project is to assess whether the hydrothermal system is playing an active role in the current activity at Long Valley. Repeated micro-gravity measurements can discriminate between magmatic intrusion on the one hand and, thermal expansion or pressurization of the hydrothermal system on the other. Before gravity changes can be interpreted, however, they must be corrected for the effects of uplift, and changes to the depth of the water table. The second aspect of the project is to investigate the poro-thermo-elastic effects of intrusion on ground uplift and subsidence in volcanic areas.

**Results:** Precise relative gravity measurements conducted in Long Valley in 1982 and 1998 reveal a decrease in gravity of as much as  $-107 \pm 6$  microgal ( $1 \text{ gal} = 0.01 \text{ m/s}^2$ ) centered on the uplifting resurgent dome. A positive residual gravity change of up to  $64 \pm 15$  microgal was found after correcting for the effects of uplift and water table fluctuations. Assuming a point source of intrusion, the density of the intruding material is 2.7 to 4.1 gm/cc at 95% confidence. The gravity results require intrusion of silicate magma, and exclude *in situ* thermal expansion or pressurization of the hydrothermal system as the cause of uplift and seismicity. To improve upon these results, in July 1999 we resurveyed 39 precise gravity stations in Long Valley, as well as 45 leveling monuments using dual-frequency GPS receivers. All sites were occupied at least twice, and data from continuous GPS sites were included in the analysis. Our estimated ellipsoidal heights have standard errors of 1.7 cm. The GPS ellipsoidal heights are converted to orthometric heights using the NGS geoid. The combined gravity change/deformation data set will be used in simultaneous inversions to estimate the magma chamber geometry and average density.

## GRANTEE: TEMPLE UNIVERSITY

Department of Chemistry  
Philadelphia, PA

**Grant:** DE-FG02-96ER14644

### Surface Chemistry of Pyrite: An Interdisciplinary Approach

*D. R. Strongin 215-204-7119, fax 215-204-1532, dstrongi@nimbus.ocis.temple.edu; M. A. A. Schoonen, State University of New York, 516-632-8007; schoonen@sbmpo4.ess.sunysb.edu*

**Objectives:** The primary goal of this research program is to understand the microscopic aspects of pyrite oxidation. Determining the charge development on pyrite surfaces and evaluating the interaction of the pyrite surface with an array of simple inorganic and organic molecules are the immediate goals. Through a combination of macroscopic observations and observations at the atomic/molecular level new insights are gained that will lead to a better understanding how pyrite reacts in a range of chemical environments.

**Project Description:** The charge development, interaction with inorganic and organic constituents, and the reactivity of pyrite are being investigated. Emphasis is placed on integrating macroscopic information from low-temperature techniques such as electrophoresis and microscopic information from modern surface science techniques that are used in the ultra high vacuum (UHV) environment. Using model, atomically clean “as-grown” surfaces of pyrite, electron spectroscopies in UHV are used to understand the atomic composition and the nature of the functional groups on pyrite after exposure to the aqueous solutions. The integration of the UHV and low-temperature studies will provide a complete picture of the type of surface functional groups at the pyrite surface, their acid-base behavior, and interaction with selected aqueous constituents.

**Results:** *Surface Science Studies of pyrite structure and oxidation.* Photoelectron Spectroscopy was used to investigate the surface structure and reactivity of {100} planes of pyrite that have been prepared by two commonly employed means. Specifically, synchrotron-based photoelectron spectroscopy was used to investigate the structure of two {100} pyrite surfaces. One was prepared by exposing a {100} pyrite growth surface to HCl, and one was produced by mechanical fracture. Results show that acid-washed growth surface (*i.e.*, exposed to HCl) showed a higher concentration of elemental sulfur and/or polysulfide impurities. Perhaps, surprisingly, the surfaces showed similar initial oxidation reactivity under well-controlled H<sub>2</sub>O/O<sub>2</sub> gaseous environments. This result implied that the fraction of both surfaces that underwent the initial oxidation reaction were similar in structure. The oxidation activity of these surfaces were, however, were experimentally determined to be significantly less than the initial oxidation activity of an acid-washed {111} growth surface. Photoelectron and ion scattering spectroscopy suggest that a reason for this structure sensitivity may be due to differences in the concentration of Fe in the outermost layer of the different crystallographic planes of pyrite.

*Studies of the pyrite-phosphate interaction.* Electrophoresis and surface science experiments have been carried out to understand the interaction between phosphate and pyrite. Electrophoresis experiments show that under anoxic conditions only a relatively small fraction (no more than 10 %) of dissolved phosphate irreversibly sorbs onto the pyrite surface. Surface science studies suggest that this irreversibly bound pyrite adsorbs to non-stoichiometric sites on pyrite. Results to date indicate that phosphate is preferentially bound to sulfur-deficient (possibly Fe<sup>3+</sup>) defect sites. Research carried out in

prior funding cycles suggests that these sites play a critical role in the oxidation of pyrite by dissolved  $O_2$ . Aqueous-based oxidation experiments and experiments carried out in a combined ultra-high vacuum/high pressure apparatus suggest that this relatively small amount of adsorbed phosphate results in a significant oxidation suppression of pyrite. This result emphasizes how minority sites (non-stoichiometric sites) control the oxidation reactivity of pyrite.

## **GRANTEE: THE UNIVERSITY OF TENNESSEE**

Institute for Rare Isotope Measurements  
10521 Research Drive, #300  
Knoxville, TN 37932

**Grant:** DE-FG05-95ER14497

### **Development of Laser-Based Resonance Ionization Techniques for $^{81}\text{Kr}$ and $^{85}\text{Kr}$ in the Geosciences**

*N. Thonnard, 865-974-9702, fax 865-974-8289, nthonnar@utk.edu; T.C. Labotka; L.D. McKay*

**Website:** <http://web.utk.edu/~irim>

**Objectives:** (1) Bring into operation a new analytical methodology for Kr-81 and Kr-85, (2) identify performance limitations and implement improvements in reproducibility, accuracy, throughput and sample size, and (3) initiate research in the geosciences.

**Project Description:** Cosmogenic Kr-81 (229,000 year half-life; 20,000 to 1,000,000 year dating range) and anthropogenic Kr-85 (10.8 year half-life; 0.1 to 40 year dating range) are potentially significant in our understanding of processes in the environment, including dating of polar ice and very old ground water, ocean circulation, and modern water flow patterns. Their chemical inertness should simplify interpretation of results. The only Kr-81 measurements from natural samples to date are a handful of results from old groundwater and polar ice using the laser-based analytical technique under development here that used approximately 50 liters of water, and a recent (2000) measurement of old groundwater from Australia using 16,000 liters of water per point with a Cyclotron-based Accelerator Mass Spectrometry technique. A few measurements of Kr-85 from ~200 liter water samples using decay counting have also been made, demonstrating the promise of this isotope. This new analytical technique will permit Kr-85 measurements using only 1 to ~5 liter samples and Kr-81 measurements from 10-20 liter samples. It is a multi-step process starting with (1) degassing of the water sample, (2) separating Kr from the recovered gas, (3 & 4) two isotopic enrichments reducing interfering isotopes by  $>10^8$ , and (5) detecting the rare krypton isotope in a time-of-flight mass spectrometer, where the sensitivity, element specificity, and immunity to isobaric interference of resonance ionization (~100 Kr-85 atom detection limit) is utilized to detect the few thousand analyte atoms remaining in the sample.

**Results:** Although the DOE-sponsored part of this program ended only two months into FY2000 on 11/30/99, the overall goals were co-funded with NSF, which continued through 8/31/00. We therefore report below progress for the entire Fiscal Year through 9/30/00.

As mentioned in previous reports, delays in space availability resulted in postponement of most of the laser and optical aspects of this project. Resonance ionization of krypton with the new, dedicated laser system was not possible until the Fall of 1999, while integration and synchronization of the new laser system with other components of the krypton detector was completed in January of 2000. A major fraction of the effort during this past year has been in bringing the RIS-TOF (resonance ionization spectroscopy time-of-flight) mass spectrometer system back into operation. High-resolution (~1200) ultra-sensitive RIS-TOF mass spectra are now obtainable on a routine basis. The careful design of the dedicated krypton RIS laser system has paid-off with very routine and reproducible operation. After numerous on/off cycles, and even after having been off for six weeks, upon restarting, the position and

wavelength of the multiple laser beams required for Kr RIS has not changed. Therefore, on most occasions, operation is possible after less than five minutes of performance verification and minor “peak-up” adjustments. This is in marked contrast to the older system, where the norm was many days of excruciating alignment being required before data could be taken, if you were lucky. All tests indicate that the sensitivity of the system is the same, if not better, than it was when the 100 Kr-85 atom detection limit was demonstrated before this major re-build.

Although mass resolution and sensitivity of the RIS-TOF system is at the expected performance level, it has not been possible to measure the Kr-85 concentration in samples because of a very rapid build-up of background krypton. The sensitivity is more than adequate to measure environmental levels of Kr-85, but the rapid in-growth of krypton blank raises the total Kr signal to saturation before sufficient Kr-85 counts have been registered to make a detection. Tests indicate that the blank is due to an extremely small leak that can only be found by a process of elimination, which is very time-consuming. Nevertheless, this is not a fundamental problem. The blank was 200 to 500 times less before the upgrades; therefore, we are confident that the earlier blank level will be achievable.

The equipment for all of the other five steps in the analytical process has been completed, thoroughly tested and meets the design goals. Calibration samples and hydrogeologic samples have been processed to various levels of completion, and are in the queue awaiting final counting with the RIS-TOF system as soon the cause of the blank is isolated and repaired.

Collaboration with hydrogeologist at the Universities of Bern, Memphis, Utah, and Waterloo continues and are at the stage where Kr-85 and Kr-81 analyses will commence as soon as feasible. New collaborations are under discussion with researchers at the Danish Geological Survey, the University of Nebraska and the USGS. The prospect of making Kr-85 and Kr-81 measurements from hydrogeologic samples has generated considerable interest in the community.

## **GRANTEE: TEXAS A&M UNIVERSITY**

Department of Petroleum Engineering, 3116 TAMU  
College Station TX 77843

**Grant:** DE-FG03-00ER15034

### **Time-Lapse Seismic Monitoring and Performance Assessment of CO<sub>2</sub> Sequestration in Hydrocarbon Reservoirs**

*Akhil Datta-Gupta, 979-847-9030, fax 979-845-1307, data-gupta@tamu.edu; Richard L. Gibson, gibson@geo.tamu.edu; Bruce Herbert, herbert@geo.tamu.edu*

**Objectives:** The primary goal of this project is twofold. First, we want to assess the feasibility of time-lapse seismic monitoring of CO<sub>2</sub> sequestration in hydrocarbon reservoirs using coupled fluid flow, geochemical and seismic modeling. Second, we want to develop a formalism for assimilation of static and dynamic data sources in the reservoir for performance assessment and quantifying uncertainty in performance predictions.

**Project Description:** Recent data obtained from both laboratory and field experiments suggest that the influence of CO<sub>2</sub> on seismic properties is sufficiently strong to be detectable, confirming that seismic methods are viable monitoring tools. Seismic monitoring of two basic categories of changes in reservoir conditions may be possible over the long term. First, seismic response may be affected by changes in pore fluid properties, because the injected CO<sub>2</sub> can exist in three separate phases, supercritical fluid (SCF) CO<sub>2</sub>, gaseous CO<sub>2</sub>, or dissolved in aqueous solutions, depending on the pore pressures and temperatures in the reservoir. Second, the seismic response may change in response to petrophysical alterations such as cementation, second porosity formation and compaction. We will develop an integrated modeling scheme whereby we can simultaneously simulate the geochemistry, fluid flow, and seismic data acquired over the reservoir. Our approach combines rapid streamline-based fluid flow simulations with high speed, three-dimensional seismic modeling using a ray-Born algorithm. A critical component of performance assessment of a CO<sub>2</sub> sequestration project will be accurate characterization of reservoir properties such as porosity and permeability by integrating a wide variety of data sources. A second component of our research is to systematically incorporate all the static and dynamic data sources into reservoir models and characterize the uncertainty about physical parameters, in particular, porosity and permeability that control the performance predictions of fluid flow simulation models.

**Results:** We constructed a reference heterogeneous reservoir model using geostatistical methods and laboratory measurements of rock and CO<sub>2</sub> parameters. Changes in rock velocities caused by variations in pore fluids were computed using the Gassmann's equation, and empirical equations based on laboratory data were used to model the dependence of velocities on pressure. The velocity of CO<sub>2</sub> in the liquid phase (T = 27 °C, P = 14 MPa) is as low as 31 % of brine velocity, but the density of CO<sub>2</sub> under the same conditions is as high as 80 % of brine density. Under supercritical conditions (T = 77 °C, P = 14 MPa), the velocity and the density of CO<sub>2</sub> are only 16% and 39% of brine's, respectively. We computed the seismic response before and after CO<sub>2</sub> injection for both of these scenarios, and the CO<sub>2</sub> saturated region can be easily detected in both cases. In particular, regions of the reservoir with high porosity (about 30%) show amplitude differences of about 23%. The model results also clearly indicate that time-lapse amplitude variation with offset (AVO) analysis has strong potential to assist in sequestration monitoring programs. For example, the AVO responses are quite different if only pressure

or only fluid saturation changes in the reservoir, allowing an inference of changing reservoir conditions from analysis of seismic data. The simulations also demonstrate that it should be possible to distinguish between liquid and supercritical fluid phases of CO<sub>2</sub> using AVO measurements. As part of our effort to construct reservoir models by integrating multiscale data sources, we have developed a hierarchical approach to spatial modeling based on Markov Random Fields (MRF) and multi-resolution algorithms in image analysis. Our proposed method is computationally efficient and well suited to reconstruct fine scale spatial fields from coarser, multi-scale samples (*e.g.*, based on seismic and production data) and sparse fine scale conditioning data (*e.g.*, well data). It is easy to implement and can account for the complex, non-linear interactions between different scales as well as precision of the data at various scales in a consistent fashion.

## GRANTEE: TEXAS A&M UNIVERSITY

Center for Tectonophysics  
Geology & Geophysics Dept.  
College Station, TX 77843-3115

**Grant:** DE-FG03-98ER14887

### Fluid-Assisted Compaction and Deformation of Reservoir Lithologies

*A.K. Kronenberg, 979-845-0132, fax 979-845-6162, a-kronenberg@tamu.edu; F.M. Chester;  
J.S. Chester; A. Hajash*

**Objectives:** This research addresses the volumetric creep compaction, chemical reaction processes, and distortional deformation of fine-grained quartz aggregates and quartz-clay mixtures subjected to aqueous fluids at temperatures, effective pressures and stress states representative of diagenetic conditions. Specific goals include 1) determination of the transition from isochemical brittle deformation to fluid-assisted solution-transfer creep, 2) identification of the mechanisms of solution-transfer creep, and 3) evaluation of mechanical and chemical rate laws for clastic reservoir lithologies.

**Project Description:** The compaction and diagenesis of sandstones that form reservoirs to hydrocarbons depend on mechanical compaction processes, fluid flow at local and regional scales, and chemical processes of dissolution, precipitation and diffusional solution transport. Using an experimental approach, the rates of compaction and distortional deformation of quartz and quartz-clay aggregates exposed to reactive aqueous fluids at varying stress states are under investigation. Pore fluid compositions and reaction rates during deformation are measured and compared with creep rates, and acoustic emissions and microstructures of specimens are used to determine the contributions of mechanical and chemical processes to deformation and pore-structure evolution.

**Results:** Significant progress has been made towards characterizing critical conditions required for rapid cataclastic compaction of St. Peter sand, and measuring long-term compaction of St. Peter sand and Arkansas novaculite (1) in the absence of a reactive pore fluid, (2) with H<sub>2</sub>O vapor present, (3) with liquid H<sub>2</sub>O saturating pores under static conditions, and (4) with aqueous fluid slowly percolating (0.12 ml/hr) through the specimens. Room temperature values of  $Pe^*$  associated with Hertzian cracking at grain contacts for St. Peter sand (of 80 MPa) are marked by curvature in pressure-volume curves and are well above the effective pressures applied in the long-term experiments. At  $Pe = 34.5$  MPa, quartz aggregates are observed to creep at low strain rates. Specimens vented to atmosphere exhibit transient logarithmic creep at rates down to  $\sim 3 \times 10^{-10} \text{ s}^{-1}$  and show little grain size sensitivity. Quartz aggregates loaded sequentially while vented, exposed to H<sub>2</sub>O vapor, and saturated by liquid H<sub>2</sub>O exhibit systematic increases in creep rate (from  $\sim 3 \times 10^{-10} \text{ s}^{-1}$  to  $\sim 4 \times 10^{-9} \text{ s}^{-1}$  and  $\sim 6 \times 10^{-9} \text{ s}^{-1}$ , respectively). Strain rates under wet conditions follow logarithmic creep relations of similar form but quantitatively distinct from the relation exhibited under dry conditions. Creep rates of samples with percolating fluid are yet another order of magnitude greater than those measured with static fluids saturating pores.

During closed system, wet, experiments static pore fluids become highly supersaturated (195 ppm) with respect to  $\alpha$ -quartz at T and  $P_p$  (equilibrium SiO<sub>2</sub> at 160 ppm). During open system, slow-flow experiments, fluids exiting specimens remain supersaturated though at lower levels ( $\sim 170$  ppm). We conclude that creep under open-system conditions is limited by the dissolution rate at loaded grain

contacts and that rates under closed-system conditions may ultimately be governed by much slower precipitation kinetics.

A)

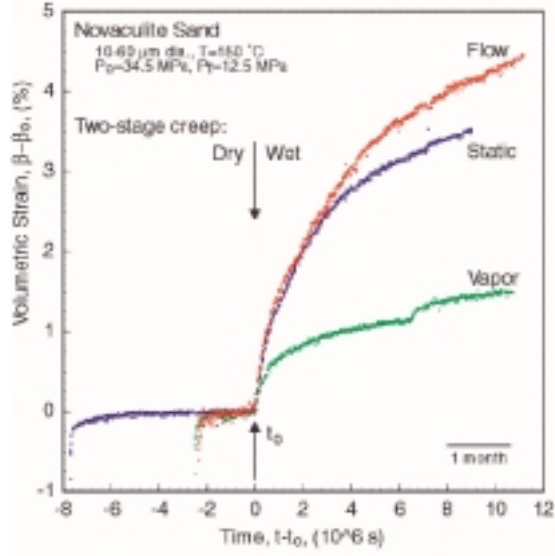
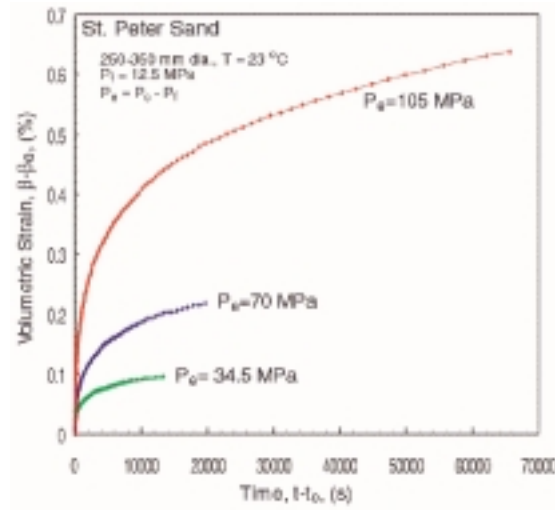
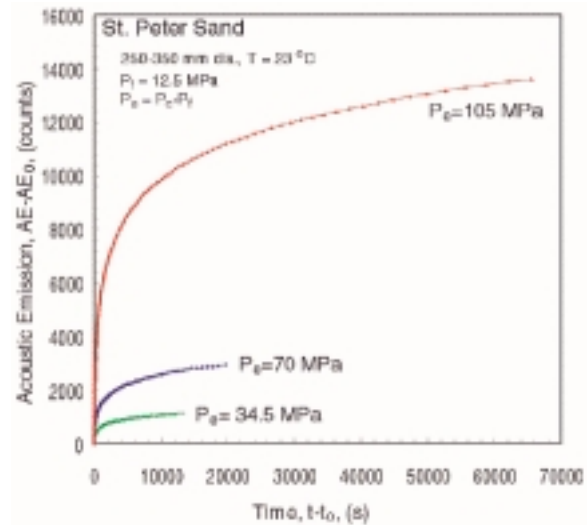


Figure 1. Hydrostatic compaction results for quartz aggregates. A) Volumetric strains measured in long-term experiments performed on disaggregated Arkansas novaculite grains under dry conditions and with H<sub>2</sub>O present, as a vapor, as a static liquid saturating pores, and as a percolating pore fluid. B) Volumetric creep strains for St Peter sand specimens saturated with H<sub>2</sub>O and subjected to three different effective pressures  $P_e \leq P_e^*$  closely fit a logarithmic creep relation with respect to time of loading. C) Acoustic emissions for the same St Peter sand experiments exhibit a similar logarithmic relation with time of loading, and acoustic emission rates at room temperature correlate well with creep rates.

B)



C)



**GRANTEE: TEXAS A&M UNIVERSITY**

Center for Tectonophysics, Geology & Geophysics Dept.  
College Station, TX 77843-3115

**Grant:** DE-FG03-00ER15033

**Experimental and Analytic Studies to Model Reaction Kinetics and Mass Transport of Carbon Dioxide Sequestration in Depleted Carbonate Reservoirs**

*John W. Morse, 979-845-9630, fax 979-845-9631, morse@ocean.tamu.edu; Daulat Mamora*

**Objectives:** 1) to determine and model the reaction kinetics of dissolution of carbonate minerals in saline waters under temperature and pressure conditions approximating those in gas-bearing carbonate reservoirs; 2) study the displacement of natural gas by supercritical carbon dioxide, and 3) develop an integrated model for the sequestration of carbon dioxide in carbonate gas reservoirs.

**Project Description:** Sequestration of carbon dioxide in depleted gas reservoirs appears to be a viable option, with a possible economic spin-off from the recovery of significant gas reserves. At the elevated temperatures and pressures encountered in reservoirs, carbon dioxide behaves as a supercritical fluid. Under these conditions, little is known regarding the kinetics of calcite dissolution by carbon dioxide, diffusion of carbon dioxide in natural gas, and displacement of natural gas by carbon dioxide. This project is conducting research to better understand these phenomena through experimental determination of the reaction kinetics for calcite dissolution, coefficient of dispersion, and displacement mechanisms in respect to supercritical carbon dioxide at temperatures and pressures typically found in reservoirs. The requisite data will be used to develop a model for mass transport and reaction kinetics for the injection and storage of carbon dioxide in carbonate or carbonate-bearing depleted gas reservoirs.

**Results:** Construction of a newly designed computer-controlled experimental apparatus necessary to conduct "free-drift" and chemostat dissolution experiments at 1 bar pressures has been completed and experimental studies started of calcite dissolution kinetics in brines. The experimental design currently implemented has involved a reconnaissance of the effects of  $p\text{CO}_2$ , temperature and ionic strength on the dissolution kinetics of calcite. Dissolution has been conducted at various  $p\text{CO}_2$ 's ranging from 0.01 to 1.0 and at two different temperatures (25°C and 80°C). Experiments that have included triplicate runs under each of these conditions have demonstrated high precision in the rate measurements and that mass-normalized rates are independent of the mass of the sample. Additionally the high-pressure experimental system reaction vessel was modified to provide more than an order of magnitude more solution for analytical studies.

The development of the apparatus for investigation of displacement of natural gas by supercritical  $\text{CO}_2$  has also proceeded well. A hoop analysis was performed to arrive at a safe design and construction of the injection cell with a water bath for temperature control. An Austin chalk core was pressurized to simulate an overburden pressure differential of 500 psi,  $\text{CO}_2$  was injected into the accumulator, and a Ruska pump was successfully tested for compression of the carbon dioxide.

## **GRANTEE: UNIVERSITY OF TEXAS**

Department of Geological Sciences  
P.O. Box 7726  
Austin, TX 78713-7726

**Grant:** DE-FG03-97ER14812

### **High-Resolution Temporal Variations in Groundwater Chemistry: Tracing the Links between Climate, Hydrology, and Element Mobility in the Vadose Zone.**

*Jay L. Banner, 512-471-5016, fax 512-471-9425, banner@mail.utexas.edu*

**Objectives:** To evaluate the extent to which radiogenic and stable isotopic and trace element variations in speleothems and modern groundwater from the same aquifer provide a means to reconstruct temporal changes in groundwater geochemistry, flow routes, and corresponding climatic controlling processes.

**Project Description:** This study is using cave calcite deposits (speleothems) and modern groundwater samples to develop a new approach, integrating Sr, Nd, C, O, H and U-series isotope variations with other geochemical and hydrologic tracing tools, to provide 1) improved sensitivity in reconstructing temporal records of groundwater evolution, and 2) a new perspective on the links between climate variability, hydrology, soil evolution, and groundwater chemistry. An understanding of controls on the modern hydrologic system provides a framework within which to interpret the speleothem record. Groundwater, soils, rainfall, speleothem and aquifer rocks are sampled in selected catchments using low-contamination procedures, and analyzed by mass spectrometry. Two karst aquifers were selected for intensive study to achieve the aims of this project. Results presented below highlight our study of the Edwards aquifer.

**Results:** We have constructed a comprehensive chronology for cave speleothems from widely-separated caves across central Texas that provides a 71,000-year record of temporal changes in hydrology and climate. High-precision ages were determined for fifty-three samples by two separate radiometric dating schemes: uranium-238/thorium-230 and uranium-235/protactinium-231 analyses. The accuracy of the ages and the closed-system behavior of uranium, thorium, and protactinium in these deposits of paleo-groundwater are indicated by inter-laboratory comparisons and the concordance of ages determined by the independent dating schemes. Over the last 71,000 years, the speleothems have similar growth histories. The growth rates vary over nearly three orders-of-magnitude, with three periods of rapid growth from 71-60 ka, 39-33 ka, and 24-12 ka. These growth rate shifts correspond in part with global glacial-interglacial climatic shifts. The most recent of these rapid growth periods corresponds with proposed wetter climatic conditions in Texas during the Last Glacial Maximum (20 ka). The temporal shift in wetness has been proposed to result from a southward deflection of the jet stream by the presence of a continental ice sheet in central North America. This mechanism also may have governed in part the two earlier intervals of fast growth in the speleothems (and inferred wetter climate). These results illustrate that speleothem growth rates can reflect the regional response of a hydrologic system to regional and global climate variability.

## **GRANTEE: THE UNIVERSITY OF TEXAS**

Department of Geological Sciences  
Austin, Texas 78712-1101 U.S.A.

**Grant:** DE-FG03-97ER14772

### **Thermohaline Convection in the Gulf of Mexico Sedimentary Basin, South Texas**

*John M. Sharp, Jr. 512-471-3317 or 512-471-5172, fax 512-471-9425,  
jmsharp@mail.utexas.edu; Craig T. Simmons, Flinders University,  
Craig.Simmons@es.flinders.edu.au*

**Objectives:** The initial three research tasks were: 1.) The selection and development of models of thermohaline convection and cross-formational diffusion; 2.) Evaluation of the evolution of thermohaline convection above and within the overpressured zone; and 3.) Modeling the effects of the hydrostratigraphic framework of the Gulf of Mexico Basin and its effects on thermohaline convection scenarios. To accomplish these objectives, we had to add: 4.) Evaluation of the effects of sediment heterogeneity, including fractures on free convection.

**Results:** 1. We selected the U. S. Geological Survey code SUTRA as the primary model and created simplified pre- and post-processors for the system and extensions for the graphics. We, including Dr. Simmons, our collaborating scientist at Flinders University of South Australia (FUSA), and colleagues, evaluated several models. SUTRA was found to be the most robust and also allowed us full access to the code. The initial set of simulations was completed by the end of November 1998.

2. These simulations documented the appropriate ranges of parameters for the processes that create the salinity inversions in the Gulf of Mexico Basin. This upwelling of brines into the permeable rocks creates lateral salinity variations and observed density inversions. These are largely responsible for the instability that creates thermohaline convection. In the Gulf of Mexico Basin, we can infer that:

2.1. Shale permeabilities below the top of overpressures, on geological time and spatial scales, are greater by an order of magnitude or more than above the overpressures. This is created by natural hydraulic fracturing.

2.2. Salinity inversions do not appear to be maintainable for long (>104 years) in the extremely overpressured or the hydro pressured zones.

2.3 There exists a transition between diffusion and convection dominated solute transport. Free convection, at least in this setting, is not a simple "on-off" process.

2.4 The transition zone, between over pressures and hydrostatic pressures, is sufficient to arrest thermohaline convection in Gulf Coast sediments.

2.5 The results demonstrate the process by which sedimentary basins become density stratified with geologic time.

3. The gathering of data on the hydrostratigraphic framework proved unexpectedly difficult. All existing stratigraphic interpretations are far too large in scale to be meaningful in modeling efforts and salinity data spatial distributions were both spotty and sparse. Shale permeability variations have never been documented, although petrographic and seismic data show significant heterogeneity. We resorted

to numerical simulations of high permeability zones caused either by zones of microfractures or by facies changes. We recommend a detailed program of data gathering be attempted to provide the requisite details.

4. The model simulations show several significant results. These are, perhaps, the most interesting and intriguing results of this research:

4.1. Traditional Rayleigh Number criteria, commonly used to estimate whether or not a system will freely convect, are of questionable validity in this or similar settings (Simmons et al., 1999; Simmons and Sharp, 2000; Sharp et al., in press; Simmons et al., in press).

4.2. The effects of permeability and salinity field heterogeneities can dominate the determination of a system's stability or instability (Sharp and Simmons, 2000). Hitherto, this has been rarely addressed. The onset and subsequent growth or decay of convective instabilities is intimately related to the style or structure of the heterogeneous porous media under consideration. Heterogeneity is important for two principle, but opposing reasons. Heterogeneity (i) serves as the triggering mechanism for the onset of instabilities, and (ii) is the most important factor controlling whether instabilities, once generated, will grow or decay.

Vertically continuous high permeability regions enhance growth conditions (*e.g.*, vertical fracturing or conduits, sinusoidal horizontal conductivity distributions). The effects of fractures on thermohaline convection were evaluated, and we prepared a closed form analytical solution on this process (Simmons et al., 1999). These calculations demonstrate that fracture sets with even minimal aperture are enough to dissipate salinity inversions. However, intermediate low permeability regions provide resistance to horizontal dispersive mixing. In lenticular or layered structures (*e.g.*, stochastic distributions), increased variance and increased horizontal correlation in the permeability field create laterally extensive low permeability barriers to the vertical upflow and downflow necessary to maintain convective flow.

## **GRANTEE: THE UNIVERSITY OF TEXAS AT DALLAS**

Center for Lithospheric Studies  
P.O. Box 830688 (FA31)  
Richardson, TX 75083-0688

**Grant:** DE-FG03-96ER14596

### **Integrated 3-D, Ground-penetrating Radar, Outcrop, and Borehole Data Applied to Reservoir Characterization and Flow Simulation**

*George A. McMechan, 972-883-2419, fax 972-883-2829, mcmec@utdallas.edu; Janok Bhattacharya 972-883-2449, fax 972-883-2537, janokb@utdallas.edu; Craig Forster, 801-581-3864, fax 801-581-7065, cforster@mines.utah.edu*

**Objectives:** 3-D ground-penetrating radar (GPR) is used for characterization of the geometry of a clastic hydrocarbon reservoir analog. Sedimentologic mapping and porosity and permeability measurements from core plugs extracted from cliff-faces and boreholes allow population of the model with realistic flow parameters. The final step is 3-D flow simulation through the model to evaluate the effects of flow barriers and baffles to hydrocarbon production.

**Project Description:** Existing reservoir models are based on 2-D outcrop studies; their 3-D aspects are inferred from correlation between well data, and so are inadequately constrained for reservoir simulations. Field study sites are in the Cretaceous Ferron Sandstone in Utah. Detailed sedimentary facies maps of cliff faces define the geometry and distribution of potential reservoir flow units, barriers, and baffles at the outcrop. High-resolution 3-D ground-penetrating radar (GPR) images extend these reservoir characteristics into 3-D, to allow development of realistic 3-D reservoir models. Models use geometrical information from the mapping and the GPR data, petrophysical data from surface and cliff-face outcrops, lab analyses of outcrop and core samples, and petrography. Flow simulation in the final models will illustrate the applicability of reservoir analog studies to well siting and reservoir engineering for maximization of hydrocarbon production.

**Results:** The focus of activity in this third project year was on 3-D GPR data imaging, constructing 3-D permeability models, sedimentologic interpretation, and flow modeling. Preliminary results indicate the existence of four main architectural elements, which, from bottom to top are (1) sand-dominated delta plain channels, (2) tidally-influenced delta plain distributary channels, (3) sand-dominated incised channel, and finally, (4) tidal. The main feature of interest is an extensive set of lateral accretion beds in element 2, related to a migrating tide-influenced point bar. The outcrops and 3-D GPR data clearly show that these lateral accretion beds extend for hundreds of meters and are partially draped by thin mudstones forming inclined heterolithic cross strata. The lateral accretion beds internally contain cross bedded to rippled sandstones. Mudstone drapes are locally cut by scours forming layers of mud-chip conglomerates. These features are tied to their corresponding permeability distributions to complete the 3-D model and provide the input for 3-D flow simulations that are now in progress. The flow is substantially anisotropic.

A novel aspect of the project is extensive use of Global Positioning System (GPS) technology in two ways. Differential GPS was used to position all data types to a precision of decimeters in 3-D. This allows us to render all data and interpretations in 3-D. The second application is direct mapping of bounding surfaces, mudstone drapes, and mud-chip horizons in 3-D, remotely, using a reflectorless laser

rangfinder. By combining photomosaics with laser mapping, undistorted bounding surfaces are correctly mapped in the same 3-D coordinate system as the GPR data. GOCAD software is used to display the lateral accretion surfaces in 3-D.

The main advance in this project is production of the ‘first-ever’ detailed 3-D images of an ancient point bar deposit, in which we can compare predictions made from theoretical considerations and from models developed from 2-D outcrops. These results motivate similar applications in other environments.

## **GRANTEE: TEXAS TECH UNIVERSITY**

Dept. of Chemical Engineering  
Lubbock, TX 79409

**Grant:** DE-FG03-99ER14932

### **Continuum and Particle Level Modeling of Concentrated Suspension Flows**

*A. Graham 806-742-3553, agraaham@ttacs.ttu.edu; L. Mondy, Sandia National Laboratories; M. Ingber, University of New Mexico*

**Objectives:** The purpose of this program is to combine experiments, computations, and theory to make fundamental advances in our ability to predict transport phenomena in concentrated, multiphase, disperse systems, particularly when flowing through geologic media.

**Project Description:** The proposed research will elucidate the underlying physical principles that govern concentrated multiphase systems in areas essential to continued progress in geosciences. In order to be of use in real world applications, significant enhancements to currently available continuum-level suspension flow models will be required. We will use both experimentation and high performance computing to obtain microstructural information that is necessary to the development and refinement of the continuum models. For example, we expect to use this microstructural information to gain insight into the physics of particle interactions and particle sedimentation, which are particularly important in sand control issues found in petroleum production. Further, we expect that continuum-level modeling could eventually be directly implemented in codes currently used to predict hydraulic fracturing operations in the petroleum industry. The understanding gained about the physics of multiphase flows will, however, have much broader application in geosciences.

**Results:** The continuum models originally developed by Phillips *et al.*(1992) and Nott and Brady (1994) have been extended to account for normal stress contributions in general three-dimensional flows. The Phillips-type model currently also allows for non-neutrally buoyant particles and non-Newtonian suspending liquids. However, we have found that without the enhancement of the suspension flow model with an anisotropic flow tensor, the results for the non-Newtonian suspending fluid are qualitatively incorrect in some cases. Results from the newest model, which have been implemented into a general-purpose finite element computer code, are being compared with experimental measurements based on nuclear magnetic resonance (NMR) imaging to test our theory that effects of a shear-thinning suspending fluid are also influenced by the particle-induced normal stress contributions. For Newtonian suspending liquids, we have concentrated on modeling viscous resuspension of a settled bed of particles -- a phenomenon important in many geologic flows. Although the model works extremely well for most flows influenced by gravity, numerical instabilities appear when the particle concentration, and hence the viscosity, changes abruptly. We are currently implementing a porous Brinkman source term that will slow the flow depending on the particle volume fraction. This is known to be a more robust approach to phase-change than that of solely ramping the viscosity.

In addition, massively parallel computing has allowed particle level simulations, based on the boundary element method (BEM), with up to a thousand particles. These simulations were used to determine the magnitude of the normal stresses developing from particle interactions. Currently they are being use, as well, to develop more accurate hindered settling functions for particles interacting with other types of particles or in a porous medium. These simulations lead to detailed information on individual particle

and fluid motion that is unobtainable through experiments. In addition, a multipole-accelerated boundary element method (BEM) has been developed to simulate many thousands of individual interacting particles. Three-dimensional simulations are now possible for dynamically interacting particles.

## **GRANTEE: UNIVERSITY OF UTAH**

Department of Geology and Geophysics  
135 S. 1460 S.  
Salt Lake City, Utah 84112-0101

**Grant:** DE-FG03-00ER15043

### **A Comparative Study of the Feasibility for CO<sub>2</sub> Sequestration in Faulted and Fractured Sandstones in Eolian and Fluvial Deltaic Deposits**

*Craig Forster, 801-581-7162, 801-581-7065, cforster@geofluid.esri.utah.edu; J. P. Evans Utah State Univ, jpevans@cc.usu.edu*

**Objectives:** The goals of this integrated project are to complete a reservoir characterization of faulted Aeolian Jurassic Navajo Sandstone, and the Ferron Sandstone in Central Utah, in order to determine its feasibility as a long-term sequestration site for CO<sub>2</sub>-charged fluids. This project is a collaboration between Utah State University and the University of Utah, and the following is a summary of the entire project work performed to date. The Utah State group is working on reservoir characterization issues, while the University of Utah group is examining the geochemistry of the system and will perform flow models of the candidate sites. In addition, we examine faults of the Colorado Plateau along which CO<sub>2</sub>-charged springs, geysers, and travertine deposits are common, in order to evaluate how a CO<sub>2</sub> storage site might fail.

**Project Description:** We have used a multi-scale, multifaceted approach to determine the hydraulic structure of a fault zone in aeolian sandstone. We have shown that identifying the fault zone components and their properties are important in determining the bulk hydraulic properties of the fault zone. In this section, we summarise the key results from the Big Hole fault drilling project.

**Results:** By careful observations of core, minipermeameter tests, permeability tests at confining pressures, and an analysis of the bulk permeability of the faulted volume, we show that a four-component system best represents the structure of the Big Hole fault.

The host rock exhibits considerable variability in properties, despite being within one unit of aeolian sandstone. We have characterised four main sub-facies within the Navajo Sandstone, each with distinct petrophysical properties.

Deformation bands are zones of cataclasis, rarely more than a few mm's wide that accommodate mm's to cm's of slip.

Slip-surfaces are planes upon which the majority of the slip (strain) has been taken up within zones of deformation bands. At the surface, they are usually planes of parting; within our core samples, they may be planes of parting or mated surfaces. Thus, the permeability significance is poorly understood. They have previously been modelled as high permeability features.

The fault core consists of tightly packed deformation bands and highly crushed rock with a very low overall porosity (down to 1%, Shipton, 1999; Shipton and Cowie, in press). The width of the fault core is highly variable both along strike and down dip, and cannot be correlated with the displacement on the main fault.

We estimate the transverse bulk permeability of the fault zone to be 7-57 md for the faults sampled by our boreholes. Sensitivity analyses shows that bulk fault zone permeability is most dependant on the thickness of the amalgamated deformation bands and slip surfaces that make up the fault core, suggesting that where present, such fault cores should be identified and thicknesses estimated for use in reservoir simulators. Our data also indicate that thicknesses of the fault core may vary *in situ*, and do not correlate with the amount of slip.

The fault core and fault zone cluster thickness exhibit no correlation with the amount of slip on the fault. However damage zone thickness, as determined from the first deformation band recognized in the hanging wall through the ends of the drill holes varies from 10 to 24 m, does correlate with the amount of displacement. For our data set, this relationship would predict that the fault should be about 4.7 cm thick at site 2 where the fault has 8 m of slip; and at site 1 with approximately 3 m of slip, the fault should be only 1.8 cm thick. Clearly, caution should be used when applying “global” data sets to specific cases, and it may be more accurate to restrict the use of such relationships to the specific rock types and geologic settings under consideration (Evans, 1990). We do not examine the effects of changes in continuity of the fault structure in this paper (*cf.*, Antonellini and Aydin, 1994; Hesthammer and Fossen, 2000). However, we do recognize the importance of variations in fault architecture parallel to the fault plane (see section 2). The *in situ* flow tests show that such variations may significantly alter the macroscopic hydrologic properties of the fault zone.

We examine evidence for long-term leakage from natural CO<sub>2</sub> reservoirs in southeastern Utah. CO<sub>2</sub>-charged springs and geysers are localised along fault zones throughout the region, and have deposited travertines, some of which may be as old as 200,000 years. These are either natural springs or springs that were induced by recent drilling. The faults cut siltstones, shales, and sandstones, and their outcrop appearance suggests they should be effective barriers to cross-fault flow (fine grained, clay-rich fault gouge). Abundant large calcite veins cut the faults, suggesting that fluid pressures in the past were high enough to rupture the faults. The spring waters are highly saline and high in Na, Cl, Ca, and dissolved CO<sub>2</sub>. Modelling of the water chemistry indicates that the water is either saturated or supersaturated in aragonite, calcite, dolomite, fluorite and gypsum, all of which are observed in the veins along the faults, and that the water from both areas is likely to have come from organic decomposition of a sequence of marine evaporates at depth. Preliminary isotopic data from calcite veins show that the veins are highly enriched in <sup>13</sup>C. This can only be explained if the veins have a fluid source in Palaeozoic marine rocks. The heavy  $\delta^{13}\text{C}$  values provide further evidence for thermal decomposition of organic material or development of methane. Structural analyses of the system show that the faults sole into Pennsylvanian salt beds 2-3 km deep. This suggests that the spring waters are sourced in Palaeozoic rocks and flow along the faults to the surface. Past evidence for rupture of the fault seals indicates that reservoir pressures may exceed lithostatic pressure, causing the reservoir to leak repeatedly over time. These data indicate that injection of CO<sub>2</sub> -rich fluids into geologic reservoirs must be carefully designed and monitored to avoid slow seepage or fast rupture to the biosphere.

## **GRANTEE: UNIVERSITY OF UTAH**

Department of Geology and Geophysics  
135 S. 1460 S.  
Salt Lake City, Utah 84112-0101

**Grant:** DE-FG03-93ER14313

### **High Resolution Imaging of Electrical Conductivity using Low-Frequency Electromagnetic Fields**

*Alan C. Tripp, 801-462-2112 or 801-587-9856, fax 801-581-7065; actripp@mines.utah.edu*

**Objectives:** The project seeks to determine means of increasing the resolution of low frequency electromagnetic techniques by means of an optimal use of *a-priori* information

**Project Description:** The research concentrates on enhancing the resolution of EM probing without sacrificing depth of investigation through better understanding the nature of the EM response and its relationship with other sources of geological information. This is accomplished through:

*1) Improvement of Modeling Algorithms:*

Forward and inverse modeling algorithms of increasing power and versatility permit subtle data features to be modelled, thus increasing the amount of resolution provided by a given data set.

*2) Knowledge Adaptive EM Survey Design:*

EM experimental design should use the known conductivity structure to optimize resolution of the unknown target. Borehole information, baseline data, or hypothesized structure can all be used to optimize source waveforms, array weighting, or array phasing.

*3) Solution Space Characterization:*

Geophysical targets should be refined as much as possible using independent geological or engineering information.

**Results:** In the past year we have extended our investigations of knowledge - adaptive EM probing to include the probing of fractal conductivity structures. The research strategy is to find representations of fractal conductivity distributions whose EM response can be calculated in an efficient manner, and then to investigate the relationship of the EM response of these fractal conductivity distributions to the fractal geometry. The goal is to establish how much information can be derived ultimately about petrophysical structure from borehole induction studies. This investigation has relevance to any process in which petrophysical correlation of an EM response to electrical conductivity and permeability is important, particularly in a fractured environment.

To date we have established a theoretical framework for approximate forward and inverse modeling for active sources and plane waves of media whose conductivity profile is fractal in one direction. Our research continues into modeling the response of tensor fractal conductivities. We are also examining the concept of optimized fractal antennas for petrophysical probing from a borehole.

In other work, we have continued the modeling of triaxial inductive logging, including "on the fly" source array focusing. Integral equations modeling demonstrates that conductive boreholes indeed obscure the response of fracture structures in formation, but adaptive focusing can enhance the response for source arrays.

## **GRANTEE: UTAH STATE UNIVERSITY**

Department of Geology  
Logan, UT 84322-4505

**Grant:** DE-FG03-00ER15042

### **A Comparative Study of the Feasibility for CO<sub>2</sub> Sequestration in Faulted and Fractured Sandstones in Eolian and Fluvial Deltaic Deposits**

*J. P. Evans 801-797-2826, fax 801-797-1588, jpevans@cc.usu.edu; Craig Forster, Univ. of Utah; cforster@geofluid.esri.utah.edu*

**Objectives:** The goals of this integrated project are to complete a reservoir characterization of faulted Aeolian Jurassic Navajo Sandstone, and the Ferron Sandstone in Central Utah, in order to determine its feasibility as a long-term sequestration site for CO<sub>2</sub>-charged fluids. This project is a collaboration between Utah State University and the University of Utah, and the following is a summary of the entire project work performed to date. The Utah State group is working on reservoir characterization issues, while the University of Utah group is examining the geochemistry of the system and will perform flow models of the candidate sites. In addition, we examine faults of the Colorado Plateau along which CO<sub>2</sub>-charged springs, geysers, and travertine deposits are common, in order to evaluate how a CO<sub>2</sub> storage site might fail.

**Project Description:** We have used a multi-scale, multifaceted approach to determine the hydraulic structure of a fault zone in aeolian sandstone. We have shown that identifying the fault zone components and their properties are important in determining the bulk hydraulic properties of the fault zone. In this section we summarise the key results from the Big Hole fault drilling project.

**Results:** By careful observations of core, minipermeameter tests, permeability tests at confining pressures, and an analysis of the bulk permeability of the faulted volume, we show that a four-component system best represents the structure of the Big Hole fault.

The host rock exhibits considerable variability in properties, despite being within one unit of aeolian sandstone. We have characterised four main sub-facies within the Navajo Sandstone, each with distinct petrophysical properties.

Deformation bands are zones of cataclasis, rarely more than a few mm's wide that accommodate mm's to cm's of slip.

Slip-surfaces are planes upon which the majority of the slip (strain) has been taken up within zones of deformation bands. At the surface, they are usually planes of parting; within our core samples, they may be planes of parting or mated surfaces. Thus, the permeability significance is poorly understood. They have previously been modelled as high permeability features.

The fault core consists of tightly packed deformation bands and highly crushed rock with a very low overall porosity (down to 1%, Shipton, 1999; Shipton and Cowie, in press). The width of the fault core is highly variable both along strike and down dip, and cannot be correlated with the displacement on the main fault.

We estimate the transverse bulk permeability of the fault zone to be 7-57 md for the faults sampled by our boreholes. Sensitivity analyses shows that bulk fault zone permeability is most dependant on the

thickness of the amalgamated deformation bands and slip surfaces that make up the fault core, suggesting that where present, such fault cores should be identified and thicknesses estimated for use in reservoir simulators. Our data also indicate that thicknesses of the fault core may vary *in situ*, and do not correlate with the amount of slip.

The fault core and fault zone cluster thickness exhibit no correlation with the amount of slip on the fault. However damage zone thickness, as determined from the first deformation band recognized in the hanging wall through the ends of the drill holes varies from 10 to 24 m, does correlate with the amount of displacement. For our data set, this relationship would predict that the fault should be about 4.7 cm thick at site 2 where the fault has 8 m of slip; and at site 1 with approximately 3 m of slip, the fault should be only 1.8 cm thick. Clearly, caution should be used when applying “global” data sets to specific cases, and it may be more accurate to restrict the use of such relationships to the specific rock types and geologic settings under consideration (Evans, 1990). We do not examine the effects of changes in continuity of the fault structure in this paper (*cf.*, Antonellini and Aydin, 1994; Hesthammer and Fossen, 2000). However, we do recognize the importance of variations in fault architecture parallel to the fault plane (see section 2). The *in situ* flow tests (section 6) show that such variations may significantly alter the macroscopic hydrologic properties of the fault zone.

We examine evidence for long-term leakage from natural CO<sub>2</sub> reservoirs in southeastern Utah. CO<sub>2</sub>-charged springs and geysers are localised along fault zones throughout the region, and have deposited travertines, some of which may be as old as 200,000 years. These are either natural springs or springs that were induced by recent drilling. The faults cut siltstones, shales, and sandstones, and their outcrop appearance suggests they should be effective barriers to cross-fault flow (fine grained, clay-rich fault gouge). Abundant large calcite veins cut the faults, suggesting that fluid pressures in the past were high enough to rupture the faults. The spring waters are highly saline and high in Na, Cl, Ca, and dissolved CO<sub>2</sub>. Modelling of the water chemistry indicates that the water is either saturated or supersaturated in aragonite, calcite, dolomite, fluorite and gypsum, all of which are observed in the veins along the faults, and that the water from both areas is likely to have come from organic decomposition of a sequence of marine evaporates at depth. Preliminary isotopic data from calcite veins show that the veins are highly enriched in <sup>13</sup>C. This can only be explained if the veins have a fluid source in Palaeozoic marine rocks. The heavy δ<sup>13</sup>C values provide further evidence for thermal decomposition of organic material or development of methane. Structural analyses of the system show that the faults sole into Pennsylvanian salt beds 2-3 km deep. This suggests that the spring waters are sourced in Palaeozoic rocks and flow along the faults to the surface. Past evidence for rupture of the fault seals indicates that reservoir pressures may exceed lithostatic pressure, causing the reservoir to leak repeatedly over time. These data indicate that injection of CO<sub>2</sub> -rich fluids into geologic reservoirs must be carefully designed and monitored to avoid slow seepage or fast rupture to the biosphere.

## **GRANTEE: UTAH STATE UNIVERSITY**

Department of Mathematics and Statistics, and  
Department of Geology  
Logan, UT 84322-4505

**Grant :** DE-FG03-95ER14526

### **Growth of Faults and Scaling of Fault Structure**

*J. P. Evans, 801-797-2826, fax 801-797-1588, jpevans@cc.usu.edu; K. Hestir 801-797-2826, fax 801-797-1822, hestir@sunfs.math.usu.edu; S. Martel, University of Hawaii, 808-956-7797, fax 808-956-5512, martel@soest.hawaii.edu; J.C.S. Long, University of Nevada at Reno, 702-784-6987, fax 702-784-1766, jcslong@mines.unr.edu*

**Objectives:** We examine faults up to 10 km long in two localities to determine how fault structure scales, and develop a mechanically based stochastic model of fault growth that appears to represent the structure of faults, when conditioned by the field data and understanding of the three-dimensional mechanics of the faults.

**Project description:** Left-lateral strike slip faults in the central Sierra Nevada have long been used as a natural laboratory for the study of fault mechanics (Segall and Pollard, 1983; Martel et al., 1988, Martel, 1990). We examined faults that have 10's cm of slip and have trace lengths of 10's m to faults up to 10 km long and that have over 100 m of slip in order to determine the processes of fault growth near the base of the seismogenic zone. We also develop methods to invert structural data in order to infer the three-dimensional structure of the faults.

**Results:** *Small fault data:* Field mapping of small-displacement, well-exposed faults in granitic rocks of the Sierra Nevada, California, provide data on the three-dimensional structure of faults. The faults have up to 1 m of slip, formed at depths of 8-15 km, and represent brittle faults that formed at the earliest stages of development. The small faults are characterized by quartz-epidote-chlorite mineralization on narrow slip surfaces with numerous faults and fractures at fault tips. Splays in the tip regions have abundant quartz-epidote-chlorite mineralization. Data on the length, shape, orientation, and density of the splay faults show that the splays are planar fractures whose trace lengths do not exceed 10 – 20 % of the starting fault trace. Angles between the splays and the starting fault range between 35-45°. Inversion of the data using a stochastic method of conditional coding which creates models based on field data and mechanics indicates that the small faults can be modeled as a circular starting crack with an annular ring of cohesion that is 5-10% of the diameter of the fault. Splay faults within the cohesive zone are best represented as planar faults whose length is a function of the position along the tip line of the fault. This cohesive zone may represent the cohesive or breakdown zone on faults that slip seismically, and thus, these faults reflect the geometry and composition of dynamic crack propagation and arrest.

*Large faults:* Field-based structural analysis of the exhumed, 10 km-long Gemini and Glacier lakes strike-slip fault zones elucidates processes of growth, linkage, and termination for moderately sized strike-slip fault zones in granitic rocks. The Gemini fault zone is a 9.3 km-long left-lateral fault system that was active at depths of 8-11 km within the transpressive Late-Cretaceous Sierran magmatic arc. The fault zone cuts four granitic plutons and is composed of three steeply dipping northeast- and southwest-striking noncoplanar segments that nucleated and grew along preexisting cooling joints. The

fault core is bounded by sub-parallel fault planes that separate highly fractured epidote-, chlorite-, and quartz-breccias from undeformed protolith. The displacement-distance profile shows that the Gemini fault zone is segmented into three 2-3 km-long segments by two zones of displacement minima. Displacement is highest (131 m) on the western third of the fault zone and tapers to zero at the eastern termination. Slip vectors plunge shallowly west-southwest and show significant variability along strike and across segment boundaries. Four types of microstructures reflect thermal and compositional changes along strike, and show that deformation was concentrated on narrow slip surfaces at, or below, greenschist facies conditions. Taken together, we interpret the fault zone to be a segmented, hard-linked fault zone in which geometrical complexities of the faults and compositional variations of protolith and host rock resulted in non-uniform slip orientations, complex fault segment interactions, and asymmetric displacement-distance profiles.

*Slip Localization:* Our examination of small individual faults reveal that, similar to other workers, the fault surfaces are marked by foliated chlorite-epidote-quartz zones. In detail, the microstructures of the small faults reveal the evolution from brittle Mode I fracture filled by chlorite, epidote, and quartz to brittle fracture and cataclastically deformed rocks to the development of very fine-grained cataclasites and ultracataclasites. The initial shear-induced microstructures are developed on faults with as little as several mm of slip, and the transition to the foliated textures may occur for as little as 10-20 cm of slip. Fault surfaces with chlorite-epidote-quartz assemblages display a strongly developed foliation foliated texture and what appear to be thin dark regions that represent a narrow slip zone.

We have also conducted whole-rock geochemical analyses of these small faults, and the data show that these small faults exhibit subdued, but notable changes similar to those observed in much larger faults. The small faults exhibit a 1-3 wt % reduction in  $\text{SiO}_2$ , small increases in  $\text{MgO}$ ,  $\text{CaO}$ , and  $\text{TiO}_2$ . Similar, but much larger, changes have been documented for faults of the SAF system (Evans and Chester, 1995) and are interpreted to be the result of reactions that take place in the fault zone while it is active. These reactions are reaction-softening reactions that transform feldspars to micas and hornblende and biotite to chlorite.

These microstructures are remarkably similar to the much larger faults, such as those seen on the San Gabriel and Punchbowl faults, where displacements are up to 44 km. With only 1 m of slip, the Sierran faults exhibit very fine-grained dark cataclasite fault rocks with opaque matrix, and often develop the thin slip surfaces several mm thick. We draw an analogy with the direct shear experiments in which well developed shear fabrics form with only mm of displacement, and subsequent slip is often accommodated by the development of stable microstructures that include foliated cataclasites and ultracataclasites, and the creation of a narrow slip zone, typically at the margin of the small fault. Experiments of shearing of phyllosilicate-rich gouge in an environment where slip in phyllosilicates and pressure solution is promoted also show that slip may be localized very early in the history of the system, and leads to a strain weakening response. We suggest that slip in faults that form at depths of 4-13 km, in a wet environment, seems to localize very early, and strain-softening mechanisms associated with hydrothermal and reactive fluids may be activated in the earliest stages of faulting.

## **GRANTEE: VIRGINIA POLYTECHNIC INSTITUTE & STATE UNIVERSITY**

Fluids Research Laboratory  
Department of Geological Sciences  
Blacksburg, Virginia 24061

**Grant:** DE-FG05-89ER14065

### **Experimental Studies in the System H<sub>2</sub>O-CH<sub>4</sub>-“Petroleum”-Salt Using Synthetic Fluid Inclusions**

*R. J. Bodnar, 540-231-7455, fax 540-231-3386, bubbles@vt.edu*

**Objectives:** The objective of this project is to experimentally determine the pressure-volume-temperature-composition (PVTX) relationships of fluids in the C-O-H-NaCl system over the complete range of PTX conditions encountered in crustal energy, resource and hazardous waste-related environments. These data are used to develop equations of state to predict the behavior of fluids during crustal water-rock interactions.

**Project Description:** Volumetric (PVT) data provide the fundamental information needed to understand the physical and chemical behavior of fluids in shallow crustal environments. These data represent the basis for developing empirical or theoretical equations of state to predict the thermodynamic properties of fluids over crustal PTX conditions. In this study the PVTX properties of fluids in the C-O-H-NaCl system are being experimentally determined using the synthetic fluid inclusion technique as well as a newly designed high-pressure cell for use on the Raman microprobe. These combined techniques permit determination of phase equilibria and PVT properties of fluids over a wide range of PTX conditions.

**Results:** Significant progress has been made in the following areas:

*Development of a numerical model for methane solubility in water.* One of the goals of this research is to develop a quantitative model that can be used to interpret results from fluid inclusions from petroleum and natural gas environments. We have developed a numerical model based on the compilation of Haas (1978) for methane solubility in water and brines. This model calculates the pressure corresponding to a given temperature and methane concentration.

*Quantitative analysis of H<sub>2</sub>O-CH<sub>4</sub> fluid inclusions using Raman spectroscopy.* In order to use the numerical model for methane solubility described above, it is necessary to know the concentration of methane in a fluid inclusion. We have developed a technique based on the Raman spectrum that allows the composition of aqueous methane-bearing inclusions to be determined non-destructively, using the measured peak areas for the methane and water bands.

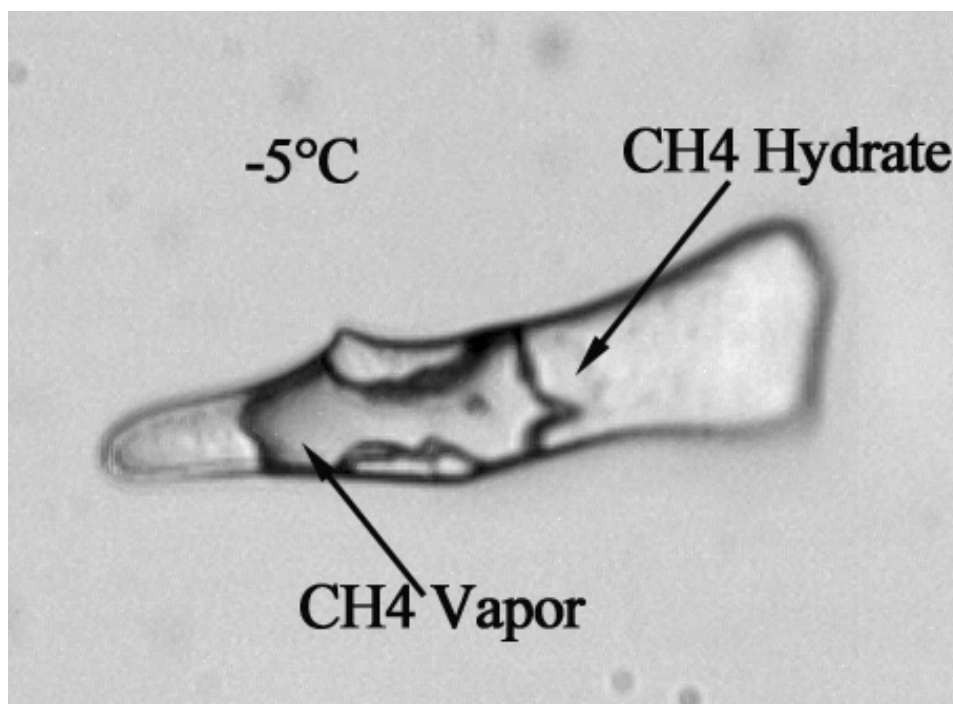
*Determination of pressure (depth) of hydrocarbon trapping based on Raman analysis of CH<sub>4</sub>-bearing aqueous inclusions.* One of the most poorly constrained variables in petroleum exploration is the pressure (or depth) at which petroleum generation, migration and accumulation occurred. Combining results from (1) and (2) above, we have developed a procedure to determine the pressure at homogenization of methane-bearing fluid inclusions in natural samples. The model has been tested using synthetic fluid inclusions of known composition and trapping temperature and pressure, and used to interpret results from natural inclusions from petroleum basins in which the history is well-known.

The results are in good agreement and confirm that the model can be used to constrain the pressure in hydrocarbon environments.

*Determination of methane clathrate stability relations in aqueous solutions using Raman spectroscopy.*

Methane hydrate research has increased significantly in the past decade owing to the potential contributions to the world's energy supply by methane hydrate, as well as by recent reports that methane is a major contributor to global warming. Methane hydrate has also been invoked to explain geologically recent climate fluctuations and has even been suspected as the cause of mysterious disappearances of ships at sea. Using synthetic  $\text{H}_2\text{O}-\text{CH}_4$  fluid inclusions (see figure below) and Raman spectroscopy, we have confirmed the P-T stability limits of methane hydrate over a wide range of conditions. Having documented that the technique is valid for determining methane hydrate stability, this work is being extended to include the complete range of aqueous fluid compositions expected in submarine and permafrost regions of the earth.

**Figure:** Synthetic inclusion containing  $\text{H}_2\text{O}-\text{CH}_4$  showing methane vapor, methane hydrate and ice at  $-5^\circ\text{C}$ . The inclusion is about 25 microns long.



## **GRANTEE: VIRGINIA POLYTECHNIC INSTITUTE & STATE UNIVERSITY**

Department of Geological Sciences  
NanoGeoscience and Technology Laboratory  
Blacksburg, Virginia 24061

**Grant:** DE-FG02-99ER15002

### **Microbial Community Acquisition of Nutrients from Mineral Surfaces**

*M. F. Hochella, Jr., 540-231-6227, fax 540-231-3386, hochella@vt.edu; D. Berry, M. Eick, Dept. of Crop and Soil Environmental Sciences; J. Little, Dept. of Civil and Environmental Engineering; M. Potts, Dept. of Biochemistry; C. Tadanier, Dept. of Geological Sciences*

**Objectives:** Minerals and microbes undergo complex interactions in nature that impact broad aspects of near-surface Earth chemistry. Our primary objective in this project is to gain insight into how microbial communities acquire critical but tightly held nutrients residing on or within minerals common in soils.

**Project Description:** The overall purpose of this project is to search for and delineate fundamental physiological strategies and/or environmental conditions by which microbial consortia, as a collection of taxa, mediate release of strongly bound nutrients/contaminants from mineral surfaces. The underlying hypothesis is that microbial consortia employ specific physiological strategies and/or take advantage of specific environmental circumstances that result in release of chemical components tightly bound to mineral surfaces. This is being studied using a model nutrient-mineral system of orthophosphate sorbed to goethite in the presence of a soil derived microbial consortium. Experiments involving this model system are run in chemostat bioreactors, and various aspects of the system are being characterized by scanning probe and scanning laser confocal microscopies, molecular biochemistry, and mineral surface/aqueous geochemistry.

**Results:** We have now run a few long-term (several weeks to two months) chemostat experiments using a soil inoculum and synthetic goethite with sorbed orthophosphate. In these runs, we determined that the consortium utilized about 80% of the sorbed phosphate during the four-day hydraulic retention time in the chemostat. A low molecular-weight organic acid produced by one or more members of the consortia was tentatively identified as citric or gluconic acid. Goethite was also reductively dissolving, and it aggregated at low glucose concentrations in the chemostat bioreactor.

Methods were optimized to allow direct extraction of DNA from microorganisms in our soil inoculum and chemostat effluent. The dominant player in our chemostat runs was identified as *Burkholderia cepacia*. We are currently developing and testing a 16S rRNA probe specific to this species so that we can use scanning laser confocal microscopy to help track its role in the phosphate extraction process.

We also continued to develop biological force microscopy, a variation of atomic force microscopy. Native cells are linked to an atomic force cantilever that in turn is used to measure the forces between the cells and mineral surfaces. The measurements, which are performed in solution, are quantitative down to the nanoNewton range over distances of zero (contact) to hundreds of nanometers.

## **GRANTEE: UNIVERSITY OF WASHINGTON**

Department of Earth and Space Science  
Box 351650  
Seattle WA 98195

**Grant:** DE-FG03-99ER14976

### **Two and Three-dimensional Magnetotelluric and Controlled Source Electromagnetic Inversion**

*J. R. Booker, 206-543-9492, fax 206-543-0489, booker@geophys.washington.edu; M. Unsworth, 780-492-3041, fax 780-492-0714, unsworth@Phys.UAlberta.CA*

**Objectives:** Develop practical algorithms for imaging multi-dimensional underground structure using natural or controlled source very low frequency electromagnetic energy. Emphasis is on implementations suitable for computer resources widely available.

**Project Description:** Electrical conductivity in the sub-surface depends primarily on the presence of ionic fluids and metallic films or objects. Imaging electrical conductivity structure has applications in the exploration for water, where it is particularly sensitive to quality, temperature and permeability, for minerals, where it is directly sensitive to the target and for petroleum, where conductivity (or its lack) is diagnostic of trapping structure such as salt, volcanics and limestone that are often difficult to penetrate with seismic energy. Electrical conductivity is particularly useful in a wide variety of waste remediation targets and in the determination of permeability in reservoir rocks. Determining conductivity in the subsurface is a problem in electromagnetic (EM) remote sensing with deeper targets requiring lower frequency. The EM signal can be natural, or in noisy industrial situations, may be artificial. If both electric and magnetic fields are measured, the data are termed magnetotelluric (MT). Modern understanding of sub-surface structure has made evident its fundamental three-dimensional (3D) character. Recent developments in equipment make it possible to collect MT data on dense surface grids. However, the inverse problem of extracting 3D structure from such data is computationally formidable even with the largest and fastest modern computers. Such resources are not often available to industrial contractors and certainly not appropriate in the field, where imaging can result in important feedback to the data collection process. This has led to the search for algorithms that can fully invert the data, but require very small fractions of the computer resources that standard approaches entail. Our basic approach involves approximate iterative schemes that have the property that their error goes to zero as convergence is approached.

**Results:** In the past year, work was completed on an implementation of the magnetotelluric (MT) Rapid Relaxation Inverse (RRI) for three-dimensional (3D) structure using a magnetic field finite difference implementation of the forward problem. To test this inversion, we developed several noisy data sets for known structure with increasingly strong 3D effects. We have provided these to other people working on 3D inversion. 3D RRI works extremely well when the data are collected on a 2D grid of closely spaced sites. It has difficulty when site spacing increases or consists of widely spaced profiles. RRI requires interpolation of structure between sites and profiles. Schemes that do 3D interpolation properly computationally overwhelm the efficiency of RRI. We recognized this difficulty in our original proposal and it remains to be solved. A strong competitor for RRI is Conjugate Gradient (CG) inversion, which does not require the problematic interpolation step. Theoretically, CG requires only twice as many forward problems and thus should take only twice as long. However, experiments with an existing

implementation of CG concluded that it was 20 times slower for a real data set and could be caught in local minima of the object function, a well-known problem for RRI. We are pursuing methods to accelerate CG using techniques we found effective for RRI and are developing a hybrid RRI/CG code since the difficulties of each algorithm tend to be orthogonal.

## **GRANTEE: UNIVERSITY OF WASHINGTON**

Department of Earth and Space Science  
Box 351650  
Seattle WA 98195

**Grant:** DE-EG03-97ER-14781

### **Electromagnetic Imaging of Fluids in the San Andreas Fault**

*M. Unsworth, 206-543-4980, unsworth@geophys.washington.edu*

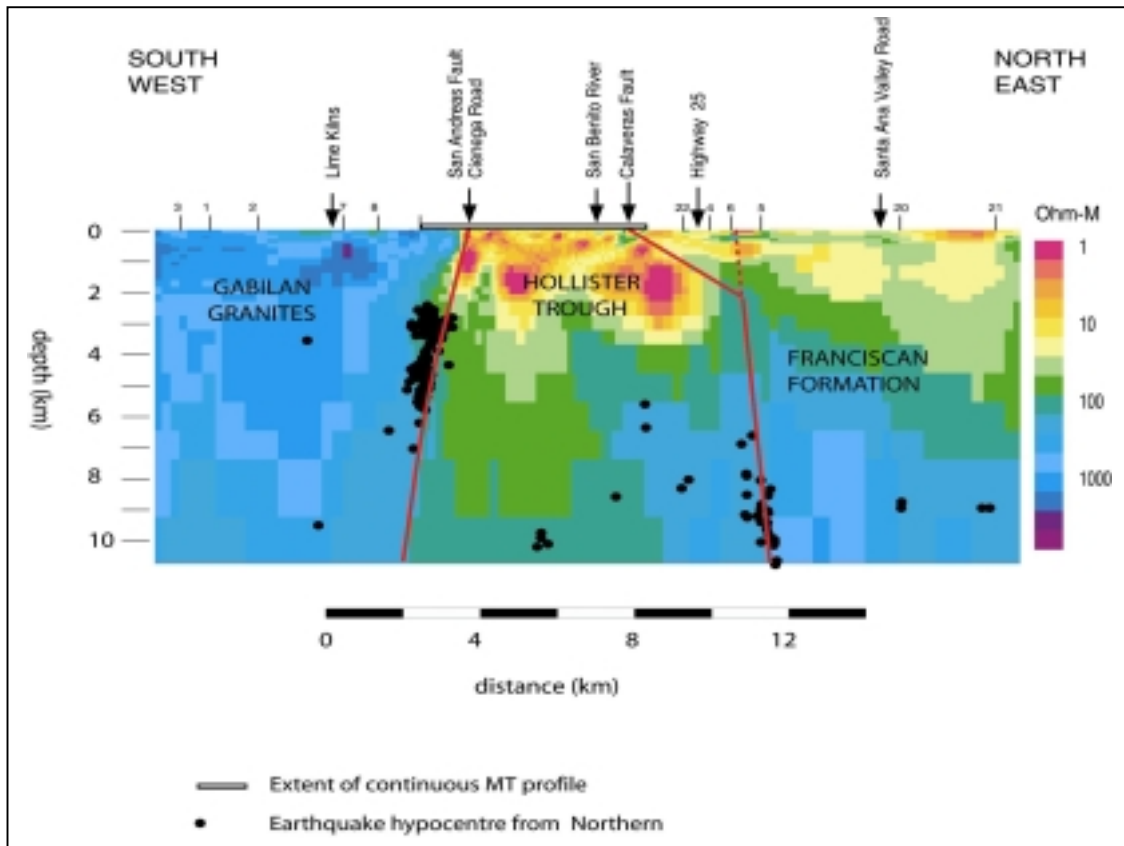
**Objectives:** To obtain high-resolution images of the electrical resistivity of the San Andreas fault (SAF) zone. This will permit the fault zone architecture and fluid distribution to be constrained.

**Project description:** There is increasing evidence that fluids may play a significant role in the earthquake rupture process. However, the difficulty of directly observing fluids in active fault zones currently limits progress in understanding these processes. Magnetotelluric (MT) data collected in 1994 at Parkfield and Carrizo Plain showed that the fault zone at these locations has very different electrical structure.

To further examine how these differences might be related to fault zone seismicity, a two-phase program of MT data acquisition and interpretation is being undertaken. In the first phase, data will be collected on additional profiles across the SAF at Middle Mountain, Parkfield to obtain a three-dimensional image of the electrical resistivity in this area. In the second phase, a three-dimensional survey of the central creeping section of the SAF near Hollister will be undertaken.

**Results:** During this period the second phase of data acquisition took place. Magnetotelluric data were collected on two profiles that crossed the creeping section of the San Andreas Fault south of Hollister. After careful analysis to remove the effects of cultural noise, the electrical resistivity model shown in the figure on the following page was produced by inversion of the data. The following features can be observed in the model

1. The San Andreas Fault forms a steeply dipping boundary between the granites of the Gabilan Range and the lower resistivity rocks of Franciscan formation. The earthquake hypocenters are coincident with the electrically imaged fault.
2. Low resistivity units are found between the San Andreas and Calaveras Fault, extending to a depth of around 4 km. The lowest resistivities (and by inference, the highest fluid contents) are associated with the San Andreas and Calaveras Faults. As at Parkfield, the active fault trace is found on the edge of the low resistivity fault zone in the upper 3 km.
3. As at Parkfield, the conductive feature in the shallow structure is probably due to a zone of fractured rock, permeated with saline groundwater. This appears to be common to all locations at which the fault is creeping. The origin of the groundwater is uncertain. It may have an origin in the deep crust, or could be due to infiltration from the surface.
4. A zone of low resistivity is located between the San Andreas and Calaveras faults. The precise location of the surface trace of the Calaveras Fault, and its relationship to the resistivity anomaly is being investigated.



**GRANTEE: UNIVERSITY OF WISCONSIN**

Department of Civil and Environmental Engineering  
Madison, Wisconsin 53706

**Grant:** DE-FG02-99ER14995

**Three Dimensional Transient Electromagnetic Inversion**

*D. L. Alumbaugh, 608-262-3835, fax 608-26-2453, alumbaugh@engr.wisc.edu; G. A. Newman, Sandia National Laboratories*

**Objectives:** This project seeks to develop a three-dimensional imaging capability for transient electromagnetic fields in a manner similarly developed for seismic wavefields for high resolution imaging of the subsurface. Specific applications considered include the characterization of DOE hazardous waste sites and nuclear waste repositories and monitoring of sequestered CO<sub>2</sub> in depleted gas reservoirs.

**Project Description:** The objective of this project is to develop a full 3D inversion capability for transient electromagnetic fields. Although the development of practical multidimensional TEM inversion methods are just beginning, seismic imaging techniques have advanced the idea of back propagating or migrating the wavefield into the earth in order to image the subsurface. By applying a similar concept for electromagnetic fields, an imaging algorithm will be developed, which employs a conjugate gradient search for an optimal solution. This algorithm will be governed by the diffusive Maxwell's equations and is efficiently implemented by back propagating the data residuals into the model. To achieve realistic model complexity, the algorithm will use finite difference methods for computing predicted data and cost functional gradients. Parallel computing platforms will also be utilized for reasonable computation times. Finally, the algorithm will be tested on TEM data acquired over hazardous waste sites and nuclear waste repositories. It will also be used in an experiment design to determine its resolving power for monitoring the sequestration of CO<sub>2</sub> in gas-depleted reservoirs.

**Results:** Implementation of the 3D finite difference modeling code on single processor workstations is now completed. This code solves the diffusive Maxwell equations, in the presence of the air-earth interface, using explicit time stepping scheme and has been checked for a range of simple earth models. A borehole version of the code, which neglects that air-earth interface condition, is also available. This later code is now being employed in an experiment design study to access the applicability of TEM method for monitoring sequestered CO<sub>2</sub>. A nonlinear conjugate-gradient solution, using the finite difference code, is also under development. The code will employ back propagation to efficiently compute functional gradients. Parallelization of this code and of the finite difference solution mentioned earlier remains to be implemented.

For high-resolution TEM imaging, monitoring of the transmitter waveform is a necessity. Because the nature of current system induced in the ground depends on the transmitter turn-off time, and because an accurate inversion scheme requires a detailed knowledge of the current distribution at all times, having and accurate knowledge of the transmitter waveform will be crucial to the success of the project. To address the question of transmitter stability and waveform monitoring, we have been employing a Zonge nanoTEM system at the University of Wisconsin to test a computer controlled 'virtual oscilloscope' acquisition system produced by Pico-systems. The oscilloscope has a minimum sampling interval of 20ns which is fast enough for TEM systems that would be employed in a sequestration monitoring

scenario, and it allows for the 'captured' waveform to be written directly to lap-top computer memory. Initial testing has yielded interesting results as preliminary surveys have shown that the transmitter waveform can change significantly depending on the subsurface characteristics of the site under investigation. In this case, we tested the system over two different locations, one of which is known from a magnetometer survey to have significant amounts of metal present. The transmitter at this second site was shown to produce a significant negative side lobe in the waveform in its effort to turn off the source-current when compared to the first site. Thus, it appears that transmitter monitoring will be required for accurate 3D inversion.

## **GRANTEE: UNIVERSITY OF WISCONSIN**

Department of Geology and Geophysics  
Madison, Wisconsin 53706

**Grant:** DE-FG02-93ER14328

### **Precipitation at the Microbe-Mineral Interface**

*J. F. Banfield, 608-265-9528, fax 608-262-0693, jill@geology.wisc.edu*

**Objectives:** Microbial biomineralization can dramatically modify the distribution of metals in the environment. The goals of this research are to determine the mechanisms by which cell surfaces, enzymatic activity, and microbial byproducts impact metal speciation and induce mineral precipitation.

**Project Description:** This work focuses on biogeochemical processes in metal-contaminated environments associated with two abandoned mines. Fieldwork has been carried out in Washington, where uranium contamination of soils and sediments has occurred, and in a flooded, underground mine tunnel in SW Wisconsin, where Zn, Pb, and U contaminants are cycled across a redox boundary. We are analyzing how microbial activity in oxic and anoxic zones results in formation of metal-oxide, -sulfide, and -phosphate biominerals in proximity to, and within, cells. These precipitation reactions occur as the result of enzymatic reactions involved in energy generation, sequestration of toxic ions, and adsorption onto cell polymers. The research combines molecular biological characterization of the microbial communities, experiments involving cultured microorganisms, and high-resolution mineralogical and geochemical analysis.

**Results:** The Midnite Mine is an inactive open-pit uranium mine located northwest of Wellpinit on the Spokane Tribe Reservation, WA. Unleached ores with high uranium content remain on site and pit and ground waters are heavily contaminated with uranium in addition to heavy metals. Surface waters and sediments were collected aseptically from pit sites and the retention pond. Temperature, pH, Eh and conductivity of the water samples were measured on site. Samples were returned for the laboratory for geochemical and mineralogical characterization, DNA extraction for DNA sequence-based identification of members of microbial communities, microbial cultivation, and isolation of uranium-resistant species. The site allows the evaluation of long-term interactions between microbial communities and metals necessary to validate results of our short-term laboratory studies.

In the laboratory work conducted in the past 12 months, we have obtained 16S rRNA sequence for microorganisms in samples from pit sediments. Five isolates from the site, plus 2 reference strains, *Escherichia coli* and *Deinococcus radiodurans*, were tested for their ability to accumulate U. Cultures were incubated in 80 ppm of U nitrate solution at pH 4. Colony forming units (CFU) inoculated in experimental solutions and CFU active after incubation with and without uranium were counted and compared. Transmission electron microscopy (TEM) was used to determine the location of uranium within the bacterial cells. Energy-dispersive spectroscopic analysis was carried out to characterize elemental compositions of uranium phases. Isolate S2 closely related to *B. pumilis* and *B. subtilis*, takes up 160.94 mgU/g dry cells, whereas *E. coli* accumulated 112.18 mgU/g dry cells. However, the bacteria became inactive after incubation with uranium. *D. radiodurans*, the most radiation-resistant organism known, precipitated uranyl phosphate crystals outside the outer membrane. However, only 20% of the cells were viable after incubation with uranium. Eighty-nine percent of isolate S3 cells, closely related to *Arthrobacter ilicis*, was active after incubation with uranium. TEM observation and EDS

analysis revealed that uranium in *Arthrobacter* isolate S3 is concentrated in intracellular granules containing phosphorous and calcium. Mineralogical characterization *via* electron diffraction and synchrotron-based X-ray analysis is underway. *Arthrobacter* spp. are remarkably resistant to desiccation, starvation, and in some cases, radiation, and can degrade aromatic compounds and humic substances. Thus, this organism may be suitable for bioremediation of actinide-contaminated sites.

Research conducted at the Tennyson Mine has focused on microbial communities that induce the precipitation of essentially pure ZnS from dilute groundwater solutions (< 3 ppm Zn). Extensive mineralogical and biological characterization and geochemical modeling has been completed. Our results demonstrate that anaerobic respiration leads to build up of sulfide concentrations in proximity to the cell, resulting in supersaturation with respect to ZnS and precipitation of 1- 3 nm diameter particles consisting of sphalerite+wurtzite. The ZnS contains 0.009 wt % As and 0.004 wt% Se. The Zn and As are concentrated by a factor of  $\sim 10^5$ - $10^6$  times relative to solution. The ZnS nanoparticles flocculate to form spherical, micron-scale aggregates. Within the aggregates, crystal growth appears to proceed primarily via oriented aggregation. Sulfate-reducing microorganisms detected by sequencing of 16S rRNA genes from organisms in the biofilm are phylogenetically placed within the *Desulfobacteriaceae*. *In situ* hybridization of group specific oligonucleotide probes to mineralized cells in biofilm samples confirmed that these organisms are associated with sulfate-reduction and mineral precipitation. Cultures of sulfate-reducing bacteria induce exclusive precipitation of ZnS from Fe-Zn-sulfate solutions under moderately anaerobic conditions.

Organic compounds necessary to sustain the sulfate-reducing bacteria are released by adjacent communities of anaerobic fermentative bacteria that degrade cellulose in mine timbers. We have modeled the geochemical changes induced by release of organics and the resulting production of sulfide. Results demonstrate that monomineralic ZnS precipitation is expected from these solutions. Precipitation of ZnS titrates out all sulfide released, preventing the decrease in redox potential necessary to saturate the solution with a second metal sulfide compound. In the environment, Zn is continuously supplied by slow groundwater flow, so other sulfides never form. The redox condition determined by ZnS formation selects for (and is set by) a microbial community able to tolerate relatively oxidizing conditions. Ongoing work is testing the predictions made by this model for their relevance to groundwater treatment and ore deposit formation.

The fate of Zn, U, and Pb in the more aerobic groundwater regions is controlled largely by microbially produced ferric iron oxyhydroxides. Initial geochemical and mineralogical studies indicate that U and Pb and Zn are in solid solution, and Zn is surface adsorbed. These ions are released by microbially controlled reductive dissolution of the ferric iron minerals.

## GRANTEE: UNIVERSITY OF WISCONSIN

Department of Materials Science and Engineering  
Madison, WI 53706

**Grant:** DE-FGO2-98ER14850

### Deformation and Fracture of Poorly Consolidated Media

*B. C. Haimson, 608-262-2563, fax 608-262-8353, haimson@enr.wisc.edu*

**Objectives:** The objective of this research is to investigate the process of hydraulic fracturing and of borehole breakout formation in high porosity sandstones. Specifically we investigate the potential mechanisms leading to these two types of borehole failure, with the practical goal of establishing whether they can serve as *in situ* stress indicators in granular rocks.

**Project description:** For borehole breakout studies we employ a specially fabricated biaxial loading cell mounted inside a compression loading machine, which allow us to carry out drilling of axial boreholes (diameters of 14–40 mm) in rock blocks (150×150×230 mm) already subjected to a state of true triaxial *in situ* stress. Berea sandstone of various porosities, other sandstones, and artificial granular material of high porosity are tested. For hydraulic fracturing experiments we use cylindrical rock specimens (100 mm dia.×150 mm long) mounted in a triaxial vessel through which we apply lateral and axial loads, as well as pore pressure and borehole fluid pressure.

**Results:** *Borehole Breakouts.* We induced borehole breakouts in a 25%-porosity Berea sandstone (BSs25) by drilling 23 mm diameter holes into rectangular prismatic specimens subjected to constant true triaxial far-field stresses. BSs25 consists of large quartz grains (0.5 mm) cemented mainly by sutured grain contacts. Breakouts in BSs25 are demonstratively different from those observed in granite, limestone, and lower porosity sandstones. Rather than the typically short ‘V’-shaped breakouts, BSs25 displays long fracture-like tabular slots, which counterintuitively, develop orthogonally to  $\sigma_H$ . These breakouts originate at the points of highest compressive stress at the borehole wall, along the  $\sigma_H$  spring line. Micrographs of BSs25 breakouts show an apparent compaction band created just ahead of the breakout tip in the form of a narrow layer of grains that are compacted normal to  $\sigma_H$ . The compaction band characteristics are nearly identical to those recently observed in the field. The mechanism leading to fracture-like breakouts is seen as anti-dilatant, and related directly to grain debonding and porosity reduction accompanying the formation of the compaction band. Some compacted grains at the borehole wall are expelled because of the line of tangential loading and the radial expansion of adjacent grains. The circulating drilling fluid flushes out the remaining compacted loose grains at the borehole-rock interface. As the breakout tip advances, the stress concentration ahead of it persists, extending the compaction band, which in turn leads to additional grain removal and breakout lengthening. By extrapolation, this process may continue for considerable distance (at least several times the wellbore diameter) in field situations, leading potentially to substantial sand production.

A most remarkable finding is that fracture-like breakouts have a consistent width of 5-10 grain diameters regardless of test variables (such as far-field stress condition, borehole diameter, drilling fluid flow rate, bit penetration rate). This finding reinforces the suggestion that the fracture-like breakouts are “emptied compaction bands” (which typically are several grain diameters thick).

From initial testing of other high porosity sandstones, it appears that the creation of the compaction bands is limited to rocks in which grain cementation is primarily through sutured contacts. Other sandstones may develop long breakouts, but they are also much wider, sometimes reaching the full diameter of the borehole.

*Hydraulic Fracturing.* We carried out several series of hydraulic fracturing (HF) tests in axial holes drilled into cylindrical specimens of high porosity (29%) Tablerock sandstone (TR30). Specimens were subjected to confining pressure (simulating the far-field horizontal stress) and a vertical stress inside a pressure vessel that also enables the application of pore pressure  $P_o$ . Hydraulic oil was used as injection fluid. An acoustic emission recording system was installed for monitoring fracture initiation.

One important result was that all tests yielded vertical hydraulic fractures similar to those in crystalline rocks in which hydrofrac stress measurements are routinely performed. Fractures propagated intergranularly, often following a tortuous path seeking the weakest resistance. The breakdown pressure  $P_c$  was interpreted as the inflection point in a plot of borehole pressurization rate ( $dP/dt$ ) as a function of  $P$ . A series of tests in which  $\sigma_h$ ,  $\sigma_v$ , and  $P_o$  were kept constant revealed that  $P_c$  increased significantly with  $dP/dt$ , and appeared to asymptotically tend to an upper and lower bound corresponding to fast and slow rates, respectively. This behavior suggested that classical Hubbert and Willis, and Haimson and Fairhurst, hydraulic fracturing criteria were unsuitable for Tablerock sandstone, since they disregard the effect of pressurization rate. On the other hand, the Detournay and Cheng criterion, which incorporates that effect, was deemed an appropriate model. However, hydraulic fracturing tests for a preset pressurization rate inunjacketed specimens ( $\sigma_h = P_o$ ) revealed that  $(P_c - P_o)$  increased with confining/pore pressure, contrary to the constant  $(P_c - P_o)$  predicted by the Detournay and Cheng criterion. By adjusting this criterion so that the Terzaghi effective stress ( $\sigma' = \sigma - P_o$ ) is replaced by the more general Nur and Byerlee effective stress ( $\sigma' = \sigma - \alpha P_o$ ) (where  $\alpha$  is the Biot coefficient), and determining  $\alpha$  experimentally, the modified D-C criterion satisfactorily models the  $(P_c - P_o)$  behavior when  $\sigma_h = P_o$ . Two additional series of HF tests, one in which the only variable was  $\sigma_h$  and the other in which the only variable was  $P_o$ , reinforced the capacity of the modified Detournay and Cheng criterion to correctly estimate the far-field stress  $\sigma_h$  in Tablerock sandstone when  $P_c$ ,  $P_o$  and  $dP/dt$  are known. It thus appears that high porosity rocks such as Tablerock sandstone is amenable to the estimation of the *in situ* stress from hydraulic fracturing, provided material parameters such as the Biot constant, hydrofrac tensile strength, and initial pore pressure can be determined independently.

## **GRANTEE: UNIVERSITY OF WISCONSIN**

Department of Geology and Geophysics  
Madison, Wisconsin 53706

**Grant:** DE-FG02-93ER14389

### **Microanalysis of Stable Isotope Ratios in Low Temperature Rocks**

*J. W. Valley, 608-263-5659, fax 608-262-0693, valley@geology.wisc.edu*

**Objectives:** To further develop microanalytical techniques for stable isotope analysis and to employ them to decipher the complex effects of superimposed hydrothermal events in modern and fossil geothermal systems (Long Valley, Yellowstone, BTIP/Skye, Timber/Yucca Mtn.).

**Project Description:** This study focuses on samples of altered volcanic rocks from the Long Valley caldera, Timber Mountain caldera complex, Yellowstone, and on hydrothermally altered granites from related rocks from the British Tertiary Igneous Province (BTIP). New techniques allow analysis of stable isotope ratios in ultra-small samples of refractory and of highly reactive samples; and oxygen isotope ratio can now be contoured across single crystals. Mineral zonation patterns provide new insights into the process of water/rock interaction: mechanisms of exchange, timing, degree of equilibration, variability of fluid fluxes, and fluid sources. Enhanced understanding of these processes is essential for improving computer models of fluid flow through hot rocks.

At the Long Valley and Yellowstone, these results provide information on the nature of magma chambers at depth, the size of the modern geothermal resource, and the volcanic hazards. At Timber Mountain, the results restrict theories of ancient *vs.* on-going hydrothermal activity. On the Isle of Skye, Scotland, samples of granite from beneath an ancient, deeply eroded caldera provide further insights for active systems.

**Results:** At Long Valley, analysis of samples from additional wells has greatly expanded our coverage (from our previous study; McConnell *et al.* 1997) and extended our study to the west of the Resurgent Dome. These results document shallow lateral flow of heated meteoric waters radially outwards from the Resurgent Dome due to convection driven by post 500Ka intrusions.

At Yellowstone, 400 analyses of zircons and quartz have been made from 24 units erupted over the past 2Ma. Zircon preserves the best record of primary magmatic composition and some quartz is altered. In common with earlier studies of quartz, extreme depletions of oxygen isotope ratio occur after caldera forming eruptions. In contrast to earlier studies, analysis of zircons reveals periods of extreme disequilibrium in oxygen isotope fractionation that correlate to the periods of isotopic depletion. Some zircons were found (by air abrasion/ laser analysis and by ion microprobe), to be zoned in oxygen isotope ratio. The zonation and low oxygen isotope ratios record wholesale melting of hydrothermally altered rocks from the down-dropped cauldron after major eruptions and not assimilation as previously proposed. The shape and depth of these isotopic gradients provides a timescale for the longevity of the melt and rules out rapid or explosive processes.

Low  $\delta^{18}\text{O}$  igneous zircons have been found in rhyolites from Yellowstone (-0.4 to 5.8, Bindeman and Valley 2000 Geology, 2001 J Petrology) and the Ammonia Tanks and Tiva Canyon tuffs, Timber Mtn ( $\delta^{18}\text{O}$ =4.3, 5.7, respectively, Bindeman and Valley 2000a,b GSA). At Yellowstone, the low values are restricted to relatively small, post-caldera eruptions. These units have low  $\delta^{18}\text{O}$  quartz and zircon,

disequilibrium  $\Delta(\text{Qt-Zc})$ , and zoning of  $\delta^{18}\text{O}$  in zircon. Zircon cores are xenocrystic and normal in  $\delta^{18}\text{O}$ , while rims are low in  $\delta^{18}\text{O}$ . Estimates of zircon residence in low  $\delta^{18}\text{O}$  magma are on the order of 500-5000 years, ruling out catastrophic phreatic interactions of magma and meteoric water as have been proposed. A new model is proposed to form low  $\delta^{18}\text{O}$  rhyolites involving caldera subsidence followed by wholesale melting of the hydrothermally altered, down-dropped roof.

In the BTIP, oxygen isotope analysis of zircons from 22 rock units has shown that most granites formed from isotopically light magmas (Monani and Valley 2001 EPSL). These data document a more complex and protracted history of hydrothermal alteration and magmatic interaction than was previously detected by analysis of quartz or feldspar. Samples have been analyzed from four magmatic centers on the Isle of Skye and from other plutons of the BTIP (Arran, Mull) that stitch domains with basement ages from Archean to Phanerozoic. The evolved oxygen isotope compositions are decoupled from trends seen in Pb or Sr isotopes, do not correlate to basement, and are dominated by processes in the shallow crust.

At Timber Mountain/ Oasis Valley caldera complex, we have collected samples and separated zircons and quartz. Preliminary analysis confirms earlier reports that magmas were low in oxygen isotope ratio. While the amount of isotopic depletion is smaller, the size of the anomalous magmas is suggested to be much larger, up to 1000 cubic km. We plan to test our new model for the genesis of such magmas.

Zircons from Yucca Mtn, near Timber Mtn also provide boundary conditions for estimating post-magmatic hydrothermal alteration. Zircons were separated from carbonate fault gouge in Trench 14. The proposal of hydrothermal zircons has lead to concerns about the proposed nuclear waste repository at Yucca Mtn. The  $\delta^{18}\text{O}$  values of zircon in carbonate gouge are similar to those from adjacent Tiva and Rainier Mesa tuffs and provide no evidence of hydrothermal activity (Bindeman and Valley GSA 2000).

**GRANTEE: UNIVERSITY OF WISCONSIN**

Department of Geology and Geophysics  
Madison, Wisconsin 53706

**Grant:** DE-FG02-98ER14852

**Pore-Scale Simulations of Rock Deformation, Fracture, and Fluid Flow in Three Dimensions**

*H. F. Wang, 608-262-5932, fax 608-262-0693, wang@geology.wisc.edu*

**Objectives:** The objective is to develop a numerical, percolation model on the geologic scale for two-phase, immiscible fluid displacement in a porous medium.

**Project Description:** Two-phase displacement in a porous medium occurs in many geologic processes. Although pore scale mechanics can be readily understood in terms of the relevant viscous, capillary, and buoyancy forces, geologic scale, multiphase flows (large and slow) remain beyond the capabilities of current models. Conceptual and computational methods are being developed to separate a geologic-scale percolation model into a series of simulations that capture appropriately the dominant percolation behavior. The product of our research will be an understanding of the controls on the spatial distribution of the non-wetting fluid clusters.

**Results:** The Invasion-Percolation-in-a-Gradient (IPG) model is capable of incorporating all forces --- viscous, buoyancy, and capillary forces --- relevant to geologic problems of two-phase flow in a porous medium. Our calibration of the IPG model to a data set of two-phase flow experiments on glass bead packs showed that the characteristic throat radius is about 10% of the site radius, assuming that the site radius is approximately the grain size. Two-dimensional model results of the fractal dimension and the invasion probability of a throat on the interface are in excellent agreement with predictions for limiting cases of Capillary number and Bond number. In moving from two to three-dimensional media, trapped wetting clusters do not scale with the extent of the invading cluster, remaining under 5 to 8 pores in size.

## **GRANTEE: WOODS HOLE OCEANOGRAPHIC INSTITUTION**

Department of Marine Chemistry and Geochemistry  
Woods Hole, MA 02543

**Grant:** DE-FG02-97ER14746

### **Laboratory Constraints on the Stability of Petroleum at Elevated Temperatures: Implications for the Origin of Natural Gas**

*Jeffrey Seewald 508-289-2966, fax 508-457-2164, jseewald@whoi.edu*

**Objectives:** Constrain the role of water and minerals during organic transformations responsible for the conversion of oil to natural gas at elevated temperatures and pressures.

**Project Description:** Factors that regulate the generation and composition of natural gas during the thermal maturation of petroleum are poorly understood. The origin of natural gas is being investigated by conducting a series of laboratory heating experiments to constrain the stability of petroleum and its degradation products in the presence of water and minerals at elevated temperatures and pressures. These experiments will assess carbon isotope fractionation and the catalytic activity of minerals, aqueous species, and water during oxidative decomposition of hydrocarbons and organic acids. Theoretical modeling is being used to evaluate thermodynamic and mass balance constraints on the production of carboxylic acids and dry natural gas.

**Results:** During the past year we have focused on experimental investigations of decomposition reactions that affect aqueous carboxylic acids to assess how such processes influence natural gas composition. Results demonstrate that reaction mechanisms responsible for carboxylic acid decomposition are strongly redox and carbon chain length dependent. Under relatively oxidizing conditions, acetic acid undergoes complete oxidation to CO<sub>2</sub> while under more reducing conditions, decarboxylation produces equal amounts of CO<sub>2</sub> and CH<sub>4</sub> despite a strong thermodynamic drive for complete oxidation. Longer chain acids decompose *via* decarboxylation under both oxidizing and reducing conditions.

Additional experiments have demonstrated that formic acid rapidly attains a metastable state of thermodynamic equilibrium with CO<sub>2</sub> but remains out of equilibrium with methane. This result suggests that the absence of formate in oil-field brines reflects thermodynamic equilibration with CO<sub>2</sub> at the prevailing subsurface pH and redox conditions.

A theoretical model based on *n*-alkanes oxidation has been developed that accounts for the uniform distribution of carboxylic acids in petroleum producing basins. A major implication of this model is that quantities of carboxylic acid generated during the thermal maturation of sedimentary organic matter are not limited by the initial kerogen oxygen content and may be substantially greater than amounts predicted by conventional models.

## **GRANTEE: WOODS HOLE OCEANOGRAPHIC INSTITUTION**

Department of Marine Chemistry and Geochemistry  
Woods Hole Oceanographic Institution  
Woods Hole, Massachusetts 02543

**Grant:** DE-FG02-89ER13466

### **Organic Geochemistry of Outer Continental Margins and Deep-Water Sediments**

*J.K. Whelan, 508-289-2819, fax 508-457-2164, [jwhelan@whoi.edu](mailto:jwhelan@whoi.edu)*

**Website:** <http://dynatog.whoi.edu/>

**Objectives:** The objective of this program is to develop a better understanding of processes of hydrocarbon generation and migration in coastal and offshore sedimentary basins as an aid in predicting favorable exploration areas for oil and gas.

**Project Description:** Current research focuses on utilization of organic compounds in elucidating mechanisms, rates, and consequences of subsurface fluid flow. A particular interest is understanding the role of gas in driving fluid movement in sedimentary basin processes in collaboration with scientists at Cornell University, Louisiana State University and oil companies (Global Basin Research Network); the Geochemical and Environmental Research Group (GERG) at Texas A&M; and U. Mass, Boston.

**Results:** Previous work provided evidence for on-going oil and gas injection (termed dynamic migration) into reservoirs of Eugene Island Block 330 (EI330) and areas to the south along the Louisiana Gulf Coast shelf edge and slope. Alterations to reservoir oils are produced by "gas washing", in which oil in reservoirs is "washed" with multiple volumes of upward migrating gas. Gas washing, together with oil biodegradation, is probably responsible for the hydrocarbon compositional changes that occur in some, but not all, EI330 oils on short time-scales (5-10 year). The result of gas washing working together with biodegradation is a very dynamic system where heavier n-alkanes are lost by on-going biodegradation in the reservoir and are replaced by the lighter n-alkanes, which accompany gas washing.

Many lines of evidence indicate this on-going upward gas flow may not be restricted to the Gulf of Mexico, but might be part of a much larger phenomenon which occurs worldwide, particularly over active oil and gas generation areas in actively subsiding basins such as many of the world's major river deltas and continental margins. Even though this upward gas flow is probably very large volumetrically, it is often difficult to detect and quantify because the upward gas flow involved is highly localized and probably episodic. Part of our research is aimed toward developing better *in situ* seafloor methods for continuous detection and measurement of the gas amounts, compositions, and fluxes involved. *In situ* measurements of gases would provide a crucial missing link in quantifying the importance of gas flux both at the sediment-water interface and in the subsurface - it is much easier to make these measurements at the sediment surface than in the subsurface. Furthermore, only 2% of generated oil and gas is ever trapped in a producible reservoir, while about 54% of the remainder is discharged at the sediment surface into the overlying ocean.

During the past year, we participated in a cruise to two areas where gas bubble streams continuously stream through seafloor gas hydrates in the Gulf of Mexico. We were successful in making *in situ* measurements of gases both in bottom waters and in sediment pore waters. These show a high degree of

methane undersaturation very near the seeps. In addition, observations of: a) an active biota associated with the seeps, b) rapid formation of solid ice-like methane hydrates from gas bubbles under *in situ* seafloor conditions, and c) the presence of oil coated gas bubbles which persist to within 100 ft of the air sea interface, are all consistent with the very dynamic gas flow system which we have found for the subsurface oil-gas system underlying this area.

## **GRANTEE: WOODS HOLE OCEANOGRAPHIC INSTITUTION**

Department of Geology and Geophysics  
Woods Hole, MA 02543

**Grant:** DE-FG02-00ER15058

### **Evolution of Pore Structure and Permeability of Rocks under Hydrothermal Conditions**

*W. Zhu, 508-289-3355, fax 508-457-2183, wzhu@whoi.edu; J. B. Evans, Massachusetts Institute of Technology*

**Objectives:** The pore structure and transport properties of rocks, including fluid permeability and electrical conductivity, can be altered by a wide variety of diagenetic, metamorphic, and tectonic processes. We are studying the interrelationships among permeability, mechanical properties, and the pore shape, under hydrothermal conditions, in mineral aggregates, with and without reactions.

**Project Description:** A better understanding of the processes that change porosity in the Earth is important for improving resource recovery, predicting rates of metamorphism, understanding fault mechanics and fault stability, and estimating rates of deformation by pressure solution. Laboratory results indicate that the measurements of macroscopic transport properties can be rationalized by considering the evolution of the pore space. As the mineral aggregates react and lithify, a larger fraction of porosity becomes ineffective for fluid or electrical transport. In this study, we use an integrated approach consisting of experimental testing, quantitative microscopy, and theoretical and numerical analyses to quantify changes in surface roughness, porosity, and pore dimensions. Detailed microstructure study will be made using standard optical, scanning electron, and laser confocal scanning optical microscopes. The image data will then be used in network models to predict the permeability.

**Results:** This project has only recently been initiated and awarded since July 2000. Up to date, we have conducted a series of experiments on calcite aggregates to investigate the effect of water on the evolution of pore geometry and permeability during hot pressing. Quantitative characterization of the pore geometry of 6 hot isostatically pressed calcite samples with final porosities ranging from 4% to 12% are complete using a scanning electron microscope (SEM). We obtained preliminary data to elucidate the 3-dimensional geometry and connectivity of the pore space using a laser scanning confocal microscope (LSCM). Incorporating the important constraints on geometric attributes of these samples, we also developed a new network model that is more realistic in modeling permeability and fluid transport in partially molten systems.

## GRANTEE: UNIVERSITY OF WYOMING

Department of Geology and Geophysics  
Laramie, WY 82071-3006

**Grant:** DE-FG03-96SF14623/A000

### Mineral Dissolution and Precipitation Kinetics: A Combined Atomic-Scale and Macro-Scale Investigation Targeted toward CO<sub>2</sub> Sequestration Data Needs

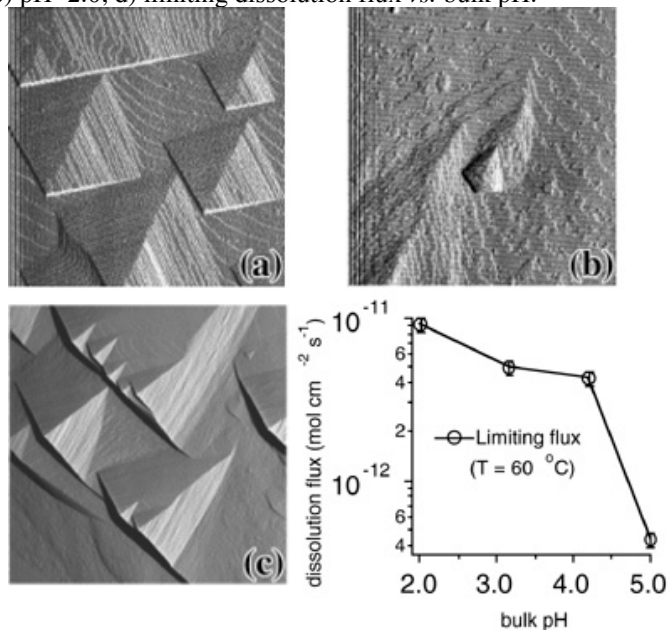
*C. M. Eggleston, 307-766-6769, fax 307-766-6679, carrick@uwyo.edu; S. R. Higgins, 307-766-3318, fax 307-766-6679, shiggins@uwyo.edu; K. G. Knauss, 925-422-1372, fax 925-422-0209, knauss@s19.es.llnl.gov*

**Objectives:** The primary objective for this research program is to develop an appropriate mechanistic understanding of carbonate mineral dissolution and growth through extensive experimentation at both microscopic and macroscopic length-scales.

**Project Description:** This project utilizes a combined atomic-scale and macro-scale study of mineral/fluid interaction that is designed to improve our understanding of, and ability to predict the course of, mineral dissolution and precipitation processes specifically affecting coupled silicate mineral dissolution and carbonate mineral growth expected as part of a CO<sub>2</sub> sequestration strategy of injection into deep aquifers. Our atomic-scale studies utilize a Hydrothermal Atomic Force Microscope (HAFM) for molecular-level experiments on the kinetics of nucleation, step motion and other phenomena on mineral surfaces under conditions relevant to CO<sub>2</sub>-sequestration. The same conditions used in HAFM experiments will also be investigated with macroscopic hydrothermal reactors (for stoichiometric rate data) and geochemical reactive transport codes. This approach will allow us to address many still-open questions concerning the exact forms for rate laws near and far from equilibrium, the microscopic interpretation of these rate laws, the activation energies and formation energies for key microscopic surface structures (*e.g.*, steps, kinks), and the impact of specific aquifer solute catalysts and inhibitors on the dissolution and growth processes.

**Results:** Our objectives for FY 2000 involved both research and instrumentation development. On the research front, our goal was to obtain experimental data on the dissolution and precipitation kinetics of magnesite and calcite as a function of solution composition and temperature, all in well-

**Figure:** Magnesite *in situ* etch-pit morphology (6000nm x 6000 nm images) at 60°C using the HAFM. a) pH = 4.2; b) pH = 3.1; c) pH=2.0; d) limiting dissolution flux vs. bulk pH.



defined hydrodynamics. These experimental goals required that significant improvements to the fluid delivery system be made to the original HAFM developed earlier under this grant number.

We have updated and improved the HAFM technology with a new fluid inlet that creates hydrodynamic conditions, modeled extensively by Dr. Richard Compton's group at Oxford University. This improvement permits well-constrained kinetic data to be obtained from the HAFM. We have conducted studies of magnesite and calcite dissolution in aqueous solution at temperatures up to 90 °C. The step directions defining etch pits on magnesite (see Figure 1) are sensitive to the extent of surface protonation with little resultant change in overall dissolution flux. The experimental results suggest a fundamental difference in mechanism between acidic dissolution of calcite and magnesite – calcite follows a first-order heterogeneous proton promoted mechanism whereas magnesite displays a much weaker dependence on surface proton concentration; indicative of a pre-equilibrium or surface complexation mechanism.

## **GRANTEE: YALE UNIVERSITY**

Department of Geology and Geophysics  
New Haven, Connecticut 06520-8109

**Grant:** DE-FG02-95ER14522

### **A Field Experiment on Plants and Weathering**

*R. A. Berner, 203-432-3183, fax 203-432-3134, [berner@hess.geology.yale.edu](mailto:berner@hess.geology.yale.edu)*

**Objectives:** For the year 2000 objectives were to: (1) complete our study of the effects on geochemical cycling resulting from experimental deforestation, (2) continue our theoretical calculations of long-term carbon cycling and atmospheric CO<sub>2</sub>, (3) Continue our study of the stomatal density of fossil leaves as an indicator of past levels of atmospheric CO<sub>2</sub> and (4) continue our study of the effects of varying O<sub>2</sub>/CO<sub>2</sub> on the fractionation of carbon isotopes during photosynthesis and how results can be applied to theoretical calculations of the evolution of atmospheric oxygen.

**Project description:** (1) Results on drainage water chemistry, subsequent to the cutdown of pine trees from experimental plots at the Hubbard Brook Experimental Forest Station, have been brought to a close. (2) GEOCARB computer modeling of the long-term carbon cycle and atmospheric CO<sub>2</sub> has been modified to include new data on erosion over Phanerozoic time, the latest results of atmospheric GCM modeling, and new data on the quantitative role of plants in weathering. (3) Ginkgo leaves from herbarium collections have been studied to calibrate the paleo-CO<sub>2</sub> stomatal method and fossil Ginkgo leaves from rocks have been measured. (4) In collaboration with Dr. David Beerling (Univ. Sheffield, UK), we have undertaken plant growth experiments under varying O<sub>2</sub>/CO<sub>2</sub> and combined results with the analysis of the carbon isotopic composition of fossil plants, to make deductions about ancient O<sub>2</sub> levels.

**Results:** (1) Since the pine trees were cut down at Hubbard Brook, there has been a great release of dissolved chloride, which presumably represents earlier root storage during growth of the trees. The pattern is totally different in timing from the release of the essential nutrient nitrate. (2) Our new GEOCARB calculations indicate that past levels of CO<sub>2</sub> probably varied more (but with the same overall pattern) than thought previously, with generally higher levels during the Mesozoic era. (3) The stomatal density for Ginkgo leaves collected over the past 140 years correlates very closely, in an inverse manner, with known atmospheric CO<sub>2</sub> level. Using this calibration, values of paleo-CO<sub>2</sub> have been determined for portions of the Cretaceous, Paleocene and Eocene periods (70-45 Ma). (4) In two papers (Berner *et al.*, 2000, *Science*, v.287, p.1630; Beerling *et al.*, 2001, submitted to *Nature*) the effect of changes in atmospheric O<sub>2</sub> on the fractionation of carbon isotopes during photosynthesis is demonstrated for both land plants and marine plankton. These results have enabled the theoretical calculation of O<sub>2</sub> levels over the Phanerozoic that show a maximum level of about 35% during the Permo-Carboniferous (Berner, 2001, *Geochimica et Cosmochimica Acta*--in press). This agrees with our independent study based on the isotopic analysis of fossil plants.

**GRANTEE: YALE UNIVERSITY**

Department of Geology and Geophysics  
P.O. Box 208109  
New Haven, Connecticut 06520-8109

**Grant:** DE-FG02-90ER14153

**Reactive Fluid Flow and Applications to Diagenesis, Mineral Deposits, and Crustal Rocks**

*D. M. Rye, 203-432-3174, fax 203-432-3134, danny.rye@yale.edu; E. W. Bolton 203-342-3149, edward.bolton@yale.edu*

**Objectives:** To initiate new modeling of coupled fluid flow and chemical reactions of geologic environments; experimental and theoretical studies of water-rock reactions and collection and interpretation of stable isotopic and geochemical field data at many spatial scales of systems involving fluid flow and reaction in environments ranging from soils to metamorphic rocks.

**Project Description:** Theoretical modeling of coupled fluid flow and chemical reactions involving kinetics, has been employed to understand the differences between equilibrium, steady state, and non-steady-state behavior of the chemical evolution of open fluid-rock systems. The numerical codes developed in this project treat multi-component, finite-rate reactions combined with advective and dispersive transport in multi-dimensions. The code incorporates heat, mass, and isotopic transfer in both porous and fractured media. Experimental work has obtained the kinetic rate laws of pertinent silicate-water reactions and the rates of Sr release during chemical weathering. *Ab-initio* quantum mechanical techniques to obtain the kinetics and mechanisms of silicate surface reactions. Geochemical field-based studies were carried out on the Wepawaug metamorphic schist, on the Irish base-metal sediment-hosted ore system, in the Dalradian metamorphic complex in Scotland, and on weathering in the Columbia River flood basalts. The geochemical and isotopic field data, and the experimental and theoretical rate data, were used as constraints on the numerical models and to determine the length and timescales relevant to each of the field areas.

**Results:** Analytical and numerical models were extended for metamorphic processes in the presence of mixed volatiles (CO<sub>2</sub> and water). Depending on the rates of heating and fluid flow, these open-system, kinetic models can exhibit reaction histories with significant departures from equilibrium and can produce quite different fluid flux estimates from those based on the equilibrium approach. Besides underscoring the central role of kinetic control, these models also illustrate the importance of metastable reactions. Localized heating can drive fluid flows by either reaction induced volatile production, or by buoyancy driven convection.

A grain-scale oxygen isotope exchange model was developed. The results indicate that the standard method of utilizing a  $k_{\text{effective}}$  for the rate of exchange is only useful for slow flow rates and/or very fast diffusion rates. Further results indicate that complex zoning patterns both within grains and along the exchange front can result from the fact that different minerals exchange at different rates.

A white-light interferometric system directly measured dissolution rates of anorthite. These measurements revealed strong spatial variations of dissolution and they circumvented ambiguities associated with BET surface area measurements. The development of an absolute reference on the

mineral surface showed, for the first time, that the etch pits and the entire surface each retreat at separate characteristic rates. This observation has led to a new theory of dissolution kinetics.

*Ab initio* methods indicate that a Grotthus type of reaction path is energetically reasonable for hydrogen isotope exchange between water and dissolved silica. Calculated equilibrium values were in good agreement with experiments. Oxygen isotope exchange between water and silica was found to proceed at a reasonable rate via a five-fold coordinated transition state.

Field studies indicated that weathering rates of basalt were about three times those of either diorite or granite. Strontium fluxes were approximately equal in all three rock types, with Sr isotopic ratios similar to the parent rock. A coupled flow and mass transfer model showed that weathering of large volumes of fresh flood basalts will tend to lower the strontium isotopic composition of seawater, and at the same time tend to draw down the CO<sub>2</sub> concentration of the atmosphere.

Pb isotopic results from all possible source rocks in the Irish Midlands demonstrate unequivocally that the Pb in these world class ore bodies was largely derived from the underlying basement rocks and delivered to the ore deposition site by fluid flow in nearly vertical fractures. By implication, the low temperature fluid flow in the ore-formation part of the basin was profoundly affected by injection of fluid and heat of deep origin.

## Subject Index

- Acids, 16, 44, 47, 50, 67, 72, 101, 139, 140, 141, 144, 161, 162, 216, 241, 255  
  organic, 66, 241, 255
- Actinides, 249
- Activity coefficients, 44, 153
- Age dating, 28, 45, 58, 59, 100, 109, 179, 180, 189, 218, 225
- Age dating  
  exposure ages, 100
- Air-water interface, 27
- Aluminum, 31, 44, 45, 46, 47, 101, 102, 103, 112, 146, 156, 157, 162, 175, 192, 193, 197
- Amphiboles, 64, 68, 105
- Aqueous, 12, 26, 31, 33, 44, 45, 48, 50, 65, 66, 67, 69, 70, 72, 74, 103, 116, 121, 136, 139, 140, 146, 147, 153, 154, 159, 161, 162, 182, 195, 199, 200, 206, 216, 220, 222, 239, 240, 241, 255, 260
- Aqueous geochemistry, 241
- Aquifer, 26, 31, 32, 33, 47, 48, 97, 101, 131, 192, 214, 225, 259
- Atomic Force Microscopy, 12, 32, 49, 50, 60, 69, 70, 71, 72, 75, 76, 106, 127, 143, 156, 157, 158, 192, 194, 241
- Bacteria, 60, 65, 74, 75, 101, 156, 157, 158, 206, 248, 249
- Basalt, 14, 19, 24, 94, 116, 145, 172, 181, 262, 263
- Basalts  
  MORB, 58, 116
- Beamlines, 117
- Biofilms, 206, 207, 249
- Biomineralization, 49, 75, 143, 144, 161, 248
- Birnessite, 16
- Bonding, chemical, 69, 80, 89, 120, 146, 153, 162, 206
- Borehole, 17, 18, 19, 43, 53, 77, 78, 90, 168, 196, 246, 250, 251  
  stability, 250
- Boron, 91, 92
- Brines, 26, 44, 67, 118, 208, 209, 220, 224, 226, 239, 255
- Brucite, 62
- Calorimetry, 105
- Capillarity, 24, 86, 87, 128, 129, 148, 168, 187, 188, 211, 254
- Carbon, 29, 33, 34, 35, 40, 43, 46, 49, 53, 58, 65, 67, 70, 79, 84, 90, 99, 100, 108, 109, 118, 131, 136, 146, 150, 151, 184, 197, 201, 224, 255, 261
- Carbon  
  carbon cycle, 58, 261
- Carbon 14, 45
- Carbon dioxide, 17, 19, 22, 26, 29, 33, 40, 41, 42, 43, 45, 46, 47, 48, 51, 61, 62, 65, 66, 67, 70, 78, 84, 86, 94, 95, 98, 99, 100, 106, 127, 128, 131, 146, 147, 168, 187, 197, 199, 206, 211, 220, 224, 232, 233, 235, 236, 246, 255, 259, 261, 262, 263
- Carbon dioxide sequestration, 17, 26, 33, 41, 46, 47, 48, 86, 106, 127, 128, 187, 220, 259
- Carbonates, 14, 22, 29, 47, 48, 49, 51, 65, 70, 72, 86, 105, 106, 108, 110, 118, 121, 122, 127, 143, 144, 146, 147, 152, 178, 179, 184, 189, 206, 208, 224, 253, 259  
  minerals  
    calcite, 43, 48, 49, 50, 53, 63, 65, 66, 67, 70, 71, 72, 89, 90, 106, 108, 121, 127, 142, 143, 144, 179, 180, 224, 225, 233, 236, 258, 259, 260
- Carbonates  
  minerals, 47, 49, 65, 70, 108, 143, 224  
  minerals  
    dolomite, 65, 89, 106, 108, 120, 233, 236
- Catalysis, 16
- Cesium, 154, 159
- Chemical potential, 139, 140
- Chromatography, 16, 201, 202
- Chromium, 15, 35, 117, 121, 154, 159, 207, 241
- Clays, 17, 27, 30, 35, 43, 53, 66, 88, 90, 91, 105, 121, 158, 189, 190, 210, 222, 233, 236  
  kaolinite, 27, 89, 121, 156, 157, 158  
  smectite, 89, 91, 110, 152, 189
- Clays  
  illite, 27, 91, 110, 152, 189  
  montmorillonite, 27, 30, 31, 66, 89

Climate, 11, 28, 49, 64, 79, 96, 109, 131, 134, 184, 225, 240  
 Climate Change, 28, 49, 79, 109, 184  
 Colloid transport, 27, 69  
 Colloids, 27, 69, 96  
 Compaction, 20, 80, 84, 119, 164, 184, 186, 210, 220, 222, 223, 250, 251  
 Conductivity  
     electrical, 17, 41, 43, 53, 90, 164, 210, 242, 258  
     hydraulic, 83, 166, 191  
 Constitutive relationships, 87, 129, 188  
 Convection, 112, 141, 169, 226, 252, 262  
     thermohaline, 112, 226, 227  
 Cosmic rays, 45, 57  
 Creep, 170, 222, 223, 244  
 Crust, 35, 43, 53, 55, 63, 90, 112, 138, 169, 186, 199, 206, 244, 253  
 Crystallography, 117  
     deep saline aquifer, 51, 197  
 Defects, 64, 70, 75, 76, 143, 155, 160, 192, 216  
 Deforestation, 261  
 Diagenesis, 16, 91, 110, 127, 148, 152, 153, 189, 190, 201, 222  
 Diamond anvil, 117  
 Diffusion, 28, 35, 44, 45, 63, 64, 67, 68, 83, 113, 116, 118, 121, 125, 141, 146, 147, 166, 170, 191, 199, 211, 224, 226, 262  
 Diffusion  
     coefficients, 44, 64, 68, 116, 121, 125, 147, 211  
 Dissolution, 12, 26, 28, 29, 42, 44, 46, 47, 48, 59, 60, 66, 70, 71, 72, 75, 76, 87, 88, 95, 101, 102, 116, 121, 129, 141, 153, 154, 155, 156, 157, 158, 159, 160, 161, 188, 192, 194, 199, 211, 222, 224, 249, 259, 260, 262  
 Earth materials, 54, 79, 120, 184  
 Earthquakes, 19, 39, 54, 93, 124, 244  
 Elastic Properties, 209, 210  
 Electric double layers, 72  
 Electrical properties, 41, 42, 203  
 Electrolytes, 44, 72, 139, 140, 153  
 Electron transfer, 75, 76, 182  
 Energetic particles, 57  
 Energy transport, 125  
 Enthalpy, 26, 112, 161  
 Entropy, 113  
 Environment, 19, 28, 49, 56, 57, 58, 74, 75, 96, 120, 121, 125, 127, 182, 195, 196, 203, 216, 218, 238, 248, 249  
 Epidote, 64, 68, 237, 238  
 Equation of state, 44, 140  
 Erosion, 37, 59, 141, 142, 167, 261  
     rates, 59  
 Fault, 110, 152, 196, 214, 237, 238, 244  
 faults, 26, 93, 110, 124, 125, 145, 152, 172, 196, 213, 214, 232, 233, 235, 236, 237, 238, 244  
 Faults and faulting, 28, 93, 110, 112, 124, 145, 148, 152, 164, 169, 172, 185, 196, 213, 214, 232, 233, 235, 236, 237, 238, 244, 253, 258  
     gouge, 214, 233, 236, 253  
     mechanics, 164, 237, 258  
     San Andreas Fault, 244  
 Feldspars, 63, 68, 127, 164, 192, 210, 238, 253  
     albite, 68, 192, 193  
     anorthite, 262  
     orthoclase, 12, 127  
 Feldspars  
     plagioclase, 68, 110, 152, 192  
 Ferric iron oxides, 75  
 Fingering, 87, 111, 129, 188  
 Fluid conductivity, 18  
 Fluid flow, 14, 15, 33, 37, 55, 79, 84, 86, 88, 110, 118, 123, 125, 127, 128, 129, 130, 136, 141, 152, 168, 181, 184, 186, 187, 188, 189, 199, 208, 210, 213, 220, 222, 250, 252, 256, 262, 263  
     fast flow, 39, 125, 194  
     multiphase, 26, 82, 86, 128, 148, 175, 181, 187, 230, 254  
     porous media, 111, 205  
     reactive, 42, 213  
     unsaturated, 24, 87, 129, 188  
 Fluid inclusions, 63, 118, 120, 239, 240  
 Fluid migration, 29, 33, 64, 84, 189, 213  
 Fluid-rock interactions, x, 14, 62, 63, 68, 108  
 Fluorescence, 14, 32, 117, 120, 206  
 Fractional derivatives, 55

Fractionation, 62, 63, 65, 67, 91, 94, 108, 116, 121, 261  
 Fractures, 14, 20, 24, 26, 29, 37, 39, 42, 43, 80, 81, 86, 87, 88, 123, 125, 128, 129, 132, 133, 141, 142, 148, 173, 174, 184, 187, 188, 194, 196, 197, 208, 213, 214, 216, 227, 238, 250, 251  
     aperture, 24, 42, 43, 88, 125, 129, 188, 194, 214  
     mechanics, 26, 184  
     systems, 123, 132  
 Friction, 93, 123, 124  
 Gas  
     hydrates, 210, 256  
     Hydrates, 147, 240  
     natural, 34, 95, 137, 201, 224, 239, 255  
     noble, 29, 33, 34, 45, 51, 100, 136, 137, 138  
 Gassmann technique, 39, 40, 208, 209, 220  
 Geochemical transport, x, 12, 199  
 Geochemistry low temperature geochemistry, x, 45, 58, 62, 94, 108, 117, 204, 206, 220, 225, 232, 235  
 Geomorphology, 45, 134  
 Geophysics, x, 17, 19  
 Geothermal, 28, 42, 61, 62, 65, 66, 108, 109, 110, 152, 215, 252  
 GIXAS, 32  
 Glaciation, 134  
 Glass, 24, 64, 80, 81, 83, 94, 112, 161, 162, 164, 165, 166, 168, 173, 191, 192, 193, 205, 254  
 Glasses  
     aluminosilicate, 30, 161, 162, 192  
 Gold, 64, 118, 162  
 Grain boundaries, 43, 53, 90, 154, 155, 159, 160, 199  
 Granite, 54, 145, 168, 172, 244, 250, 252, 253, 263  
 Granular flow, 123  
 Gravity, 17, 26, 49, 82, 87, 111, 123, 128, 129, 175, 187, 188, 205, 215, 230  
 Ground-penetrating radar, 228, 229  
 Groundwater, 17, 28, 29, 33, 34, 65, 110, 125, 136, 137, 152, 168, 218, 225, 244, 249  
     hydrocarbon movement, 35, 91, 138  
     Hydrocarbon source, 33, 34, 98, 136, 137  
 Hydrocarbons, 33, 34, 35, 39, 66, 84, 91, 98, 108, 136, 137, 138, 140, 168, 220, 228, 239, 256  
 Hydrology, x, 29, 213, 225  
 Hydrolysis, 66, 192, 193  
 Hydrothermal, 42, 48, 62, 63, 64, 65, 67, 96, 108, 109, 117, 118, 120, 164, 189, 215, 238, 252, 253, 258, 259  
     fluids, 96, 117, 120, 189  
     systems, 42, 108, 109, 215  
 hydroxyl, 30, 103, 116, 192  
 Imaging, x, 19, 22, 33, 40, 42, 78, 82, 114, 118, 119, 122, 154, 155, 157, 159, 160, 168, 173, 175, 194, 197, 228, 230, 242, 246  
     seismic, 19, 78, 246  
     subsurface, x  
     subsurface geophysical imaging, x  
 Instability, 56, 109, 111, 169, 170, 226, 227  
 Inverse methods, 17, 18, 19, 77, 78, 132, 203, 242, 244, 246  
 Iron, 15, 31, 32, 59, 60, 64, 65, 73, 74, 75, 76, 101, 102, 105, 106, 120, 121, 154, 156, 157, 158, 159, 216, 249  
     oxides, 16, 59, 117, 182  
         goethite, 32, 60, 72, 75, 101, 102, 121, 156, 206, 241  
         hematite, 32, 59, 60, 72, 75, 76, 106, 117, 121, 156  
         magnetite, 66, 72, 73, 75, 121, 189  
 Iron  
     oxides, 32, 60, 121  
     oxides  
         hematite, 107  
         magnetite, 66  
 isotope partitioning, 63, 65, 66, 94  
 Isotopes, 29, 33, 34, 51, 62, 91, 94, 96, 108, 109, 131, 136, 137, 192, 204, 218, 253  
     argon, 108  
     carbon, 65, 66, 94, 109, 146, 233, 236  
     chlorine, 51, 100  
     cosmogenic, 45, 59, 100  
     fractionation, 62, 63, 65, 67, 91, 94, 116, 252, 255  
     helium, 29, 137

hydrogen, 62, 68, 116, 150, 151, 263  
 Iodine, 51  
 oxygen, 63, 64, 65, 66, 94, 108, 109, 204, 252, 253, 262  
 stable isotopes, 62, 67, 94, 108, 151, 252  
 Isotopes  
   carbon, 108, 109, 131, 261  
   cosmogenic, 34, 51, 138  
   exchange, 67, 150  
   osmium, 96  
   uranium, 29, 51  
 Joint inversion, 17, 18, 132, 203  
 Kerogen, 16, 98, 99, 150, 255  
 Kinetics, 12, 35, 47, 48, 49, 50, 64, 65, 66, 70, 75, 101, 116, 118, 127, 142, 143, 144, 153, 156, 164, 223, 224, 259, 260, 262, 263  
 Krypton, 34, 136, 137, 218, 219  
 Lattice-Boltzman models, 79, 123, 141, 173  
 Lead, 28, 105, 108, 109, 121, 122, 162, 179, 180, 206, 207, 248, 249, 253, 263  
 Lithology, 17, 38, 114, 197, 208  
 Magmatism, 28, 29, 58, 94, 109, 112, 113, 169, 215, 237, 252, 253  
 Magnetosphere, 56, 57  
 Manganese oxide, 105, 121  
 Mantle, 39, 40, 43, 53, 80, 90, 96, 98, 112, 117, 137, 169, 170, 199  
 Marble, 43, 141  
 Mass spectrometry, 16, 43, 45, 51, 53, 90, 94, 108, 192, 225  
   accelerator mass spectrometry, 45, 46, 51  
   inductively coupled plasma, 101  
   ion microprobes, 63, 67, 68, 91, 108, 109, 192, 252  
   resonance ionization, 218  
   time-of-flight, 218, 219  
   time-of-flight Seismic crosswell tomography, 43, 53, 90, 218  
 Mass transfer, 35, 63, 83, 87, 88, 98, 99, 110, 128, 129, 152, 166, 187, 188, 191, 263  
 Mechanics  
   damage, 185  
   micromechanics, 55, 80  
 Melts, 94, 112, 121, 169  
 Mercury, 162  
 Metamorphism, 29, 43, 53, 90, 91, 164, 204, 258  
 Methane, 33, 61, 131, 201, 210, 233, 236, 239, 240, 255, 257  
 Micas, 105, 127, 154, 159, 185, 238  
   biotite, 64, 154, 155, 159, 160, 238  
 Micas  
   muscovite, 13, 127  
 Microorganisms, 16, 59, 60, 65, 74, 76, 118, 156, 157, 158, 206, 241, 248, 249  
 Microorganisms  
   microbes, 241  
 Microstructure, 15, 40, 54, 79, 184, 199, 258  
 Mineral-fluid interface, 12, 154, 159  
 Minerals  
   dissolution, 28, 47, 66, 156, 157, 158, 259  
   growth, 48, 50, 259  
   solubility, 144  
   surface chemistry, 12, 35, 48, 66, 67, 70, 74, 106, 117, 121, 143, 144, 146, 153, 156, 161, 182, 195, 206, 207, 241, 259, 263  
 Molecular dynamics, 72, 74, 88, 140, 146, 169  
 Molecular modeling, 88, 161  
 NaCl, 26, 44, 45, 63, 67, 68, 146, 147, 239  
 Nanoscale, 55, 169  
 Neodymium, 28, 29, 225  
 Nitrogen, 29, 150  
 Nonlinear, 54  
 nonlinear behavior, 54  
 Nuclear Magnetic Resonance (NMR), 82, 103, 146, 150, 162, 168, 175, 192, 230  
 Numerical simulation numerical modeling, 26, 42, 59, 80, 83, 86, 87, 111, 123, 128, 166, 168, 187, 191, 205, 227  
 Oceans, 29, 42, 49, 58, 95, 96, 116, 118, 211, 218, 224, 256  
 Olivine, 94, 100, 170  
 Organic sulfur, 16  
 Oxidation state, 35, 120, 121  
 Paleoclimate, 58, 108, 109  
 Paleomagnetism, 189  
 Peclet number, 111, 125  
 Permeability, 14, 15, 17, 24, 37, 38, 39, 42, 47, 55, 80, 83, 84, 85, 86, 108, 110, 111, 118, 123, 125, 148, 152, 164, 166, 168, 177, 178,

185, 186, 191, 194, 197, 199, 205, 210, 213,  
 214, 220, 226, 227, 228, 232, 233, 235, 242,  
 258  
 measurement, 85, 86, 177, 178, 232, 235  
 Petroleum, 16, 17, 34, 52, 82, 86, 98, 108, 110,  
 128, 136, 151, 152, 175, 187, 196, 201, 230,  
 239, 242, 255  
 migration, 110, 152  
 pH, 12, 27, 29, 31, 47, 65, 66, 67, 68, 69, 70,  
 75, 101, 154, 158, 159, 162, 182, 192, 207,  
 248, 255  
 Phase  
   relationships, 61  
 Plasma instabilities, 56  
 Platinum, 64  
 Pore structure, 118, 119, 164, 168, 181, 184,  
 258  
 Poroelastic properties, 38, 39  
 Porosity, 14, 17, 18, 20, 34, 39, 40, 42, 47, 80,  
 84, 86, 113, 119, 137, 164, 165, 178, 181,  
 184, 194, 209, 210, 213, 220, 228, 232, 235,  
 250, 251, 258  
 Porous media, 27, 41, 55, 87, 111, 112, 123,  
 127, 128, 168, 169, 187, 205, 214, 227  
 Precipitation, 12, 26, 28, 29, 42, 44, 46, 47, 48,  
 58, 65, 66, 71, 118, 134, 143, 146, 189, 199,  
 206, 222, 223, 248, 249, 259  
 pressure-volume-temperature, 239  
 Protonation, 48, 66, 153, 195, 260  
 Pyrite, 120, 182, 216  
 Pyrolysis, 98, 150  
   hydrous, 150  
 Quantum mechanics, 139, 161, 162, 262  
 Quartz, 31, 32, 45, 46, 63, 66, 100, 118, 127,  
 153, 164, 199, 210, 222, 223, 237, 238, 250,  
 252, 253  
 Reactive transport, 35, 36, 48, 259  
 Reduction, 12, 35, 37, 46, 60, 74, 75, 76, 80,  
 98, 111, 118, 119, 154, 159, 164, 206, 209,  
 214, 238, 249, 250  
 Remediation, 17, 28, 42, 79, 86, 106, 117, 128,  
 184, 187, 242  
 Reservoirs  
   characterization, 39, 232, 235  
   dynamics, 62  
 Resolution, 12, 14, 15, 22, 35, 40, 41, 42, 63,  
 72, 75, 78, 79, 80, 86, 87, 108, 109, 118,  
 120, 127, 128, 132, 141, 142, 154, 155, 159,  
 160, 168, 181, 183, 187, 194, 201, 203, 218,  
 219, 221, 225, 228, 234, 244, 246, 248  
 Retrograde metamorphism, 43, 53, 90  
 Reynolds  
   equation, 173  
   number, 80, 125  
 Rheology, 112, 169, 170  
 Richard's equation, 87, 129, 188  
 Rivers, 167, 256  
 Rock mechanics, x  
 Rock mechanics, x, 79, 184  
 Rock physics, 22, 38  
 Sandstone, 14, 20, 21, 22, 54, 80, 84, 85, 86,  
 164, 165, 168, 177, 178, 181, 184, 194, 213,  
 214, 232, 235, 250, 251  
 scanning probe microscopy, 70  
 Sedimentology, 15, 29, 35, 110, 122, 127, 152,  
 226, 256, 262  
 Sediments, 14, 15, 16, 29, 31, 34, 49, 60, 64,  
 117, 120, 122, 134, 137, 179, 201, 207, 226,  
 248  
 Seepage, 233, 236  
 seismic absorption, 22  
 Seismic velocity, 17, 39, 119  
 Seismic wave propagation, 20, 52, 54, 77, 197  
 Seismology, 19  
   computational, 19  
   seismic anisotropy, 197  
 Selenium, 35  
 Shale, 91, 120, 164, 214  
 Shear localization, 186  
 Silica, 20, 31, 47, 116, 153, 161, 162, 263  
 Silicates, 20, 21, 29, 47, 91, 94, 105, 112, 116,  
 153, 154, 155, 159, 160, 199, 215, 259, 262  
 Soils, 16, 35, 106, 117, 121, 195, 207, 225,  
 241, 248, 262  
 Solar wind, 56  
 Solid solutions, 105, 106, 108, 122, 249  
 Solubility, 34, 44, 66, 67, 118, 136, 137, 144,  
 147, 161, 239

Sorption, 12, 13, 31, 32, 35, 66, 69, 71, 74, 88, 117, 120, 121, 146, 147, 153, 154, 159, 168, 182, 183, 195, 206, 207, 248  
 Space plasmas, 56  
 Speciation, 16, 26, 35, 67, 72, 112, 118, 120, 122, 153, 206, 207, 248  
 Spectrometry  
   infrared, 94  
   Mössbauer, 75  
 Spectroscopy, 12, 14, 16, 31, 43, 53, 90, 94, 103, 117, 127, 146, 154, 158, 159, 182, 183, 192, 195, 206, 207, 216, 218, 239, 240  
   electron spectroscopy  
     electron energy loss spectroscopy (EELS), 154, 159  
   XANES, 16, 35, 122, 162  
   X-ray, 195  
   X-ray photoelectron spectroscopy, 154, 158, 159, 182, 183  
 Speleothems, 109, 225  
 Strontium, 28, 29, 69, 96, 105, 118, 189, 192, 207, 225, 253, 262, 263  
 Sulfates, 16, 44, 45, 67, 105, 139, 183, 206, 249  
 Sulfides, 118, 120, 248, 249  
 Sulfur, 16, 182, 183, 216  
 Surface  
   charge, 72, 127, 153, 206  
   chemistry, 31, 70, 121, 130  
 Synchrotron, 12, 14, 16, 31, 35, 71, 75, 89, 117, 120, 184, 195, 206, 216, 249  
 Synchrotron radiation, 12, 117  
 Tectonics, 28, 84, 110, 148, 152, 164, 196, 258  
 Thermochronometry, 108  
 Thermodynamics, 44, 49, 50, 61, 62, 74, 75, 98, 105, 106, 112, 139, 144, 147, 153, 202, 239, 255  
 Thorium, 51, 64, 96, 97  
 Tomography, 14, 15, 40, 41, 132, 181, 184  
 Trace elements, 35, 113, 120, 204, 225  
 Transmission Electron Microscopy (TEM), 32, 154, 159  
 Transport coefficients, 44, 123  
 Transport properties, 41, 112, 154, 159, 164, 169, 194, 210, 258  
 TRXRF, 32  
 Tuff, 85, 177  
 Uranium series, 58, 109, 225  
 vadose, 24, 27, 28, 97, 225  
 Vertical-scanning interferometry, 72  
 Viscoelasticity, 39, 170  
 Volcanoes, 14, 28, 58, 100, 109, 204, 215, 252  
 Water, 61, 62, 94, 95, 98, 99, 107, 116, 146, 147, 199, 216, 222, 223, 239  
 Water-rock interaction, 239  
 Wave equation one way wave equation, 52, 114  
 Wave propagation, 19, 20, 40, 52, 53, 54, 77, 197, 209  
 Weathering, 29, 47, 96, 97, 120, 121, 127, 153, 197, 261, 262, 263  
   rock varnish, 134  
 Xenon, 28, 34, 136, 137  
 X-ray diffraction, 71, 207  
 X-ray scattering, 12  
 Zeolites, 105

## Author Index

<u>Contributor</u>	<u>Organization</u>	<u>Page</u>
Aldridge, David. F.	Sandia National Laboratories	73
Alumbaugh, David. L.	University of Wisconsin	252
Amonette, J. E.	Pacific Northwest National Laboratory	65
Anovitz, L. M.	Oak Ridge National Laboratory	55
Aydin, A.	Stanford University	217
Baer, D. R.	Pacific Northwest National Laboratory	65
Banfield, J. F.	University of Wisconsin	254
Banner, J. L.	University of Texas	230
Bedzyk, Michael. J.	Northwestern University	2
Bénézech, P.	Oak Ridge National Laboratory	60,63
Benson, D.	Desert Research Institute	132
Berge, P. A.	Lawrence Livermore National Laboratory	30,211
Bernabé, Yves	Université Louie Pasteur, France	164
Berner, R. A.	Yale University	267
Berry, D.	Virginia Polytechnic Institute & State University	247
Berryman, James. G.	Lawrence Livermore National Laboratory	30,31
Beveridge, T.	University of Guelph	71
Bhattacharya, Janok	University of Texas	233
Birn, J.	Los Alamos National Laboratory	49
Blair, S. C.	Lawrence Livermore National Laboratory	29
Blencoe, J. G.	Oak Ridge National Laboratory	55
Bodnar, R. J.	Virginia Polytechnic Inst. & State Univ.	245
Boles, James. R.	University of California at Santa Barbara	107,150
Bolton, E. W.	Yale University	268
Booker, J. R.	University of Washington	248
Bourcier, W. L.	Lawrence Livermore National Laboratory	34,
Brantley, Susan. L.	The Pennsylvania State University	194,196
Broecker, Wallace. S.	Columbia University	132
Brown Jr., Gordon. E.	Stanford University	209
Brown, Stephen.R.	New England Research	77,175
Burns, Daniel R.	Massachusetts Institute of Technology	169
Burton, E.A.	Lawrence Livermore National Laboratory	34
Caffee, M.	Lawrence Livermore National Laboratory	37,43,52,97
Caprihan, Arvind.	New Mexico Resonance	77
Carroll, Susan. A.	Lawrence Livermore National Laboratory	39,
Casey, William.H.	University of California at Davis	100,103
Chester, F. M.	Texas A&M University	227
Chester, J. S.	Texas A&M University	227
Chialvo, A.A.	Oak Ridge National Laboratory	63
Cole, D. R.	Oak Ridge National Laboratory	56,57,59,62
Constable, Steven	Scripps Institute of Oceanography, UCSD	206

Cygan, R. T.	Sandia National Laboratories	85
Daily, William D.	Lawrence Livermore National Laboratory	32
Datta-Gupta, Akhil	Texas A & M University	225
Davis, James.A.	U. S. Geological Survey	23
de Groot-Hedlin, Cathrine	Scripps Institute of Oceanography, UCSD	206
DePaolo, Donald. J.	Lawrence Berkeley National Laboratory	19
de Souza, Anthony R.	National Academy of Sciences	173
De Yoreo, Jim	Lawrence Livermore National Laboratory	41
Dietrich, W. E.	University of California, Berkeley	52,97
Dixon, D. A.	Pacific Northwest National Laboratory	67,70
Dove, Patricia. M.	Georgia Institute of Technology	41,141
Duba, A. G.	Lawrence Livermore National Laboratory	35,46,87
Dupuis, M.	Pacific Northwest National Laboratory	67
Durham, W. B.	Lawrence Livermore National Laboratory	34
Dvorkin, Jack.	Stanford University	214
Eggleston, Carrick M.	University of Wyoming	40,265
Eick, M.	Virginia Polytechnic Institute & State University	247
Elmore, R. D.	University of Oklahoma	191
Elsworth, Derek	The Pennsylvania State University	196
Engel, M. H.	University of Oklahoma	191
Epstein, S.	California Institute of Technology	91
Evans, J. Brian	Massachusetts Institute of Technology	164,264
Evans, James. P.	Utah State University	143,174,237,241,243
Fehler, Michael.	Los Alamos National Laboratory	45,
Felmy, A. R.	Pacific Northwest National Laboratory	70
Fenter, Paul.	Argonne National Laboratory	2
Finkel, R.C.	Lawrence Livermore National Laboratory	37,52,97
Forster, Craig.	University of Utah	233,237,241
Fredrich, Joanne T.	Sandia National Laboratories	76,186
Fredrickson, J. K.	Pacific Northwest National Laboratory	71
Garven, Grant T.	Johns Hopkins University	107,150
Gary, S. P.	Los Alamos National Laboratory	49
Ge, Shemin.	University of Colorado	122
Gibson, Richard L.	Texas A & M University	225
Glass, R. J.	Sandia National Laboratories	84,125,189
Goldstein, S. J.	Los Alamos National Laboratory	51
Gorby, Y.	Pacific Northwest National Laboratory	71
Grader, Abraham S.	The Pennsylvania State University	196
Graham, A.	Texas Tech University	79,177,235
Grechka, Vladimir.	University of Colorado	130
Guyer, R. A.	Los Alamos National Laboratory	47,
Haggerty, Roy	Oregon State University	80,166,193
Haimson, B. C.	University of Wisconsin	256
Hajash, A.	Texas A&M University	227
Hamilton, W.	Oak Ridge National Laboratory	63

Hanson, G. N.	State University of New York, Stony Brook	181,
Harrison, T. M.	University of California at Los Angeles	105
Harvey, Charles	Massachusetts Institute of Technology	80,166,193
Helgerud, M.	Stanford University	163
Helgeson, Harold C.	University of California, Berkeley	95
Herbert, Bruce	Texas A & M University	225
Hersman, Larry E.	Los Alamos National Laboratory	53,98,155
Hervig, Richard. L.	Arizona State University	68
Hestir, Kevin.	Utah State University	143,174,243
Higgins, Steven. R.	University of Wyoming	40,265
Hochella Jr., M.F.	Virginia Polytechnic Institute & State University	247
Holcomb, D. J.	Sandia National Laboratories	81
Horita, J.	Oak Ridge National Laboratory	56,59,62
Hoversten, G. Michael	Lawrence Berkeley National Laboratory	8
Hudson, G.B.	Lawrence Livermore National Laboratory	43
Ilton, Eugene S.	Lehigh University	153,159
Ingber, M.	University of New Mexico	79,177,235
Johnson, A.M.	Purdue University	198
Johnson, L. R.	Lawrence Berkeley National Laboratory	10
Johnson, Paul A.	Los Alamos National Laboratory	46
Jones, K. W.	Brookhaven National Laboratory	4
Kennedy, B. Mack	Lawrence Berkeley National Laboratory	19,25,134
Kirkpatrick, R.James	University of Illinois at Urbana-Champaign	144
Klein, W.	Boston University	90,121
Klusman, Ronald W.	Colorado School of Mines	128
Knauss, Kevin G.	Lawrence Livermore National Laboratory	39,40,265
Koplik, Joel	City College of the City University of NY	120
Kronenberg, A. K.	Texas A&M University	227
Labotka, T. C.	University of Tennessee	223
Ladd, Anthony, JC	University of Florida	29,139
Larner, Kenneth L.	Colorado School of Mines	130
Lay, T.	University of California at Santa Cruz	111
Lee, Ki Ha	Lawrence Berkeley National Laboratory	8
Lindquist, W.Brent	State University of New York, Stony Brook	183
Lins Neto, R. D.	Pacific Northwest National Laboratory	70
Little, J.	Virginia Polytechnic Institute & State University	247
Liu, Tanzhuo.	Columbia University	132
Liyang, L.	Oak Ridge National Laboratory	63
Long, Jane. C. S.	University of Nevada at Reno	143,174,243
Majer, E. L.	Lawrence Berkeley National Laboratory	10
Mamora, Daulat	Texas A & M University	229
Mango, Frank. D.	Rice University	204
Martel, Stephen	University of Hawaii	143,174,243
Mastalerz, M.	Indiana University	148
Mathez, E. A.	American Museum of Natural History	35,46,87

Maurice, Patricia A.	Kent State University	53,98,155
Mavko, G. M.	Stanford University	211
Maxworthy, Tony	University of Southern California	208
McEvelly, Thomas V.	Lawrence Berkeley National Laboratory	10
McKay, L. D.	University of Tennessee	223
McMechan, George. A.	University of Texas at Dallas	233
Meiburg, Eckart	University of California at Santa Barbara	108
Meigs, Lucy	Sandia National Laboratories	80,166,193
Meyers, W. J.	State University of New York, Stony Brook	181,
Miller, Donald.G.	Lawrence Livermore National Laboratory	36
Mok, Ulrich	Massachusetts Institute of Technology	164
Mondy, L.	Sandia National Laboratories	79,177,235
Morris, J.P.	Lawrence Livermore National Laboratory	29
Morrison, H. Frank	Lawrence Berkeley National Laboratory	8
Morse, John W.	Texas A & M University	229
Muir, Francis	Stanford University	211
Murrell, M. T.	Los Alamos National Laboratory	51
Myer, Larry R.	Lawrence Berkeley National Laboratory	11,13
Myneni, Satish, C.B.	Princeton University	197
Nagy, Kathryn, L.	University of Colorado	124
Naney, M.T.	Oak Ridge National Laboratory	55
Navrotsky, Alexandra	University of California at Davis	102
Newman, Gregory A.	Sandia National Laboratories	74,252
Newmark, Robin L.	Lawrence Livermore National Laboratory	32,
Nicholl, M. J.	Oklahoma State University	84,125,189
Nihei, Kurt. T.	Lawrence Berkeley National Laboratory	13
Nimz, G.J.	Lawrence Livermore National Laboratory	43
Nishiizumi, K.	University of California at Berkeley	52,97
Nur, Amos.	Stanford University	214
Olsson, W. A.	Sandia National Laboratories	81
Orr, Franklin.M.	Stanford University	215
Ortoleva, Peter J.	Indiana University	146
Palmer, D.A.	Oak Ridge National Laboratory	63
Pantano, Carlo.	The Pennsylvania State University	194
Parks, G. A.	Stanford University	209
Phillips, Brian L.	University of California at Davis	100
Pollard, D. D.	Stanford University	217
Potts, M.	Virginia Polytechnic Institute & State University	247
Pruess, Karsten	Lawrence Berkeley National Laboratory	17
Pyrak-Nolte, Laura J.	Purdue University	200
Rajaram, H.	University of Colorado	84,125,189
Ramirez, A.L.	Lawrence Livermore National Laboratory	32
Rard, Joseph. A.	Lawrence Livermore National Laboratory	36
Reedy, Robert	Los Alamos National Laboratory	52,97
Reeves, G. D.	Los Alamos National Laboratory	50

Reitmeyer, Rebecca	U. S. Geological Survey	23
Richter, Frank M.	University of Chicago	113
Riciputi, L. R.	Oak Ridge National Laboratory	57,62
Rivers, Mark L.	University of Chicago	114
Roberts, J. J.	Lawrence Livermore National Laboratory	33
Rock, Peter A.	University of California at Davis	103
Rothman, Daniel H.	Massachusetts Institute of Technology	167
Rudnicki, J. W.	Northwestern University	188
Rundle, John. B.	University of Colorado	90,121
Rustad, J. R.	Pacific Northwest National Laboratory	67,70
Rye, D. M.	Yale University	268
Schimmelmann, A.	Indiana University	148
Schoonen, Martin A. A.	State University of New York, Stony Brook	184,221
Seewald, Jeffrey.	Woods Hole Oceanographic Institution	261
Segall, P.	Stanford University	220
Shankland, T. J.	Los Alamos National Laboratory	35,46,47,87
Sharp, John M.	University of Texas	231
Shock, Everett. L.	Washington University	137
Silver, E.	University of California at Santa Cruz	111
Simmons, Craig T.	Flinders University, South Australia	231
Smith, E.	Los Alamos National Laboratory	47,
Sorensen, Sorena S.	Smithsonian Institution	207
Spera, F. J.	University of California at Santa Barbara	109,171
Spetzler, Hartmut	University of Colorado	122,127
Sposito, Garrison	Lawrence Berkeley National Laboratory	22,53,98,155
Stockman, Harlan W.	Sandia National Laboratories	77,175
Stolper, E.	California Institute of Technology	91
Straatsma, T. P.	Pacific Northwest National Laboratory	70
Strongin, Daniel R.	Temple University	184,221
Sturchio, Neil C.	Argonne National Laboratory	12
Sutton, Stephen R.	University of Chicago	114,117
Sverjensky, Dimitri A.	Johns Hopkins University	151
Symons, N.P.	Sandia National Laboratories	73
Tadanier, C.	Virginia Polytechnic Institute & State University	247
TenCate, J. A.	Los Alamos National Laboratory	47,
Thonnard, N.	University of Tennessee	223
Tidwell, Vincent C.	Sandia National Laboratories	82,179
Toksöz, M. N.	Massachusetts Institute of Technology	45,169
Tokunaga, T. K.	Lawrence Berkeley National Laboratory	15,27
Torgerson, Thomas	University of Connecticut	25,134
Tossell, J. A.	University of Maryland	161
Travis, B. J.	Los Alamos National Laboratory	48
Tripp, Alan C.	University of Utah	239
Tsang, Chin-Fu	Lawrence Berkeley National Laboratories	17
Tsvankin, Ilya	Colorado School of Mines	130,211

Unsworth, M.	University of Washington	248,250
Vairavamurthy, Murthy A.	Brookhaven National Laboratory	6
Valley, J. W.	University of Wisconsin	258
Vasco, D.	Lawrence Berkeley National Laboratory	8
Veblen, David R.	Johns Hopkins University	153,159
Wan, Jiamin	Lawrence Berkeley National Laboratory	18
Wang, H. F.	University of Wisconsin	29,260
Wasserburg, G. J.	California Institute of Technology	93
Watson, E. B.	Rensselaer Polytechnic Institute	202
Waychunas, Glenn A.	Lawrence Berkeley National Laboratory	23
Wesolowski, D. J.	Oak Ridge National Laboratory	60,63
Whelan, J. K.	Woods Hole Oceanographic Institution	262
Williams, Lynda	Arizona State University	68
Wilson, John L.	New Mexico Institute of Mining and Technology	82,179
Wong, Teng-fong	State University of New York at Stony Brook	76,
Wood, R. H.	University of Delaware	137
Wu, Ru-Shan	University of California at Santa Cruz	111,
Wu, X. Y.	University of California at Santa Cruz	111
Xie, X. B.	University of California at Santa Cruz	111
Yuen, David A.	University of Minnesota	48,171
Zachara, J. M.	Pacific Northwest National Laboratory	71
Zhu, Wenlu	Woods Hole Oceanographic Institution	164,264

## DOE/OBES Geosciences Research: Historical Budget Summary

(Thousands of dollars)

ON-SITE INSTITUTION	FY 96	FY 97	FY 98	FY 99	FY00
Argonne National Laboratory	600	620	620	740	438
Brookhaven National Laboratory	528	350	425	595	870
Idaho National Laboratory	65	40	40	0	0
Los Alamos National Laboratory	1960	2096	1509	1260	1235
Lawrence Berkeley National Laboratory	2197	2170	2320	2160	2332
Lawrence Livermore National Laboratory	1940	1915	1421	1445	1736
Oak Ridge Inst for Sci and Ed			85	110	155
Oak Ridge National Laboratory	1251	1195	1228	1235	1145
Pacific Northwest Laboratory	684	600	770	760	815
Sandia National Laboratory	1616	1725	1845	1635	1324
total, on-site published	10865	10826	10263	9940	10050
total, off-site published	8815 0	9705 0	11226	12851	10649
total, operating published	19680	20521	21489	22791	20699
total, equipment	1258	1450	1256	1235	1340
Total GEOSCIENCES-published	20938	21971	22745	24026	22039
<b>OFF-SITE INSTITUTION</b>					
AM. Mus. NY (Mathez)	69	85	98	87	
Arizona (Harpalani - Conf)					10
Arizona St. (Buseck)	132	139			
Arizona St. (Hervig/Williams)	59	74	83	70	
Boston Univ. (Klein)	74	77	123	129	116
Brown U (Yund)	152				

Cal Tech. (Stolper)	140	142	146	150	135
Cal Tech. (Wasserburg)	400	400	465	400	325
Calif, Univ. of Berkeley (Helgeson)	185	192	195	197	190
Calif, Univ. of Berkeley (Nishiizumi)		160	164	160	144
Calif, Univ of Berkeley (Sposito)		67	70	73	74
Calif. Univ. of Davis (Casey)	110	108	104	121	108
Calif, Univ of Davis (Navrotsky)		150		169	160
Calif, Univ. of Davis (Rock)	151	134	138		
Calif, Univ. of LA (Harrison)	111	119	123	124	126
Calif, Univ. of LA (McKeegan)	44				
Calif. Univ. of SB (Boles)	20	31	16		70
Calif. Univ of SM (Meiburg)					69
Calif. Univ. of SB (Spera)	75	76	89	92	82
Calif, Univ of Santa Cruz (Wu)			278	267	251
Calif, Univ of San Diego (DeGroot-Hedlin)		49	58		
Carnegie Inst of Wash (Hemley)			37		
Chicago, Univ. of (Richter)		183	141		
Chicago, Univ. of (Sutton/Rivers)	341	418	429	440	475
Chicago, Univ. of (Sutton)	159	131	137	299	
Colo, Univ. of (Ge)	13	86		120	101
Colo, Univ of (Nagy)				99	128
Colo, Univ. of (Rajaram)	79	124		60	54
--					
Colo, Univ. of (Rundle)	114	120	130	136	122
Colo, Univ. of (Spetzler)	132	152	161	168	
Col. Sch of Mines (Klusman)					159
Col Sch of Mines (Tsvankin)			230	240	216
Columbia Univ. (Broecker)	137	134	154	130	

Conn. Univ. of (Torgersen)	65	68	79	188	
Delaware, Univ. of (Wood)	109	111	124	236	
Desert Res. Inst. (Tyler)	80	148			
Duke Univ (Malin)			44		
Florida, Univ. of (Ladd)			85	70	63
Georgia Tech (Dove)	91	39	86	145	
Hawaii, Univ. of (Martel)	79	84	130		117
Illinois, Univ of (T. Johnson)		138			
Illinois, Univ. of (Kirkpatrick)					395
I.R.I.S. (Simpson)	211				
Indiana, Univ. of (Ortoleva)	102	108	141	124	112
John Hopkins Univ.(Garven)	67	70	77		77
Johns Hopkins Univ.(Sverjenski)	118	105	108	110	100
Johns Hopkins Univ.(Veblen)	156	163	110	110	99
Kent State Univ (Maurice)		33	34	69	
Lehigh Univ. (Ilton)	44	37	115	115	104
Lehigh Univ. (Moses)	123				
Maine Science & Tech (Shehata)		340			
Maryland, Univ. of (Tossell)	28	56	47	48	63
Michigan, Univ. of (Ballentine)	69	71	69		
Michigan, Univ. of (Halliday)	207	226	200		
Minn. Univ of (Yuen)	78	76	91	100	90
MIT (B. Evans)		185	188	198	185
MIT (Harvey)					35
MIT (Rothman)				134	135
MIT (Toksoz)			150	160	144
MIT (Toksoz)					240
NASA (Blankston)	113	95	113		

NAS/NRC (Schiffries/DeSouza)	100	100	100	100	90
Nevada, Univ of (Long)			106	106	96
New England Res (S. Brown)			211	372	
New Mexico Inst. Min. Tech.(Wilson)	30	64		72	65
New Mexico, Univ of (Ingber)			76	80	71
New Mexico, Univ. of (Miller)	100				
NY, City Univ. of CC (Koplik)	98	98	100	99	89
NY, State Univ. of SB (Hanson)	131		155	164	155
NY, State Univ. of SB (Lindquist)	33	35	50	95	
NY, State Univ. of SB (Schoonen)	48	51	54	65	60
NY, State Univ. of SB (Wong)	71	99	100	106	95
Northwestern Univ. (Rudnicki)		88	148	91	89
Notre-Dame, Univ. of (Maurice)					70
Notre Dame Univ (Pyrak-Nolte)	78	81	83		
Ohio St. Univ (Adler)	43				
Okla, Univ. of (Elmore)	158		219	131	127
Okla Sate (Nicholl)				40	36
Oregon St. Univ (Egbert)	41				
Oregon State Univ (Haggerty)					76
Penn St. Univ. (Barnes)	81	87	93		
Penn St. Univ. (Brantley)	117	107	200	142	110
Penn St. Univ. (Brantley) conf.	10				
Penn St. Univ. (Elsworth)					109
Princeton (Myneni)					102
Princeton Univ (Navrotsky)	150				
Purdue Univ. of (Johnson)			130	238	

Purdue Univ. (Pyrak-Nolte)				180	
Rensselaer Polytech. Inst. (Watson)	146		181	179	161
Rice Univ. (Mango)	105	109	111	213	
Rust Geotech, Inc. (Fukui)	87	35			
Rutger Univ (Cheney)		75	75		
Smithsonian Institution (Sorensen)					88
Southern Calif. Univ. of (Aki)	112				
Southern Calif. Univ of (Maxworthy)					85
Stanford Univ. (Brown)		247	259	268	
Stanford Univ. (Harris)	120	125			
Stanford Univ (Mavko)				115	104
Stanford Univ. (Nur)	193	196	211	219	200
Stanford Univ. (Nur)			150	150	135
Stanford Univ (Orr)				136	
Standard Univ. (Pollard)	232	250	195	199	179
Stanford Univ. (Segall)				93	97
Temple Univ. (Strongin)	76	49	52	60	60
Tennessee Univ. of (Thonnard)	82	69			
Texas, Univ of (Banner)			152	152	
Texas, Univ. of (Hardage)	175	175			
Texas, Univ of (Sharp)		61	58	59	
Texas, Univ of Dallas (McMechan/Bhattacharya)	164	124	162	137	124
Texas, A&M Univ. (Kronenberg)			184	350	
Texas A & M Univ (Datta-Gupta)					304
Texas A&M Univ (Morse)					259
Texas Tech Univ (Graham)				100	90
Utah, Univ. of (Forster)					25

Utah, Univ. of (Tripp)	55	57	60	80	73
Utah St. (Hestir)	160	157	73	84	
Utah St (Evans)			129	147	85
VPI & SU (Bodnar)	100	104	122	118	108
VPI & SU (Dove)					202
VPI & SU (Hochella)				161	159
Washington, Univ. of (Booker)	116				
Washington, Univ of (Booker-conf)			8		
Wasington, Univ. of (Unsworth/Booker)		96	97	205	
Washington Univ, St. Louis (Shock)	75	80	106	201	
Wisconsin (Alumbaugh)				52	50
Wisconsin (Alumbaugh - conf)					10
Wisconsin, Univ of (Banfield)	104	139	149	114	103
Wisconsin, Univ of (Haimson)			125	127	115
Wisconsin, Univ. of (Valley)		148	153	147	336
Wisconsin, Univ of (Wang)			50	95	
WHOI (Chave)	55				
WHOI (Eglinton)	135				
WHOI (Seewald)		130	79	134	120
WHOI (Whelan)	195	200	205	377	
WHOI (Zhu)					41
Wyoming, Univ. of (Eggleston)	81	56	56		95
Yale Univ. (Berner)	91	92	177	197	
Yale Univ. (Lasaga/Rye)	290	295	240	247	222
Other	90	244	222	316	505
OFF-SITE TOTALS	8815	9705	11226	12851	10649